Design of Reinforced Concrete Buildings for Restrained and Imposed Deformations

By

Nontavat Aroonsiri
B.E. (Civil) Hons

Supervisor: Professor R.F. Warner

A thesis submitted for the Degree of Master of Engineering Science

Department of Civil and Environmental Engineering
The University of Adelaide
Australia
March 2000

CONTENTS

Abstract

In general, a building structure is designed so that it has adequate strength and robustness to resist the external applied loads. This can be achieved most efficiently by making the structure continuous and indeterminate. On the other hand, deformations which are either internally induced (eg. by shrinkage) or externally imposed (eg. by differential foundation movements) are restrained in an indeterminate structure, and the effects are often overlooked or underestimated by the designers. This can easily result in excessive cracking.

In this case, cracking which lead to a loss of serviceability and those which are aesthetically unacceptable are considered in this thesis. In many situations, it will be necessary to incorporate movement joints to minimise cracking. Usually a successful design requires a compromise between the two conflicting requirements of continuity and articulation.

The main objective of this research is to propose recommendations for the design of reinforced concrete buildings to accommodate the effects of restrained and imposed deformations. This mainly involves investigations into the causes of deformations and the relevant factors that affect shrinkage and creep. Literature view of different methods to predict the magnitude of both shrinkage and creep previously proposed by a number of researchers and design codes is also conducted.

It is also important to understand cracking mechanisms of reinforced concrete member due to applied tensile forces and shrinkage and temperature effects. These involve a study of the effects of bond stress on the behaviour of cracking and the analysis of bond stresses which are based on two approaches, namely "bond stress-slip relation" and " bond stress distribution". Having established the relationships between bond stress and development of cracking, it is then possible to deal with the formulation of crack spacing and crack width equations. From these findings, an analytical model is developed as a simple design tool to determine whether excessive cracking would occur in one-way reinforced concrete slabs. Several conditions of end supports are investigated to determine their effects on the development of cracking. A number of examples are presented in the Appendix.

Various methods proposed by researchers and design codes are reviewed, including the Australian Concrete Structures Standard, AS 3600 (SAA, 1994). In all cases, a minimum amount of reinforcement is recommended for all reinforced concrete members, in order to minimise cracking. These reinforcement requirements are compared critically.

Statement of Originality

This work contains no material which has been accepted for the award of any other degree or diploma in any university and, to the best of my knowledge and belief, contains no material previously published or written by another person, except where due reference has been made in the text. I consent to this thesis being made available for loan and photocopying if accepted for the award of the degree

Nontavat Aroonsiri

Date 12/3/2000

Acknowledgments

The author wishes to thank Professor R. F. Warner of the University of Adelaide for his supervision of the research project presented in this thesis. Without his guidance and sound advice, this thesis would have never been completed. I also appreciate his assistant in providing some part-time employment during my stay at the university.

Many thanks also to all the Civil and Environmental Engineering staff , post graduate researchers and students in particular Mrs Berni Gollege, the departmental secretary. I am very grateful for your friendship and assistant through out those years.

Finally I thank my family especially my grand mother and mother for their patience and continual support through out the years. I know it has taken a very long time. Special thanks also go to my girl friend for her understanding and encouragement.

Notations

β	Factor depending on spacing of transverse reinforcement and average spacing, S_m
β_H	Constant obtained using relative humidity and member size,
β_{sc}	Coefficient which is influenced by the type of cements
α	Constant depends on type of curing method, constant defining member shape and size, air content (% of volume), coefficients of thermal expansion of material
ζ	Coefficient accounts for the effects of tension stiffening in concrete in tension
κ_1	Coefficient accounting for bond properties of reinforcement
κ_2	Coefficient accounting for the distribution of tensile stress within the section
ε	Strain
ε_t	Total strain a member
ε_e	Elastic strain
ε_c	Total strain in concrete, Creep strain
ε_c^*	Maximum value for creep strain
ε_s	Strain in reinforcement
ε_{st}	Total resultant shrinkage strain and thermal strain
ε_t'	Ultimate tensile strain in concrete
ε_{sh}^*	Final shrinkage strain, ultimate shrinkage strain at time infinity commencing after the time of curing, free shrinkage strain in slab
$\varepsilon_{sh}(t)$	Shrinkage strain at time t measured from the commencement of drying
δ_{sh_A}	Free shrinkage at A
δ_{sh_B}	Free shrinkage at B

δ_{sp_A}	Deformation in spring A
δ_{sp_B}	Deformation in spring B
δ_A	Deformation of section A from shrinkage, zero force, position
δ_B	Deformation of section B from shrinkage, zero force position
δ_{slab1}	Extension of span 1
δ_{slab2}	Extension of span 2
$\varepsilon\ (t,t_s)$	Shrinkage strain at any time, t for drying that commenced at an age t_s
$\varepsilon_{sh}(28)$	Shrinkage strain at 28 days
ε_{sho}	notional or ultimate shrinkage strain
ε_{sc}	Compressive strain in reinforcement
ε_{ct}	Tensile strain in concrete
ε_{s2}	Strain in reinforcement at the crack, steel strain within the cracked region
ε_{c2}	Strain in concrete at the crack
ε_m	Mean reinforcement strain, measured over the cracks
ε_{sm}	Average strain in the reinforcement over fully cracked state
ε_{cm}	Average tensile strain in concrete
ε_w	Average crack strain
σ_c	Stress in concrete
σ_s	Tensile stress in reinforcement
σ_{c1}	Tensile stress in concrete of uncracked region, concrete strain in the uncracked region
σ_{c2}	Compressive stress in concrete of cracked region
σ_{s1}	Compressive stress in reinforcement of uncracked region, tensile stress between two cracks
σ_{s2}	Tensile stress in the reinforcement at the crack
$\sigma_{s2,c}$	Tensile stress in the reinforcement at the crack when the tensile stress exceeds the tensile strength in concrete

σ_{sc}	Compressive stress in the reinforcement
σ_{sf}	Tensile stress in reinforcement prior to establishment of stabilised cracking stage
σ_{ct}	Tensile stress in the concrete
ϕ	Creep coefficient
ϕ_o^*	Creep coefficient at time infinity
ϕ_{cc}	Long term value as time t approaches infinity for design creep factor
$\phi_{cc.b}$	Basic creep factor (AS3600)
$\Phi(t,t_o)$	Creep function ψ Ratio of fine aggregate to total aggregate content (%), number of days, factor which averages tensile stress in concrete, σ_{ct} over the area, A_c
γ_{sh}	Correction factor depending on various concrete properties
γ_λ	Correction factor accounts for the influence of relative humidity
γ_h	Correction factor accounts for the size and shape of the member and depends on the average thickness of member under consideration
γ_s	Correction factor depending on concrete slump, S
γ_ψ	Correction factor depending on ratio of fine aggregate to total aggregate concrete, ψ
γ_c	Correction factor depending on cement content, c, correction factor depending on several conditions
γ_α	Correction factor depending on air content, α
γ_{cp}	Correction factor for variations in period of initial moist curing, T_c
γ_{la}	Correction factor for the age of concrete at the time at first loading, t_o
λ	Relative humidity (%)
δ	Total deformation/displacement in a member
δ_c	Deformation/displacement in concrete, concrete stress before 1st crack
δ_s	Deformation/displacement in reinforcement

δ_{sh}	Total deformation in unrestrained slab
δ_{sp}	Deformation in spring
δ_{slab}	Deformation in slab
ρ	Reinforcement ratio
$\rho_{\min}$	Minimum reinforcement ratio
ρ_r	Reinforcement ratio
ρ_{crit}	Critical reinforcement ratio
ρ_{eff}	Effective reinforcement ration relating to the concrete area A_{ct}
$\hat{t}$	Duration of drying (t - t_{sh})
τ	Average bond stress, bond stress
τ_{ave}	Average bond strength between concrete and reinforcement
$\tau(x)$	Bond stress at a distance x from the end of the member, average bond stress measured at a point distance x from the face of the crack
$\tau_{\max}$	Maximum bond stress
τ_{sh}	Shrinkage square half time
Δ	Slip at reinforcement and concrete interface
$\Delta\varepsilon_{s2}$	Change in strain of reinforcement in cracked region
$\Delta\varepsilon_{c2}$	Change in strain of concrete in cracked region
ΔL	Change in length of member
ΔT	Different in temperature
Δ_x	Local slip at a distance x from the crack
a	Reinforcement spacing, "no bond length" for the reinforcement near a crack
a_{cr}	Distance from the point considered to the surface of the nearest longitudinal reinforcement
A	Slope of bond stress-slip curve or slip modulus, a constant depending on a set of boundary conditions
A_s	Cross section area of steel
A_{ct}	Area of concrete under tension before cracking
A_c	Cross section area of concrete

A_s	Cross section area of steel
$A_{c,ef}$	Effect cross section area of concrete
A_{c1}	Cross section area of concrete in uncracked region
A_{s1}	Cross section area of reinforcement in uncracked region
B	A constant depending on a set of boundary conditions
c	Cement content (kg/m^3), concrete cover
c_{min}	Minimum concrete cover
C	Specific Creep, factor depending on shape of bond stress-slip curve and bond strength, a constant depending a set of boundary conditions
C_o	Specific creep
C_1^{ref}	Coefficient taken as 10 mm^2 per day
$C_1(t)$	Coefficient which is proportional to the drying diffusivity at the commencement of drying
$C_d(t,t_o,t_{sh})$	Increase in specific creep due to drying
$C_p(t,t_o,t_{sh})$	Decrease in specific creep after drying
d	Diameter of reinforcement, constant defining shape and size
d_{max}	Maximum diameter of reinforcing bar
D	A constant depending a set of boundary conditions
E	A constant depending a set of boundary conditions
E_c	Elastic modulus of concrete
E_s	Elastic modulus of steel
E_e	Effective modulus for concrete
E_o	Asymptotic modulus
F	Restraining force in member, applied axial force
F_c	Reactive force at C
F_{sp}	Tensile force in the spring
F_{slab}	Tensile force in the slab
F_{sp_A}	Tensile force in spring at A
F_{sp_B}	Tensile force in spring at B
F_{slab1}	Tensile force in span 1
F_{slab2}	Tensile force in span 2

f_{sy}	Yield strength in reinforcement
f	Number of days
$f_t^{'}$	Tensile strength of concrete
f_{cm}	Mean compressive strength of concrete at the age 28 days (MPa)
$f_c^{'}$	Characteristic strength of concrete at 28 days
h	Humidity (%), depth of member
h_o	Initial relative humidity before drying commences, average thickness of member
k	Slope of bond stress-slip curve
k_{sp_A}	Stiffness of spring A
k_{sp_B}	Stiffness of spring B
k_{slab1}	Axial stiffness of span 1
k_{slab2}	Axial stiffness of span 2
K	Bond constant, factor depending on the type of reinforcement, modulus of elasticity of reinforcement, reinforcement ratio and tensile strength f concrete
K_1	A factor accounting for the effects of concrete cover c and reinforcement spacing a, a factor to provide for the possible variation in materials properties
k_{slab}	Axial stiffness of the slab
k_{nslab}	New axial stiffness after cracking
k_{nslab1}	New axial stiffness in span 1
k_{nslab2}	New axial stiffness in span 2
k_{sp}	Stiffness of the spring
k_s	Shape factor
k_h	Coefficient which depends on relative humidity h (%)
k_1	Factor accounts for the age of concrete (AS3600)
k_2	Factor accounts for the duration of loading (t-t_o) (AS3600), factor depending on the type of reinforcement used.
k_3	Factor accounts for the age of the concrete at the time of loading, factor depending on the shape of tensile stress diagram
k_4	Scatter factor accounts for variation of concrete and bond

	strength
k_5	Factor accounts for load repetition or sustained load
k_1 (c,a)	Factor representing influence of concrete cover c and spacing of reinforcement a.
RH	Relative humidity of the ambient atmosphere (%)
L	Length of member
L_1	Length of span 1
L_2	Length of span 2
l_o	Length of lost bond
m	Number cracks at any time
n	Modulus ratio
n_e	Modulus ratio
N	Factor depending on shape of bond stress-slip curve and bond strength, number of cracks
N_{bar}	Number of reinforcing bars
R	Restraint factor, a factor of 1 is used for fully restraint member
S	Surface area, crack spacing
S_o	Minimum crack spacing, length of transfer
S_m	Average crack spacing
S_{min}	Minimum crack spacing
S_{max}	Maximum crack spacing
$S_d(t, t_o)$	Time shape function
$S_p(t, t_{sh})$	Time shape function
t	Time measured from commencement of drying (days) or from the end of the initial curing
t_e	Effective concrete cover
t_{sh}	Age/time at which drying commences
t_o	Time at which constant sustained stress is applied, time at first loading
t_{sh}, t_s	Time in which drying begins
u	Perimeter of the member in contact with the atmosphere
V	Volume

W_{cr}	Length of cracked region
W_{cr1}	Cracked length in span 1 and is equal to $2S_o$
W_{cr2}	Cracked length in span 2 and is equal to $2S_o$
w	Crack width
w_{ave}	Average crack width
w_{max}	Maximum crack width
w_k	Design crack width (95 percent fractile)
w_m	Average crack width
w_{95}	95 % fractile of maximum crack width
x	Distance measured from reference point or distance between two cracks

List of tables

Chapter 2

Chapter 3

Chapter 4

Chapter 5

Chapter 7

List of figures

Chapter 2

Chapter 3

Chapter 4

Chapter 5

Chapter 6

Chapter 7

Chapter 1

Introduction

1.1 Introduction

The structural behaviour of a reinforced concrete structure is not only influenced by the applied loads, but also by various time-dependent effects such as temperature changes, shrinkage and creep of concrete and differential movement of the foundation. These factors can seriously affect the overall performance and adequacy of reinforced concrete buildings and structures. If each reinforced concrete member in a building were free to move or deform as a result of these effects, no internal stresses would develop. In practice however this is not possible. Some degree of restraint is always imposed on an element by the rest of the structure, even in the smallest building. As a result, when a member undergoes contraction and expansion as a result of time-dependent deformation, there is a build up of internal forces which eventually can result in excessive cracking in both the structural and non structural members of the building.

In general, a building structure is designed so that it has adequate strength and robustness to resist the external applied loads. This can be achieved most efficiently by making the structure continuous and indeterminate. On the other hand, deformations which are either internally induced (eg. by shrinkage) or externally imposed (eg. by differential foundation movements) are restrained in an indeterminate structure, and the effects often tend to be overlooked or underestimated by the designers. This can easily result in excessive cracking.

In all circumstances, designers need to understand the effects of restrained and imposed deformations and their origins. In some cases, special design provisions

need to be incorporated in order to produce a design which does not result in excessive cracking. For example, a form of articulation of the structure through the introduction of movement joints can allow relative movements to occur within the structure and thus relieve the restraints within the members.

1.2 Continuity and Articulation in Building Structures

While it may seem rational to include movement joints to reduce internal stresses in a structure, it is often very difficult in practice to achieve the intended function of the movement joints, which is to reduce the internal stresses that lead to excessive cracking. Problems can stem from the incorrect choice of joint detail during the design process or from poor detailing in design and construction (Rüth , 1995). Apart from these problems, there are other significant disadvantages to the use of movement joints. These include:

a) regular maintenance or replacement is required which can be costly;
b) the construction time and cost are increased due to the high precision required during construction;
c) overall stiffness of the structure is reduced which can result in vibration and deflection problems;
d) if not properly sealed, leakage problems can occur at the joint; and
e) the visual impact can be adversely affected by the discontinuity in the structure.

On the other hand, continuity in building structures offers a number of structural advantages. These include:

(a) reduction in member sizes due to a decrease in the magnitudes of bending moments and shears;
(b) smaller bending moments also lead to significant increase in allowable span;
(c) reduction in deflection and vibration;
(d) increase structural stiffness of the structure;
(e) higher fire resistance;
(f) improved earth-quake resistance; and
(g) time saved during construction to cater for movement joints.

With these factors under consideration, most designers remain adamant that movement joints are necessary in reinforced concrete buildings, but the number of these joints should be kept absolutely to a minimum. From the practical design point of view, it is also often very difficult to obtain full continuity, particularly at the connections. This is because once cracks form in the member or connections, the degree of continuity can reduce drastically. A study conducted by Oesterle et.al (1989) found that cracks forming over the support region of a continuous bridge girder could drastically reduce the degree of continuity. In addition, numerous tests have shown that joints and connections tend to perform poorly at overload and are weak points in concrete structures.

Usually a successful design requires a compromise between the two conflicting requirements of continuity and articulation. Ultimately, the form of the compromise will depend on the magnitude of the restraining forces and deformations occurring under the various factors mentioned earlier. They will decide on the necessity of movement joints, and of their number and locations.

1.3 Cracking in Building Structures

In the design of a building, cracking plays a major role in determining which design alternative to adopt. Cracking problems mainly relate to serviceability problems, and only cracks which lead to a loss of serviceability and those which are aesthetically unacceptable are considered in this thesis. The former may result in excessive crack widths which lead to corrosion of the reinforcement or leakage of water or heat, as well as sound transfer and damage to finishes. Acceptable crack widths are difficult to specify, although guidelines are available (CEB Manual, 1985 and CEB-FIP, 1993).

Since the types of cracking being considered generally occur in the serviceability state or in the range where reinforcement has not yielded, flexural cracking is rarely a problem as long as adequate reinforcement is provided and good bond is achieved. In effect, cracking associated with shrinkage and temperature often dominate. For most buildings, cracking associated with shrinkage and temperature effects is accommodated by providing sufficient reinforcement so that the crack widths are maintained at an acceptable level. However, this is not always the case as the

magnitudes of the tensile forces are often too large and a design alternative is necessary, in the form of movement joints.

1.4 Purpose for this research

The purpose of this research is to propose recommendations for the design of reinforced concrete buildings to accommodate the effects of restrained and imposed deformations. This involves investigations into the following:

1) causes of deformations and their effects on building structures;
2) cracking mechanisms in members subjected to restrained and imposed deformations;
3) analytical methods which can be used to determine the restraining forces in reinforced concrete members subjected to varying degrees of restraint in a building;
4) methods of crack control as recommended by various design and building codes;
5) different design provisions to control restrained deformation in building structures;
6) current practice in the use of movement joints; and
7) recommendations for the design of reinforced concrete buildings to resist restrained and imposed deformations.

1.5 Thesis Contents

This thesis consists of 8 chapters. Following on from this introductory chapter, the contents of the various chapters are as follows:

Chapter 2 Time dependent deformations in reinforced concrete

The main objective of Chapter 2 is to study the causes of time dependent deformations which result in restrained and imposed deformations in building structures. These are: shrinkage, creep, temperature changes and differential movement of foundations. Particular attention is paid to shrinkage and creep effects which form a major part of this chapter. Temperature effects and differential foundation movement are dealt with in less detail. The main part of this chapter

contains a study of the relevant factors that affect shrinkage and creep, as well as a literature review of methods used to predict the magnitude of both shrinkage and creep previously proposed by a number of researchers and design codes.

Chapter 3 Cracking mechanism for reinforced concrete members in tension

This chapter investigates the mechanism of cracking caused by restrained and imposed deformations. Cracking of this nature is different to cracking due to flexure and therefore alternative available theories are reviewed. These include cracking mechanisms of reinforced concrete member due to applied tensile forces and shrinkage and temperature effects. These involve a study of the effects of bond stress on the behaviour of cracking and the analysis of bond stresses which are based on two approaches, namely "bond stress-slip relation" and " bond stress distribution". Having established the relationships between bond stress and development of cracking, it is then possible to deal with the formulation of crack spacing and crack width equations. Accordingly, a literature review of works on crack spacing and crack width equations for both cases is presented.

Chapter 4 Analysis of restrained and imposed deformations in reinforced concrete buildings

Chapter 4 contains the main analytical study undertaken in this research. An analytical model is developed to determine whether excessive cracking would occur in one-way reinforced concrete slabs. The main criterion used for this model is a limit on the cracking caused by time-dependent deformations. Shrinkage and creep are assumed to be the dominant sources, and bending moment is ignored. Several conditions of end supports are investigated to determine their effects on the development of cracking. There are also a number of numerical calculations shown as examples.

Chapter 5 Control of cracking due to restrained and imposed deformations

Chapter 5 presents different recommendations as to how excessive cracking can be controlled. Various methods proposed by researchers and design codes are reviewed, including the Australian Concrete Structures Standard, AS 3600 (SAA, 1994). In all cases, a minimum amount of reinforcement is recommended for all

reinforced concrete members, in order to minimise cracking. These reinforcement requirements are compared critically.

Chapter 6 Design of reinforced concrete buildings for restrained and imposed deformations

Having identified causes and effects of restrained and imposed deformations, Chapter 6 presents design methods to control the effects of restrained and imposed deformations. This can be accomplished by either carefully controlling the causes of deformation and design the continuous structures to accommodate the deformations or to introduce specially design to relieve the restraining forces.

Chapter 7 Movement joints in reinforced concrete buildings

Chapter 7 presents a literature review of the use of movement joints in reinforced concrete buildings. Two types of movement joints are discussed namely, contraction and expansion joints. There is also a discussion of factors affecting the locations of movement joints. In general, there are no reliable rules for determining the spacing of the joints. In practice, these design decisions are usually based on experience and judgment. However, two analytical methods of calculating the maximum spacing of movement joints are discussed. The results obtained from these methods are used to compare with the current practice.

Chapter 8 Conclusions and recommendations

The conclusions and recommendations for the research are summarised in this chapter. Specific recommendations for design of restrained and imposed deformations in reinforced concrete building due to what ever causes are made with considerations drawn from findings through out this research. The analytical model proposed in Chapter 4 provides a simple procedure which can be incorporated in analysing restrained members subjected to time dependent deformations.

Chapter 2

Time dependent deformations in reinforced concrete

2.1 Introduction

Reinforced concrete buildings are subjected to various load independent and time-dependent deformations. The deformations which to be considered here are:

- shrinkage
- creep
- temperature changes
- differential foundation movements

The main objective of this chapter is to investigate the factors that affect the magnitude of these deformations and their development with time. This information is needed and must be properly assessed, so that designers can predict their magnitudes. Currently there are numerous methods to predict the magnitude of shrinkage and creep in concrete structures. Thus a literature review is also conducted to study and compare these methods. Over the years, an enormous number of papers have been published on shrinkage and creep, and it has been necessary to discuss only the ones most relevant to this thesis.

Although temperature changes and differential foundation movements are equally as important as creep and shrinkage in their effects on deformations, they are only briefly discussed because their physical processes are relatively simple.

2.2 Shrinkage

2.2.1 Definition

Shrinkage can be described as a reduction in volume of concrete due to the loss of water during the drying process. It can occur within weeks or many months or even years after construction and some occur on a random basis corresponding to random temperature changes. Various types of shrinkage have been identified in concrete structures, namely:

- drying shrinkage
- plastic shrinkage
- carbonation shrinkage
- autogenous shrinkage.

Drying shrinkage is often regarded as the most serious problem to be considered in the design and construction of concrete structures. Consequently, the main discussion on the topic of shrinkage is concentrated on drying shrinkage. The term "shrinkage" used later in this chapter and in other parts of this thesis therefore refers to drying shrinkage. Other types of shrinkage, if mentioned, are referred to in their full terminology.

A brief summary of each type of shrinkage is presented here, before dealing in some detail with drying shrinkage.

Plastic shrinkage

Plastic shrinkage develops during early stages of hydration, often thirty minutes to six hours after concrete pouring. It occurs as a result of rapid drying of the concrete surface during the plastic stage such that water evaporates from the surface faster than it reaches by bleeding. In general, cracks due to plastic shrinkage are more of an aesthetic rather a structural problem, but in some cases, they can subsequently act as starters for more serious cracks.

Carbonation shrinkage

Concrete can also undergo shrinkage due to carbonation. This process is due to the carbon dioxide in the atmosphere. In the presence of moisture, it proceeds slowly through the surface layer of the concrete and chemically reacts with the hydrated

cement. The rate of carbonation increases with an increase in the concentration of carbon dioxide. If both drying and carbonation shrinkage occur simultaneously, less shrinkage develops. The effect of carbonation shrinkage alone is more pronounced in the vicinity of 50 percent humidity, and is very small at 100 percent and 25 percent humidity.

Autogenous shrinkage

Autogenous shrinkage generally occurs in the interior of a large concrete mass even when no moisture movement to or from the member is possible. This is caused by the hydration of cement where an autogenous volume reduction in the cement plus water system takes place. Typically, the magnitude of autogenous shrinkage is between 50 to 100 microstrains (Neville and Brooks, 1987).

2.2.2 Composition of hardened cement paste

To understand the basic mechanism of drying shrinkage, it is useful first to consider shrinkage in plain concrete (the influence of reinforcement will be discussed in Chapter 3) and study the structural components that make up a hardened concrete. The shrinkage process in hardened cement paste is very complex because of diverse components, with largely different properties, combined together (Bazant, 1986).

When dry cement paste is mixed with water, several chemical reactions take place. These reactions are called hydration. Once the cement paste has hardened, some of the water remains in the capillary pores, but a large amount is contained in a continuous matrix component, known as Calcium Silicate Hydrate (C-S-H). This component occupies approximately two thirds of the total volume. The remainder of the cement paste contains other hydrated products such as Calcium Hydroxide (CH), Calcium Sulfoaluminate hydrates and some unhydrated residues of the original cement grains are all embedded within the C-S-H matrix. The components are summarised in Table 2.1 and illustrated in Figure 2.1.

It was suggested by W. Hansen (and reported by Bazant, 1986) that only the Calcium Silicate Hydrate and the capillary pores components contribute significantly to the process of shrinkage (as well as creep) and that it is therefore

justified to ignore the influence of both Calcium Hydroxide and Calcium Aluminate on concrete shrinkage.

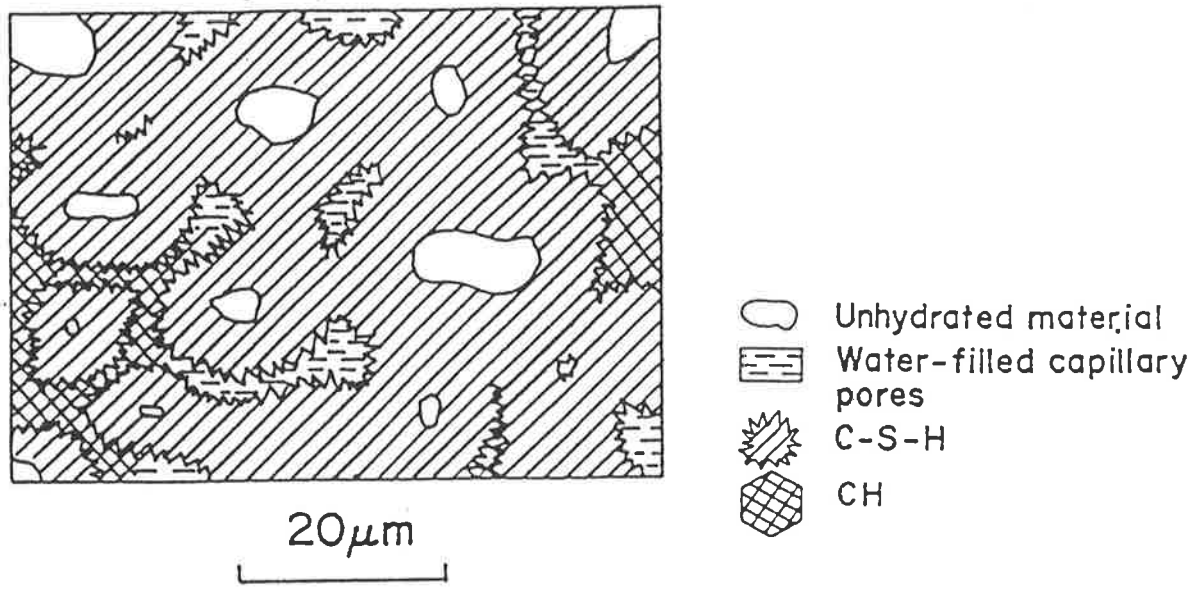

Figure 2.1 Schematic view of hardened cement paste microstructure (reproduced from Bazant, 1986)

Table 2.1 Summary of components in hardened Portland Cement Paste (modified from Bazant, 1986)

Components	Description
Calcium Silicate Hydrate (C-S-H)	Amorphous, methastable gel
Capillary pores	Remnants of water-filled space
Calcium Hydroxide (CH)	Relatively large crystal (approximately 10 μm – 1mm)
Calcium Aluminate	Very small crystals (approximately 1- 10 μm)

2.2.3 Physical mechanism of drying shrinkage in plain concrete

Drying shrinkage is caused by the withdrawal of water from hardened concrete in an unsaturated or dry atmosphere. The process is largely irreversible. Even after an extensive period of storage in water, concrete can not recover the entire initial drying shrinkage.

For a concrete member undergoing shrinkage, the general pattern of behaviour in the irreversible part of the shrinkage can be described as follows:

- during the drying process of concrete, the exposed surface loses water by evaporation. Initially, the water molecules held in the large capillary pores of the hardened cement paste are removed, as they are not physically bonded to any components. The loss of this water does not significantly alter the volume or cause any shrinkage,
- however, this process induces a relative humidity gradient within the cement paste structure (Neville and Brooks, 1987). As drying continues, the water molecules from the Calcium Silicate Hydrate are transferred into the empty capillaries and hence are removed by evaporation,
- unlike the initial loss of water molecules which does not induce any volumetric changes, this time the cement paste contracts, resulting in shrinkage of the concrete member. However it should be realised that the reduction in volume of drying concrete is not equal to the volume of water removed. This is because the initial loss of free water does not cause a significant volumetric contraction of the paste and the Calcium Silicate Hydrate structure provides some internal restraint against consolidation.

2.2.4 Factors influencing shrinkage

Numerous factors can affect shrinkage in concrete members, and can be both external and internal. Member shape and size, humidity, temperature, and the area of the exposed surface of the concrete are treated as external factors, while water-cement ratio, composition of the cement, aggregate, characteristics and amount of admixtures used, the proportions of the mix and the amount of reinforcement are the main internal factors affecting shrinkage.

Extensive experimental information is available in the literature concerning the effect of these factors on shrinkage. The following is a brief summary:

2.2.4.1 Properties and types of aggregate

As water molecules are removed from the cement paste, concrete begins to shrink. The presence of aggregate in the concrete provides internal restraint which

significantly reduces the magnitude of volume changes. Campbell-Allen (1979) commented that without aggregate, cement paste could shrink from 5 to 15 times as much as concrete. As a result, the effect of aggregate is a very important factor. Neville (1981) and Neville and Brooks (1987) considered it to be the most important factor. This view is also supported by many researchers, including Roper (1974b). Although Neville (1981) suggested that size and grading of aggregates do not directly influence the magnitude of shrinkage, increasing the size of aggregate allows the use of a leaner mix which results in lower shrinkage.

In addition, the degree of restraint to shrinkage is affected by the elastic properties of the aggregate. Aggregates with a low modulus of elasticity are easier to compress and therefore offer less restraint to the shrinkage of the cement. Neville (1981) reported that lightweight aggregate generally results in higher shrinkage because of a lower modulus of elasticity. Lightweight aggregate with a lower modulus of elasticity generally results in higher shrinkage because of the smaller restraint against shrinkage of the cement paste (Neville, 1981).

Aggregates of various types are also known to exhibit different shrinkage characteristics. Quartz, granite, feldspars and some basalts can be regarded as low shrinkage type, while sand-stone like materials, shale and volcanic breccia materials are considered to have high shrinkage. Roper (1974b and c) found that aggregates like breccia aggregates used in NSW were dimensionally unstable and were leading to very large shrinkage.

Samarin (1996) suggested that aggregate of a specific origin, rather than the generic aggregate type should be assigned to be the influential factor. Moreover, Samarin (1985) suggested that blending aggregate of different types could actually produce desirable shrinkage values. Gilbert (1988) also reported that an increase in aggregate content should reduce shrinkage due to the additional restraint between aggregates and cement paste.

It should be noted that even though the restraining effect of the coarse aggregate reduces overall shrinkage in the concrete, but it also produces significant tensile

stress in the concrete matrix. Residual stresses are thus built up in the concrete as the result of shrinkage.

In summary, it can be concluded that the main factors to influence the ability of the aggregate to restrain shrinkage are as follows:

- Volume fraction of aggregates
- Compressibility or modulus of elasticity
- Source and type of the materials
- Shrinkage characteristics of the aggregate upon drying

2.2.4.2 Water-Cement Ratio

Campbell-Allen (1979) singled out the amount of water per unit volume of concrete as the dominating factor. A significant increase in drying shrinkage in a given environment can occur if the water-cement ratio is increased. However this increase is influenced more by the total amount of water present in the concrete, and less by the cement content. In fact, this idea is reinforced by Neville (1981) who did not believe that the properties of cement exert any large influence on the shrinkage of concrete. In contrast, he commented that the water content of a concrete mix affects shrinkage such that the volume of aggregate is reduced and did not believe water-cement ratio to be a primary factor.

2.2.4.3 Chemical admixtures

Admixtures used in concrete may be categorised into three different types, namely accelerators, water-reducing agents, and air entraining agents. Water-reducing agents are widely used in Australia whereas air-entrainment agents are more common in the United States (Campbell, 1992).

In general, it is often very difficult to establish a clear conclusion as to how these admixtures affect shrinkage because each type of admixture and the interaction with the concrete mix are different to a varying degree. Nevertheless, a study conducted by Morgan (1975) indicated that accelerators such as calcium chloride triethanolamine caused substantial increase in drying shrinkage. This is also supported by tests conducted by California Department of Transportation in the United States as reported by ACI 224 (1989), which showed that concrete

humidities exhibited different volume changes due to shrinkage. This can be demonstrated in Figure 2.2 where shrinkage strains, obtained from concrete specimens stored under prescribed conditions of temperature and humidity, are plotted against time.

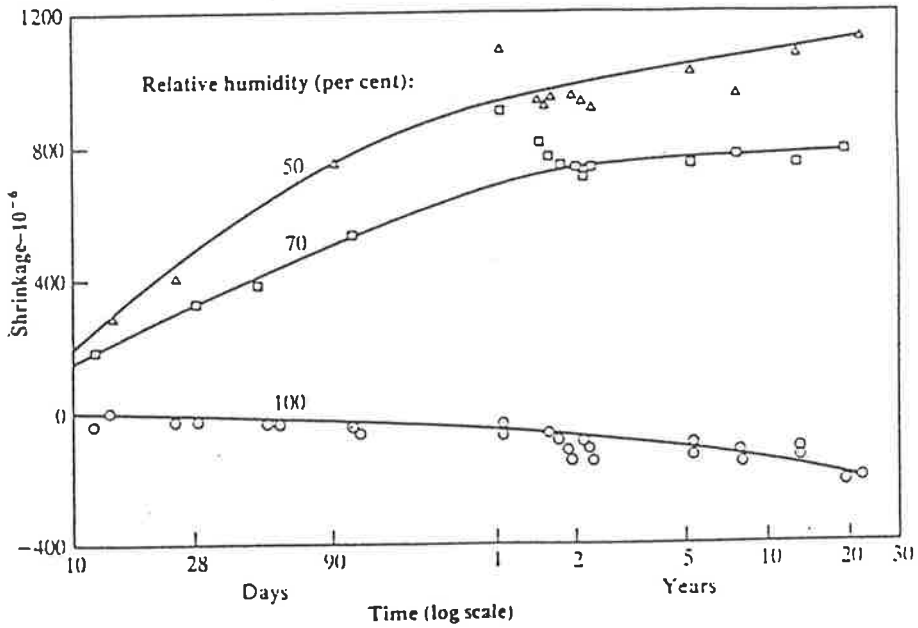

Figure 2.2 Relation between shrinkage and time for concrete specimens stored at 50, 70 and 100 percent relative humidity respectively (Reproduced from Neville & Brooks, 1987)

It is also important to consider any fluctuations in the environmental conditions and the ambient relative humidity. Unfortunately, there is only a limited amount of information concerning this topic. Nevertheless, test results from Muller and Pristl (1993) demonstrated that constant ambient relative humidity results in higher shrinkage than variable humidity. This observation also agreed with those of Al-Alusi et al, as reported by Muller and Pristl (1993)

2.2.4.7 Type and Duration of Curing

By lengthening the curing time, it is possible to delay the commencement of shrinkage and allow the concrete member to gain higher concrete strength. However, it is uncertain whether this practice actually affects the magnitude of shrinkage once drying commences. A report published by ACI 224 (1989) indicated that the duration of moist curing of concrete does not significantly affect the final drying shrinkage. The reasons for this were based on experiments conducted by the

California Department of Transportation, as reported by ACI 224 (1989) which found that concrete having been moist cured for 7, 14 and 28 days exhibited essentially the same amount of total shrinkage.

Neville (1981) also demonstrated theoretically that prolonged curing might not necessarily be beneficial as far as cracking tendency is concerned. He suggested that shrinkage in a well cured concrete progresses more rapidly, thus the relief of shrinkage by creep is smaller. In his view, it is not justified in lengthening the curing period and delaying the commencement of drying as the disadvantages far outweigh the advantages.

In contrast to cast-in-place concrete, precast concrete can benefit from curing to minimise shrinkage. ACI 224 (1989) suggested that steam curing at atmospheric pressure can help to reduce drying shrinkage. This is because steam curing assists in high early-age strength of concrete, thus it will minimise the possibility of cracking since precast members are usually unrestrained.

2.2.5 Summary

From the previous discussion, it can be seen that the magnitude of shrinkage in a concrete member is influenced by many variables. Concretes with large aggregate content undergo less shrinkage, and aggregates with a high modulus of elasticity or with rough surfaces provide a greater restraint to shrinkage. While the type of cement can affect shrinkage, the full extent of this effect is not completely determined. However, several investigators, including Neville and Brooks (1987) and Neville (1981), suggested that it is the water-cement ratio which is of more importance because a higher water-cement content can increase the amount of shrinkage. In fact, this increase is influenced more by the total amount of water present in the concrete and to a lesser extent by the cement content. In addition, the use of chemical admixtures in concrete can be another factor that affects shrinkage, but the effect is complex and depends on the admixtures' chemical formulation, the interaction with the cement and other admixtures in the concrete.

In summary, shrinkage of concrete can be minimised in several ways. First, the water content of a mix should be kept to a minimum. Second, aggregate of large size

and with low shrinkage properties should be selected. Other factors such as curing may not be beneficial to the suppression of shrinkage, unless the members are precast. As a result, it is not advantageous to delay the commencement of drying by lengthening the curing period.

2.2.6 Typical Shrinkage Strains

2.2.6.1 Unreinforced concrete

It can be seen that shrinkage strains in unreinforced concrete vary with the mix constituents, especially on the amount and type of aggregate. A concrete member that is unrestrained, does not usually exhibit any visible cracking because the member is allowed to freely deformed. However, because of the tensile stresses which develop in the matrix, very fine bond cracks always exist at the interface between the coarse aggregate and hydrated cement even before any visible cracking has occurred. Such bond cracks are known as microcracks and they occur as a result of differential volume changes between the cement paste and the aggregate, and in the thermal and moisture movements (Neville and Brooks, 1987).

Tests conducted by Roper (1974b and c) showed that ultimate shrinkage strains can range between 600 to 1600 microstrain, depending on the type of aggregate used. Campbell-Allen (1992) reported that shrinkage strain in concrete can range between 500 and 1000 microstrain and in some cases, shrinkage strains up to 1200 microstrain can occur. Nevertheless, these values are varied from country to country.

2.2.6.2 Reinforced concrete

The presence of reinforcement in concrete section contributes to the internal restraint against shrinkage. Therefore, it can be expected that the ultimate shrinkage strain in reinforced concrete is lower than in plain concrete. As with plain concrete, it is not possible to establish any reliable typical values for shrinkage strains.

Alexander and Lawson (1981) reported that shrinkage strains in most reinforced concrete sections could be estimated in the range of 150 microstrain and 300 microstrain depending on the amount of reinforcement. They further suggested a net long-term shrinkage of 200 microstrain for a floor slab of a building. However they did not specified the countries which these values apply to.

On the other hand, Woodside (1989) and Samarin (1996) recommended shrinkage strain in Australia is substantially larger. Samarin (1996) suggested a shrinkage strain of about 800 microstrain to be used, in the absence of any specific shrinkage data from the concrete supplier and for non-critical structural elements. If the dimensional change in structure is going to have a significant effect on the performance of the structure, then it is necessary to obtain test results of shrinkage values from the suppliers. Woodside (1989) recommended a slightly lower ultimate shrinkage strain of 750 microstrain for concrete structures in Adelaide otherwise this value is further reduced to 600 microstrain for precast structures.

If shrinkage strain takes place rapidly in very young concrete, it is possible for the tensile stress to exceed the tensile strength of concrete which may have not attained its maximum value. In effect, cracking is expected to develop. When this happens, Campbell-Allen (1979) found that the ultimate tensile strain of concrete is in the order of 100 microstrain otherwise it can become three or four times this magnitude if shrinkage takes place slowly. Hence, it is critical for engineers to realise that both long term and short term cracking can occur. The topic of cracking will be discussed in more detail in Chapter 3.

In addition to the internal restraint provided by reinforcement, the magnitude of shrinkage strain that can occur in reinforced concrete members also depends on external restraint such as member end supports. This topic will be covered later in the Chapter 3.

Table 2.2 summarises various design recommendations for typical shrinkage strains. However these values are estimates and a more accurate method of prediction should be adopted whenever local condition and environment directly affects the design.

2.2.7 Methods for Predicting Shrinkage

Over the years, various methods have been proposed to predict the amount of shrinkage in concrete structures. Current procedures for predicting shrinkage strain are largely derived from empirical formulae, and at best are only rough estimates.

Gilbert (1988) suggested that the most accurate means for obtaining shrinkage strain (as well as the final creep coefficient) is to extrapolate from short term test results. Generally, shrinkage strain is measured over a short period of time in an unloaded concrete specimen, thus the name "free shrinkage strain". Based on these short-term measurements, the long-term values of shrinkage strains can then be estimated. In order to improve the accuracy of the long-term shrinkage, the measurement can also be extended over long period of time.

Nonetheless, designers often can not afford to carry out proper testing of shrinkage because of time and cost constraints. Hence, they must rely on one of the numerical methods which have been developed over a number of years.

Table 2.2 Typical shrinkage strain in concrete members as reported by authors

Author	Typical shrinkage strain
Campbell-Allen (1973)	200-600 $\mu\varepsilon$ in unrestrained concrete depending on humidity of the environment
Alexander and Lawson (1981)	200 $\mu\varepsilon$ for typical building slab or 150-300 $\mu\varepsilon$, depending on the amount of reinforcement for most concrete structures
Thornton and Lew (1982)	Typical value of 800 $\mu\varepsilon$
Woodside (1989)	Limited to 700 $\mu\varepsilon$ for concrete structures and 600 $\mu\varepsilon$ for precast structures
Campbell-Allen (1992)	500-1000 $\mu\varepsilon$ for long term values
AS 3600 (1994)	assume a median value of 700 $\mu\varepsilon$ in the absence of any data
ACI Committee 224 (1995)	500 $\mu\varepsilon$ for building slabs and can be less than 100 $\mu\varepsilon$ for an exposed slab on grade
Samarin (1996)	A typical value of 800 $\mu\varepsilon$ as a guide

Mostly, numerical expressions for shrinkage are in the form of exponential or hyperbolic functions that approach a limiting value as time approaches infinity (Neville et al, 1983 and Gilbert, 1988). This is because drying shrinkage of concrete is believed to approach a limiting value with time. The majority of the equations in well known model codes are hyperbolic functions.

Some equations proposed for estimating shrinkage in concrete as a function of time are as follows:

2.2.7.1 Meyers et al. (1970)

Meyers et al. (1970) presented the following equation to calculate shrinkage strain $\varepsilon_{sh}(t)$ at time t :

$$\varepsilon_{sh}(t) = \frac{t}{\alpha + t}\varepsilon^{*}_{sh} \tag{2.1}$$

where t = time measured from commencement of drying (days)

α = a constant taken to be 35 for moist cured concrete and 55 for steam cured concrete

ε^{*}_{sh} = the final shrinkage strain

From equation (2.1) shrinkage strains at 28 days may be measured and used to predict long term shrinkage using the following equations:

For moist cured concrete:

$$\varepsilon_{sh}(t) = \frac{2.25}{35 + t}\varepsilon_{sh}(28) \tag{2.2}$$

For steam cured concrete:

$$\varepsilon_{sh}(t) = \frac{3.0t}{55 + t}\varepsilon_{sh}(28) \tag{2.3}$$

2.2.7.2 Neville et al (1983)

Neville et al (1983) proposed the following equations to calculate long term shrinkage, $\varepsilon_{sh}(t)$ for moist cured concrete.

$$\varepsilon_{sh}(t) = \alpha \varepsilon_{sh}(28)^{\beta} \tag{2.4}$$

In the above equation

$$\alpha = (1.53 \ln t - 4.17)^2 \tag{2.5}$$

$$\beta = \frac{100}{2.9 + 29.2 \ln t} \tag{2.6}$$

In addition to the above methods, there are numerous methods that are widely used and accepted for predicting shrinkage in concrete, including:

- Bazant and Panula (1978, 1982)
- ACI Committee 209 (ACI Committee 209, 1982)
- CEB-FIP Model Code 1990 (CEB-FIP, 1993)
- AS3600-1994 (SAA, 1994)

For simplicity, the methods of predictions for shrinkage by the Australian Code AS3600-1994 (1994) will be referred as AS3600. Similarly, the methods reported by ACI Committee 209 under the title "Prediction of creep, shrinkage and temperature effects in concrete structures", ACI Committee, 1982 will be identified as ACI 209. Likewise, methods developed by CEB-FIP Model Code 1990 (CEB-FIP, 1993) will be called CEB-FIP 1990. Methods presented by Bazant and Panula (1978 & 1982) will also be referred as BP model.

2.2.7.3 Bazant and Panula (1978, 1982)

Based mostly from experimental work conducted by Bazant, Osman and Thonguthai (1976), the BP model was derived utilising extensive published experimental data as a basis to achieve highest accuracy in the prediction. The model employs a square root hyperbolic law to represent the behaviour of shrinkage at various times.

The general form of equation for shrinkage strain at time t measured from the commencement of drying is given in the BP model as;

$$\varepsilon_{sh}(\hat{t}, t_{sh}) = \varepsilon^{*}_{sh} k_h S(\hat{t}) \tag{2.7}$$

In the above equation, $S(\hat{t})$ is expressed in square root hyperbolic law with time as;

$$S(\hat{t}) = \sqrt{\frac{\hat{t}}{\tau_{sh} + \hat{t}}} \tag{2.8}$$

where $\hat{t}$ = duration of drying $(t - t_{sh})$

t_{sh} = the time in which drying begins

k_h = coefficient which depends on relative humidity h (%)

and can be taken as;

$$k_h = 1 - h^3 \quad \text{for } h \leq 98 \tag{2.9}$$

$$k_h = -0.2 \quad \text{for } h = 100 \tag{2.10}$$

τ_{sh} = shrinkage square half time which depends on the size, shape and age of the member and is given by;

$$\tau_{sh} = 600\left(\frac{k_s}{75}\frac{V}{S}\right)^2 \frac{C_1^{ref}}{C_1(t_{sh})} \tag{2.11}$$

where k_s = the shape factor equal to 1.0 for a slab, 1.15 for a long square prism, 1.30 for a sphere, and 1.55 for a cube.

C_1^{ref} = taken as 10 mm^2 per day

$C_1(t)$ = coefficient which is proportional to the drying diffusivity at the commencement of drying (refer to the actual papers for more detail)

$\frac{V}{S}$ = volume to surface ratio

2.2.7.4 ACI 209 (1982)

The American Concrete Institute recommended a standard equation for predicting drying shrinkage in concrete as;

$$\varepsilon_{sh}(t) = \frac{t^{\alpha}}{f + t^{\alpha}} \varepsilon_{sh}^{*} \tag{2.12}$$

where $\varepsilon_{sh}(t)$ = Shrinkage at time t measured from the commencement of drying

f = number of days

ε_{sh}^{*} = ultimate shrinkage strain at time infinity commencing after the time of curing

t = time from the end of the initial curing

α = a constant defining member shape and size

Based on standard conditions set out by ACI 209 (1982), it was found that normal ranges of these constants were to be:

f = 20 to 130 days

ε_{sh}^{*} = 415 to 1070 microstrain

α = 0.9 to 1.10

Equation (2.12) basically represents an estimate for shrinkage strain at time t where the ultimate shrinkage strain obtained is modified by time-ratio to yield the desire result.

By modifying equation (2.12) further, ACI 209 recommended the following shrinkage strain equations at various time including ultimate values after casting of concrete member as given below;

Shrinkage after age 7 days for moist cured concrete is given by:

$$\varepsilon_{sh}(t) = \frac{t}{35 + t} \varepsilon_{sh}^{*} \tag{2.13}$$

Shrinkage after age 1 to 3 days for steam cured concrete is given by:

$$\varepsilon_{sh}(t) = \frac{t}{55+t}\varepsilon^{*}_{sh} \tag{2.14}$$

When determining shrinkage strain less than 7 days for moist cured concrete and other than 1-3 days for steam cured concrete, ACI 209 suggested the difference between equation (2.13) and (2.14) should be calculated starting from this time.

It is important to recognise that the ultimate shrinkage strains given are average values only and should be used in the absence of any specific shrinkage data of local aggregates and condition. Additional correction factors also have to be applied to the ultimate shrinkage strains to account for various environmental factors such as humidity, member shape and sizes. Thus, the ultimate shrinkage strain at time infinity can be determined by:

$$\varepsilon^{*}_{sh} = 780\gamma_{sh} \tag{2.15}$$

where γ_{sh} is the product of various correction factors as given below;

(a) Ambient relative humidity

γ_{λ} factor accounts for the influence of relative humidity. For relative humidity > 40%, then;

$$\gamma_{\lambda} = 1.40 - 0.01\lambda \quad \text{when} \quad 40 \le \lambda \le 80 \tag{2.16}$$

$$\gamma_{\lambda} = 3.00 - 0.03\lambda \quad \text{when} \quad 80 \le \lambda \le 100 \tag{2.17}$$

where λ is relative humidity in percent.

When relative humidity < 40%, values higher than 1.0 should be used.

(b) Size and shape of member

γ_{h} accounts for the size and shape of the member and depends on the average thickness of member under consideration, $h_o = 4V/S$. When $50\ mm \le h_o \le 150mm$, γ_{h} can be determined in Table 2.3 as;

Table 2.3 γ_h correction factors for various average thickness h_o

h_o (mm)	50	75	100	125	150
γ_h	1.35	1.25	1.17	1.08	1.00

When 150 $mm < h_o \leq 380$ mm;

$$\gamma_h = 1.23 - 0.0015h_o \quad \text{for } t \leq 356 \text{ days} \tag{2.19}$$

$$\gamma_h = 1.17 - 0.00114h_o \quad \text{for } t > 365 \text{ days} \tag{2.20}$$

These equations treat the effect of member size in terms of the average thickness and is referred as "average thickness" method by ACI 209

Alternatively, ACI 209 provided another method called "volume surface ratio" method and is given by;

When $h_o \geq 380$ mm;

$$\gamma_h = 1.2^{e\text{-}0.00472V/S} \tag{2.21}$$

where V/S is the volume to surface ratio

(c) Concrete composition

The influences of concrete slump s, ratio of fine aggregate to total aggregate concrete ψ (percent), cement content c (kg/m^3) and air content α (percent of volume) are expressed as $\gamma_s, \gamma_\psi, \gamma_c$ and γ_α respectively;

$$\gamma_s = 0.89 + 0.00161s \tag{2.22}$$

$$\gamma_\psi = 0.30 + 0.014\psi \quad \text{for } \psi \leq 50\% \tag{2.23}$$

$$\gamma_\psi = 0.90 + 0.002\psi \quad \text{for } \psi > 50\% \tag{2.24}$$

$$\gamma_c = 0.75 + 0.00061c \tag{2.25}$$

$$\gamma_\alpha = 0.95 + 0.008\alpha \tag{2.26}$$

It is possible to neglect the composition factors because concrete mix characteristics are not usually known at the design stage and have to be estimated.

(d) Initial moist curing

γ_{cp} is included to account for variations in period of initial moist curing T_c in days and is given in Table 2.4 as shown;

Table 2.4 γ_{cp} correction factors for various initial moist curing T_c

T_c	1.0	3.0	7.0	14.0	28.0	90.0
γ_{cp}	1.2	1.1	1.0	0.93	0.86	0.75

For steam cured concrete between a period of one and three days, γ_{cp} is equal to 1.

2.2.7.5 CEB-FIP Model Code 1990

Similar to ACI 209 method, the CEB-FIP 1990 equations for shrinkage are in hyperbolic power forms. The equation to calculate shrinkage $\varepsilon_{sh}(t,t_s)$ at any time can be given as;

$$\varepsilon_{sh}(t,t_s) = \varepsilon_{sho}\left[\frac{(t-t_s)}{350\left(\frac{h}{100}\right)^2 + (t-t_s)}\right]^{0.5} \tag{2.27}$$

In the above equation;

$$\varepsilon_{sho} = \left([160 + 10\beta_{sc}(9 - \frac{f_{cm}}{10})] \times 10^{-6}\right)\beta_{RH} \tag{2.28}$$

where f_{cm} = the mean compressive strength of concrete at the age 28 days (MPa)

β_{sc} = a coefficient which is influenced by the type of cements:

β_{sc} = 4 for slowly hardening cements SL,

β_{sc} = 5 for normal or rapid hardening cements N and R,

β_{sc} = 8 for rapid hardening high strength cements RS.

$$\beta_{RH} = -1.55[1-\left(\frac{RH}{RH_o}\right)^3] \text{ for } 40\ \% \leq \text{RH} < 99 \qquad (2.29)$$

β_{RH} = + 0.25 for RH ≥99%

RH = the relative humidity of the ambient atmosphere (%)

Rh_o = 100%

h = $2A_c/u$ where A_c is the cross section area and u is the perimeter of the member in contact with the atmosphere.

Like the ACI 209, CEB-FIP 1990 incorporated various terms including relative humidity, type of cement and concrete compressive strength as multiplication factors to the creep coefficient. Unlike ACI 209, CEB-FIP 1990 did not consider the effect of curing contributes to the predicted shrinkage value. Table 2.5 shown below is used to demonstrate the shrinkage strain ε_{sh} for an ordinary concrete structures after a duration of drying for 70 years using the method adopted by CEB-FIP 1990.

Table 2.5 Final shrinkage strains after 70 years of drying (CEB-FIP, 1993)

Relative humidity (RH) at 50 %			Relative humidity (RH) at 80 %		
Notional size $2A_c/u$ (mm)					
50	150	600	50	150	600
0.00057	0.00056	0.00047	0.00032	0.00031	0.00026

2.2.7.6 Australian Standard (AS 3600, 1994)

The Australian Standard AS 3600 (1994) provides three approaches for determining the basic shrinkage strain. First approach is to assume a median value of 700 microstrain, although it is also reasonable that the value can vary between 500 to 1000 microstrain. Second is to obtain the results directly from measurements on similar local concrete and third is to conduct shrinkage tests in accordance with AS 1012.13 after eight weeks of drying.

To calculate design shrinkage strain, the shrinkage strain which is obtained from one of the three approaches must be modified by a factor, k_1. Thus, a shrinkage strain at any time after the commencement of drying is expressed as;

$$\varepsilon_{sh}(t) = 0.0007k_1 \tag{2.30}$$

This factor is incorporated to account for the age of the concrete when shrinkage strain is to be evaluated by considering various environment effects, namely the environmental conditions and the size and shape of the member. Values for k_1 are presented graphically in Clause 6.1.7.2 of the code. This is reproduced here in Figure 2.3. It can be seen also that this graphical representation relates very closely to the methods presented by CEB-FIP (1970). In fact, the method by AS3600 was initially developed using CEB-FIP (1970) as a basis, but contained several modifications to account for the local concrete and local environment (Gilbert, 1988 and O'Moore, 1996).

Based on a shrinkage strain of 700 $\mu\varepsilon$, AS 3600 provides some typical design shrinkage strains under given four hypothetical thickness and four exposure conditions in Table 6.1.7.2. However it is likely that these design shrinkage strain values can vary within the range of ± 30 percent.

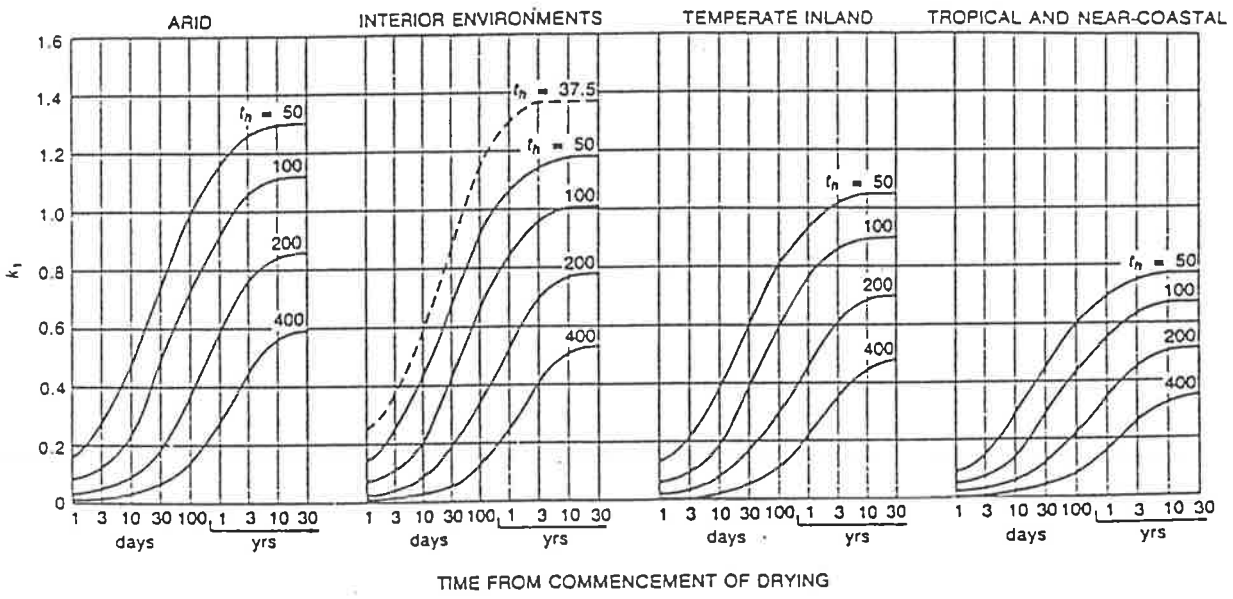

Figure 2.3 Shrinkage factor coefficient (k_1) for various environment in AS 3600

2.3 Creep

2.3.1 Definition

Test shows that stress and strain of concrete are functions of time. A gradual application of loading with time will result in gradual increase in concrete strain due to creep. Thus, creep can be defined as an increase in concrete strain with time under sustained loading. On the other hand creep can be considered as a progressive reduction of stress with time when subjected to constant application of strain (Neville, 1981).

As in the case of shrinkage, creep has both recoverable and irrecoverable components. When concrete is unloaded, the accumulated creep strain is only partially recovered, whereas the elastic strain is nearly complete. Creep can even be further categorised as basic and drying creep. Basic creep is considered as creep in concrete under the conditions of no moisture movement to or from the ambient medium. Drying creep is considered as the additional creep which occurs due to drying of concrete. In this review, the magnitude of creep will be considered as a time dependent deformation in excess of shrinkage.

2.3.2 Physical mechanism of creep in plain concrete

Several attempts have been made to explain the mechanism of creep in concrete, but none can be used to fully explain all the observations made during experiments and practice. The subject of this topic can be found in a number of references, namely Neville (1981), Bazant and Wittman (1982) and Gilbert (1988).

Nevertheless, it is generally believed that the physical process of creep under sustained load, is contributed, in a varying degree, to a number of mechanisms (Wittmann, 1982 and Gilbert, 1988). These include:

- the consequence of displacement of hydrated cement paste components, in particular the Calcium Silicate Hydrate components between the layers of absorbed water (viscous flow);
- the expulsion and redistribution of the inter-layer water within the hardened cement paste;

- elastic deformation of the aggregate and the cement paste as viscous flow and seepage occur with the cement paste (delayed elasticity);
- local fracture with the hardened cement paste which may occur as a result of microcracks; and
- additional deformation also occurs due to the bond break down between hardened cement paste and aggregate components at high stresses.

In addition, the magnitude and rate of creep in concrete are known to be influenced by a number of factors. As with shrinkage, concrete mix and environmental conditions affect the magnitude of creep. Unlike shrinkage, creep also depends on the loading conditions.

2.3.3 Factors affecting creep

Similar to shrinkage, factors influencing creep can be both internal and external. Internal factors include those that occur as a result of chemical reactions between all the concrete constituents. External factors are mainly contributed from environmental conditions and loading conditions.

2.3.3.1 Concrete mix

It should be realised at the onset that in proportioning of concrete mix, it is not possible to modify one factor without altering at least one other. Nonetheless, all the relevant factors governing the concrete mix will be treated separately as follows:

2.3.3.1.1 Concrete strength

The compositions of concrete affect creep primarily through their influence upon the magnitude of concrete strength. Thus, an increase in concrete strength generally reduces creep and concrete of higher strength therefore creeps less. One explanation of this is that the removal of water from the hydrated cement paste becomes more difficult as the porosity is decreased through hydration. Since the extent of hydration reflects on the strength of concrete, it can be stated that creep varies inversely as the concrete strength.

The above statement can be supported by many experimental observations, including one obtained by Ngab et al.(1981). Their experiments on creep in concrete

confirmed that increasing compressive strength of concrete can reduce the creep coefficient and specific creep.

2.3.3.1.2 Aggregate

It should be realised that aggregate does not undergo creep, but it is the cement paste which is affected by creep. Since aggregate is stiffer than the cement paste, its primary role is to restrain the creep in the cement paste. The situation is therefore identical to that of shrinkage. In effect, the increase in aggregate content and size and use a stiffer aggregate type would generally reduce creep.

Neville, Dilger and Brooks (1983) found that aggregates with higher modulus provide greater restraint and therefore offer higher resistance to creep. As with shrinkage, the elastic modulus of the aggregate can be considered as one of the most important factor. Rusch, Kordina and Hildorf (1963), as reported by Neville, Dilger and Brooks (1983) also found the reduction of creep strains under different types of aggregate.

2.3.3.1.3 Water-cement ratio

The water-cement ratio of concrete affects creep such that its magnitude is decreased when the water-cement ratio is reduced. This is because a higher water-cement ratio increases the size of the pores in the cement paste, so that the water molecules may be easily escaped. This is particular significant for concrete member under sustained load as more water is expelled, thus resulting in a higher rate of creep.

On the other hand, it can be argued that, its influence is related more with the concrete strength since the amount of water-cement ratio is inversely proportional to the concrete strength. Similarly, for a wide range of concrete mixes, creep is inversely proportional to the strength of concrete. Thus, it is reasonable to say that creep, strength of concrete and water-cement ratio are all related.

Perenchio and Klieger (1978), as reported by O'Moore (1996) investigated the properties and behaviour of high strength concrete and concluded that specific creep increases with water-cement ratio. In addition, the decrease in specific creep can

also be related to the compressive strength which is governed by the water-cement ratio.

2.3.3.1.4 Chemical admixtures

Tests conducted by Morgan (1974) found that the influence of water-reducing admixtures with or without accelerators is to increase the creep. Newbegin & Bruere (1992) reported that lignosulphonates and modified lignosulphonates (types of water-reducing admixtures) increased creep by up to 30 percent and between 50 to 70 percent respectively without any adjustments to the concrete mix proportions and the water-reducing benefits were not taken into consideration.

2.3.3.2 Loading conditions

The magnitude of creep is depended on the age of the concrete at the time of loading. By delaying the age at first loading, creep can be reduced. This should be expected because strength gained in concrete can offer greater resistance against creep.

2.3.3.3 Environmental conditions

2.3.3.3.1 Relative humidity

Relative humidity can also influence the magnitude of creep. Concrete exhibits higher creep as the relative humidity increases. However tests conducted by various researchers, including Bernhardt in 1969 and Hansen and Al-Alusi et al, as reported by Muller & Pristl (1993) indicated that creeps in concrete members when subjected to variable ambient humidity are significantly higher than those exposed to constant ambient relative humidity. Moreover, experiment results by Muller & Pristl (1993) suggested that the effect of variable humidity in the concrete specimens is to accelerate creep.

2.3.3.3.2 Temperature changes

A rise in temperature also increases creep because the cement paste deforms at a higher temperature and drying is accelerated. Gilbert (1988) suggested that temperature effect on creep is more prominent at elevated temperature and is negligible for temperature variations between $0^{o}C$ and $20^{o}C$.

2.3.3.4 *Effects of shrinkage on creep*

Creep and shrinkage are considered to be closely related, as both phenomena are associated to the structure of hydrated cement paste. As a general rule, concrete that exhibits high shrinkage is also expected to have high creep tendency. In fact creep when accompanied by shrinkage can be significantly larger (Neville, 1981).

To summarise, creep and shrinkage effects are interrelated and should not be analyse without one another. It is also reasonable to assume that the total amount of strain in a concrete member to consist of:

Total strain (ε_t) = elastic strain (ε_e) + creep strain (ε_c) + shrinkage strain (ε_{sh})

2.3.3.5 *Member shape and size*

Larger concrete members tend to creep less than small ones. This is because concrete at the surface creeps faster under condition of drying than concrete remoted from the surface where conditions approximate to curing (Neville, 1981). In general, the effect of member size is expressed in terms of volume/surface ratio. Similar to shrinkage, the shape of the member plays an insignificant role on creep, but a reduction in creep is less than the case in shrinkage when the member size is increased.

2.3.3.6 *Type and duration of curing*

It is possible to reduce the creep strains by using steam curing to accelerate hydration of the cementitious content, thus achieving desire concrete strength prior to loading. However it should be recognised that the advantage gained in reducing creep may be offset by an increase in shrinkage.

2.3.4 Summary

According to the study from the preceding sections, it is possible to draw some firm conclusions concerning factors affecting creep. Since concrete strength is inversely proportional to creep, therefore cement content, cement fineness, water-cement ratio affect creep in as far that they influence the concrete strength. The role that the aggregate plays in creep, is very much similar to shrinkage. Thus, the amount, type and properties of the aggregate can directly influence the magnitude of creep. Just

like shrinkage, the effects of chemical admixtures can vary depending on the type and the overall adjustments to the concrete mix proportions.

Moreover, creep is affected by the time at first loading. Generally, a delayed application of loading affects creep such that concrete has sufficient time to gain additional strength. Thus, concrete member creeps less when loaded at older age. Another external influence is the relative humidity of the surrounding environment. Concrete members which are subjected to variable ambient relative humidities usually exhibit larger creep than those subjected to constant humidity. In contrast, the influence of curing remains argumentative and is rather inconclusive. So it would be more appropriate to consider the process of drying leading up to the application of load to be more important.

2.3.5 Time effect on creep

Under sustained loading as illustrated in Figure 2.4, creep increases at a decreasing rate. When loading is suddenly removed, there is a gradual reduction in creep strain with time. However, only small proportion of creep strain would be recovered as the majority of the concrete had permanently deformed. The recoverable part of creep is referred as recoverable creep or delayed elastic strain while the irrecoverable part is known as irrecoverable creep or flow. Therefore, creep strain can often be divided into two major components, irrecoverable and recoverable creeps.

To calculate the capacity of concrete creep, a stress-independent quantity known as creep coefficient $\phi(t,t_o)$ is introduced and defined as the ratio of creep strain at time t to instantaneous elastic strain in a specimen subjected to constant sustained stress at time t_o. This is expressed as;

$$\phi(t,t_o)=\frac{\varepsilon_c(t,t_o)}{\varepsilon_e(t_o)} \tag{2.31}$$

Thus creep coefficient at time infinity where creep attains its maximum value $\varepsilon_c^*(t_o)$, is assumed to approach the value ϕ_o^* where;

$$\phi_o^*=\frac{\varepsilon_c^*(t_o)}{\varepsilon_e(t_o)} \tag{2.32}$$

As well as the time t_o at first loading which influences the value of creep coefficient ϕ_o^*, other influencing factors include the ambient conditions and size and shape of the member. Since the value of creep coefficient is independent on any stresses, creep coefficient at the time infinity can be used as a convenient mean to measure creep in concrete. Thus knowing the value for creep coefficient allows the rapid determination of creep strain in concrete subjected to constant sustained loading.

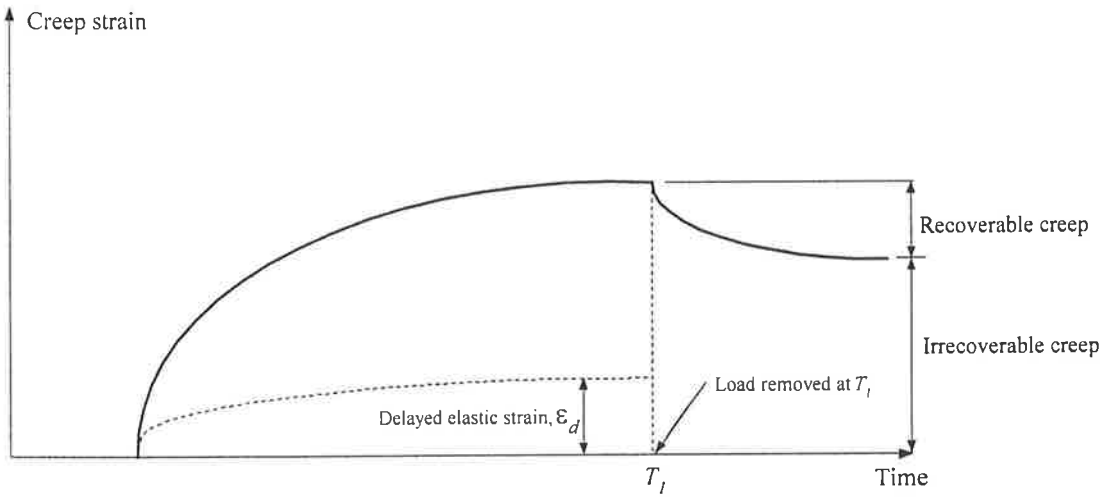

Figure 2.4 Recoverable and irrecoverable creep components

Another method which is commonly used, relies on a linear relationship between creep strain and stress. This is known as specific creep $C(t, t_o)$ where creep strain is produced by a unit stress. It is obtained by dividing $\varepsilon_c(t,t_o)$ by the constant sustained stress σ_o at time t_o. ie.

$$C(t,t_o) = \frac{\varepsilon_c(t,t_o)}{\sigma_o} \tag{2.33}$$

Furthermore, the relationship between specific creep and creep coefficient can be used to include the effect of elastic modulus of concrete. Thus;

$$C(t,t_o) = \frac{1}{E_c(t_o)}\phi(t,t_o) \tag{2.34}$$

By combining equation (2.33) and (2.34), it is possible to obtain creep strain at any time using the expression below;

$$\varepsilon_c(t,t_o) = \frac{\sigma_o}{E_c(t,t_o)} \tag{2.35}$$

As creep develops with time, its effect is also known to cause a reduction in stiffness of concrete member. Hence the magnitude of stiffness in concrete has to be adjusted with time in order to precisely estimate the creep strain. The effect of elastic modulus of concrete have been incorporated into several techniques in time deformation analysis including "the effective modulus" and "ages-adjusted modulus" methods. This topic however is beyond the scope of this research, so reader is suggested to refer the relevant references.

The choice of either creep coefficient $\phi(t,t_o)$ or specific creep $C(t,t_o)$ is largely depended on whether it is necessary to apply the creep coefficient to stress or strain, (Neville, 1981). Generally specific creep is more convenient for calculation of deflections and prestressing losses.

Since internal forces caused by restrained and imposed deformation in an indeterminate structure are proportional to stiffness, the internal forces would eventually decrease with time in all concrete and reinforced concrete members.

2.3.6 Methods of predicting creep

There are a number of mathematical expressions that can be used to predict creep in concrete. In all cases, it is necessary to collect data for concrete properties which in turn are used to form creep curves in order to obtain the coefficients and constants for the mathematical expressions. Typically, the experimental data are collected over a relatively short period of time. O'Moore (1996) reported that it may only take several months. Based on these short-term data, long-term creep values can then be predicted. The chosen mathematical expression is only valid for the experimented concrete since the data obtained, is only generated for the specific concrete mix in question.

Neville, Dilger and Brooks (1983) reviewed several types of mathematical expressions using short-term experimental data. They summarised that essentially creep time functions can be categorised into four major types;

- Hyperbolic
- Logarithmic
- Power
- Exponential

Exponential and hyperbolic functions can be used to models the development of creep where their values reach a limit as time approaches infinity. On the other hand, logarithmic and power functions that increase indefinitely can be used to estimate long-term deformations from the short-term tests. Neville (1981) suggested that for periods under load up to five years, the power expression is more suitable to fit experimental data for basic creep, and for basic plus drying creep, a logarithmic power function appears most appropriate.

Nevertheless it is the hyperbolic function which is perhaps the most widely used creep time functions, (Neville, 1981 and Gilbert, 1988). A number of authors and concrete codes including ACI Committee 209 (1982), based their equations on this function. As previously discussed in section 2.2.7, majorities of mathematical expressions for predicting shrinkage are likewise expressed in hyperbolic forms.

The aim of this research is not to conduct a detail literature review of various creep functions since they can be quite mathematically complicated. In addition, tests required to obtain experimental data for various creep curves are not part of the research and are clearly beyond the scope of this research. The purpose of this research however is to review alternative approaches to predict creep when experimental data is not readily available. These approaches are readily available in most reinforced concrete codes and several of them form a major part of this literature review.

Similar to the prediction of shrinkage strain, in the absence of any experimental data, designers have to rely on general prediction methods that do not require any experimental investigations. Most of these methods can be found in the existing

concrete codes and some published literature. A number of influencing factors such as compressive strength, environmental conditions, loading conditions and modulus of elasticity are incorporated as input data.

The general prediction methods being considered for review include:

- Bazant & Panula (1978, 1982)
- ACI Committee 209 (ACI Committee 209, 1982)
- CEB-FIP Model Code 1990 (CEB-FIP, 1993)
- AS3600-1994 (SAA, 1994)

2.3.6.1 Bazant and Panula (1978, 1982)

Bazant and Panula (1982) presented mathematical equations which separates creep components into basic creep and drying creep. The effects of the influencing factors are also depended on the type of creep component being considered. The coefficients relating to relative humidity and temperature are only incorporated into the drying creep components while the basic creep component of the equation is unaffected by the member size. Even though they studied the influence of cyclic loading, it does not form part of this research and therefore is not reviewed in this chapter.

From experiment measurements, basic creep usually increases at a constant or increasing slope in log-time for the duration of the test. Unlike ACI 209 and CEB-FIP 1990 which are discussed later, BP model does not consider hyperbolic function to be appropriate since there is no experimental result which would confirm that basic creep actually approaches a finite value at time infinity. As a result, a double power law with no limiting value is adopted to model the basic creep. Nonetheless, Bazant and Panula (1978 &1982) acknowledged that it is possible for designers to assume a finite creep value on a basis of practicality when the duration of loading becomes reasonably large, say 50 to 100 years.

It is often difficult to differentiate between instantaneous strain and creep strain during loading. As a result, BP model introduced a basic creep function $\Phi(t,t_0)$

which can be considered as an instantaneous strain plus creep strain at time t caused by sustained unit stress first applied at age t_o as;

$$\Phi_b(t,t_o)=\frac{1}{E_o}+C_o(t,t_o) \tag{2.36}$$

and

$$C_o(t,t_o)=\frac{\varphi_1}{E_o}\left(t_o^{-m}+\alpha\right)(t-t_o)^n \tag{2.37}$$

where $C_o(t,t_o)$ = the specific creep

In addition, Gilbert (1988) further modified the empirical equations given in BP model so that material properties in S.I. units can be used such that;

$$\varphi_1 = 0.30+152.2[f_c(28)]^{-1.2} \tag{2.38}$$

$$m = 0.28+47.541[f_c(28)]^{-2} \tag{2.39}$$

$$n = 0.115+0.61[f_c(28)]^3 10^{-6} \tag{2.40}$$

$$\frac{1}{E_o} = [0.0145+3.447(f_c(28))^{-2}]10^{-3} \tag{2.41}$$

It is important not to confuse E_o with modulus of elasticity. In fact, E_o is much larger than the actual elastic modulus and is referred as asymptotic modulus. $\frac{1}{E_o}$ can be considered as a constant which indicates the left hand asymptote of the creep curve when plotted in log-time scale.

When the component of drying creep is included, the total creep function $\Phi(t,t_o)$ in equation (2.36) can be modified by adding a drying creep term to the right hand side of the equation as shown in equation (2.42);

$$\Phi(t,t_o)=\frac{1}{E_o}+C_o(t,t_o)+C_d(t,t_o,t_{sh})-C_p(t,t_o,t_{sh}) \tag{2.42}$$

where $C_d(t,t_o,t_{sh})$ = the increase in specific creep due to drying

$C_p(t,t_o,t_{sh})$ = the decrease in specific creep after drying

t_{sh} = age at which drying commences

In the equation (2.42), both $C_d(t,t_o,t_{sh})$ and $C_p(t,t_o,t_{sh})$ can then be expressed as follows;

$$C_d(t,t_o,t_{sh}) = \frac{\varphi_d^{'}}{E_o} t_o^{-\frac{m}{2}} k_h^{'} \varepsilon_{sh}^{*} S_d(t,t_o) \tag{2.43}$$

where

$$\varphi_d^{'} = \left(1 + \frac{t_o - t_{sh}}{10\tau_{sh}}\right)^{-\frac{1}{2}} \varphi_d \tag{2.44}$$

$$S_d(t,t_o) = \left(1 + \frac{10\tau_{sh}}{t - t_o}\right)^{-C_d n} \tag{2.45}$$

and also

$$C_p(t,t_o,t_{sh}) = c_p k_h^{''} S_p(t,t_o) C_o(t,t_o) \tag{2.46}$$

where

$$S_p(t,t_o) = \left(1 + \frac{100\tau_{sh}}{t - t_o}\right)^{-n} \tag{2.47}$$

In both equation (2.43) and (2.46), the influence of relative humidity is defined as;

$$k_h^{'} = \left|h_o^{1.5} - h^{1.5}\right| \tag{2.48}$$

$$k_h^{''} = \left|h_o^{2} - h^{2}\right| \tag{2.49}$$

where h = relative humidity of environment and is assumed to be constant

h_o = initial relative humidity before drying commences,

i.e. $t_{sh} \leq t_o$ and usually is between 0.98 to 1.00

It can be seen from the set of equations above that drying creep is very much dependent on the environmental humidity and member size similar to shrinkage, as reflected in $k_h^{'}$ and τ_{sh} terms. The terms $S_d(t, t_o)$ and $S_p(t, t_{sh})$ represent the time shape function similar to shrinkage. The inclusion of shrinkage effect into equation

(2.43) further reinforced the idea that Bazant and Panula (1978, 1982) do not regard creep and shrinkage as independent phenomenon and simply can not be superimposed to obtain the value of concrete strain.

Other material parameters c_d and φ_d can be obtained empirically while c_p was set at 0.83. The terms for shrinkage square half-time τ_{sh} and ultimate shrinkage strain ε^*_{sh} were already defined and thoroughly discussed in Section 2.2.7.2

It can be seen that the BP model is quite complicated when compare with other models being reviewed here. The equations were derived as a result of extensive data correlation and fitting from various experiments. Since the model attempts to account for variation in long term behaviour due to fundamental concrete and environment parameters, this model may not be suitable to estimate long-term strains by using short-term data (O'Moore, 1996). Due to the complexity nature of this model, hand calculation is not also practical.

2.3.6.2 ACI 209 (1982)

ACI 209 used hyperbolic expressions and proposed a general equation to determine the creep coefficient $\phi(t,t_o)$ as;

$$\phi(t,t_o) = \frac{(t-t_o)^{\psi}}{d+(t-t_o)^{\psi}}\phi^*_o \qquad (2.50)$$

where
ϕ_o^* = ultimate creep coefficient at time infinity
d = constant defining shape and size
ψ = number of days
t_o = time at first loading
$(t\text{-}t_o)$ = duration of loading (days)

Ideally, ACI 209 prefers these constants to be obtained through testing. Based on standard conditions set out by ACI 209 (1982), it was found that normal ranges of these constants were to be:

d = 6 to 30 days,
ψ = 0.4 to 0.8,

$$\phi_o^* = 1.3 \text{ to } 4.15$$

For concrete loaded at the age of 7 days, either for moist cured concrete at 7 days or steam cured for 1-3 days, equation (2.50) then can be written as;

$$\phi(t,t_o) = \frac{(t-t_o)^{0.6}}{10+(t-t_o)^{0.6}}\phi_o^* \tag{2.51}$$

O'Moore (1996) suggested that problems associated with the equation above is that for conditions which are not within the range or not specified in the above paragraph, no additional information is provided to assist in obtaining the values of d and ψ. It is critical that these values are determined as accurate as possible as they have large bearing on the rate at which creep strains develop.

In the absence of any specific creep data for local aggregates and conditions, ACI 209 recommended an average value for ultimate creep coefficient ϕ_o^* which is given as;

$$\phi_o^* = 2.35\gamma_c \tag{2.52}$$

where γ_c is the product of the correction factors which accounts for various factors as given below;

(a) Age at first loading, t_o

γ_{la} accounts for the age of concrete at the time at first loading, t_o;

For moist cured concrete

$$\gamma_{la} = 1.25(t_o)^{-0.118} \qquad \text{when } (t\text{-}t_o) > 7 \text{ days} \tag{2.53}$$

For steam cured concrete

$$\gamma_{la} = 1.13(t_o)^{-0.094} \qquad \text{when } (t\text{-}t_o) > 3 \text{ days} \tag{2.54}$$

(b) Ambient relative humidity

When ambient relative humidity is greater than 40 %, ACI 209 included the correction factor γ_λ as;

$$\gamma_{\lambda} = 1.27 - 0.0067\lambda \tag{2.55}$$

where λ is the relative humidity in percent

(c) Size and shape of member

Similar to shrinkage, ACI 209 presented two techniques to estimate the correction factor γ_h. First technique is based on the average thickness h while the second technique is based on the volume-surface ratio (V/S)

In "average thickness" technique, the effect of member size is expressed in terms of average thickness. When the average member thickness is < 150 mm, γ_h can be obtained from Table 2.6 shown below;

Table 2.6 Correction factor for the average member thickness (modified from ACI Committee 209, 1982)

$h\ (mm)$	50	75	100	125	150
γ_h	1.30	1.17	1.11	1.04	1.00

When the average member thickness is between 150 mm and 380 mm, then;

$$\gamma_h = 1.14 - 0.00092h \quad \text{when } (t\text{-}t_o) \leq 365 \text{ days} \tag{2.56}$$

$$\gamma_h = 1.10 - 0.00067h \quad \text{when } (t\text{-}t_o) > 365 \text{ days} \tag{2.57}$$

Alternatively, "volume-surface ratio" technique expressed the relationship between the correction factor and (V/S) as;

$$\gamma_h = \frac{2}{3}\left(1 + 1.13e^{-0.0213\frac{V}{S}}\right) \tag{2.58}$$

where V/S is the volume surface ratio of member (mm)

(d)Concrete composition

The effects of concrete slump γ_s, percent of fine aggregate γ_ψ and air content γ_α are incorporated into the equation. Hence;

$\gamma_s = 0.82 + 0.00264s$ where s is the observed slump in mm (2.59)

$\gamma_\psi = 0.88 + 0.0024\psi$ where ψ is the ratio of the fine aggregate to total aggregate by weight (%) (2.60)

$\gamma_\alpha = 0.46 + 0.09\alpha$ where α is the air content in percent (2.61)

2.3.6.3 CEB-FIP Model Code 1990

Based on data collected from the laboratory tests, CEB-FIP 1990 model obtains empirical relationships as a mean to calculate the creep coefficient in concrete structures. The code however includes only parameters which are known to the designer during the time of analysis. This would largely eliminate the needs to measure the creep data by conducting experiments. Similar to ACI 209, the parameters incorporated into the respective equations are identical, only with the exception of the type of cement which also forms part of the correction factors in the equations.

As with ACI 209, CEB-FIP 1990 adopted hyperbolic time function which approaches an asymptotic value as time reaches infinity to estimate creep, even though CEB-FIP commented on the lack of evidence which demonstrates that this is valid. Thus the expressions for the creep coefficient $\phi(t,t_o)$ can be given as;

$$\phi(t,t_o) = \phi_o \left[\frac{(t-t_o)}{\beta_H + (t-t_o)} \right]^{0.3} \tag{2.62}$$

where β_H = a constant obtained using relative humidity and member size, where;

$$\beta_H = 150\left[1 + \left(1.2\frac{RH}{100}\right)^{18}\right]\frac{h}{100} + 250 \le 1500 \tag{2.63}$$

where RH = relative humidity of the ambient environment (%)

h = the notional size of member (mm), equals to $2A_C/u$ where A_c is the cross section and u is the perimeter of the member in contact with the atmosphere.

ϕ_O^* = the notional or ultimate creep coefficient

The ultimate or notional creep coefficient therefore can be estimated from;

$$\phi_o^* = \phi_{RH}\,\beta(f_{cm})\beta(t_o) \tag{2.64}$$

and in the above equation;

$$\phi_{RH} = 1 + \frac{1 - \frac{RH}{100}}{0.46\left(\frac{h}{100}\right)^{\frac{1}{3}}} \tag{2.65}$$

$$\beta(f_{cm}) = \frac{5.3}{(f_{cm}/10)^{0.5}} \tag{2.66}$$

$$\beta(t_o) = \frac{1}{0.1 + (t_o)^{0.2}} \tag{2.67}$$

where f_{cm} = the mean compressive strength of concrete at the age of 28 days (MPa)

CEB-FIP 1990 suggested the equations above should provide good estimation of creep for up to 70 years of loading. For loading in excess of this duration, the code expects a variation of 5%.

Alternatively, when the degree of accuracy does not warrant detail analysis, CEB-FIP 1990 provides a set of values for creep coefficient which can be valid after 70 years.

2.3.6.4 AS3600-1994

Base initially on CEB-FIP 1970, the Australian Standard provides a simple approach to calculate design creep factor (referred as design creep coefficient elsewhere) at time t due to a sustained loading at age t_o as;

$$\phi_{cc} = k_2 k_3 \phi_{cc,b} \tag{2.68}$$

where ϕ_{cc} = long term value as time t approaches infinity for design creep factor

$\phi_{cc,b}$ = basic creep factor which can be obtained from the Table 2.7 below;

Table 2.7 Creep coefficient of an ordinary structural concrete after 70 years of loading

Age at loading t_o (days)	Dry atmospheric conditions (indoors) (RH = 50%)			Humid atmospheric conditions (out of doors) (RH = 80%)		
	Notional size $2Ac/u$ (mm)					
	50	150	600	50	150	600
1	5.8	4.8	3.9	3.8	3.4	3.0
7	4.1	3.3	2.7	2.7	2.4	2.1
28	3.1	2.6	2.1	2.0	1.8	1.6
90	2.5	2.1	1.7	1.6	1.5	1.3
365	1.9	1.6	1.3	1.2	1.1	1.0

Table 2.8 Values of basic creep factor (reproduced from AS3600-1994)

f_c' MPa	20	25	32	40	50
$\phi_{cc,b}$	5.2	4.2	3.4	2.5	2.0

The data above are median values and were obtained from test at 28 days, thus some variations of plus or minus 30 % can be expected. Walsh (1988) commented that the values of basic creep are relatively high and are based on limited experiment data. Alternatively, the quantity ϕ_{cc} can be determined from creep tests conducted in accordance with AS 1012, Part 16.

The constant k_2 is incorporated to account for the duration of loading (t-t_o), the relative humidity and hypothetical thickness of the member. This value is comparable to the constant k_1 used in shrinkage prediction. Identical to shrinkage, the values of k_2 are presented graphically in Clause 6.1.8.2 of the code and is reproduced here in Figure 2.8

The constant k_3 depends on the age of the concrete at the time of loading. The values are expressed in terms of the ratio of mean concrete strength f_{cm} at time of loading and the characteristic strength f_c' of 28 days. Again this is shown in Figure 2.6.

2.4 Comparisons of the predictive methods for shrinkage and creep

With so many alternative methods available, the question which arises is, which ones should be used. Neville, Dilger and Brooks (1983) advised that any of the predictive methods could be adopted on the basis of published comparisons. Due to the variability of material properties and environmental conditions, designers need to recognised that these methods only give rough estimates.

Symon (1989) commented that good correlation between predicted and measured values should not be expected. The degree of correlation nonetheless can be improved if the prediction is based on tests of the actual materials used, under environmental and loading conditions similar to those expected in the field. Neville (1981) further emphasised that there still remains a lack of reliable test data for both the development of creep with time and the final creep coefficient for varying effective thickness.

In addition, it is probably best to make use of local materials with the knowledge of local data and experience. It is suggested that the knowledge of local concrete and conditions can be much more reliable means for determining material properties than any of the predictive methods contained in structural codes and reviewed here.

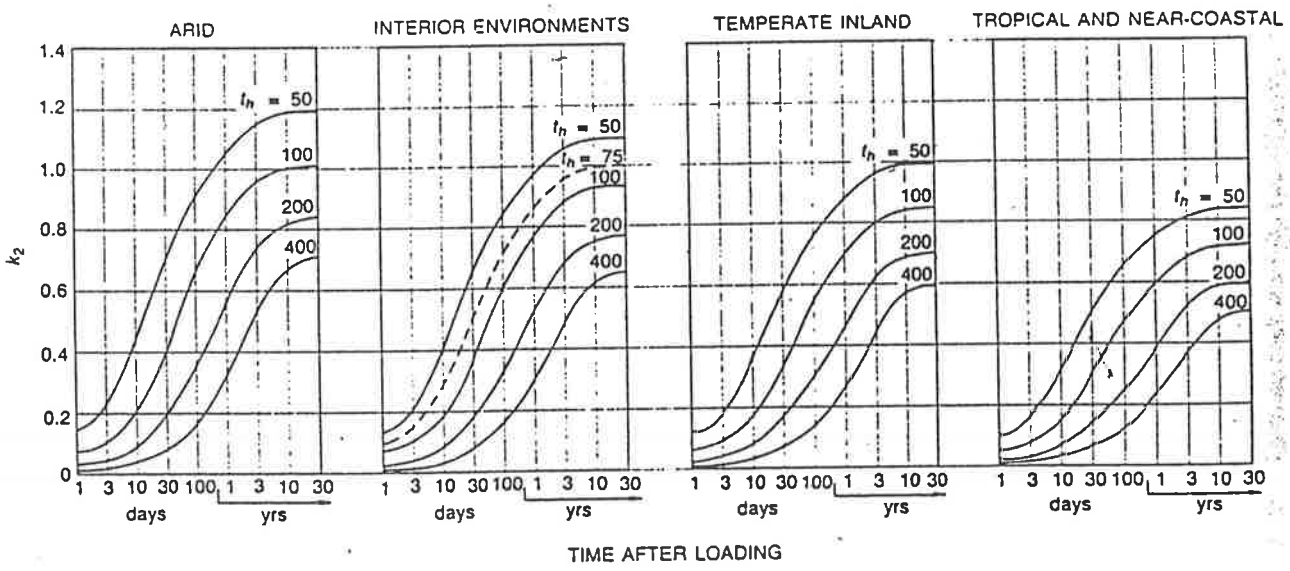

Figure 2.5 Creep factor coefficient (k_2) for various environments in AS 3600

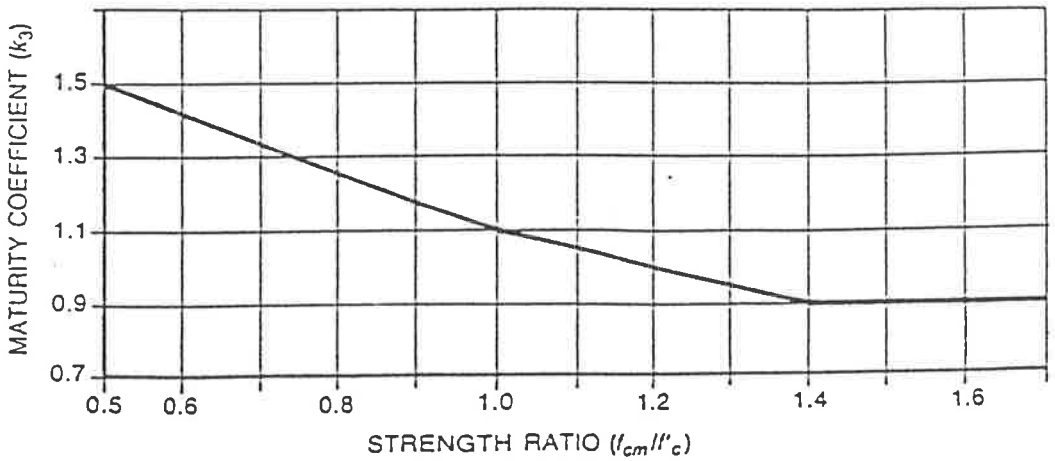

Figure 2.6 Maturity coefficient (k_3) versus strength ratio by AS 3600

Methods proposed by Bazant and Panula (1978 & 1982) were derived using large amount of shrinkage and creep data collected during laboratory tests. It can be quite complicated and require extensive calculation. Thus, this is not really suitable to use in preliminary or even in detail design where precise accuracy does not justified the extra effort to carry out the analysis. On the other hand, methods recommended by AS3600, ACI 209 and CEB-FIP 1990 require minimal effort to accomplish simple analysis with a hand held calculator.

It is apparent that numerically accurate estimates of creep, shrinkage and their effects on structural behaviour can not be achieved. The increase in complexity in the predictive models does not always guarantee a superior or more accurate results.

This was confirmed by investigations conducted by Müller and Hildorf (1982) and McDonald and Roper (1993). Gilbert (1988) recommended a simple method with no pretence to great accuracy should be adopted and he suggested the AS3600 is one of those methods.

In their research, Müller and Hildorf (1982) compared the reliability and accuracy of various predictive methods including ACI 209 and BP model. They found that ACI 209 yielded poor results for concrete at higher ages at loading and for basic

creep. BP model on the other hand was inaccurate for very young concrete. Furthermore, BP model tended to underestimate the effect of member size whereas ACI 209 method in many cases overestimated the influence of this factor. Müller and Hildorf (1982) also suggested both ACI 209 and BP model underestimated the effect of relative humidity.

Gilbert (1988) further reported that ACI 209 and BP model produce the smallest estimates of creep. In contrast, Bakoss et al. (1982) found that creep of some Australian concrete was best predicted by CEB-FIP models. Generally, creep coefficient can vary between 2.0 and 4.0 for most practical situations.

Recent studies by McDonald and Roper (1993) reported that additional factors which are incorporated into various predictive methods do not always guarantee a better result, particularly if no prior information of the performance of a particular concrete is not available. McDonald and Roper (1993) also made the following observations when comparing various predictive methods for shrinkage; AS3600's accuracy is not as high during the first 10 and 100 days of prediction. Nonetheless, AS3600 achieved the best accuracy overall. Surprisingly, BP model came almost last in their rating for accuracy even though it is the most complex in terms of data requirement. BP model's prediction became even more non-conservative as drying period increased. Unfortunately, CEB-FIP 1990 model was not included for the comparison in their studies.

It should be pointed out also that all the predicting models failed to incorporate the effect of variable ambient relative humidities in their analysis. Study by Müller and Pristl (1992) showed that the reason for this omission could be due to the limited amount of test data on this matter. Thus, any predictive models would have to be derived based on these limited existing data.

Since the predictive methods for both shrinkage and creep can vary greatly and even worst, none can predict the results accurately. Table 2.9 summarises various influencing factors incorporated into each predictive model reviewed in this chapter.

Table 2.9 Influencing factors for prediction of shrinkage and creep (modified from Muller and Hildorf (1982), McDonald and Roper (1993))

	AS3600	ACI 209	CEB-FIP 1990	BP Model
Humidity	X	X	X	X
Temperature				X
Size	X	X	X	X
Shape	X	X		X
f'_c at 28 days	X		X	X
Strength at loading		X		
Elastic modulus			X	
W/C				X
Cement content		X		X
Cement type			X	X
Fine/coarse aggregate		X		X
Cement/sand				X
Cement/gravel				X
Air content		X		
Slump		X		
Density	X	X		X
Age at drying				X
Age at loading	X	X	X	X

According to the table, it can be seen that all models recognise the importance of different external factors such as relative humidity, member shape and size by accounting for them at some stages in the analysis of both shrinkage and creep. As already mentioned, the influence of variable ambient relative humidities is not included in any of the models, but instead constant relative humidity is assumed.

Both predictive models from CEB-FIP 1990 and AS 3600 do not require designers to obtain the information concerning compositions of concrete while BP model accounts most of the factors associated with concrete compositions. In the prediction of creep, concrete strength at 28 days is adopted for most models as a long-term value while the age and strength of concrete are still necessary to complete the analysis.

2.5 Other causes of restrained and imposed deformations

These sources are equally as important as shrinkage and creep. However, in this thesis, both temperature effect and differential foundation movement are discussed in less detail

2.5.1 Temperature effects

Temperature difference affects deformation of concrete members in two distinct ways. The difference can originate internally from within the concrete itself and externally between the surrounding environment. Each of these are briefly discussed in turn

The first case generally is associated with early-age thermal movement from a rise in concrete temperature during cement hydration. The evolution of heat from hydration of cement causes concrete to expand and upon cooling back towards the ambient temperature, it contracts. If, on cooling, contraction of the immature concrete is restrained by adjoining slabs or walls, then early-age cracking may develop.

Similar to shrinkage and creep, the rate, magnitude, and duration of the rise in temperature is dependent on a number of factors, including cement type and content, type of aggregate, possible use of cement replacement materials, as well as the ambient temperature, formwork used and section thickness (Harrison, 1981). Hughes (1978) suggested that heat would continue to dissipate as long as the concrete temperature is higher than that of its surroundings. In a thin structure, peak temperature usually takes about 15 hours to 3 days, before reaching equilibrium in 1 to 2 weeks. In large or massive structures, it may take up to 20 hours before peak

temperature is attained and several years before cooling to equilibrium condition is established.

In addition to early-age thermal effects, temperature differences can also occur between the concrete member and its surroundings. Hughes (1978) reported that temperature of a structure continued to change in an attempt to keep pace with the temperature of the surrounding environment which fluctuates daily and seasonally. As a result, strains that are larger than that of shrinkage can be expected.

Attention is frequently drawn to the need for recognising that the temperature may not be constant throughout a structural member. When the change in temperature is uniform through the depth of concrete section, uniform stress usually results, unless the structure is statically indeterminate. However in deep sections, non-linear temperature distribution is quite common and it can have adverse effects on the structure. CEB Manual (1985) considers the effect of the non-linear temperature distribution to consist essentially of three parts. They are:

- due to average temperature in the section there will be some overall movement. If the member is unrestrained a temperature strain is induced throughout the section without stress.
- due to average gradient of the non-linear temperature distribution, a strain gradient will be induced through the section causing an overall curvature of the member. If the member is free to assume this curvature, temperature strain is induced without stress.
- due to the difference between the thermal strain distribution and the strain distribution which the section can assume (plane sections are assumed to remain plane), "self-equilibrating" stresses are induced. These stresses arise due to the self-restraint of the section. Thus, the magnitude and distribution of the "self-equilibrating" stresses depends on both the form of the non-linear temperature differential and the state of the section (cracked or uncracked).

For a simple case of an unrestrained reinforced concrete member subjected to uniform change in temperature, it is possible to calculate the overall contraction or expansion as;

$$\delta = \alpha L(\Delta T) \tag{2.69}$$

where δ = total deformation

α = coefficients of thermal expansion of material

ΔT = temperature difference

L = length of member

Although, reinforced concrete is considered as a non-homogeneous material, the coefficients of thermal expansions of both concrete and steel are essentially identical, thus it is reasonable to neglect the effect of differential internal strains. The coefficient of thermal expansion in concrete can be obtained with the knowledge of the coefficient of thermal expansion in aggregates. Hence it is not possible to assume average values of coefficients of thermal expansions. However, as an indication the average value of coefficient of thermal expansion in concrete is about 12 x $10^{-6}/C^{o}$, except those with limestone and lightweight aggregate (Alexander and Lawson, 1981).

2.5.2 Differential foundation movement

Differential foundation movement can occur as a result of a number of causes. These are briefly summarised as follows:

- differential settlement under loading between two or more adjoining structures;
- consolidation of compressible soils due to changes in loading or moisture content; and
- ground subsidence due to mining or tunnelling.

In addition, differential movement is also contributed to the variations in shape, size and bearing pressure of individual foundations. The topics concerning these matters are beyond the scope of this research, but can be found in other references including Bowles (1988).

2.6 Summary

In summary, this chapter presented literature reviews of load independent and time-dependent deformations in reinforced concrete buildings. They have been identified as shrinkage, creep, temperature effects and differential foundation movements. All of which need to be considered seriously so that the structure does not encounter problems during the design life.

All the factors that affect the magnitude of both shrinkage and creep were presented. Those factors which affect both shrinkage and creep include the concrete mix and environmental conditions, but creep also depends on the duration of loading. Thus creep can be considered as time and load dependent deformation phenomenon. In addition, different methods of predicting shrinkage and creep were discussed. However, due to the variability of the material properties and environmental conditions, it should be recognised that these methods only produce rough estimates. There are other methods which may provide results with greater precision, but they require greater effort and time in order to achieve such outcomes. Unless these effects are very serious and require very accurate means to obtain the results, any of the methods presented should be suitable for the majority of building structures.

Chapter 3

Cracking mechanism in RC slabs in tension

3.1 Introduction

In reinforced concrete structures, cracking is generally regarded as unavoidable at service loads. Flexural cracks are rarely a problem if adequate reinforcement is provided to satisfy the deflection and ultimate strength requirements. On the other hand, the effects of pure tensile cracking are often overlooked or underestimated by designers. This type of cracking can be quite severe, whether or not the member is also subjected to flexure, and the cracks that occur can propagate over the full depth of the section. Such cracks can occur because the member is subjected shrinkage and temperature effects, which in turn generate longitudinal tensile forces as a result of restraint and imposed deformations. Because this type of cracking only occurs as a result of axial tensile force, it is commonly known as "direct tension cracking".

On the other hand, in a reinforced concrete member which is subjected to little or no restraint and imposed deformation, direct tension cracking is rarely a problem. This is best explained by considering an unrestrained reinforced concrete member subjected to uniform shrinkage strain, ε_{sh}^{*}, as shown in Figure 3.1. As shrinkage develops, a compressive stress, σ_{sc} is induced in the reinforcement, while a uniform tensile stress, σ_{st} is generated in the concrete to maintain equilibrium.

Since there is no external restraint, equilibrium imposes the following relationship between the compressive stresses in the reinforcement and concrete;

$$A_s \sigma_{sc} = A_c \sigma_{ct} \tag{3.1}$$

Moreover, the compatibility condition of the two elements must be satisfied. Thus it can be seen that the total uniform shrinkage strain, ε^*_{sh} can be expressed as follows;

$$\varepsilon^*_{sh} = \varepsilon_{sc} + \varepsilon_{ct} \tag{3.2}$$

where ε_{sc} = compressive strain in the steel reinforcement

ε_{ct} = elastic tensile strain in the concrete

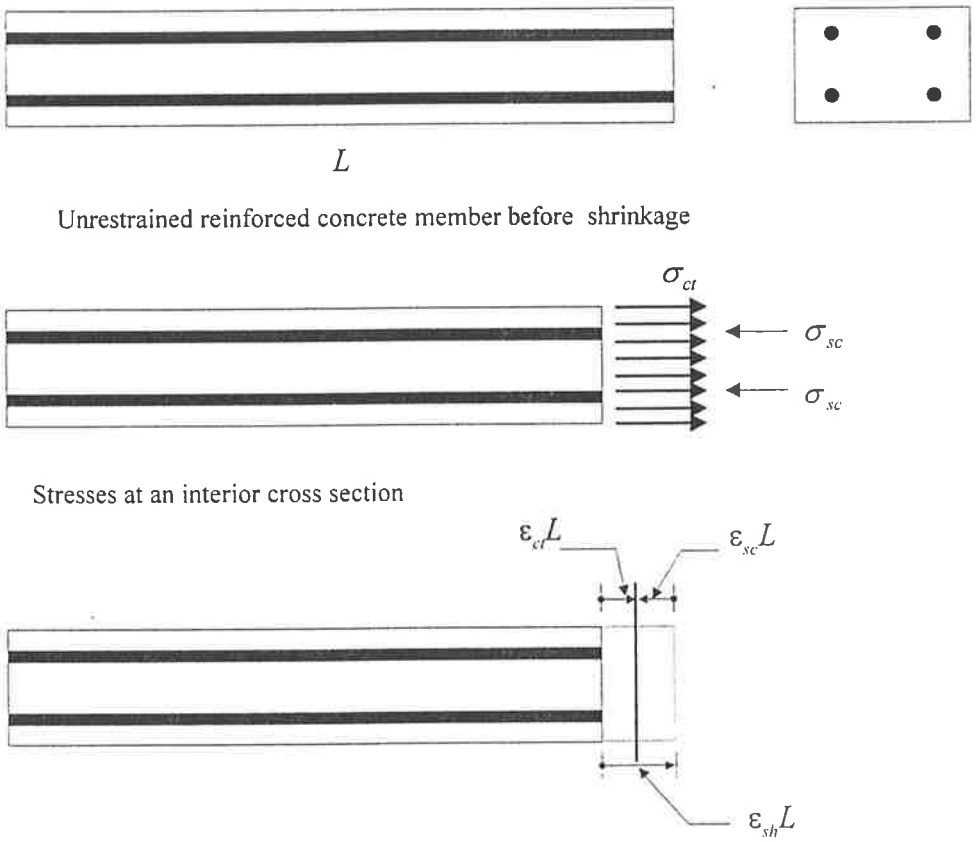

Figure 3.1 Unrestrained reinforced concrete subjected to uniform shrinkage

Equation (3.2) can be further modified as;

$$\varepsilon^*_{sh} = \frac{\sigma_{sc}}{E_s} + \frac{\sigma_{ct}}{E_c} \tag{3.3}$$

By substituting the reinforcement ratio, $\rho = \frac{A_s}{A_c}$ and eliminating σ_{sc}, the relationship in equation (3.4) is obtained. This can be used to examine the likelihood

of cracking in the externally unrestrained reinforced concrete member. If the tensile stress, σ_{ct} in concrete is greater than the concrete tensile strength, cracking should occur.

$$\sigma_{ct} = \frac{\varepsilon^*_{sh}}{\left(\frac{1}{\rho E_s} + \frac{1}{E_c}\right)} \tag{3.4}$$

In order to investigate this effect, values of σ_{ct} are calculated using the following properties:

$$\varepsilon^*_{sh} = 500 \quad \mu\varepsilon$$

$$E_s = 200{,}000 \text{ MPa}$$

and $$E_c = 28000 \text{ MPa}$$

The values of concrete tensile stresses corresponding to different reinforcement ratio are tabulated as shown in Table 3.1

Table 3.1 Values of tensile stresses in concrete for ε^*_{sh} at 500 and 1000 $\mu\varepsilon$

	$\varepsilon^*_{sh} = 500$ $\mu\varepsilon$				$\varepsilon^*_{sh} = 1000$ $\mu\varepsilon$			
Reinforcement ratio, ρ	0.0025	0.0050	0.01	0.02	0.0025	0.0050	0.01	0.02
Tensile stress in concrete, σ_{ct} (MPa)	0.20	0.39	0.75	1.75	0.5	0.97	1.9	3.5

It can be seen that for the range of reinforcement ratios, the resulting concrete stresses obtained are generally lower than the stress at which cracking would occur. Even with a shrinkage strain of 1000 $\mu\varepsilon$ and one percent of reinforcement, the concrete tensile stress would be 1.9 MPa. With two percent steel, however, the stress would be 3.5 MPa and cracking might occur at this stage. Thus, it can be concluded that unrestrained reinforced concrete members do not usually experience severe cracking as a result of shrinkage effect. This suggests that some form of restraint is needed in order to produce significant cracking due to shrinkage.

It is emphasised that this analysis is approximate, and tends to overemphasise the magnitude of the concrete stresses because the effect of shrinkage is ignored. The mechanism of cracking will be discussed in greater detail later in this chapter.

Furthermore, in partial or fully restrained reinforced concrete slabs with large spans, the effects of shrinkage are small compared to the effect of flexural loading and as a consequence flexural cracking tends to dominate. Any tensile cracks caused by shrinkage can then be absorbed by small increases in the widths of the numerous flexural cracks. In fact, Base and Murray (1982) suggested that tensile cracking due to shrinkage (and temperature changes) does not exist in flexural loaded concrete members.

On the other hand, the situation is more complex when the flexural loading is small and the restrained longitudinal deformations predominate. This occurs in the lower range of spans of fully restrained suspended concrete slabs (Gilbert, 1988). Axial tensile forces also occur in the transverse (no moment) direction of one-way slabs and can produce unsightly wide cracks if insufficient secondary reinforcement is provided.

It can be seen that the development of direct tension cracking and the effect of restrained and imposed deformations are closely related. There are also several factors which can influence the degree of cracking, namely member span, degree of restraint and amount of reinforcement. A one-way reinforced concrete slab that spans between two simple supports allows almost free movement under the effect of any deformations and hence no induced cracking. In contrast, a one-way reinforced concrete slab which is fully restrained at both ends, large longitudinal tension forces develop when the member is subjected to shrinkage or temperature strains. This can result in severe cracking throughout the span. Hence the relationships between the restraints and the development of cracking in a reinforced concrete slab can be explained by considering the following cases.

The first case considers an unrestrained reinforced concrete member subjected to applied tensile force at each end as shown in Figure 3.2a As the tensile force is increased, the member gradually elongates freely. When the stress reaches the

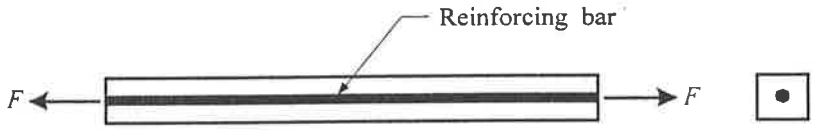

(a) Reinforced concrete member subjected to axial tensile forces

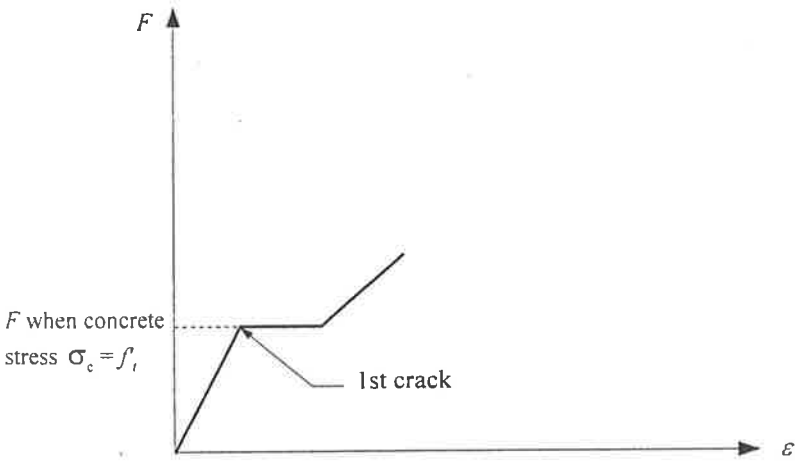

(b) Development of tensile force and average strain of the member after a first crack

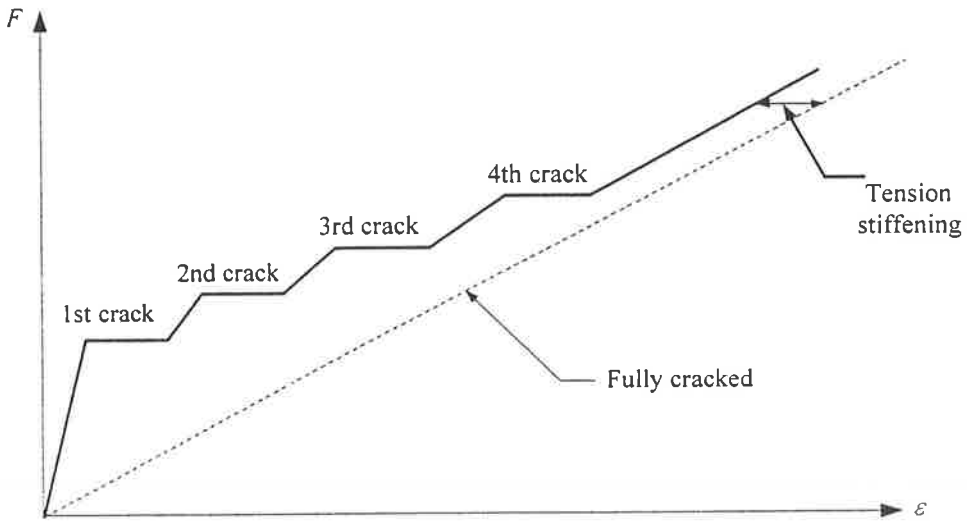

(c) Development of tensile forces and average strains of the member after several cracks

Figure 3.2 Development of cracking in a reinforced concrete member subjected to applied tensile forces

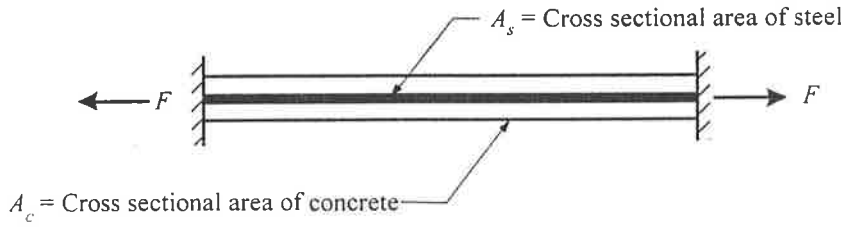

(a) Fully restrained reinforced concrete slab subjected to shrinkage

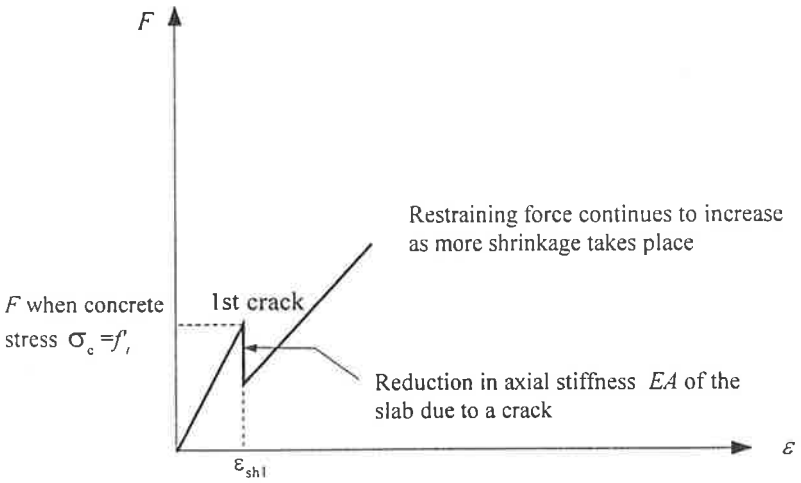

(b) Development of restraining force and shrinkage after a first crack in full restrained member subjected to shrinkage

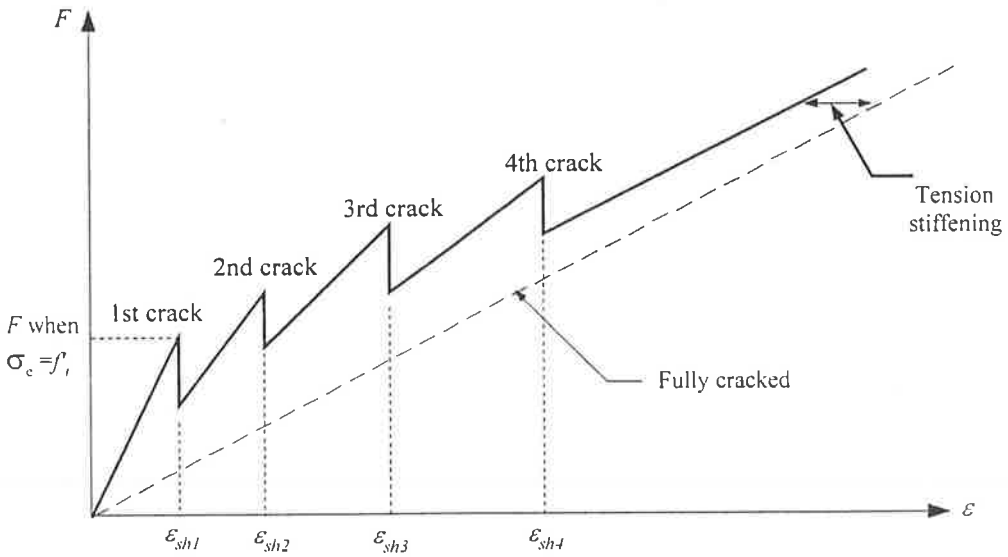

(c) Development of restraining forces and shrinkage strains after several cracks have occured

Figure 3.3 Development of cracking in a fully restrained reinforced concrete member sujbected to uniform shrinkage

tensile strength of concrete, the first crack abruptly forms. This is further shown in Figure 3.2b and 3.2c. As the tensile force is gradually increased, more cracks form along the member until a freely developed pattern of cracks exists. As more tensile forces are applied, there is a subsequent increase in widths of the existing cracks. When the reinforcement starts to yield, these crack widths can be excessive. As each crack forms, there is an increase in deformation of the member. However, the internal forces of the member remain unchanged as long as there is no change in the applied tensile stresses.

The second case considers a reinforced concrete slab spanning between two rigid supports subjected to uniform shrinkage as shown in Figure 3.3a. As the structure is indeterminate, cracking can influence the reactions, internal forces, and area properties, and, therefore, the stresses and strains in individual cross sections (Elbadry and Ghali, 1995). The creep effect that generally occurs simultaneously is ignored for simplicity. As the shrinkage strain increases with time, the restraining forces continue to increase. Due to the initiation of the first crack, there is a sudden reduction of member axial stiffness, *EA* (This analysis is discussed in details in Chapter 4) and so the restraining forces decrease immediately after first cracking. This is illustrated in Figure 3.3b. The magnitude of this reduction depends on the stiffness and the length of the member. When the slab undergoes further shrinkage, the restraining forces again increase until the second crack forms. The same process continues to repeat itself with third and subsequent cracks and accompanying immediately after each crack, there is a sudden loss in member stiffness and a reduction in the magnitude of restraining forces, as shown in Figure 3.3c. As with the reinforced concrete member subjected to applied tensile forces, the number of cracks continues to increase until a fully stabilised cracking pattern develops. Any further increase in shrinkage in the slab simply leads to a widening of the existing cracks, and, possibly, yielding of the reinforcement.

In continuous building structures, situations of unrestrained slabs as explained in the first case rarely occur. In most cases, one or both of the support conditions are in the form of exterior or interior columns or transverse beams. Elbadry & Ghali (1995) reported that it is often difficult to attain stabilised cracking patterns in a fully

restrained slab whereas stabilised cracking pattern in unrestrained reinforced concrete members can be expected in most cases. This is attributed to the fact that as more cracks develop along the span, larger restraining forces (after each crack) are required to cause the subsequent cracks to occur. In a real structure, a restraining force of such magnitude may not be attainable because shrinkage is decreasing with time. For these situations, a small number of very wide cracks at large spacing may instead exist along the member (Leonhardt, 1977).

In this chapter, the aim is to study cracking mechanisms in a reinforced concrete slab due to a direct tensile force, and also due to tension induced by restrained and imposed deformation. Since the formation of this type of cracking is quite complex because of the contribution from various factors such as concrete properties, bond strength, time dependent effects in concrete etc, this chapter also investigates the influence of bond stress on cracking behaviour.

At present, there are relatively few research publications on the subjects of cracking relating to bond stress and the effects of shrinkage and temperature. However there is a large number of experimental and analytical studies of the relationship between cracking and bond stress in the case of an applied axial tension. It will be shown in the following sections that these various types of cracking are closely related, and are essentially bond-related phenomenon.

Hence the first section of this chapter deals with cracking due to an applied tensile force, and reviews the work of various researchers. The review is divided to cover the following topics that affect this type of cracking:

- Cracking due to applied tension force;
- Effect of bond stress on cracking behaviour;
- Methods of calculating crack spacing and crack width due to applied tension force.

The second part of this chapter deals with cracking due to restrained and imposed deformation. A number of methods by various researchers and organisations to calculate crack spacing and crack width are discussed.

3.2 Cracking due an applied tensile force

3.2.1 Introduction

Direct tension cracking in reinforced concrete structures involves bond break down and slip at the reinforcement and concrete interface. It is therefore necessary to study the effects of bond stresses on development of cracking in order to form a proper working model.

3.2.2 The relationships between direct tension cracking, bond stress and slip at the reinforcement - concrete interface

Studies of the development of cracking were commenced in the early 1930's by Vetter in 1933 and Saliger in 1936. As reported by Rawi and Kheder (1990), Vetter's 1933 research was the first to recognise that there is slip at the reinforcement and concrete interface adjacent to the crack. However his theory did not address cracking due to temperature and shrinkage effects. In 1943, Watstein and Parsons, as reported by Cambell-Allen and Hughes (1981), developed a general theory of cracking based on axially loaded prisms which leads to the derivation of equations for crack widths and crack spacings. Their hypothesis, which is now termed the "bond-slip" hypothesis implies that cracks form in conjunction with the loss of adhesion, and "slip", between the concrete and reinforcement. Based on this hypothesis, both crack widths and crack spacings were believed to depend on the reinforcement diameter and inversely proportional to the bond strength and the reinforcement ratio.

Since the early 30's and 40's, various researchers have conducted further studies and experimental test programs in order to improve the understanding of the relationship between bond stress and cracking behaviours. Some of the significant findings include papers presented by Beeby (1979), Kemp and Wilhelm (1979), Nilson (1972), Goto (1971), Lutz and Gergely (1967), Perry and Thompson (1966) plus numerous others. Initially, the "bond-slip mechanism" was thought to be valid for concrete members in both flexure and direct tension. However, further studies by a number of researchers, including Base (1976), Campbell-Allen and Hughes, (1981) and Beeby, (1979), have shown that for flexural cracking, the hypothesis is

unacceptable. A different approach has therefore been adopted for flexural cracking (Beeby, 1979).

In order to discuss the relationship between the bond stress and direct tension cracking, the behaviour of a reinforced concrete slab will be considered at various stages of cracking under increasing tensile force.

Consider a reinforced concrete member subjected to a gradually increasing axial tensile force, F at each end as shown in Figure 3.4a. As the tensile force F increases, the reinforced concrete member remains uncracked provided that the tensile stresses are still below the tensile strength of concrete. In the pre-cracking stage, the tensile force F is resisted by both concrete and reinforcement.

ie. $$F = A_c\sigma_c + A_s\sigma_s \tag{3.5}$$

When the concrete strength f_t' is reached ($\sigma_c = f_t'$), the first crack forms. After cracking, the member consists of 2 regions, an uncracked region (1) and a cracked region (2) which includes the sections adjacent to the actual fracture where the concrete stress varies.

Consider the cracked region 2 surrounding the first crack. At the crack, the concrete stress is zero and the reinforcement alone carries the tensile force, as shown in Figure 3.4c and 3.4d

$$F = A_s\sigma_{s2} \tag{3.6}$$

where σ_{s2} = tensile stress in the reinforcement at the crack (subscript 2 corresponds to region 2 where area inside region 2 is influenced by the effect of the crack)

Within region 2, the stresses in the concrete and reinforcement vary with distance from the crack and depend on the distribution of bond stress. As the tensile stresses are transferred from the reinforcement to the concrete by bond, stress in the concrete increases, until at some distance S_o, from the crack, the concrete stress again resumes a constant value. Since the concrete surface stress within the distance S_o on

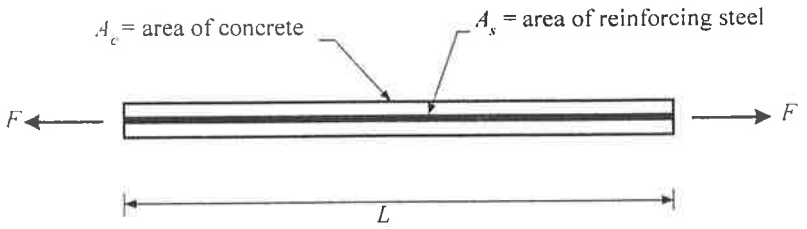

(a) Reinforced concrete member subjected to a gradually increasing tensile forces,F

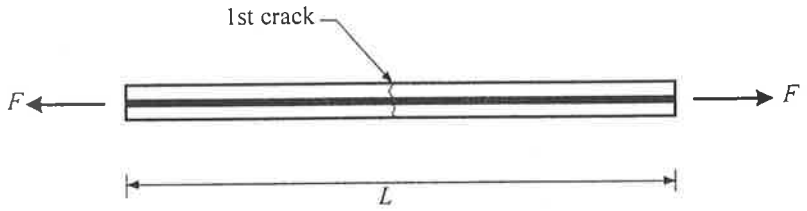

(b) Restraining forces,F at each end cause a first crack to develop

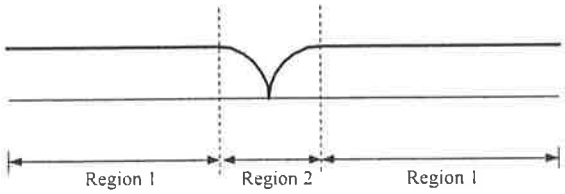

(c) Concrete stresses along the length of reinfored concrete member

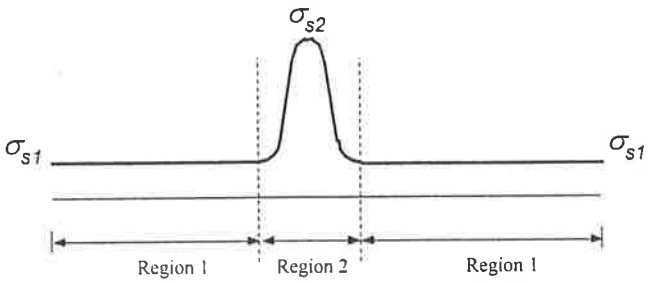

(d) Tensile stress in the reinforcement

Figure 3.4 Conditions after first cracking in a reinforced concrete member subjected to applied tensile forces

both side of the crack is below the tensile strength, no other cracks form between these distances. At some distance S_o away from either side of the crack (region 1), the stress distribution remains unaffected by the crack (Figure 3.4a) and the force F still is resisted by both concrete and reinforcement. In addition,

$$F = F_{c1} + F_{s1} \tag{3.8}$$

$$= A_{c1}\sigma_{c1} + A_{s1}\sigma_{s1} \tag{3.9}$$

$$F = A_{c1}\varepsilon_{c1}E_c + A_{s1}\varepsilon_{s1}E_s \tag{3.10}$$

For full strain compatibility,

$$\varepsilon = \varepsilon_c = \varepsilon_s \tag{3.11}$$

So that

$$F = \varepsilon\,(A_{c1}E_c + A_{s1}E_s) \tag{3.12}$$

Rearrangement gives

$$F = A_{c1}\varepsilon\,E_c(1 + n\rho) \tag{3.13}$$

$$= A_{c1}\sigma_{c1}(1 + n\rho) \tag{3.14}$$

where σ_{c1} = tensile stress in the concrete of region 1

σ_{s1} = tensile stress in the reinforcement of region 1

A_{c1} = cross-sectional area of concrete in region 1

A_{s1} = cross-section area of steel reinforcement in region 1

In order for subsequent cracks to form in uncracked region along the member, the concrete stress term σ_{c1} must be increased to the tensile concrete strength f_c' in equation (3.14) and the location must occur away from the distance S_o. It is important to note that the value of tensile strength of concrete f'_t in an uncracked region is directly proportional to the applied tensile force F. Since the magnitude of f'_t in a member is also depended on time and can vary from section to section; as a result, cracks do not form at the same level of applied tensile force F. However, it is reasonable for the purpose of this study to assume that the tensile strength of

concrete f'_t is constant through out the cracking process, thus resulting in identical force F at which each crack occurs.

If two adjacent cracks form at a distance greater than $2S_o$ as shown in Figure 3.5b, there will be an area in which the full concrete stress σ_{cl} occurs, this area is not affected by either of the cracks. This is where another cracks can form. On the other hand, if cracks form at a spacing less than $2S_o$, then the concrete stresses will be reduced over the whole length between the two cracks and cracks will not formed (Beeby,1979).

This is illustrated in Figure 3.5c. In general, the distance S_o is regarded as the minimum crack spacing between 2 cracks whereas the distance $2S_o$ is considered as the maximum crack spacing. After all the cracks have developed, it is considered that the development of cracking has reached a stabilised state. This theoretically means that no more cracks can form (with the exception of small secondary cracks) and additional increase in tensile stress simply results in widening the existing cracks or yielding of the reinforcement. In this state, cracks generally consist of those having distribution of spacing within the range of S_o and $2\ S_o$.

From the above discussion, it can be seen that bond stress has large a influence on the development of cracking, since the variation of concrete and reinforcement stresses is depended on bond stress along the distance $\pm S_o$. The following section explains the effects of bond stress on the cracking behaviour as well as the relation between bond stress, stresses in concrete and reinforcement within the cracked regions, crack spacing and crack width in reinforced concrete member.

3.2.3 Effects of bond stress on cracking

Bond stress can be considered as the shear stress at the interface of the reinforcement and concrete. For both materials to behave compositely, bond stress has to develop and transfer stresses from the reinforcement to the surrounding concrete and vice versa. Bond between concrete and reinforcement is considered to consist of three components:

- chemical adhesion;

- friction; and
- mechanical interaction between concrete and reinforcement

Even though all three components can affect the bond properties, mechanical interaction between concrete and reinforcement is thought to primarily dominate the bond properties in deformed bars (Lutz and Gergely, 1967). Hence, the attainment of satisfactory performance in bond is the most important factor in minimising cracking in reinforced concrete structures. In most cases, the studies of tensile cracking and bond stresses in reinforced concrete members have been made from axial loaded tests conducted in laboratory.

Slip between the reinforcement and concrete results in differences between strains in the reinforcement and concrete. The slip of a deformed bar is mainly caused by either crushing of the concrete at the ribs or by the ribs pushing the concrete away from the bar (Lutz and Gergely,1967). Depending on the facing angle of the ribs, one of these actions can dominate, but in the case of a reinforcing bar with good frictional properties and rib face angles greater than 40 degrees, slip mainly occurs by progressive crushing of the porous concrete paste structure in front of the rib.

When the tensile stress exceeds the tensile strength of concrete, cracks perpendicular to the member axis develop and the concrete pulls away from the reinforcement in the vicinity of the crack. At the crack, there is bond break down between the two materials. Experiments conducted on axially loaded reinforced concrete specimens by Goto (1971), found that the formation of internal cracks adjacent to the primary cracks can have a great influence on the bond mechanism between reinforcement and concrete. Within the length where these internal cracks are formed, the bond is considered almost lost. This behaviour is shown in Figure 3.6. Leonhardt (1971) roughly estimated this length of lost bond in standard deformed reinforcement to be

$$l_o = \frac{\sigma_{s2}}{45} d \tag{3.15}$$

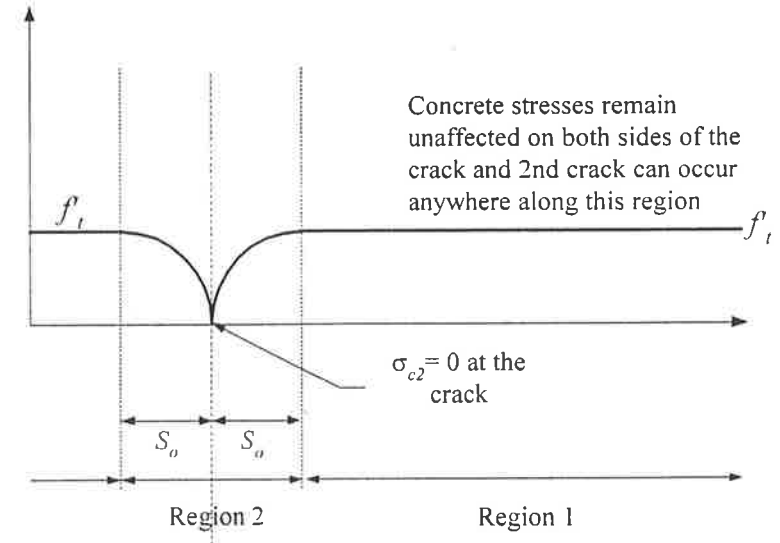

(a) The state of concrete stresses after a first crack has occurred

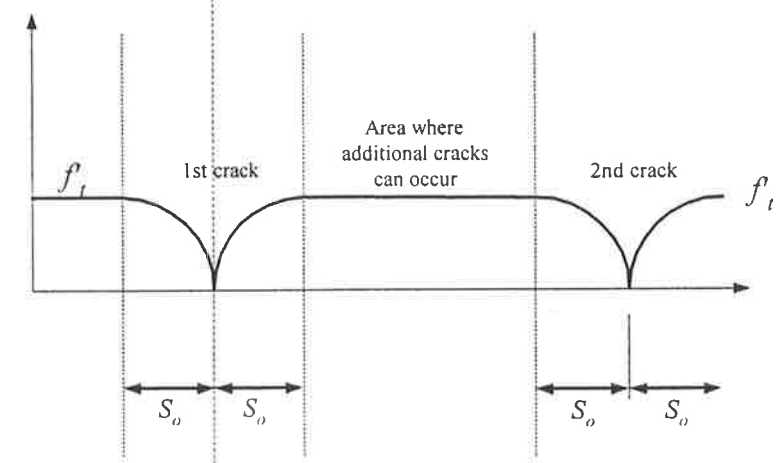

(b) The state of concrete stresses after two cracks have occurred

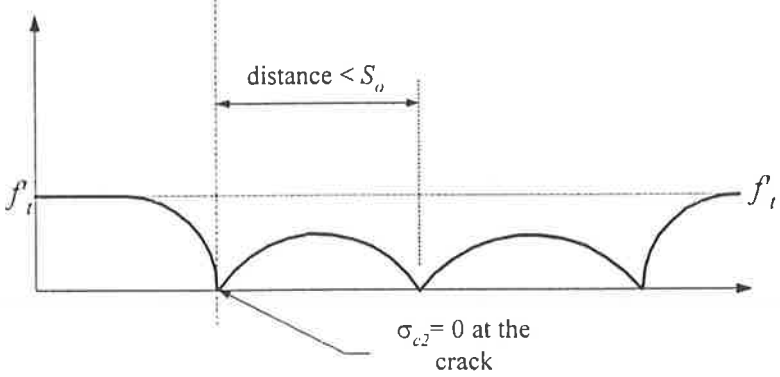

(c) The condition at a stablisd cracking stage where no additional cracks can develop

Figure 3.5 Conditions of concrete stresses during the development of cracking

ACI 224 (1986) stated that the primary cracks generally are widest at the surface of the concrete, but become narrowest at the surface of the reinforcement. The width at the concrete surface also increases at a faster rate than the width at the reinforcement as the magnitude of the tensile force is increased. In contrast, internal cracks were considered to increase in width with distance away from the reinforcement prior to narrowing and closing before reaching the surface of concrete. This is again shown in Figure 3.6.

The stress condition in the vicinity of the crack is very complex. At the crack, the tensile stresses that existed in the concrete before cracking, have disappeared and the reinforcement alone carries the tensile forces. Away from the crack, there is a gradual transfer of tensile stresses from the reinforcement to the concrete. The distance for this transfer to be effective is defined in Section 3.1.2 as S_o and is often referred as transfer length.

Three main approaches have been developed for the analysis of bond stress, the vicinity of the crack or within the distance S_o on either side of the crack. These are referred to as "the bond stress-slip relationship", "the bond stress distribution" and "the average bond stress distribution". The following sections describe these approaches and present some of the equations proposed by various authors. However for full details of the equations, the original references should be consulted.

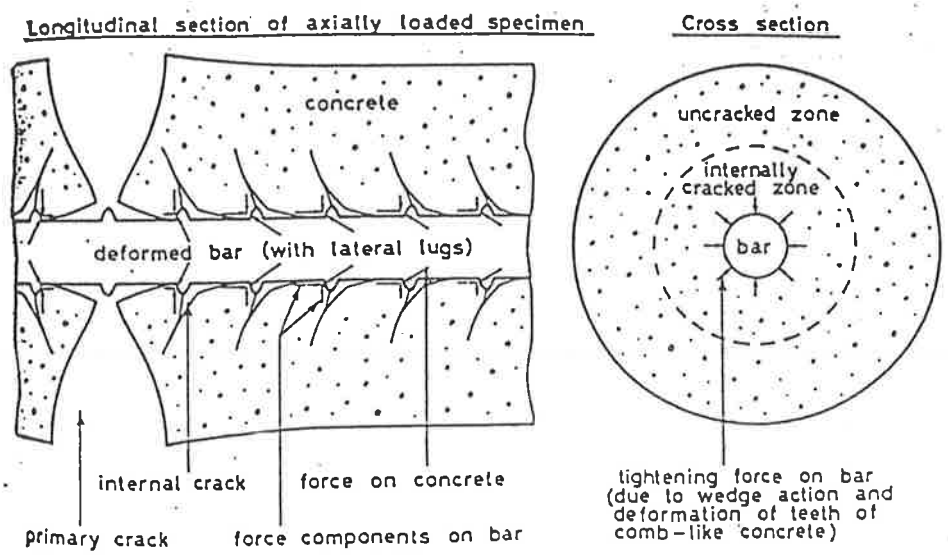

Figure 3.6 The formation of internal cracks around the reinforcing bar near the main crack (Goto, 1971)

3.2.3.1 Bond stress-slip relationship

Several researchers have studied the relationships between bond stress, slip and cracking. These include Nilson (1972), Edward and Picard (1972), Tassios and Yannopoulos (1981), Jiang et al. (1984), Yang and Chen (1988), Gupta and Maestrini (1990), and Russo and Romano (1992).

The relationships between bond stress and slip can be influenced by many factors, CEB (1981) considered the followings to be important:

- surface of reinforcing bar;
- concrete strength;
- position of the reinforcement during casting;
- type of loading;
- confinement of concrete; and
- concrete mixes.

Generally, the relationships between bond stress and slip can be determined experimentally from tests. From the test results, bond stresses and slip along the member are plotted to generate a curve which can be used to analyse the relationship between bond stress and the stresses in the reinforcement and concrete along the length of transfer S_o.

Nilson (1972) defined the average unit bond stress at any location along the interface, at any load, to be proportional to the slope of the strain distribution curve in the reinforcement at that point and load. This average unit bond stress can be taken as

$$\tau = \frac{A_s E_s}{\Sigma \pi d} \frac{d\varepsilon_s}{dx} \tag{3.16}$$

Slip at the reinforcement and concrete interface is defined as the difference in displacement of the reinforcement and concrete.

ie. $$\Delta = \delta_s - \delta_c \tag{3.17}$$

$$\Delta = \int (\varepsilon_s - \varepsilon_c) dx \tag{3.18}$$

This expression is only valid within the distance $\pm S_o$ from the crack, and displacement functions for the concrete and reinforcement can be obtained by integrating the strain functions of both materials. Since the strain in the reinforcement ε_s is continually decreasing while the strain in the concrete ε_c is increasing towards the distance S_o, these two variables are often very complicated to analyse due to the non-uniformity of bond stress distribution.

As the applied axial force is increased incrementally, a series of points can be used to construct a bond stress-slip curve. Bond stress and bond slip can be calculated from the slope of the reinforcement strain curve using equation (3.16), and equation (3.17) respectively. As an example, a typical bond stress-slip curve can be illustrated as shown in Figure 3.7

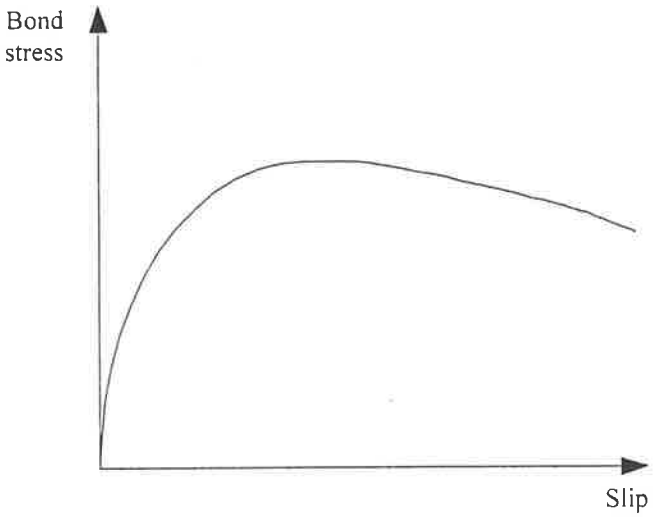

Figure 3.7 A typical bond stress-slip curve

Gupta and Maestrini (1990) further simplified the curve by approximating it as a bilinear curve as shown in Figure 3.8. For a given bilinear curve, the slope of the inclined line and the horizontal line representing the maximum bond stress are influenced by material properties, geometry, and the loading parameters. Gupta and Maestrini (1990) proposed a bond stress-slip relationship for the incline part of the curve as,

$$\tau = A\Delta \qquad (3.19)$$

where A = the slope of bond stress-slip curve and is referred as slip modulus

Furthermore, Gupta and Maestrini (1990) suggested the following displacement functions for the reinforcement and concrete along this part of the curve as,

$$\delta_s = \frac{Fx}{A_s E_s} - \frac{C_1}{1+n\rho}(kx\cosh(kS_o) - \sinh kx) \tag{3.20}$$

$$\delta_c = \frac{n\rho C_1}{1+n\rho}(kx\cosh(kS_o) - \sinh kx) \tag{3.21}$$

$$\text{where } k = \sqrt{\frac{A2\pi d}{A_s E_s}(1+n\rho)} \tag{3.22}$$

x = the distance measured from the reference point which is taken as the distance between two cracks (ie. Distance S_o from the crack)

F = applied axial force

In addition, the following boundary conditions were assumed so as to calculate the constant C_1: when $x = S_o$, force in reinforcement = F and force in concrete = 0, when $x = 0$, δ_s and $\delta_c = 0$. The expression for C_1 can be given as,

$$C_1 = \frac{F}{A_s E_s}\frac{1}{k\cosh(kS_o)} \tag{3.23}$$

In addition, the following boundary conditions were assumed so as to calculate the constant C_1: when $x = S_o$, force in reinforcement = F and force in concrete = 0, when $x = 0$, δ_s and $\delta_c = 0$. The expression for C_1 can be given as,

$$C_1 = \frac{F}{A_s E_s}\frac{1}{k\cosh(kS_o)} \tag{3.23}$$

Using similar assumptions, Edwards and Picard (1972) suggested two techniques to study the bond stress. The first technique assumes that the bond stress-slip relationship is linear up to a critical slip which they defined as the point where bond

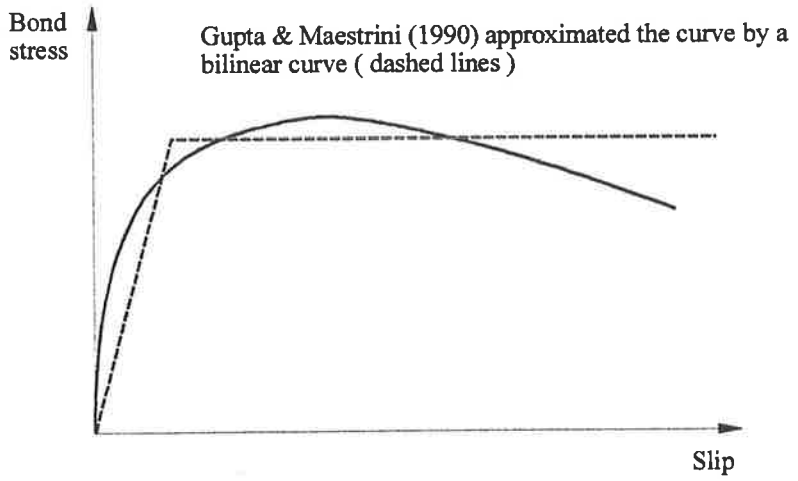

Figure 3.8 A simplified bond stress-slip curve (Gupta & Maestrini, 1990)

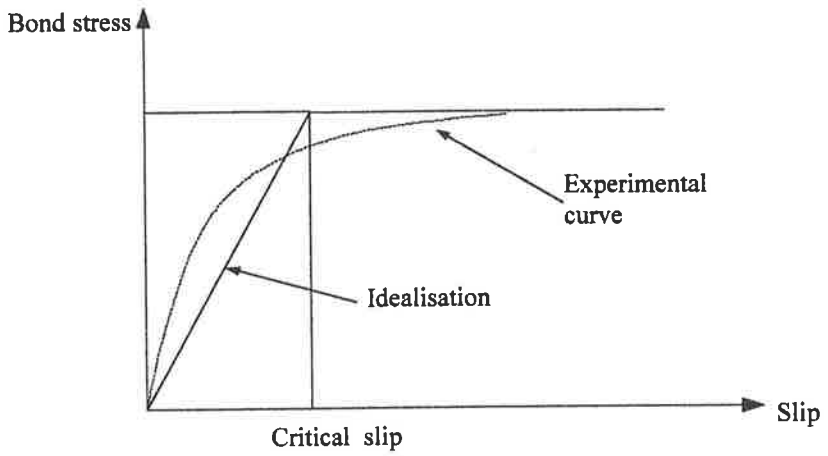

Figure 3.9 Bond stress-slip relationship assuming linear up to critcal slip (Edward & Picard, 1972)

stress becomes constant. This is shown in Figure 3.9. The analysis then proceeds with the determination of bond stress equations for cases where bond stress is assumed below its maximum value and where bond stress is constant (horizontal line).

With reference to Figure 3.10a, the bond stress distribution function where bond stress is below its maximum value can be expressed as,

$$\tau(x) = \frac{k\sigma_{s2}}{K_1 E_s}\left(\frac{e^{[K_1(2S_o - x)]} - e^{(K_1 x)}}{e^{(K_1 2S_o)} + 1}\right) \tag{3.24}$$

where $\tau(x)$ = bond stress at any distance x from the crack

k = slope of the bond stress-slip curve

σ_{s2} = tensile stress in reinforcement at the crack

$2S_o$ = assumed maximum spacing between each crack

K_1 = another expression which is given as,

$$K_1 = \sqrt{\frac{\pi dk}{A_s E_s}\left(1 + \frac{nA_s}{\psi A_c}\right)} \tag{3.25}$$

A_s = cross-sectional area of reinforcement

A_c = cross-sectional area of concrete

ψ = a factor which averages the tensile stress in concrete σ_{ct} over the area A_c

In the second technique, Edwards and Picard (1971) assumed bond stress to be constant up to the distance l_n from the crack as shown in Figure 3.10b. Beyond this distance, the distribution of bond stress remains the same as for the case previously described. However, the value of l_n is not allowed to approach the distance S_o because there is a discontinuity of bond stress distribution at distance S_o. In order to obtain a thorough understanding of the theory behind this hypothesis, readers are recommended to refer to Edwards and Picard (1972).

As with the previous authors, Tassios and Yannopoulos (1981) idealised the bond stress-slip curve by replacing the non-linearity curve by four segments. The detailed of their studies is omitted from this study.

In comparison to Edwards and Picard (1972) and Tassios and Yannopoulos (1981), the CEB-Model 1990 (CEB-FIP, 1993) provides a general law for the bond stress-slip relationship based on deformed reinforcing bars under monotonic short-term loading. The bond stress-slip curve is shown in Figure 3.11. It should be realised that this figure is only applicable for confined concrete subjected to short-term monotonic loading. According to Wicke (1990) who studied the method by CEB, cracking at the serviceability stage only occurs on the first branch of the curve and the bond stress within this range can be expressed as

$$\tau = \tau_{max}\left(\frac{\Delta}{\Delta_1}\right)^{\alpha} \tag{3.26}$$

The value of constant α are suggested to range from 0.22 to 0.40.

Furthermore, in the vicinity of the crack, there is a zone where bond between the reinforcement and concrete is reduced. As a result, Wicke (1990) advised that bond stress and slip should be reduced to within a distance of $x \leq 5\phi$ from the crack by a factor λ where

$$\lambda = \frac{x}{5\phi} \leq 1 \tag{3.27}$$

By modifying equation (3.26) further, an equation to describe the distribution of bond stress along the length of transfer S_o can be obtained:

$$\tau(x) = k_r x^{\frac{2\alpha}{1-\alpha}} \tag{3.28}$$

It is necessary to point out that the previous method by CEB is only valid for monotonic loading cases. Thus, long-term or repeated loading would need additional consideration.

By using curve fitting of the experimental data to a bond stress-slip curve, Bruggeling (1991) presented an exponential equation which can be used to calculate the length of transfer. The equation expressed bond stress as a function of the distance x away from the crack and can be written as,

$$\tau(x) = C\Delta^N \tag{3.29}$$

where C and N are factors which depend on the shape of the bond stress-slip curve and the bond strength respectively.

Bruggeling (1991) recommended the values of N to range from 0.18 to 0.28 for normal reinforcement while the values of C are expressed as the ratio of compressive strength of concrete and are between 0.38 and 0.32 for normal reinforcement. The rest of the analysis can be found in the reference provided.

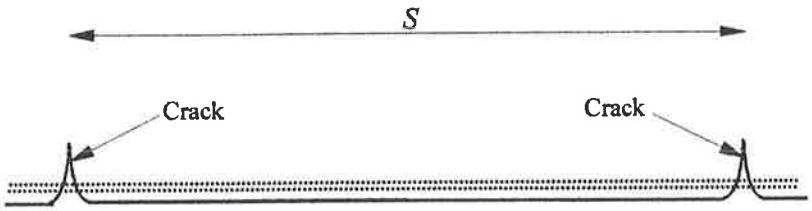

Case 1: $\tau(o) < \tau_{max}$

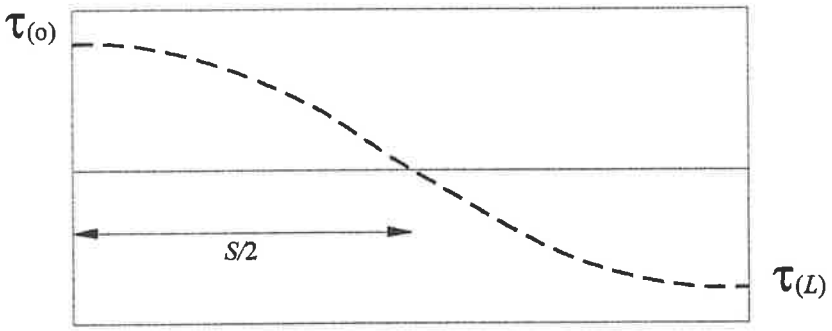

(a) Bond stress-slip relationship is assumed linear up to a critical slip

Case 2: $\tau(o) = \tau_{max}$

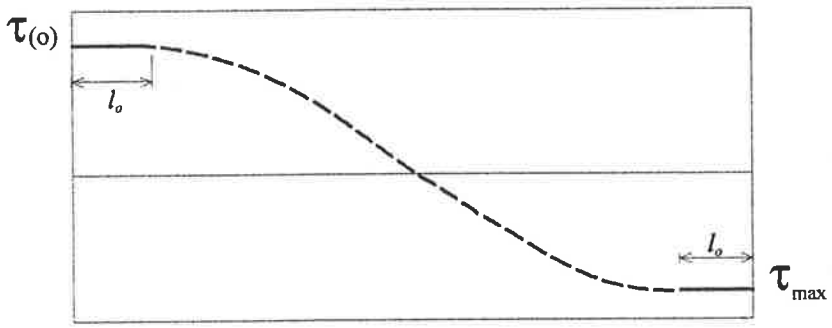

(b) Bond stress is assumed to be constant up to the distance l_o

Figure 3.10 Bond stress distribution betwen two cracks (Edwards & Picard, 1972)

Even though the relationship between bond stress and slip has been used as a basis for describing cracking behaviour in most of the analytical models mentioned herein, experimentally, it is extremely difficult to measure the local bond stress and local slip along the stressed reinforcement in a tension member. The experiments were also found to be error prone. The relationship between bond stress and local

slip has been observed to vary from section to section (Jiang et al.,1984), (Tassios and Yarnopoulos,1981) and (Somayaji and Shah, 1981).

With these objections in mind, many researchers have directed their attention towards an alternative approach based on bond stress distribution to predict the cracking behaviour. The discussion of this topic is covered in the following section.

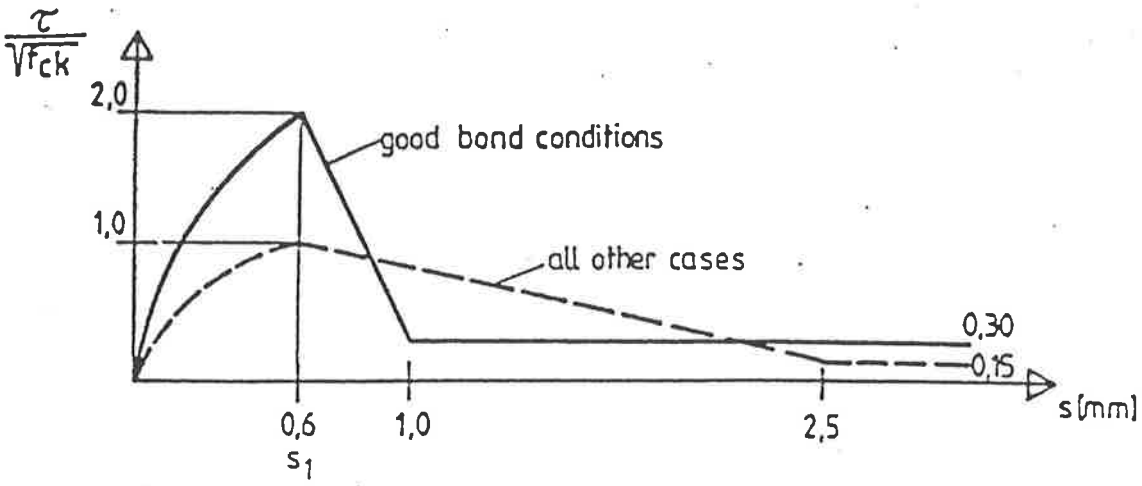

Figure 3.11 Bond stress-slip curve for deformed reinforcing bars under monotonic loading as recommended by CEB-FIP 1990 Model Code (Wicked, 1990)

3.2.3.2 Distribution of bond stress

Several analytical methods exist which can be used to predict the behaviour of cracking based on an assumed distribution of bond stress. The method is based on sets of bond stress distribution equations which must satisfy the equilibrium and compatibility conditions. These equations then are integrated or differentiated so that the reinforcement and concrete strains and bond stresses at any sections can be evaluated. These equations in turn can also be used to predict other quantities such as crack widths and tension stiffening in concrete.

In order to form a model for the analysis, bond stress distribution functions between two primary cracks are considered as shown in Figure 3.12.

The following observations are also made in order to establish the function:

- bond stress is zero and changes its sign at the centre between two cracks due to the anti-symmetry;
- bond stress at the crack face and inner end of the length of transfer is zero, and reaches its maximum value within a short distance from the cracks compared with length of transfer. This is again shown in Figure 3.10.

Somayaji and Shah (1981) proposed an analytical model using an exponential function for bond stress distribution. This is also demonstrated in Section 3.2.4.1.2 By integrating this equation further, it can be used to determine crack width. Instead of assuming a relationship between local bond stress and local slip, they proposed a general exponential bond stress distribution function as given below,

$$\frac{d^2\Delta}{dx^2} = Ae^x + Be^{-x} + C \tag{3.30}$$

The constants A, B and C can be obtained from various boundary conditions. Using this method, the maximum bond stress can generally be found at the centre of the length of transfer. Yang and Chen (1988) claimed that this improvement makes the function easier to integrate and differentiate, thus making it possible to calculate the exact distribution of stress in reinforcement and concrete. However, Yang and Chen also argued that maximum bond stresses usually occur at a section closer to the crack face than to the other end of length of transfer. Hence they developed another equation which relates bond stress to the slip, but incorporates parabolic and cosine terms to improve the shape of the bond stress distribution as shown.

$$\tau(x) = K\Delta(x) + (Cx^2 + D) + E\cos(\frac{\pi}{2}.\frac{x}{S_o}) \tag{3.31}$$

where K = bond constant (bond stress per unit slip)

A, B, C, D and E are constants and as in Somiyaji and Shah's work, they have to be determined from a set of boundary conditions.

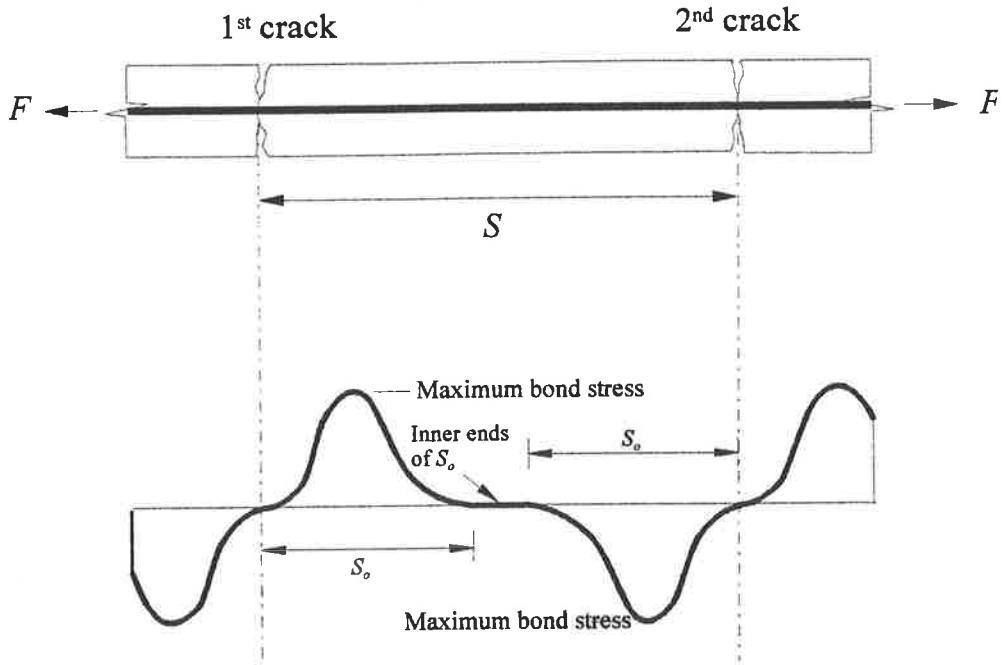

Figure 3.12 Bond stress distribution between two primary cracks as idealised to form a model for bond stress distribiton function

Despite this, Chan, Cheung and Huang (1992) commented that the Yang and Cheng (1988) model is very difficult to obtain experimentally. In their analytical model, various bond stress distribution functions are proposed for different loading stages. They claimed that the value of bond stress is zero at the end of length of transfer and develops into the peak value at a location near the crack. The distribution of the bond stress also changes its form as the tensile stresses increase. In addition, the peak bond stress also develops into the ultimate bond stress where from this point, the bond stress is assumed to be constant regardless of any axial force increased.

Another bond stress distribution function was presented by Jiang et al. (1984) who assumed a parabolic bond stress distribution function as shown,

$$\tau(x) = \tau_{max}[1-(1-\frac{4x}{2S_o})^2] \qquad (3.32)$$

where $2S_o$ = assumed distance between two primary cracks

$\tau(x)$ = bond stress at a distance x from the end of the member

τ_{max} = maximum bond stress which depends on material properties and expressed in terms of bar diameter, concrete strength, and stress in reinforcement. Thus, the equation is expressed as,

$$\tau_{max} = 0.034\sigma_{so}(1 - 0.01\sigma_{so}) \quad (3.33)$$

where σ_{so} = stress (ksi) in reinforcement at the end of member

By considering material properties, equilibrium and compatibility conditions, it is possible to calculate stresses in reinforcement and concrete slip using equation (3.33). Moreover, Jiang et al. (1984) suggested that different bond stress distribution functions do not significantly alter the results as long as identical values are selected for the maximum bond stress.

So far, it can be seen that the use of bond stress distribution functions is not any easier or less complicated when compared to the method of bond stress-slip relationships. In fact, both methods require the determination of several variables which can not be obtained accurately using empirical results. In addition, the costs associated with setting up experimental tests and the time consumed to obtain these variables may not justify the accuracy that might be obtained.

Therefore, several researchers and design codes have adopted an alternative method, which simplify the calculation of stresses in reinforcement and concrete along the cracked region. Instead of assuming a variation of bond stress along the member, bond stress is assumed constant in the region of cracking.

By using this method, many researchers have developed equations for the determination of crack spacing and crack width in reinforced concrete members spanning between both unrestrained and restrained supports. The results obtained generally agreed well with the experiments. Some of these researchers include Base (1978a, 1978b), Leonhardt (1977), Hughes (1971, 1973, 1974), and Evans and Hughes (1969). A number of design codes including CEB-FIP Model Code 1990 (1993)

adopted a similar approach in order to simplify the calculation of crack spacing and crack width.

The CEB-FIP Model Code 1990 (1993) simplified the distribution of bond stress over the length of transfer under short-term monotonic loading by assuming average bond stress over this length. The value of the average bond stress can be obtained simply by multiplying the average tensile stress of concrete by 2.0.

3.2.4 Application of bond stress theory to predict crack spacings and crack width

There are several ways in which crack width can be determined. One is by employing the bond stress-slip relationship approach discussed in Section 3.2.3.1. A second way is by adopting the bond stress distribution approach in Section 3.2.3.2. However, the simplest and probably most frequently used by engineers is the approach where average bond stress is assumed in the cracked region rather than analysing the non uniformity of the bond stress along the cracked region. All three ways are now considered.

3.2.4.1 Average bond stress

In general, a basic equation for crack width can be given as;

$$w = 2S_o(\varepsilon_s - \varepsilon_c) \tag{3.34}$$

where ε_s = tensile strain of reinforcement within the distance $2S_o$

ε_c = concrete strain within the distance $2S_o$

From the above equation, it can be seen that the magnitude of the crack width is only influenced within the area inside of the cracked region (region 2, Figure 3.4). Therefore, the distances S_o on both side of the crack are only considered. On the other hand, in some approaches, the average crack spacing and average tensile strain of steel reinforcement are used instead in equation (3.34). It is also the slip that occurs due to the difference in displacement between the reinforcement and concrete within this region which is the most concern.

In addition, several researchers also proposed other equations to calculate crack width based on either the experimental observations or modifications of the equation (3.34). These equations are examined in this section to understand the assumptions used behind their derivations. Hence, the general predicting methods for crack spacing and crack width being considered for review are those contained in the following references;

- Leonhardt (1977)
- Beeby (1979)
- CEB Manual "Cracking and Deformation" (1985)
- ACI 224 "Cracking of concrete members in direct tension" (1986)
- Christiansen and Nielsen (1997)

3.2.4.2.1 Method by Leonhardt (1977)

Leonhardt (1977) suggested that crack width should be calculated within the area of cracked region which he defined as the length of lost bond, l_o, defined earlier in equation (3.15), plus the length of transfer S_o.

ie. $$l_o + S_o$$

Using Goto (1971)'s experiments which suggested that crack width decreases from the concrete surface towards the reinforcement as a basis, Leonhardt (1977) included the effect of concrete cover in his expression for length of transfer S_o as follows;

$$S_o = \frac{f_t' A_{ct}}{\tau_{ave} \sum \pi d} + k_1(c, a) \tag{3.35}$$

The variable A_{ct} is the area of concrete under tension before cracking. The term k_1 (c,a) is the factor representing influence of concrete cover c and spacing of reinforcement a. Leonhardt (1977) suggested that this term is the length in which stresses spread out from the crack and can be expressed as;

$$k_1 = 1.2c \qquad \text{for } a \le 2c \tag{3.36}$$

$$k_1 = 1.2(c + \frac{a - 2c}{4}) \qquad \text{for } a > 2c \text{ with } a \le 14d \tag{3.37}$$

In addition, the ratio $\frac{f_c'}{\tau_{ave}}$ is now replaced by a factor k_2, which depends on the type of reinforcement being used. Leonhardt (1977) suggested a value of 0.4 and 0.74 for standard ribbed and smooth hot rolled reinforcement respectively. Likewise, the term $\frac{A_{ct}}{\sum \pi d}$ is rewritten relating it to the ratio between percentage of reinforcement and the tensioned area of concrete multiplied by a factor k_3, which depends on the shape of the tensile stress diagram.

ie. $$\frac{A_{ct}}{\sum \pi d} = k_3 \frac{d}{\rho_{eff}} \tag{3.38}$$

where k_3 = 0.25 for pure tension

ρ_{eff} = effective reinforcement ration relating to the concrete area A_{ct}

Hence, with these factors, equation (3.38) can be rewritten as;

$$S_o = k_1(c, a) + k_2 k_3 \frac{d}{\rho_{eff}} \tag{3.39}$$

Due to the assumptions for which his analysis are based on, the mean values for the tensile strength of concrete and bond strength have to be modified by a scatter factor, k_4. The crack width calculated then would be the 95% maximum crack width for cracking in the stabilised stage. For pure tension and moderate bar spacing, the value of k_4 can be taken as 1.4.

Another factor, k_5 is also introduced to accounts for load repetitions or sustained load. This generally causes the crack width to increase due to the effect of k_5 on tension stiffening. Usually, k_5 is between 0.8 to 0.4

At a stabilised cracking stage, cracks are considered to distribute having a minimum spacing equals to;

$$S_{min} = \frac{l_o}{2} + S_o \tag{3.40}$$

where both l_o and S_o were already discussed in equation (3.15) and (3.39) respectively

With the relationships between concrete, reinforcement and all the relevant factors being established, the maximum crack width can now be determined using the relationship between displacement in the distance l_o and S_o as follows;

$$w_{\max} = l_o \varepsilon_{s2} + S_o \varepsilon_m \tag{3.41}$$

where ε_m = mean reinforcement strain, measured over the cracks and can be obtained by neglecting the cracking strain in concrete as;

ε_{s2} = tensile strain at the crack

$$\varepsilon_m = \varepsilon_{s2}[1 - (\frac{\sigma_{s2,c}}{\sigma_{s2}})^2] \tag{3.42}$$

By substituting equation (3.42) into (3.41) and incorporating the factors k_4 and k_5, the following expression is obtained;

$$w_{95} = k_4 l_o \frac{\sigma_{s2}}{E_s} + k_4 S_o \frac{1}{E_s}(\sigma_{s2} - k_5 \frac{\sigma_{s2,c}^2}{E_s}) \tag{3.43}$$

where w_{95} = 95 % fractile of maximum crack width

σ_{s2} = tensile stress in the reinforcement at the crack

$\sigma_{s2,c}$ = tensile stress in the reinforcement at the crack when the tensile stress exceeds the tensile strength in concrete (ie. when crack develops)

According to Leonhardt (1977), the crack width is primarily influenced by the bond quality of the reinforcement, the ratio between diameter and reinforcement ratio and the spacing of the reinforcement.

3.2.4.1.2 Method by Beeby (1979)

Beeby (1979) developed his theory of cracking using the classical cracking theory proposed by R. Saliger and another theory by J. Ferry Borges which rather contradict the assumptions proposed by the former researchers. The basis behind this theory considers both "slip" and "non-slip" approaches from both researchers to actually provide different components of the problem.

Beeby's theory considers the development of cracking to be influenced by the concrete cover to the reinforcement and the internal cracks that develop near the main cracks. It is suggested that the degree of internal crack failure can greatly determine the magnitude of crack spacing.

With these conditions in mind, Beeby (1979) recommended the following assumptions as a basis to explain development of cracking:

- a crack initially forms with minimal width at the reinforcement surface;
- as the load is increased, there is a loss of adhesion adjacent to the crack resulting in load being transferred to the rib of the reinforcement;
- internal cracks form close to the main cracks;
- additional loads cause more internal cracks to form at successively greater distances from the main cracks;
- the spacing of the cracks would largely depend on the development of the above events;
- crack spacing can range from a minimum value of S_o close to the value of concrete cover if a significant amount of internal failure has occurred after an adjacent crack has formed to substantially larger than the concrete cover if significant internal failure has occurred prior to formation of the adjacent crack.

Using the above assumptions, Beeby (1979) gave an equation for average crack spacing which incorporated both the effects of concrete cover and average increase in the distance S_o resulting from the average amount of internal failure occurring prior to formation of the adjacent crack as;

$$S_m = K_1 c + K_2 \frac{d}{\rho} \tag{3.44}$$

The first term on the right hand side of equation (3.44) represents the effect of concrete cover c, being factored by a constant K_1. The second term on the right hand side of equation (3.44) represents the development of tensile stress along the cracked region which is considered proportional to the rate of development of internal failure. Thus, this is proportional to the ratio between the reinforcement diameter and the reinforcement ratio. In order to evaluate K_1 and K_2, Beeby (1979) provided the following table;

Table 3.2 Values of K_1 and K_2 (Beeby, 1979)

Probability of exceedence	K_1	K_2
Mean	1.33	0.08
20 %	1.59	0.12
5 %	1.86	0.20
2 %	1.94	0.28

Having established the relationship for the crack spacing, it is now possible to obtain an expression for crack width. This simply can be taken as;

$$w_m = (K_1 c + K_2 \frac{d}{\rho_{eff}})\varepsilon_m \tag{3.45}$$

where w_m = crack width over the bar

ε_m = average strain

ρ_{eff} = effective reinforcement ratio

The average strain given in equation (3.45) can be expressed as;

$$\varepsilon_m = \varepsilon_{s2} - \frac{K f_t' \sigma_{s2,cr}}{E_s \rho \sigma_{s2}} \tag{3.46}$$

The constant K depends on the type of reinforcement, the modulus of elasticity of reinforcement, the reinforcement ratio and the tensile strength of concrete.

According to the above relationships, it can be concluded that Beeby's crack width equation is influenced by several factors, namely the concrete cover to the reinforcement, diameter of the reinforcement, effective reinforcement ratio, and the bond qualities of the reinforcement.

3.2.4.1.3 Method by CEB Manual "Cracking and deformation" (1985)

The CEB Manual, "Cracking and deformations", developed a model for cracking in reinforced concrete members subjected to pure tension. As with other cracking theories, CEB considered the tensile stress and bond stress distributions after cracking to vary along the member. The actual conditions change continuously from the uncracked state at a distance S_o for each crack to the fully cracked state at the crack.

However, to reduce the complications involved in analysing the non-uniformity of both tensile and bond stress distribution functions, CEB proposed a reinforced concrete member after cracking to consist of uncracked and cracked states, which are defined as state I and II respectively. A distribution coefficient ζ is then introduced to account for the effects of tension stiffening in the concrete in tension as shown in Figure 3.13. For member with possible restraint, this can be assumed as 0.5.

This idealisation allows a fully cracked state to be equivalent to a length of $2\zeta S_o$, while the uncracked state to be the remaining length $(1-\zeta)2S_o$. Based on these assumptions, it is possible to calculate a crack width, which can be considered as the extension of the reinforcement over the length $2\zeta S_o$ minus the contraction of concrete due to shrinkage or temperature effect.

As a result, the average crack width at the stabilised cracking state can be expressed as follows;

$$w_m = S_m(\varepsilon_{sm} - \varepsilon_{sh}) \tag{3.47}$$

where S_m = the average crack spacing

ε_{sm} = the average strain in the reinforcement over fully cracked state

ε_{sh} = shrinkage strain in the concrete

According to equation (3.47), the average crack spacing, S_m is influenced by a number of factors, namely bond properties, reinforcement ratio, reinforcement spacings, reinforcement diameter, concrete cover and distribution of tensile stress within the section. As a result, an equation for average crack spacing relating to the above factors can be given as;

$$S_m = 2(c + \frac{a}{10}) + \kappa_1 \kappa_2 \frac{d}{\rho_r} \tag{3.48}$$

where c = concrete cover

a = reinforcement spacing

κ_1 = coefficient accounting for bond properties of the reinforcement and can be taken as 0.4 for normal deformed reinforcement

κ_2 = coefficient accounting for the distribution of tensile stress within the section and can be taken as 0.25

d = reinforcement diameter

ρ_r = reinforcement ratio

By observing the term on the right hand side of equation (3.48), it can be seen that effectively, it is the minimum crack spacing similar to the ones proposed by other researchers, including Hughes (1972, 1973). The two coefficients, κ_1 and κ_2 were incorporated to account for the average bond stress, τ_{ave} and tensile strength of concrete, f_t'.

With the average crack spacing determined, the relationship between the average tensile strain, ε_{sm} in reinforcement and the localised reinforcement strain, ε_{s2} at the crack can be defined as;

$$\varepsilon_{sm} = \zeta \varepsilon_{s2} \tag{3.49}$$

where ε_{s2} = tensile strain in the reinforcement at the crack and can be calculated as $\frac{\sigma_{s2}}{E_s}$

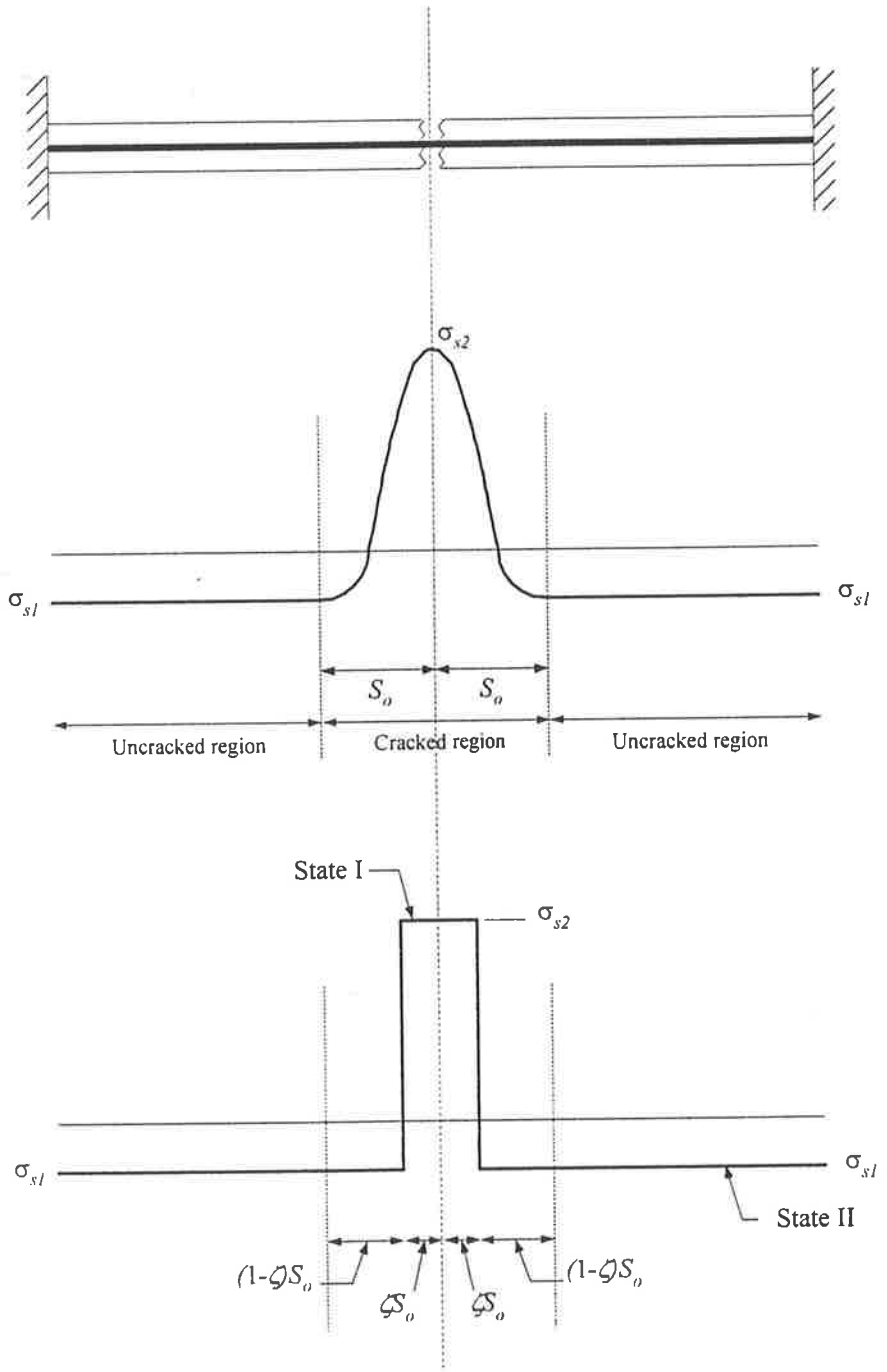

Figure 3.13 Idealisation of stress distribution in the reinforcement near a crack by CEB Manual (1985)

According to CEB, an extensive number of tests had been carried out in order to form this model and the procedure developed for calculating crack widths therefore can be considered as reliable. In general, the crack widths calculated should guarantee that the widths exist in practice will not exceed these values.

3.2.4.1.4 Method by ACI 224 (1986)

Under the title "Cracking of concrete members in direct tension", ACI Committee 224 presented another approach to determine crack spacing and crack widths. The causes of direct tension were identified as the applied loads which directly induce axial tensile stresses in the member and axial forces which occur as a result of restraint.

In both situations, the member is axially loaded. As the forces increase, the development of cracking was assumed to take place until the crack spacing is approximately twice the concrete cover which is measured from the surface to the centre of the reinforcing bar. ACI 224 estimated that the average crack spacing in normal reinforced concrete members with concrete cover ranging from 30 to 75mm would not reach the maximum value of twice the concrete cover until the tensile stress in the reinforcement reached about 138 to 200 MPa.

Furthermore, the maximum crack spacing was approximated to equal to twice that of the average crack spacing.

i.e. $$S_{max} = 2S_m \tag{3.50}$$

$$S_{max} = 4c \tag{3.51}$$

ACI 224 suggested that this range of crack spacing is generally 20 percent greater than crack spacing observed in flexural members. In order to reduce the number of cracks (which are visible), for a given tensile force, it is possible to increase the concrete cover so that a larger percentage of the cracks would remain as internal cracks.

With the crack spacing determined, the maximum crack width can be estimated by multiplying the maximum crack spacing by the average strain in the reinforcement. In addition, the actual concrete cover is replaced by an effective concrete cover t_e,

which is defined as a function of the reinforcement spacing, a, and the concrete cover measured from the centre of the reinforcing bar. ACI 224 used an expression for the effective cover t_e (in.), from a study conducted by Broms and Lutz (1965) as;

$$t_e = c\sqrt{1+\left(\frac{a}{4c}\right)^2} \tag{3.52}$$

According to equation (3.52), the effective cover, t_e is directly proportional to the reinforcement spacing, a. Therefore, a reinforced concrete member with relatively large reinforcement spacing would expect to develop in proportion larger crack widths. Similar to Brom and Lutz (1965), an expression for the maximum crack width (in.) can be estimated as;

$$w_{\max} = 4t_e\varepsilon_{sm} \tag{3.53}$$

where ε_{sm} = average strain in the reinforcement

Similar to crack spacing, the maximum crack width in direct tension is generally expected to be larger than those in flexure at the same stress level.

3.2.4.1.5 Method by Christiansen and Nielsen (1997)

A recent investigation into cracking of reinforced concrete structures by Christiansen and Nielsen (1997), has led to another physical model to predict cracking in a member subjected to axial tensile load. The basis for the theory is still very much similar to the previous models by others, but with additional modifications to further refine the model.

As a result, the average bond stress is assumed to equal to the tensile strength f_t' times a factor μ

ie. $$\tau_{ave} = \mu f_t' \tag{3.54}$$

According to the experimental data, Christiansen and Nielsen (1997) suggested that the factor μ can be taken as 1.0 in most cases.

Using Goto (1971)'s concept of internal cracking, the influence of internal cracks can have significant effect on the bond mechanism between the reinforcement and concrete. Similar to Leonhardt (1977)'s paper, it was assumed that no bond length exists between the reinforcement and concrete. This is mainly due to punching failure caused by the ribs of the reinforcement bars near the main cracks. As was the case with Leonhardt (1977), this no bond length is equal to $\frac{1}{2}l_o$ on each side of the crack. Beyond the distance $\frac{1}{2}l_o$ from each side of the crack, tensile stresses are transferred from the reinforcement to the concrete via bond stress. The stresses in concrete would reach the effective tensile strength of concrete at the distance ($\frac{1}{2}l_o$ + S_o). The distance S_o is considered as the length required for the concrete by bond to reach its effective tensile strength. It can be shown as;

$$S_o = \frac{0.5A_c}{N_{bar}\pi d} \tag{3.55}$$

where N_{bar} = number of reinforcing bars

The effective tensile strength of concrete was defined as the tensile strength of concrete multiplied by a factor introduced to account for the variation between tests and actual results.

In practice, the sum of $\frac{l_o}{2}$ and S_o is considered as the minimum crack spacing S_{min}.

The stress distribution between two cracks is illustrated in Figure 3.14a. According to this figure, it demonstrated that the concrete stress between the two length of transfer S_o, is carrying a stress equivalent to its effective tensile strength. Christiansen and Nielsen (1997) referred to this region as the yield zones. If the average crack spacing S_m becomes less than (l_o + 2S_o), stress distribution adopted in Figure 3.14a is no longer valid and the stress distribution in reinforcement as shown in Figure 3.14b is now used. This basically means that concrete stress would no longer reach its optimum value and no additional cracks would form between the two cracks.

Christiansen and Nielsen (1997) provided an equation for the no bond length l_o as;

$$l_o = (1+\frac{\sigma_{s2}}{100})d \qquad \leq \begin{cases} 1.3c \\ 0.65a \end{cases} \tag{3.56}$$

where σ_{s2} = tensile stress in reinforcement at the crack (MPa)

c = concrete cover

a = reinforcement spacing between centers

In addition, Christiansen and Nielsen (1997) identified three stages of cracking which can take place. First is the condition before cracking. Second is when cracks have already taken place, but the yield zone between the cracks still remain ($S_m > l_o + 2S_o$ in Figure 3.14b). In effect, the mean crack width can be determined as the elongation along the no bond length l_o and the length of transfer S_o on both side of the crack;

$$w_m = \frac{\sigma_{s2}}{E_s} l_o + \frac{1}{E_s}\frac{\sigma_{s2}+\sigma_{s1}}{2} 2S_o \tag{3.57}$$

Also in the above equation;

$$\sigma_{s1} = \sigma_{s2} - 4\frac{\tau_{ave} S_o}{d} \tag{3.58}$$

where σ_{s1} = tensile stress between two cracks

Thus, by substituting equation (3.58) into (3.57) and simplifying further yields;

$$w_m = \frac{1}{E_s}[\sigma_{s2}(l_o + 2S_o) - \frac{4\mu f_t' S_o^2}{d}] \tag{3.59}$$

This equation is only valid for cases where stress in the reinforcement at the crack lies between stress in reinforcement at first cracking, σ_{s2c} and stress in reinforcement prior to the establishment of stabilised cracking stage, σ_{sf}. The latter is express as;

$$\sigma_{sf} = \frac{a + b(2S_o + l_o)}{2S_o + l_o} \tag{3.60}$$

The constant a and b can be determined from a set of boundary conditions set out in Christiansen and Nielsen's paper.

A third stage recognised is when the yield zone no longer exists between the cracks (Figure 3.14b). This implies that concrete is not going to yield in this region and as a result, no addition cracks will be formed. Generally, when no yielding zone occurs throughout the member, cracking is considered to have reached a stabilised cracking stage. This is a well-known cracking phenomenon which was also explained elsewhere in this chapter.

In effect, mean crack width can be determined as the average strain in the reinforcement times the average crack spacing;

$$w_m = S_m \varepsilon_{sm} \tag{3.61}$$

$$\text{where} \quad S_m = 1.33(\frac{1}{2} l_o + S_o) \tag{3.62}$$

$$\varepsilon_{sm} = \frac{1}{E_s}(\sigma_{s2} - \frac{\mu f_t^{'}}{d}\frac{(S_m - l_o)^2}{S_m}) \tag{3.63}$$

Unlike equation (3.60), equation (3.62) is also valid in cases where $\sigma_{s2} > \sigma_{s2f}$.

3.2.4.2 *Variation of bond stress*

When bond stress is assumed to vary along the cracked region (region 2), the analysis can become quite complicated as can be seen in the bond stress functions presented earlier. Methods considered in this section include:

- Rizkalla and Hwang (1984)
- Edwards and Picard (1972)
- Somayaji and Shah (1981)

In all cases, analytical procedures were proposed and later compared and verified with the experiment results.

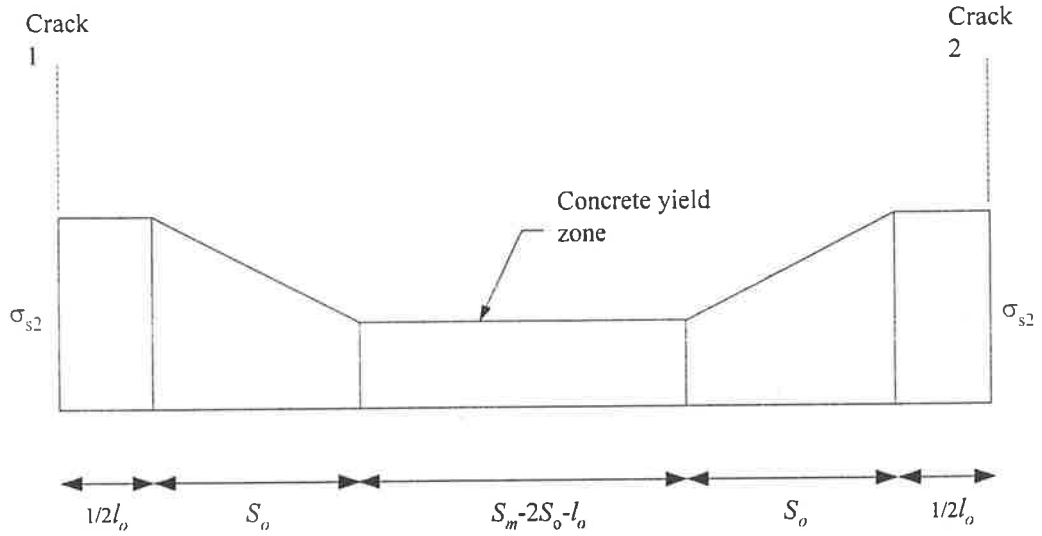

(a) Tensile stress distribution of the reinforcement between two cracks (only valid for $S_m > (2S_o - l_o)$)

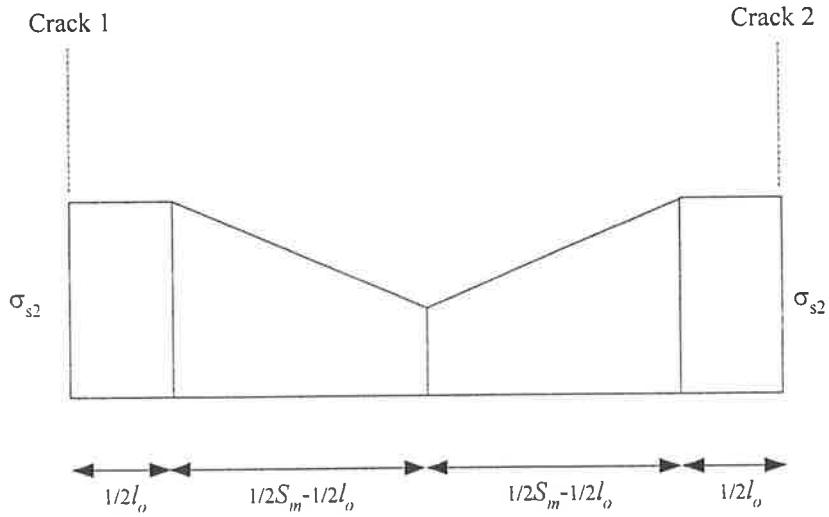

(b) Tensile stress distribution in the reinforcement when the concrete is no longer yielding (stabilised cracking stage)

Figure 3.14 Tensile stress distribution of the reinforcement during the development of cracking (Christiansen & Nelson, 1997)

3.2.4.1.1 Method by Rizkalla and Hwang (1984)

Rizkalla and Hwang (1984) proposed a methodology for predicting crack width and crack spacing subjected to tension at any given loading stage from the initiation of the first crack until the stabilised cracking stage. At the time their paper was published, it was suggested that there was no information available regarding the prediction of crack width and crack spacings between the stage at first crack and the stabilised cracking stages.

The concept of crack spacings had been discussed elsewhere in this report by Hughes (1970, 1972), Goto (1971) and others. Rizkalla and Hwang (1984) agreed that at the stabilised cracking stage, crack spacing can vary between S_{min} and $2S_{max}$. They also expressed the relationship between minimum, maximum, and average crack spacing as follows;

$$\frac{S_{\min}}{S_m} = 0.67 \tag{3.64}$$

$$\frac{S_{\max}}{S_m} = 1.34 \tag{3.65}$$

Based on experimental results and observation of cracking behaviour, the average crack spacing can be determined by adopting either Leonhardt (1977) or Beeby (1978) equations which were introduced in equation (3.39) and (3.44) respectively. Alternatively, Rizkalla and Hwang proposed their own equation as shown;

$$S_m = 5(d - 7.2) + K_1(a,c) + 0.08\frac{d}{\rho} \tag{3.66}$$

where K_1 = a factor accounting for the effects of concrete cover c and reinforcement spacing a

In addition, the presence of transverse reinforcement is considered to influence the average crack spacing at the stabilised cracking pattern, thus equation (3.66) is further modified by introducing another factor β such that;

$$S_c = \beta S_m \tag{3.67}$$

3.2.4.2.1 Method by Rizkalla and Hwang (1984)

Rizkalla and Hwang (1984) proposed a methodology for predicting crack width and crack spacing subjected to tension at any given loading stage from the initiation of the first crack until the stabilised cracking stage. At the time their paper was published, it was suggested that there was no information available regarding the prediction of crack width and crack spacings between the stage at first crack and the stabilised cracking stages.

The concept of crack spacings had been discussed elsewhere in this report by Hughes (1972, 1973), Goto (1971) and others. Rizkalla and Hwang (1984) agreed that at the stabilised cracking stage, crack spacing can vary between S_{min} and $2S_{max}$. They also expressed the relationship between minimum, maximum, and average crack spacing as follows;

$$\frac{S_{\min}}{S_m} = 0.67 \tag{3.64}$$

$$\frac{S_{\max}}{S_m} = 1.34 \tag{3.65}$$

Based on experimental results and observation of cracking behaviour, the average crack spacing can be determined by adopting either Leonhardt (1977) or Beeby (1979) equations which were introduced in equation (3.39) and (3.44) respectively. Alternatively, Rizkalla and Hwang proposed their own equation as shown;

$$S_m = 5(d - 7.2) + K_1(a,c) + 0.08\frac{d}{\rho} \tag{3.66}$$

where K_1 = a factor accounting for the effects of concrete cover c and reinforcement spacing a

In addition, the presence of transverse reinforcement is considered to influence the average crack spacing at the stabilised cracking pattern, thus equation (3.66) is further modified by introducing another factor β such that;

$$S_c = \beta S_m \tag{3.67}$$

The value of β depends the spacing of transverse reinforcement and average spacing S_m

Therefore, the total crack width at any stage of cracking can be considered as the total crack width $\sum w$ for a given length L multiplied by the average crack strain ε_w.

ie. $$\sum w = \varepsilon_w L \tag{3.68}$$

Base on experimental results,

$$\varepsilon_w = 3.145\varepsilon_m^{1.2} \tag{3.69}$$

In effect, the average crack width can be calculated as;

$$W_m = \frac{3.145\varepsilon_m^{12} L}{N} \tag{3.70}$$

The value of average strain ε_m can be evaluated using the equation (3.46) presented by Beeby (1979). N is the number of cracks at any stage until the stabilised cracking stage and can be determined according to the following conditions;

$$N_F = \frac{L}{S_c} + 1 \qquad \text{when } \varepsilon_m \cong 0.001 \tag{3.71}$$

or else

$$N = N_F \left[\frac{\varepsilon_m - \varepsilon_t'}{0.001 - \varepsilon_t'} \right] \qquad \text{when } \varepsilon_m < 0.001 \tag{3.72}$$

According to Rizkally and Hwang (1984), the first condition generally corresponds to the stabilised cracking stage and the average strain of this magnitude is assumed.

Moreover, minimum crack width w_{min} and maximum crack width w_{max} can be derived according to the following ratios;

$$w_{\min} = 0.67 w_m \tag{3.73}$$

$$w_{\max} = 1.55 w_m \tag{3.74}$$

Based on the experimental result, Rizkalla and Hwang (1984) claimed that the accuracy of using this proposed methodology is within ±a crack for most measurements of crack number, and overall average ratio for predicted to measured crack widths of 1.17 has been achieved.

3.2.4.2.2 Method by Somayaji and Shah (1981)

Earlier in Section 3.2.3.2, Somayaji and Shah (1981) developed an exponential bond stress distribution function which was given in equation (3.30). This is reproduced here as;

$$\frac{d^2\Delta}{dx^2} = Ae^x + Be^{-x} + C$$

By integrating the above function twice, an expression for crack width can be established as;

$$\Delta_x = Ae^x + Be^{-x} + C\frac{x^2}{2} + Dx + E \tag{3.75}$$

where Δ_x = the local slip at a distance x from the crack

The constants A, B, C, D and E can be determined from a set of equations given in Somayaji and Shah (1981)'s paper. These constants were found to depend on the length of transfer S_o. An equation to calculate the length of transfer S_o is given as;

$$S_o = K_p \frac{A_{eq} E_{eq} \varepsilon}{\sum \pi d} \tag{3.76}$$

The use of equation (3.76) is subjected to 2 conditions. When the member strain ε is below the strain at cracking, then the segment length is equivalent to the distance $2S_o$. On the other hand, if the member strain is large enough to cause cracking, the actual crack spacing can be assumed to be between $S_{min} = S_o$ and $S_{max} = 2S_o$.

After all the constants in equation (3.75) are determined, it is then possible to calculate the strains in reinforcement, concrete and bond stress along any section at

a distance x from the crack by successive differentiation of equation (3.71). In addition, the average crack width can be calculated when $x = 0$ as;

$$w_{ave} = 2\Delta_0 \tag{3.77}$$

With this in mind, it should be noted that other influences such as the cover and reinforcement spacing were not considered in Somayaji and Shah (1981)'s analysis. In fact, they suggested that these influences can be included in the equation for the length of transfer or the value of K_p. Furthermore, they observed that crack spacing and crack width were sensitive to the variation in the value of K_p.

3.2.4.2.3 Method by Edwards and Picard (1972)

This analytical model of cracking in concrete was previously discussed in Section 3.2.3.2. Based on bond stress-slip relationship, equation for bond stress distribution was presented in equation (3.24).

Likewise, Edwards and Picard (1972) developed an equation for crack width at the surface of the reinforcement. However, only final derivation of the equations will be given. A full derivation can be found elsewhere (Edwards and Picard, 1972). With the knowledge that crack width in general can be calculated as the difference between the displacement in reinforcement and concrete along the crack region and the bond stress distribution function presented in equation (3.24), it is possible to derive a crack width equation based on these relationships. Thus, crack width at the surface of the reinforcement can be expressed as;

$$w = \frac{2\sigma_{s2}}{K_1 E_s}\left[\frac{e^{K_1 2S_o} - 1}{e^{K_1 2S_o} + 1}\right] \tag{3.78}$$

In the above equation;

$$\sigma_{s2} = \frac{\psi + n\rho}{\rho}\left[\frac{e^{K_1 L} + 1}{e^{K_1 L} - 2e^{\frac{K_1 L}{2}} + 1}\right] \tag{3.79}$$

where σ_{s2} = tensile stress in reinforcement at the crack

ψ = a factor which averages the tensile stress in concrete σ_{ct} over the area A_c

K_1 = a constant previously defined in equation (3.25)

It is necessary to recognise that the equations present thus far are only valid for cases where bond stress is below its peak value. This criterion was already discussed in Section 3.2.3.1.

Similarly, Edwards and Picard (1972) also developed equations to determine crack width and tensile stress in reinforcement at the crack for cases where bond stress is assumed to have reached its maximum value. A complete derivation of the equations is given in their report.

From this investigation, Edwards and Picard (1972) concluded that crack width depended mainly on the maximum bond strength of the reinforcement while crack spacing is influenced by the constant ψ, reinforcement ratio ρ, tensile strength of concrete $f_t^{'}$, and the maximum bond strength.

3.3 Cracking theory due to shrinkage and temperature effects in fully restrained members

At present, there are only a few reports on the subjects of cracking relating to bond stress and the effects of shrinkage and temperature. However there are obvious similarities between this type of cracking and cracking which occurs as a result of applied tension forces, as described earlier. Both types of cracking are essentially bond-related phenomena. The effect of bond stress, as studied in the previous section, can therefore exert similar influences on this type of cracking.

Nevertheless, there are several clear distinctions between the two types of cracking. First, concrete strength in members subjected to applied axial tension force at the time of loading are generally higher or have already attained their full strength, whereas shrinkage and temperature changes usually take place when the concrete is still immature. Furthermore, the steel reinforcement of the member undergoing

shrinkage can be initially in compression, whereas the steel reinforcement in the former case always is in tension.

The case considered next is a fully restrained reinforced concrete member subjected to gradually increasing uniform shrinkage strain after it was poured. See Figure 3.15. The following discussion has similarities with applied axial tension force, discussed previously in Section 3.2

It is assumed that the structure is only subjected to uniform shrinkage strain, as shown in Figure 3.15a. As the concrete shrinks, restraining forces F develop at each restrained end. Initially, the concrete carries all the restraining force. The steel strain is zero, and $\sigma_s = 0$

$$F = A_c \sigma_c \tag{3.80}$$

When the restraining forces are large enough, and the tensile concrete strength of concrete f_t' is reached (ie. $\sigma_c = f_t'$), the first crack forms. The shrinkage strain, ε_{sh} at which the first crack occurs is therefore equalled to $\frac{f_t'}{E_c}$. As a result, the slab after cracking consists of 2 regions, the uncracked (region 1) and the cracked (region 2) which includes the sections adjacent to the actual fracture in which the concrete stress varies. As in the case of cracking due to an applied tensile force, the concrete stress is zero at the crack and the reinforcement alone carries the tensile force as shown in Figure 3.15c and 3.15d

$$F = A_s \sigma_{s2} \tag{3.81}$$

where σ_{s2} = tensile stress in the reinforcement at the crack (subscript 2 corresponds to region 2 where area inside region 2 is influenced by the effect of the crack)

The conditions within region 2 can also be explained by adopting similar assumptions as to those in Section 3.2. Within region 2, stresses in the concrete and reinforcement vary depending on the distribution of bond stress. As the tensile

stresses are transferred from the reinforcement to the concrete by bond, stress in the concrete increases, until at some distance S_o, from the crack, the concrete stress again resumes a constant value.

Since the concrete surface stress within the distance S_o on both side of the crack is below the concrete strength, no other cracks can form between these distances. At some distance S_o away from either side of the crack, the stress distribution remains unaffected by the crack (Figure 3.15d). Since the total length must remain unchanged, the reinforcement in this region must be in compression to satisfy the equilibrium condition between cracked and uncracked sections. This equilibrium relationship can be expressed as;

$$A_s\sigma_2 = A_{c1}\sigma_{c1} - A_s\sigma_{s1} \tag{3.82}$$

where σ_{c1} = tensile stress in the concrete of region 1

σ_{s1} = compressive stress in the reinforcement of region1

A_{c1} = cross-sectional area of concrete in region 1

A_s = cross-section area of steel reinforcement

In addition the equilibrium relationship in region 1 can be given as;.

ie
$$F = F_{c1} + F_{s1} \tag{3.83}$$

$$= A_{c1}\sigma_{c1} + A_s\sigma_{s1} \tag{3.84}$$

$$F = A_{c1}\varepsilon_{c1}E_c + A_s\varepsilon_{s1}E_s \tag{3.85}$$

The compatibility condition in region 1 also requires that

$$\varepsilon = \varepsilon_c = \varepsilon_s \tag{3.86}$$

where $\varepsilon_c = \varepsilon_{elastic} + \varepsilon_{sh} + \varepsilon_{creep}$

But the creep strain is ignored for now

Then

$$F = \varepsilon\,(A_{c1}E_c + A_{s1}E_s) \tag{3.87}$$

stresses are transferred from the reinforcement to the concrete by bond, stress in the concrete increases, until at some distance S_o, from the crack, the concrete stress again resumes a constant value.

Since the concrete surface stress within the distance S_o on both side of the crack is below the concrete strength, no other cracks can form between these distances. At some distance S_o away from either side of the crack, the stress distribution remains unaffected by the crack (Figure 3.15d). Since the total length must remain unchanged, the reinforcement in this region must be in compression to satisfy the equilibrium condition between cracked and uncracked sections. This equilibrium relationship can be expressed as;

$$A_s\sigma_2 = A_{c1}\sigma_{c1} - A_s\sigma_{s1} \tag{3.82}$$

where σ_{c1} = tensile stress in the concrete of region 1

σ_{s1} = compressive stress in the reinforcement of region1

A_{c1} = cross-sectional area of concrete in region 1

A_s = cross-section area of steel reinforcement

In addition the equilibrium relationship in region 1 can be given as;.

ie
$$F = F_{c1} + F_{s1} \tag{3.83}$$

$$= A_{c1}\sigma_{c1} + A_s\sigma_{s1} \tag{3.84}$$

$$F = A_{c1}\varepsilon_{c1}E_c + A_s\varepsilon_{s1}E_s \tag{3.85}$$

The compatibility condition in region 1 also requires that

$$\varepsilon = \varepsilon_c = \varepsilon_s \tag{3.86}$$

where $\varepsilon_c = \varepsilon_{elastic} + \varepsilon_{sh} + \varepsilon_{creep}$

But the creep strain is ignored for now

Then

$$F = \varepsilon\,(A_{c1}E_c + A_{s1}E_s) \tag{3.87}$$

Modifying further gives

$$F = A_{c1}\varepsilon E_c(1+n\rho) \tag{3.88}$$

$$= A_{c1}\sigma_{c1}(1+n\rho) \tag{3.89}$$

As with the case in Section 3.2, the tensile concrete strength is assumed constant for the duration of the cracking process. In effect, the force F as determined from equation (3.89) would be identical for each crack (after 1st crack) that occurs. After the first crack, the development of additional cracks is not be discussed in detail as the processes are similar to the cracking due to applied tensile force described earlier in Section 3.2. After all the cracks have developed, it is considered that the development of cracking has reached a stabilised state. In this state, cracks generally consist of those having distribution of spacing within the range of S_o and 2 S_o where So is considered as the minimum crack spacing.

3.3.4 Application of bond stress theory to predict crack spacing and Crack widths

Most of the literature studied for cracking due to shrinkage and temperature effects in restrained members assumed only the average bond stress distribution within the cracked region (region 2) discussed in Section 3.2.4. Unfortunately, no references were found which associate cracking due to time dependent deformation with variation of bond stress. As a result, the following methods being considered for review assumed average bond stress distribution within the cracked region to propose for crack spacing and crack width.

- Hughes(1972, 1973)
- Brickell and Hoadley (1976)
- Base and Murray (1978, 1982)
- Gilbert (1992)

In addition, several other references concerning cracking behaviours are also briefly discussed.

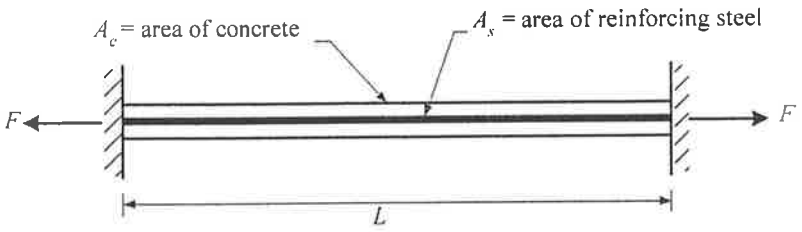

(a) Fully restrained reinforced concrete slab subjected to shrinkage

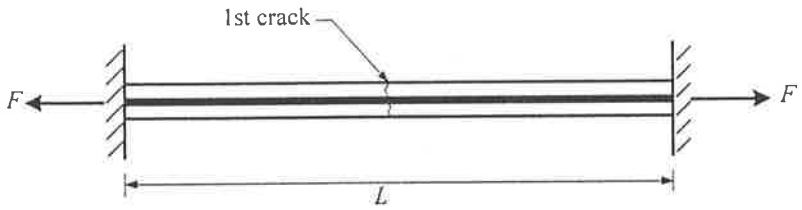

(b) Restraining forces, F at each end cause a first crack to develop , the retraining forces immediately reduce to F_{cr}

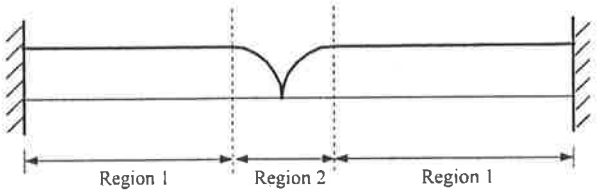

(c) Concrete stresses along the length of the slab

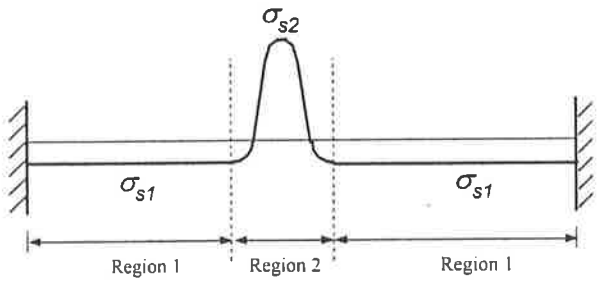

(d) Tensile stress in the reinforcement

Figure 3.15 Conditions after first cracking in fully restrained reinforced concrete slab

3.3.4.1 *Method by Hughes (1972) and (1973)*

This method was initially proposed to study early thermal cracking behaviour in fully imposed reinforced concrete member. At the crack, tensile stress is transferred from the reinforcement to the concrete by bond. The full transfer of tensile stress is established when the bond force between the reinforcement and concrete is equal to the tensile strength of concrete, thus;

$$\tau_{ave} S_o \sum \pi d = f_t' A_c \tag{3.90}$$

where τ_{ave} = the average bond strength between concrete and reinforcement

$\sum \pi d$ = sum of reinforcement perimeter

By noting that;

$$A_c = \frac{\pi d^2}{4\rho} \tag{3.91}$$

and rearranging the equation (3.91), an expression for S_o can be given as;

$$S_o = \frac{f_t' d}{4\tau_{ave}\rho} \tag{3.92}$$

The value of S_o in equation (3.92) can be considered as the minimum crack spacing in a cracked member. The ratio $\frac{f_t'}{\tau_{ave}}$ is a constant, which is determined from tests. Normally, it can be taken as 1.0 for plain round bar and 0.4 to 0.67 for deformed bars, (Hughes,1972 and Base,1981). Leonhardt (1977) suggested a value of 0.4 for standard deformed bars and 0.74 for smooth hot rolled bars.

After a stabilised crack pattern is established, the minimum crack spacing S_o, is given by the equality sign and the maximum crack spacing, is twice this value. Thus, the final crack pattern consists of cracks containing some distribution of spacing within the range;

$$S_o \le S \le 2S_o \tag{3.93}$$

ie. $$\frac{f_t' d}{4\tau_{ave}\rho} \le S \le \frac{f_t' d}{2\tau_{ave}\rho} \tag{3.94}$$

The average crack spacing is often assumed as $1.5S_o$, but Beeby (1978) suggested that there are sufficient theoretical reasons to use instead a value of $1.33S_o$.

In order to establish an equation for crack width, Hughes considered its maximum value is assumed to cause most problems. As a result, the maximum crack spacing is used as a primary factor. Since concrete strain adjacent to the crack relative to the free shrinkage strain is zero, the average concrete strain between cracks is therefore $\frac{\varepsilon_t'}{2}$. Thus, after the establishment of a stabilised crack pattern in the fully restrained member, subjected to tensile strain, a general equation for maximum crack width in its simplest form can be given:

$$w_{\max} = 2S_o(\varepsilon_{st} - \frac{\varepsilon_t'}{2}) \tag{3.95}$$

where $w_{\max}$ = maximum crack width

$2S_o$ = maximum spacing as defined in equation (3.95)

ε_{st} = total resultant shrinkage strain and thermal strain

ε_t' = ultimate tensile strain in concrete

Note also that the average crack width, w_m is assumed to be $0.75w_{max}$ for the stabilised crack pattern, since the average crack spacing is 0.75 times maximum crack spacing.

Likewise, an equation similar to (3.95) was also proposed by Evans and Hughes (1968) in which a crack width is given by the difference between the total restrained movement and the restrained movement in the concrete over the distance $\frac{S}{2}$ from both side of the crack,

$$w = S(\varepsilon_{sl} - \frac{S\dot{\varepsilon_l}}{4S_o}) \tag{3.96}$$

The distance S in equation (3.96) was recommended by Evans and Hughes (1968) as the crack spacing other than the minimum spacing S_o. The equation was also proposed to determine the crack width in a stabilised crack pattern. They further advised that it is the average width for cracks in a stabilised stage, rather than the average width for all cracks which should be given primary consideration.

3.3.4.2 Method by Brickell and Hoadley (1976)

Brickell and Hoadley (1976) proposed an expression for crack width which was given as the total relative movement between concrete and reinforcement. This can be determined by integrating the changes in strains over the transfer length, S_o , on both side of the crack;

ie. $$w = \int(\Delta\varepsilon_{s2} + \Delta\varepsilon_{c2})dx \tag{3.97}$$

By using the average bond stress over the cracked region of length l, a general equation for interface crack width is obtained as;

$$w = 2\int_0^{S_o} \Delta\varepsilon_{s2}dl + 2\int_0^{S_o} \Delta\varepsilon_{c2}dl \tag{3.98}$$

The change in strain of reinforcement $\Delta\varepsilon_{s2}$ and concrete $\Delta\varepsilon_{c2}$ at a distance l from the face of the crack can also be determined from;

$$\Delta\varepsilon_{s2} = \frac{4}{E_s d}\int_0^{S_o} \tau(x)dx \tag{3.99}$$

and

$$\Delta\varepsilon_{c2} = \frac{\pi d}{E_c A_c}\int_0^{S_o} \tau(x)dx \tag{3.100}$$

where $\tau(x)$ = average bond stress measured at a point distance x from the face of the crack

By expressing equation (3.98) in terms of the change in strains of reinforcement and concrete obtained in equation (3.99) and (3.100), another expression for the interface crack width is as shown;

$$w = \frac{8(1+n\rho)}{E_s d}\int_0^{S_o}\int_l^{S_o}\tau(x)dxdl \qquad (3.101)$$

The above equation gives the absolute maximum width of a fully developed crack and the derivation was based on the assumption that a new crack is formed only when the width of previously formed cracks reaches the fully developed value. Brickell and Hoadley (1976) further commented that this could result in over-estimation of the amount of bond slip by approximating the bond stress distribution as constant. In order to overcome this problem, an upper bound of bond slip crack width is imposed as;

$$w \le \frac{1+n\rho}{n\rho}\varepsilon_t' S_o \qquad (3.102)$$

The above equation is also based on the assumptions that reinforcement strain being less than yield and the tensile concrete strength is achieved when bond stress between reinforcement and concrete is equal to the tensile strength of concrete.

3.3.1.3 Method by Base and Murray (1978a, 1982)

In some of the crack width equations proposed thus far, crack width is directly proportional to the resultant tensile strain and inversely proportional to the reinforcement ratio. The traditional approach to crack control, as explained by Base and Murray (1982), was to reduce maximum tensile strain and thus the maximum number of cracks as a means to control crack width. However, following extensive experiments and research of thermal and shrinkage on walls, they introduced new findings which contradicted earlier proposals to determine crack width in reinforced concrete subjected to shrinkage and thermal effects.

According to their experimental observations, crack widths rapidly approach a limiting value as shrinkage increases. They also suggested that crack widths generally could not be kept very small by using a sufficiently large reinforcement ratio. As a result, Base and Murray (1978a) concluded that crack width is independent of shrinkage strain (as suggested by Hughes (1971, 1972) and also stated " the simplistic model of shrinkage cracking suggested by most researchers to date is fundamentally in error".

In addition, a new set of equations which claimed to accurately predict the relationships between crack width, reinforcement ratio and shrinkage in fully restrained concrete was proposed. Full details of this analysis and experimental results can be found in a thesis presented by Murray in 1977 and other publications including, Base and Murray (1978a, 1982) and Murray (1991).

The following set of equations was proposed by Base and Murray (1978a) to calculate the number of cracks, the stress in the reinforcement across the cracks and the average crack width of the crack, in a fully restraint reinforced concrete slab subjected to increasing shrinkage strain similar to the case shown in Figure 3.16

$$m = 1 + \frac{Lnr}{2a}\left(\frac{\varepsilon_{sh}}{\varepsilon_t'} - 1\right) \tag{3.103}$$

$$\sigma_s = \varepsilon_{sh}.E_s\left(\frac{L - 2ma}{n\rho L + 2ma}\right) \tag{3.104}$$

$$w_m = 2a\left(\frac{\sigma_{s2}}{E_s} + \varepsilon_{sh}\right) \tag{3.105}$$

where m = number cracks at any time

L = length of the member

ε_{sh} = total potential contraction shrinkage strain at any time

ε_t' = tensile cracking strain for concrete

σ_{s2} = reinforcement stress across a crack

w_m = the average crack width

a = "no bond length" for the reinforcement near a crack and for deformed bar reinforcement, it can be expressed as;

$$a = \frac{0.08d}{\rho} \tag{3.106}$$

Equation (3.103), (3.104) and (3.105) are also subjected to the condition that a crack can not reach its fully developed value unless the member has reached the stabilised

cracking pattern. A typical solution to the equations above can be represented in graphical form as shown Figure 3.16a.

It can be seen that as shrinkage increases, the crack width that starts at a threshold value approaches a limiting value while the number of cracks increases linearly. On the other hand, the steel stress increases maginally from its threshold value after the first crack and then decreases as more cracks develop.

When these equations were introduced in 1978, the effect of creep was ignored which could result in an overestimate of the number of cracks. Therefore, Base and Murray (1982) modified equations (3.103), (3.104) and (3.106) to incorporate the creep effect. This was easily achieved by reducing the shrinkage strain ε_{sh} to approximately a third of its original value, $\frac{\varepsilon_{sh}}{3}$ and can be shown as;

$$m = 1 + \frac{Lnr}{2a}\left(\frac{\varepsilon_{sh} - \varepsilon_t'}{3\varepsilon_t'}\right) \tag{3.107}$$

$$\sigma_s = \left(\frac{\varepsilon_{sh} - \varepsilon_t'}{3} + \varepsilon_t'\right).E_s\left(\frac{L - 2ma}{nrL + 2ma}\right) \tag{3.108}$$

$$w_m = 2a\left(\frac{\sigma_{s2}}{E_s} + \frac{\varepsilon_{sh}}{3}\right) \tag{3.109}$$

Similarly, equation (3.107), (3.108) and (3.109) can be presented in graphical forms as shown in Figure 3.16b and c. In addition, Base and Murray (1982) also provided a simpler equation to calculate the crack width as;

$$w_m = \frac{2a\varepsilon_t'}{3n\rho}(n\rho + 3) \tag{3.110}$$

In all cases, the modified equations generally agreed well with the observation made during the experiments

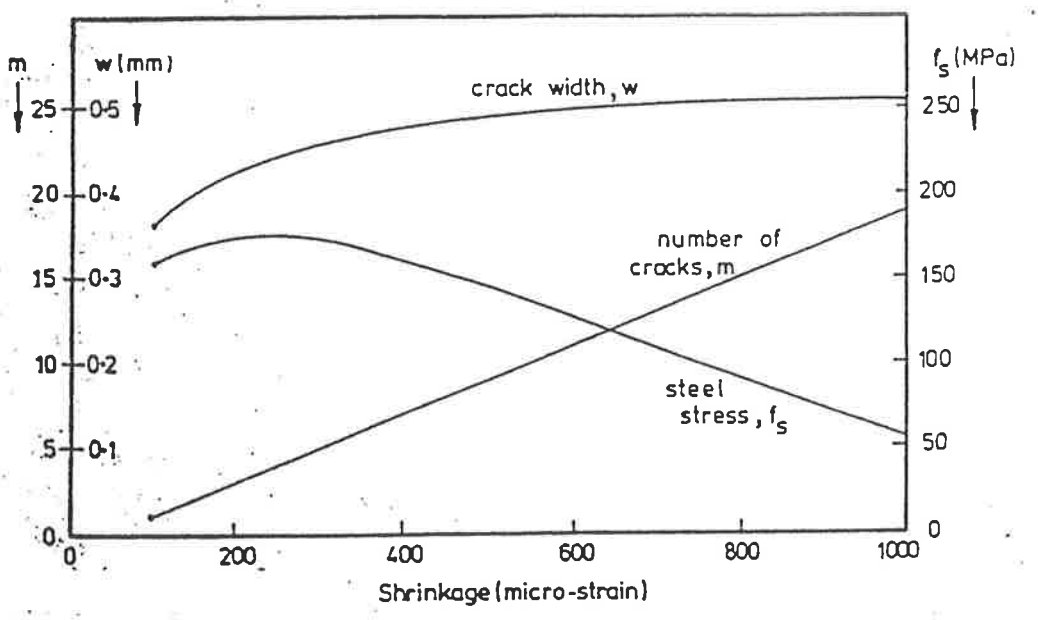

Figure 3.16a Typical solutions of equations proposed by Base & Murray (1978a) for increasing shrinkage ($L = 10000$, $n = 16$, $\rho = 0.005$, $a = 200$, $\varepsilon_t' = 100\ \varepsilon\mu$)

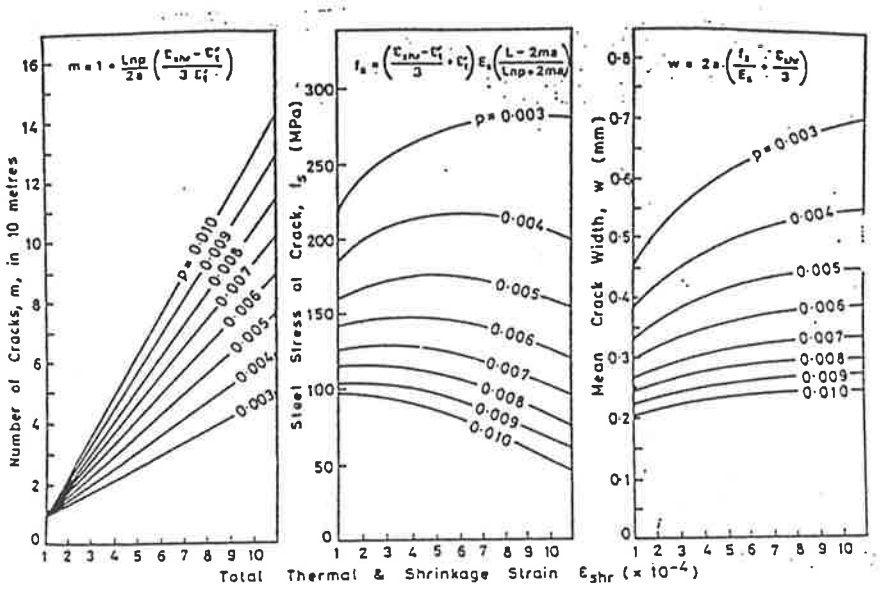

Figure 3.16b Limit of mean crack widths for various reinforcement (Base & Murray, 1982)

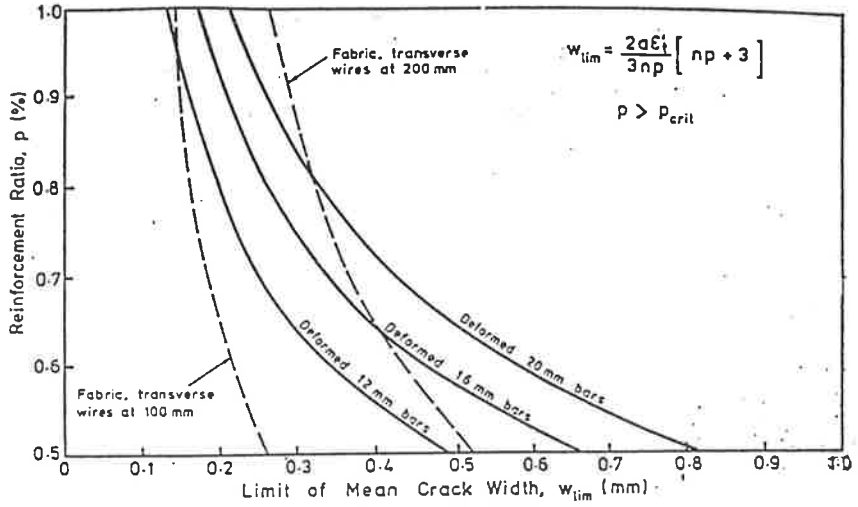

Figure 3.16c Revised design aid for the development of shrinkage cracking in fully restrained reinforced concrete (L = 10m, ε_t' = 0.0001, n = 16, a = 200) by Base & Murray (1982)

3.3.1.4 Method by Gilbert (1992)

Gilbert (1992) discussed the mechanism of cracking in a fully restrained reinforced concrete member subjected to shrinkage. He then presented an analytical method to control cracks due to shrinkage and the investigation were compared with the provisions for shrinkage and temperature reinforcement in the ACI Building Code (ACI 318-89) and the 1988 edition of AS 3600.

From the analysis, the stresses in the reinforcement and the concrete in the cracked region can be determined. It is also possible to calculate the restraining forces immediately before and after cracking. As a result, the conditions immediately after the formation of a crack can be used to determine the average crack width. Due to the length of the analysis, only basic equations are presented here. Complete information on the method should be obtained from the original paper.

The mechanism of cracking, from the first crack to the final crack (when a stabilised cracking pattern is established), is treated. At the final cracking pattern, a reinforced concrete member containing m cracks, with the distribution of stress in

the reinforcement and concrete as shown in Figure 3.17a, b and c. In the cracked region, it is assumed that stress and strain follow a parabolic function.

The average crack width is obtained by integrating the concrete strain over the length of the member. This is expressed as;

$$w_m = \left[\frac{\sigma_{c1}}{E_c} (S_m - \frac{2}{3} S_o) + \varepsilon_{sh}^* S_m \right] \tag{3.111}$$

where σ_{c1} = concrete stress in the uncracked region

ε_{sh}^* = ultimate free shrinkage strain

S_m = average crack spacing

S_o = approximated crack spacing

It should be noted that steps leading to the determination of σ_{c1}, S_m, S_o in the equation (3.110) are not included this review. Stress in the reinforcement at this stage can also be determined to ensure that the yield strength has not exceeded.

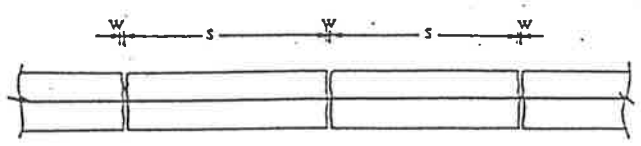

(a) Portion of a restrained member after all cracking

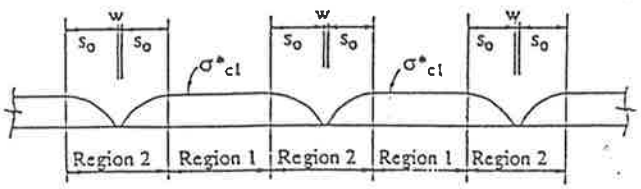

(b) Average concrete stress after all shrinkage

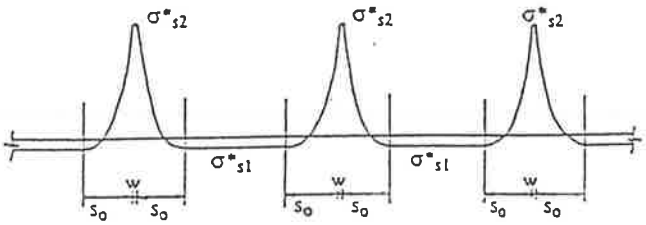

(c) Stress in reinforcement after all shrinkage cracking

Figure 3.17 Final state of cracking after shrinkage has finished (Gilbert, 1992)

Using this analysis, Gilbert (1992) claimed that the predicted number and width of shrinkage cracks generally agreed well with the observed cracking in practice and provided good guidelines for the crack control provisions in 1988 edition of AS 3600. It should be noted also that the second edition of AS 3600 (SAA, 1994), made no alteration to the section in predicting of creep and shrinkage.

3.3.4.5 Other approaches

In addition to those researchers previously discussed, there are also other cracking theories that were proposed to analyse the stress mechanism in the cracked region.

Harrison (1981) presented another method to calculate the crack width. However, his theory was very much based on Hughes's work and concentrated on early thermal cracking in concrete. The crack spacing is suggested to range from the minimum distance S_o to the maximum distance $2S_o$. As was the case with Hughes (1971, 1973), these values have already been defined in Section 3.3.4.1.

An equation to calculate maximum crack width was expressed as the difference between the restrained total movement and the restrained movement caused by the interaction between the reinforcement and concrete. The restrained total movement can consider to be influenced by the combination of shrinkage and thermal strain. This can be illustrated in the form of;

ie. $$w_{max} = 2S_o[R\varepsilon_{st} - \frac{\varepsilon_t'}{2}] \qquad (3.112)$$

where R = the restraint factor, a factor of 1 is used for fully restraint member

$2S_o$ = maximum crack spacing

ε_{st} = total resultant shrinkage and thermal strain

ε_t' = tensile strain capacity

Harrison (1981) also pointed out that in countries where early-age thermal movement dominates the cracking, early age concrete properties are mostly appropriate in equation (3.112). On the other hand, in a country like Australia,

shrinkage often is the dominant movement and the long-term values of the concrete properties should be used instead.

Another approach was also presented by Campbell-Allen and Hughes (1981), but as was the case with Hughes (1972, 1973 and 1974), crack spacing and crack width equations are similar and thus will not be shown here.

3.2 Summary

In summary, it can be seen that the restraint provided by the supporting members has a large influence on cracking of reinforced concrete members. Members that are fully restrained between supports, generally exhibit higher degree of cracking since the restraining forces being generated are much larger. However, as more cracks form along the member, the magnitude of these restraining forces reduces quite significantly due to a progressive reduction in member stiffness after each crack form.

Also immediately after each crack, there is a reduction of restraining forces as a result in loss of member axial stiffness. Therefore, additional increase in restraining forces require to develop further cracks is needed. As long as the reinforcement does not yield, cracking can progress up to a state where no additional cracks can form. This state is often referred as a stabilised state or stabilised cracking pattern. In this state, a further increase in tensile stress in the member simply causes widening of the existing cracks or yielding of the reinforcement. However, it was also observed that in member with fully restraint supports, a stabilised cracking state might not be achievable.

The phenomenon of cracking mechanism in reinforced concrete relating to direct tension cracking was explained in twofold. First, a literature review of cracking mechanism in reinforced concrete member subjected to applied axial tensile forces is conducted. This is followed by a literature review of cracking mechanism in fully restraint reinforced concrete member subjected to shrinkage and temperature effect. In general, it can be concluded that there is a strong connection between the two cracking mechanisms from the two cases and this can be directly related to the bond stress between reinforcement and concrete. At the crack, there is a bond break down between the two materials. Some researchers also considered the effect of internal cracking which occurs close to the primary cracks in the predicting models. Adjacent

from both side of the crack, the bond stress varies. The analyses of non-uniformity in bond stresses within the crack vicinity can be quite complex, depending the approach taken. This chapter investigated three approaches, namely

- Bond stress-slip relationship;
- Bond stress distribution; and
- Average bond stress.

The first two approaches using bond stress-slip relationship and bond stress distribution require the most efforts in terms of complexity and the time consumed. Both methods were found to be complicated as well as unreliable. In practical terms, both of these methods may not warrant extra effort and the time to achieve results which are in most cases, estimates. In addition the literatures found were mainly related to cracking in reinforced concrete member subjected to applied axial tensile forces.

In contrast, it was found that the best and probably the simplest approach is by assuming the average bond stress in the vicinity of each crack as proposed by a number of researchers, Hughes (1972) and (1973), Brickell & Hoadley (1976), Leonhardt (1977), Beeby (1979) Base & Murray (1978a, 1978b) and (1982), CEB Manual (1985), Gilbert (1992) and Christiansen & Nelson (1997). Based on average bond stress, several equations for crack spacings and crack widths in reinforced concrete members subjected to applied axial tensile forces and shrinkage and temperature effects were developed.

Reinforced concrete members with applied axial tensile forces are generally loaded when concrete is already mature. Most of the researchers also considered the effect of additional bond break down by introducing the length of "lost bond" at cracking, based on Goto (1971). On the other hand, reinforced concrete members subjected to shrinkage and temperature effects generally occur when concrete is still immature and the length of "lost bond" was not taken into consideration from most researchers.

Table 3.3 summarises a number of crack width equations which are proposed by various researchers using either one of the three analysis of bond stress mentioned previously.

Based on these findings, it is reasonable to conclude that crack width in member subjected to shrinkage strain should be calculated by considering only the area within cracked region. This can be shown to correspond to the extension of the reinforcement over this region minus the contraction of concrete over the same length.

ie $$w = 2S_o(\varepsilon_{s2} - \varepsilon_{c2}) \tag{3.113}$$

In order to calculate the distance S_o, it is also reasonable to used most of methods discussed even though each equation for S_o was derived based on two different types of cracking.

In addition, Table 3.4 is used to identify various influencing factors incorporated into each crack width equations reviewed in this chapter. According to the table, cracking of this nature depends on the bond properties of the reinforcement, concrete properties at the time of cracking, an increase in tensile strain of the reinforcement, arrangement and amount of reinforcement, concrete cover, and magnitude of the induced forces such as shrinkage and temperature changes. On the other hand, ACI 224 assumed that the concrete cover to the centre of reinforcement alone affects the magnitude of the crack spacing.

It can be summarised that there are a large number of methods which can be used to predict cracking in reinforced concrete members subjected only to axial tension. Each equation can differ from each other depending on the assumptions made and the importance of various parameters being considered. It seems that there is a lack of agreement amongst most researchers as to which crack width equations correctly represent the actual values on sites or in experiments. Nonetheless, all equations claimed to produce the crack widths which in general ensure the actual values do not exceed these values.

Later in Chapter 4, numerical calculations are presented to compare the results of crack widths obtained using the methods shown in Table 3.4.

Table 3.3 A summary of crack spacing and crack width equations

Authors	Crack spacing equations	Crack width equations	Causes of crack
Hughes (1972, 1973)	$S_o \le S \le 2S_o$ Eq (3.93) ie. $\frac{f_t' d}{4\tau_{ave}\rho} \le S \le \frac{f_t' d}{2\tau_{ave}\rho}$ Eq (3.94)	$w_{max} = 2S_o(\varepsilon_{st} - \frac{\varepsilon_t'}{2})$ Eq (3.95) $w_m = 1.5 w_{max}$	Shrinkage and temperature effects
Edwards and Picard (1972)		$w = \frac{2\sigma_{s2}}{K_1 E_s}\left[\frac{e^{K_1 2S_o} - 1}{e^{K_1 2S_o} + 1}\right]$ Eq (3.78) Where $\sigma_{s2} = \frac{\psi + n\rho}{\rho}\left[\frac{e^{K_1 L} + 1}{e^{K_1 L} - 2e^{\frac{K_1 L}{2}} + 1}\right]$ Eq (3.79)	Applied axial tensile force

Continue

Continue **Table 3.3** Summary of crack spacing and crack width equations

Authors	Crack spacing equations	Crack width equations	Causes of crack
Brickell & Hoadley (1976)	S_o = referred as the development length of concrete	$w \le w_{max} = \frac{1+n\rho}{n\rho}\varepsilon_t' S_o$ Eq. (3.99)	Shrinkage and temperature effects
Leonhardt (1977)	$l_o = \frac{\sigma_{s2}}{45} d$ Eq (3.15) $S_o = k_1(c,a) + k_2 k_3 \frac{d}{\rho_{eff}}$ Eq (3.39)	$w_{95} = k_4 l_o \frac{\sigma_{s2}}{E_s} + k_4 S_o \frac{1}{E_s}(\sigma_{s2} - k_5 \frac{\sigma_{s2,cr}^2}{E_s})$ Eq(3.43)	Applied axial tensile forces
Beeby (1978)	$S_m = K_1 c + K_2 \frac{d}{\rho}$ Eq (3.44)	$w_m = (K_1 c + K_2 \frac{d}{\rho_{eff}})\varepsilon_m$ Eq (3.45) Where $\varepsilon_m = \varepsilon_{s2} - \frac{K f_t' \sigma_{s2,cr}}{E_s \rho \sigma_{s2}}$ Eq (3.46)	Applied axial tensile force

Continue

Continue **Table 3.3** Summary of crack spacing and crack width equations

Authors	Crack spacing equations	Crack width equations	Causes of crack
Base and Murray (1978)	$m = 1 + \frac{Ln\rho}{2a}\left(\frac{\varepsilon_{sh}}{\varepsilon_t'} - 1\right)$ Eq (3.103) $a = \frac{0.08d}{\rho}$ Eq (3.106)	$\sigma_{s2} = \varepsilon_{sh} E_s \left(\frac{L - 2ma}{n\rho L + 2ma}\right)$ Eq (3.104) $w_m = 2a\left(\frac{\sigma_{s2}}{E_s} + \varepsilon_{sh}\right)$ Eq (3.105)	Shrinkage and temperature effects
Base and Murray (1982)	$m = 1 + \frac{Ln\rho}{2a}\left(\frac{\varepsilon_{sh} - \varepsilon_t'}{3\varepsilon_t'}\right)$ Eq (3.107) $a = \frac{0.08d}{\rho}$ Eq (3.106)	$\sigma_{s2} = \left(\frac{\varepsilon_{sh} - \varepsilon_t'}{3} + \varepsilon_t'\right) E_s \left(\frac{L - 2ma}{n\rho L + 2ma}\right)$ Eq (3.108) $w_m = 2a\left(\frac{\sigma_{s2}}{E_s} + \frac{\varepsilon_{sh}}{3}\right)$ Eq (3.109)	Shrinkage and temperature effects

Continue

Continue **Table 3.3** Summary of crack spacing and crack width equations

Authors	Crack spacing equations	Crack width equations	Causes of crack
Harrison (1981)	S_o = minimum crack spacing used in Hughes (1971, 1972)	$w_{max} = 2S_o[R\varepsilon_{sl} - \frac{\varepsilon_t^*}{2}]$ Eq (3.112)	Shrinkage and temperature effects
Rizkalla and Hwang (1984)	$S_m = 5(d-7.2) + K_1(a,c) + 0.0$ Eq (3.66)	$w_m = \frac{3.145\varepsilon_m^{1.2}L}{N}$ Eq (3.70) ε_m is obtained using Beeby's equation	Applied axial tensile force
CEB Manual (1985)	$S_m = 2(c + \frac{a}{10}) + \kappa_1\kappa_2\frac{d}{\rho_r}$ Eq (3.48)	$w_m = S_m(\varepsilon_{sm} - \varepsilon_{sh})$ Eq (3.47) $\varepsilon_{sm} = \zeta\varepsilon_{s2}$ Eq (3.49)	Applied axial tensile force
ACI 224 (1986)	$S_{max} = 4t_e$ Where $t_e = c\sqrt{1+\left(\frac{a}{4c}\right)^2}$ Eq (3.52)	$w_{max} = S_{max}\varepsilon_{sm}$ Eq (3.53)	Applied axial tensile force

Continue

Continue **Table 3.3** Summary of crack spacing and crack width equations

Authors	Crack spacing equations	Crack width equations	Causes of crack
Gilbert (1992)		$w_m = \left[\frac{\sigma_{c1}'}{E_c}(S - \frac{2}{3}S_o) + \varepsilon_{sh}{}^{*}S\right]$ Eq (3.111)	Applied axial tensile force
Christensen & Nelson (1997)	For $\sigma_{s2} > \sigma_{s2f}$ $S_m = 1.33(\frac{1}{2}l_o + S_o)$ Eq (3.59) $l_o = (1+\frac{\sigma_{s2}}{100})d \le \begin{cases}1.3c\\0.65a\end{cases}$ Eq (3.53) $S_o = \frac{0.5A_c}{N_{bar}\pi d}$ Eq (3.52)	For $\sigma_{s2c} < \sigma_{s2} < \sigma_{s2f}$ $w_m = \frac{1}{E_s}[\sigma_{s2}(l_o + 2S_o) - \frac{4\mu f_t' S_o^2}{d}]$ Eq (3.56) For $\sigma_{s2} > \sigma_{s2f}$ $w_m = S_m \varepsilon_{sm}$ Eq (3.58) Where $\varepsilon_{sm} = \frac{1}{E_s}(\sigma_{s2} - \frac{\mu f_t'}{d}\frac{(S_m - l_o)^2}{S_m})$ Eq (3.60)	Applied axial tensile forces

$$k_{nslab} = \frac{\left(A_c E_c / L\right)}{\left(\frac{W_{cr}}{L}\right)\left(\frac{1}{n\rho}\right) + \left(1 - \frac{W_{cr}}{L}\right)\left(\frac{1}{1+n\rho}\right)} \tag{4.14}$$

As a result, the equation (4.14) can be used to represent a general expression for the axial stiffness of the slab prior to and after the first crack.

(c) Subsequent cracking

After the first crack, the restraining force at each subsequent cracking case can be calculated by assuming the mean tensile strength of concrete $f_t^{'}$ to minimise the complexity. Therefore, the restraining force at concrete cracking always has the same magnitude. In effect, an expression to solve for the restraining force just before each crack after the first crack can be given as;

$$F_{cr} = f_t^{'} A_c (1 + n\rho) \tag{4.15}$$

Similar to the condition after the first crack, the analyses for subsequent formations of cracking follows the same principle. The stiffness of the slab has to be modified each time a new crack occurs in the span. An additional assumption is also made such that the cracked region of length W_{cr} is assumed to be identical for each crack that occurs. In effect, equation (4.14) can be modified to represent the axial stiffness of the slab immediately after each crack such that;

$$k_{nslab} = \frac{\left(A_c E_c / L\right)}{\left(\frac{mW_{cr}}{L}\right)\left(\frac{1}{n\rho}\right) + \left(1 - \frac{mW_{cr}}{L}\right)\left(\frac{1}{1+n\rho}\right)} \tag{4.16}$$

where $m = 0, 1, 2, \ldots\ldots$ maximum number of cracks at the stabilised cracking state in the span

Similarly, equation (4.8) has to be modified since the crack region does not contribute to any free shrinkage when the springs are disconnected even though the concrete within the crack region would undergo shrinkage. This is expressed as;

$$F\left(\frac{1}{k_{sp}}+\frac{1}{k_{nslab}}\right)=\delta_{sh} \tag{4.17}$$

$$\text{where } \delta_{sh}=(L-mW_{cr})\varepsilon_{sh} \tag{4.18}$$

Hence it is now possible to calculate the restraining force just before and immediately after each crack has formed and the corresponding shrinkage strain by using the equations (4.8), (4.18) and (4.17). By plotting the values of the restraining forces and their corresponding shrinkage strains, a graph similar to that in Figure 3.2c of Chapter 3 can be obtained. This is re-illustrated as shown in Figure 4.6.

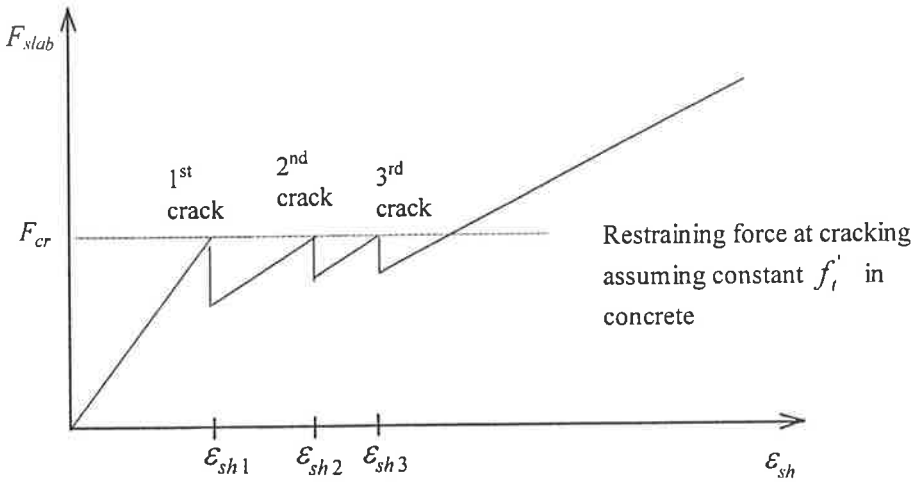

Figure 4.6 Restraining forces VS shrinkage strain after cracking in one way slab

4.2.1.2 Creep effect is included

In order to incorporate the effect of creep, a simple technique called "the effective modulus method" can be used. In this method, creep is simply treated as a delayed elastic strain and is taken in to account by reducing the elastic modulus of the concrete. As a result, the effective modulus for concrete can be defined as follows;

$$E_e=\frac{E_c}{1+\phi} \tag{4.19}$$

where ϕ = creep coefficient which is already discussed in Chapter 2

Thus, equation (4.19) can be modified to account for the effect of creep by replacing the modulus E_c with E_e as follows;

$$k_{nslab} = \frac{\left(A_c E_c / L\right)}{\left(\frac{mW_{cr}}{L}\right)\left(\frac{1}{n\rho}\right) + \left(1 - \frac{mW_{cr}}{L}\right)\left(\frac{1}{1+n\rho}\right)} \tag{4.20}$$

4.2.2 Analysis of slab wall-wall subassemblage

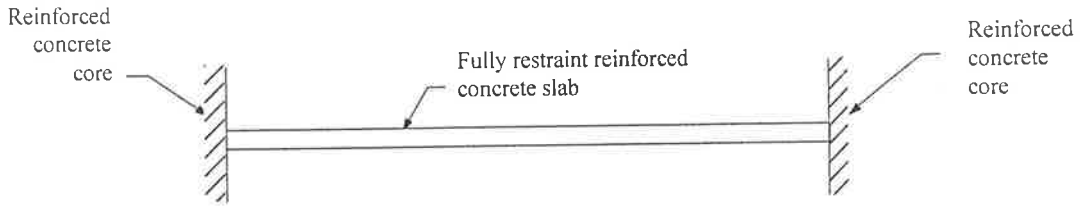

Figure 4.7 One-way reinforced concrete slab spanning between two concrete cores

The analysis now considers fully restrained supports at both ends of the span as shown in Figure 4.7. Equation (4.17) can be modified so that it accounts for the two rigid concrete cores on both ends of the span. This is easily achieved by making the spring stiffness k_{sp} term in the column infinitely large to reflect the large restraint provided by the concrete core. Hence, equation (4.17) can be rewritten as;

$$\frac{F}{k_{nslab}} = \delta_{sh} \tag{4.21}$$

$$\text{where} \quad \delta_{sh} = (L - mW_{cr})\varepsilon_{sh} \tag{4.22}$$

4.3 Two and multiple spans one-way RC slab

Consider a two span reinforced concrete slab as shown in Figure 4.8. The first slab (span 1) spans between an exterior column and an interior column while the second slab (span 2) spans between the interior column and a rigid concrete core. Uniform shrinkage is assumed to develop in both spans with time, and as a result, restraining forces develop. The amount of deformation in the slabs depends on the restraints provided by the columns and concrete core.

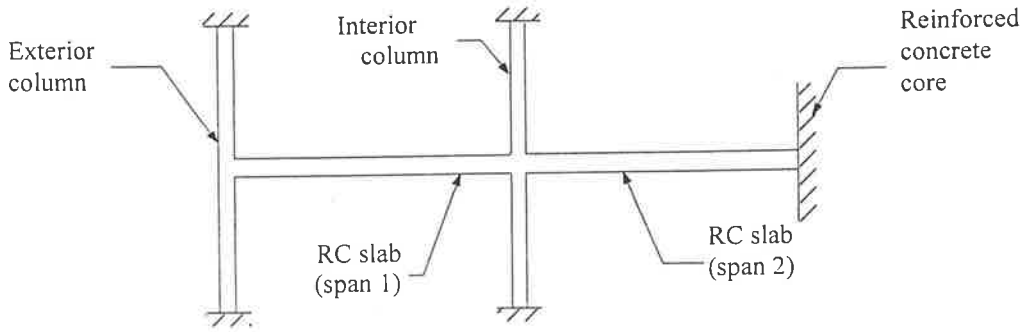

Figure 4.8 Two spans one-way reinforced concrete slab spanning between exterior column, interior column and a concrete core

For this analysis, the assumptions previously used in one-span reinforced concrete slab are applicable. The amount of restraint in the columns is represented by using a spring to represent the stiffness of each column. The deformation of each spring due to the restraining force depends on the spring stiffness and as a result, the structure can be simplified as shown in Figure 4.9.

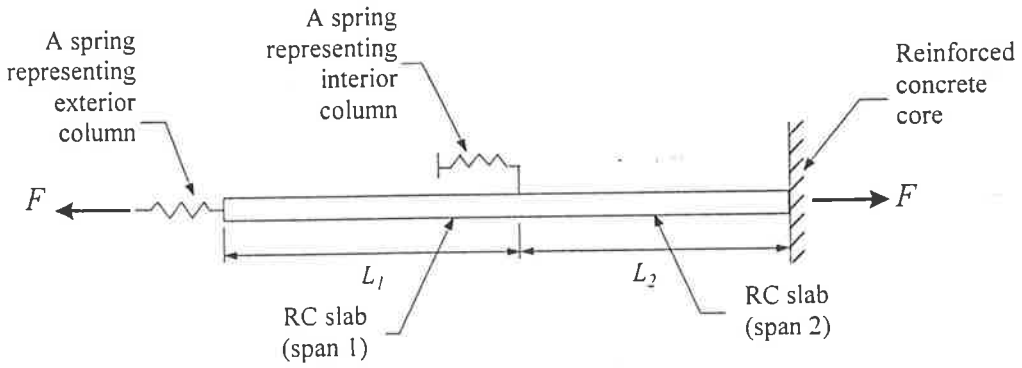

Figure 4.9 Springs are used to represent stiffness of columns

The analysis commences with an introduction of shrinkage strain into the structure similar to the single span reinforced concrete slab, resulting in restraining forces to develop at both column supports and rigid core. For the uncracked condition, both members are analysed using uncracked sections, but for post cracking condition, uncracked sections are only valid for regions which are not affected by cracking.

When the concrete begins to crack, the locations of the cracks depend mainly on the relative magnitude of the tensile forces in spans 1 and 2 and the stiffnesses of the members in the pre cracking and post cracking conditions. The first crack occurs in span 2. However, to determine subsequent cracking, it is necessary to predict the magnitude of the restraining forces in each span.

4.3.1 Creep effect is ignored

4.3.1.1 Uncracked case

The slabs are allowed to shrink freely by removing both springs as shown in Figure 4.10a. Once the slabs have fully shrunk, a force F is introduced into the springs and in the slabs to restore the compatibility. Thus, the slabs in both spans are only allowed to deform as shown in the Figure 4.10b. As can be seen from these figures, the notations used are explained as follows;

A = original position of section A

A' = position of section A, if span 1 and span 2 are free to shrink

A'' = position of section after span 1 and 2 are allowed to shrink, but are then reconnected to the springs at A and B

B = original position of section A

B' = position of section B, if span 1 and 2 are free to shrink

B'' = position of section after span 1 and 2 are allowed to shrink, but are then reconnected to the springs at A and B

C = position of section which does not move

According to Figure 4.10a, when the slabs are free to shrink in both spans, the following relationships can also be given as:

$$\delta_{sh_A} = (L_1 + L_2)\varepsilon_{sh} \tag{4.23}$$

$$\delta_{sh_B} = (L_2)\varepsilon_{sh} \tag{4.24}$$

where δ_{sh_A} = free shrinkage at A (compressive)

δ_{sh_B} = free shrinkage at B (compressive)

- adjusting maximum span lengths so that an optimum design is achieved; and
- introducing movement joints when all crack control provisions fail.

4.2 Single span one way RC slab

Consider a one-way reinforced concrete slab which spans between a reinforced concrete column and a rigid concrete core as shown in Figure 4.1. After casting of the members, shrinkage develops in the concrete and restraining forces develop as illustrated in Figure 4.2. The amount of restraint provided by the supports depends on their stiffnesses. The concrete core which is considered very rigid, provides full restraint against any movement of the slab. The amount of deformation in the slab therefore depends on the degree of restraint provided by the column, ie. by its flexural stiffness.

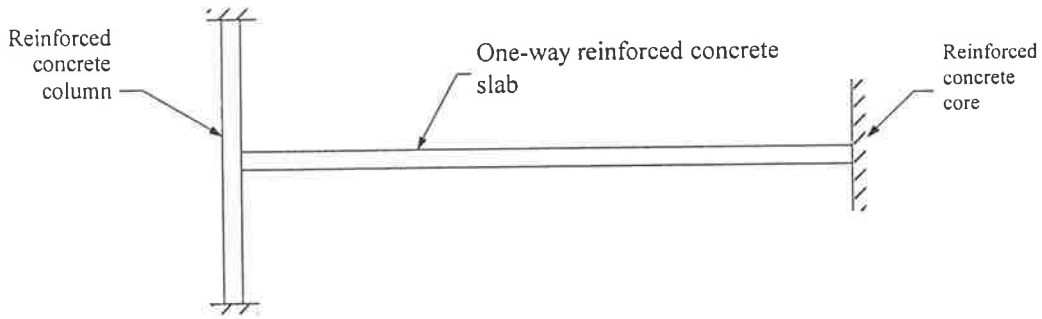

Figure 4.1 One-way reinforced concrete slab spanning between a column and concrete core prior to shrinkage

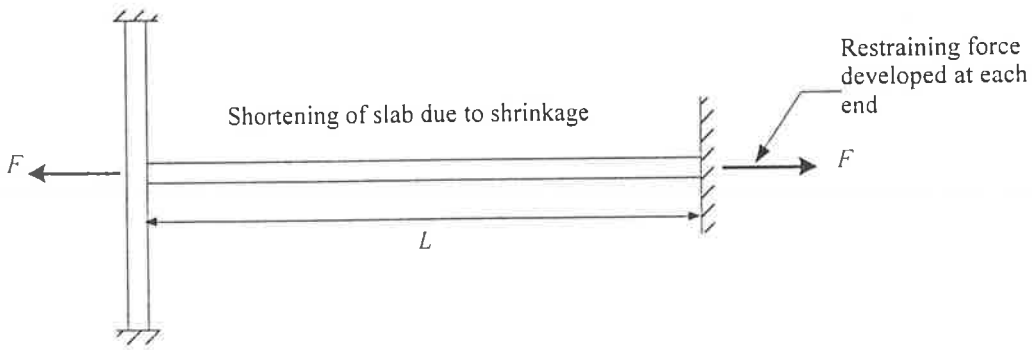

Figure 4.2 One-way reinforced concrete slab subjected to shrinkage effect with restraining force developing at both ends

In order to calculate the amount of restraint in the column, a spring is used to represent the stiffness in the column. As a result, the structure in Figure 4.1 can now be simplified as shown in Figure 4.3. The spring stiffness is essentially the flexural stiffness of the column which can be determined from basic structural mechanics.

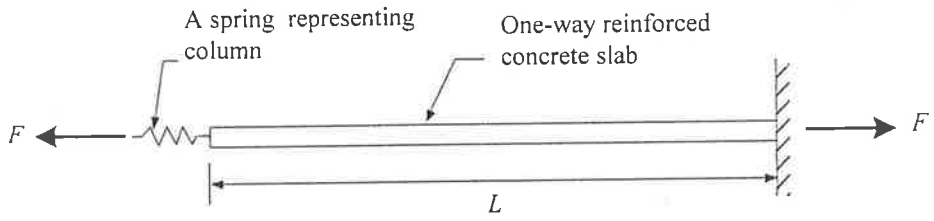

Figure 4.3 A spring is used to represent the stiffness of the column

The analysis of this model is undertaken in two steps. The first step only considers the effect of shrinkage to simplify the analysis and to demonstrate the basic mechanism behind this concept. In this case, shrinkage is the only driving force and is assumed uniform throughout the span. In fact, shrinkage and creep take place simultaneously. The second part of the analysis then considers the effect of creep to further improve the accuracy of the results.

4.2.1 Analysis of slab column-wall sub-assemblage

4.2.1.1 Creep ignored

(a) Uncracked case

To carry out the analysis, the spring in Figure 4.3 is disconnected and the slab is allowed to shrink freely. As soon as the slab attains its maximum deformation due to shrinkage, a tensile force F is introduced into the spring and in the slab to restore compatibility. See Figures 4.4a and 4.4b. The notations is as follows;

A = original position of section A

A' = position of section A, if the slab is free to shrink

A'' = position of section after the slab is allowed to shrink, but is then reconnected to the spring

B = position of section which does not move

When the slab is free to shrink, the following relationships apply:

$$\delta_{sh} = L\varepsilon_{sh} \tag{4.1}$$

where ε_{sh} = free shrinkage strain in the slab

δ_{sh} = total deformation in unrestrained slab

By reconnecting the spring to the slab, the free uniform shrinkage, is now reduced by the spring. The following compatibility equation applies:

$$\delta_{sp} + \delta_{slab} = \delta_{sh} \tag{4.2}$$

where δ_{sp} = deformation in the spring (tensile)

δ_{slab} = deformation in the slab (tensile)

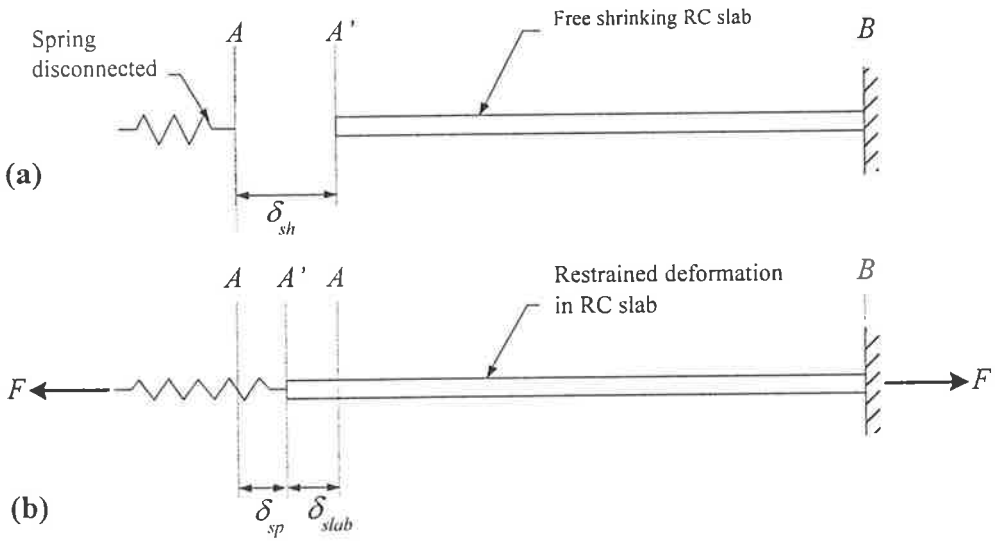

Figure 4.4 Position of the slab caused by disconnecting and reconnecting the spring

To solve for the restraining forces, the following constitutive equations are written at position A and slab;

$$F = F_{sp} = F_{slab} \tag{4.3}$$

$$F = F_{sp} = \delta_{sp} k_{sp} \tag{4.4}$$

$$F = F_{slab} = \delta_{slab} k_{slab} \tag{4.5}$$

where F = restraining forces developed at each support

F_{sp} = tensile force in the spring

F_{slab} = tensile force in the slab

k_{slab} = axial stiffness of the slab

k_{sp} = stiffness of the spring

By substituting the constitutive equations into equation (4.2), the following equations are obtained:

$$\frac{F_{sp}}{k_{sp}} + \frac{F_{slab}}{k_{slab}} = \delta_{sh} \tag{4.6}$$

$$\frac{F}{k_{sp}} + \frac{F}{k_{slab}} = \delta_{sh} \tag{4.7}$$

$$F\left(\frac{1}{k_{sp}} + \frac{1}{k_{slab}}\right) = \delta_{sh} \tag{4.8}$$

(b) Cracked case

Since the first crack develops when the shrinkage strain is equalled to the tensile strain of the concrete (ie. $\varepsilon_{sh1} = \varepsilon_t^{'} = \frac{f_t^{'}}{E_c}$), equation (4.8) can be used to determine the corresponding restraining force F_{cr}.

The analysis now considers the condition after the first crack has formed. This requires considerations of uncracked and cracked section of the slab separately. Initially, the analysis in Section 4.2.1.1(a) was carried out based on uncracked section throughout the span. The formation of first crack results in a reduction in slab stiffness and as a consequence, the magnitude of the restraining force, F_{span} immediately decreases. A more comprehensive discussion of this mechanism is contained in Chapter 3. In effect, the stiffness of the slab must be modified to account for the crack within the span.

To estimate a new axial stiffness of the slab after cracking, the following assumptions are used;

- the axial stiffness of the slab consists of an uncracked part and a cracked part as shown in Figure 4.5
- over the cracked part of length W_{cr}, concrete is insufficient and the restraining force F_{slab} is carried entirely by the steel;
- over the rest of the uncracked part (ie. (L - W_{cr}), the bond between concrete and steel is still effective and therefore behaves in the same manner as the member before cracking;
- any cracks which occur, must be at least a distance, S_o away from both side of the existing cracks;
- the length W_{cr} equals to $2\varsigma S_o$ where S_o can be regarded as the minimum crack spacing and this variable can be calculated using several methods discussed in Chapter 3. An empirical coefficient ς is introduced to account for the tension stiffening effect by CEB Manual (1985). For member with restraint, it can be taken as 0.5.

A new expression for the axial stiffness of slab can be developed using the following steps. First consider the relationship between the deformation in an uncracked and cracked region after just one crack as follows;

$$\delta_{slab} = \left(L - W_{cr}\right)\varepsilon_{c1} - W_{cr}\varepsilon_{s2} \tag{4.9}$$

where ε_{s2} = steel strain within the cracked region

ε_{c1} = concrete strain in the uncracked region

By using the relationships between restraining force, strain, area and elasticity, equation (4.9) can be expressed as:

$$\delta_{slab} = \left(L - W_{cr}\right)\frac{F_{slab}}{A_{eq}E_c} - W_{cr}\frac{F_{slab}}{A_s E_s} \tag{4.10}$$

Simplifying the equation further gives;

$$\delta_{slab} = F_{slab}\left(\frac{L - W_{cr}}{A_{eq}E_c} + \frac{W_{cr}}{A_s E_s}\right) \tag{4.11}$$

Since $k_{nslab} = \frac{F_{slab}}{\delta_{slab}}$ where k_{nslab} is the new axial stiffness after cracking, the new axial stiffness after a first crack can be given as:

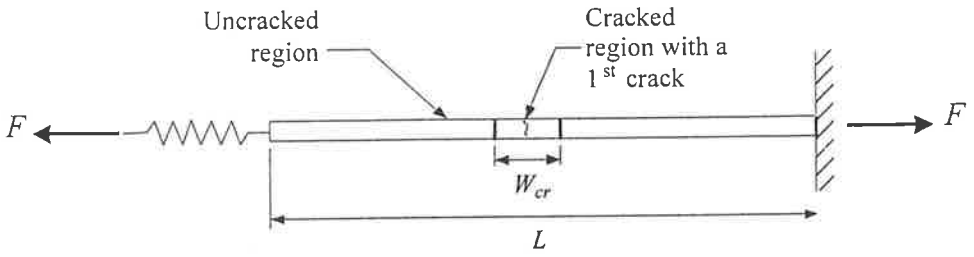

Figure 4.5a Reinforced concrete slab composes of uncracked and cracked region after a first crack

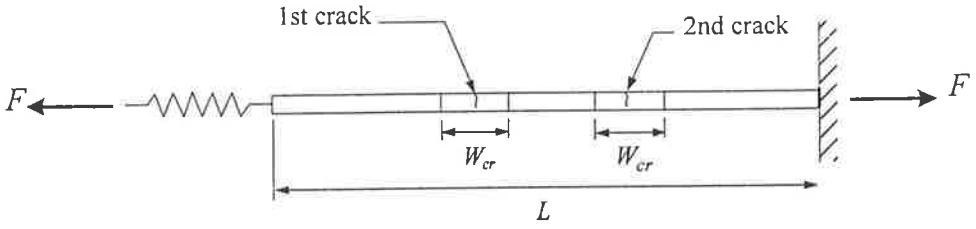

Figure 4.5b Reinforced concrete slab composes of uncracked and cracked regions after two cracks

$$k_{nslab} = \frac{1}{\left(\frac{L - W_{cr}}{A_{eq}E_c} + \frac{W_{cr}}{A_s E_s}\right)} \tag{4.12}$$

But, the area of transformed section in the uncracked region $A_{eq} = A_c(1+n\rho)$, thus:

$$k_{nslab} = \frac{1}{\left(\frac{L - W_{cr}}{A_c(1+n\rho)E_c} + \frac{W_{cr}}{A_s E_s}\right)} \tag{4.13}$$

Simplifying further gives:

$$k_{nslab} = \frac{\left(A_c E_c / L\right)}{\left(\frac{W_{cr}}{L}\right)\left(\frac{1}{n\rho}\right) + \left(1 - \frac{W_{cr}}{L}\right)\left(\frac{1}{1+n\rho}\right)} \tag{4.14}$$

As a result, the equation (4.14) can be used to represent a general expression for the axial stiffness of the slab prior to and after the first crack.

(c) Subsequent cracking

After the first crack, the restraining force at each subsequent cracking case can be calculated by assuming the mean tensile strength of concrete $f_t^{'}$ to minimise the complexity. Therefore, the restraining force at concrete cracking always has the same magnitude. In effect, an expression to solve for the restraining force just before each crack after the first crack can be given as;

$$F_{cr} = f_t^{'} A_c (1 + n\rho) \tag{4.15}$$

Similar to the condition after the first crack, the analyses for subsequent formations of cracking follows the same principle. The stiffness of the slab has to be modified each time a new crack occurs in the span. An additional assumption is also made such that the cracked region of length W_{cr} is assumed to be identical for each crack that occurs. In effect, equation (4.14) can be modified to represent the axial stiffness of the slab immediately after each crack such that;

$$k_{nslab} = \frac{\left(A_c E_c / L\right)}{\left(\frac{mW_{cr}}{L}\right)\left(\frac{1}{n\rho}\right) + \left(1 - \frac{mW_{cr}}{L}\right)\left(\frac{1}{1+n\rho}\right)} \tag{4.16}$$

where $m = 0, 1, 2, \ldots\ldots$ maximum number of cracks at the stabilised cracking state in the span

Similarly, equation (4.8) has to be modified since the crack region does not contribute to any free shrinkage when the springs are disconnected even though the concrete within the crack region would undergo shrinkage. This is expressed as;

$$F\left(\frac{1}{k_{sp}}+\frac{1}{k_{nslab}}\right)=\delta_{sh} \tag{4.17}$$

$$\text{where } \delta_{sh}=(L-mW_{cr})\varepsilon_{sh} \tag{4.18}$$

Hence it is now possible to calculate the restraining force just before and immediately after each crack has formed and the corresponding shrinkage strain by using the equations (4.8), (4.18) and (4.17). By plotting the values of the restraining forces and their corresponding shrinkage strains, a graph similar to that in Figure 3.2c of Chapter 3 can be obtained. This is re-illustrated as shown in Figure 4.6.

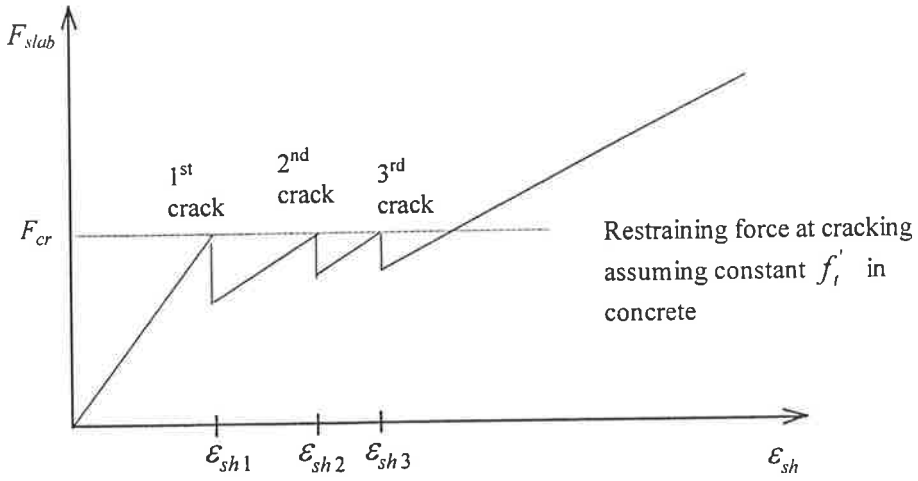

Figure 4.6 Restraining forces VS shrinkage strain after cracking in one way slab

4.2.1.2 Creep effect is included

In order to incorporate the effect of creep, a simple technique called "the effective modulus method" can be used. In this method, creep is simply treated as a delayed elastic strain and is taken in to account by reducing the elastic modulus of the concrete. As a result, the effective modulus for concrete can be defined as follows;

$$E_e=\frac{E_c}{1+\phi} \tag{4.19}$$

where ϕ = creep coefficient which is already discussed in Chapter 2

Thus, equation (4.19) can be modified to account for the effect of creep by replacing the modulus E_c with E_e as follows;

$$k_{nslab} = \frac{\left(A_c E_e / L\right)}{\left(\frac{mW_{cr}}{L}\right)\left(\frac{1}{n\rho}\right) + \left(1 - \frac{mW_{cr}}{L}\right)\left(\frac{1}{1+n\rho}\right)} \tag{4.20}$$

4.2.2 Analysis of slab wall-wall subassemblage

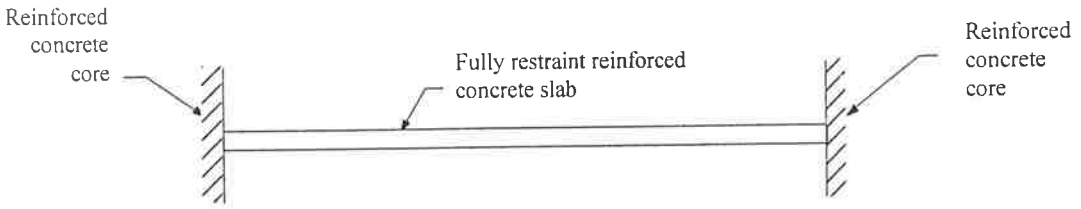

Figure 4.7 One-way reinforced concrete slab spanning between two concrete cores

The analysis now considers fully restrained supports at both ends of the span as shown in Figure 4.7. Equation (4.17) can be modified so that it accounts for the two rigid concrete cores on both ends of the span. This is easily achieved by making the spring stiffness k_{sp} term in the column infinitely large to reflect the large restraint provided by the concrete core. Hence, equation (4.17) can be rewritten as;

$$\frac{F}{k_{nslab}} = \delta_{sh} \tag{4.21}$$

$$\text{where} \quad \delta_{sh} = (L - mW_{cr})\varepsilon_{sh} \tag{4.22}$$

4.3 Two and multiple spans one-way RC slab

Consider a two span reinforced concrete slab as shown in Figure 4.8. The first slab (span 1) spans between an exterior column and an interior column while the second slab (span 2) spans between the interior column and a rigid concrete core. Uniform shrinkage is assumed to develop in both spans with time, and as a result, restraining forces develop. The amount of deformation in the slabs depends on the restraints provided by the columns and concrete core.

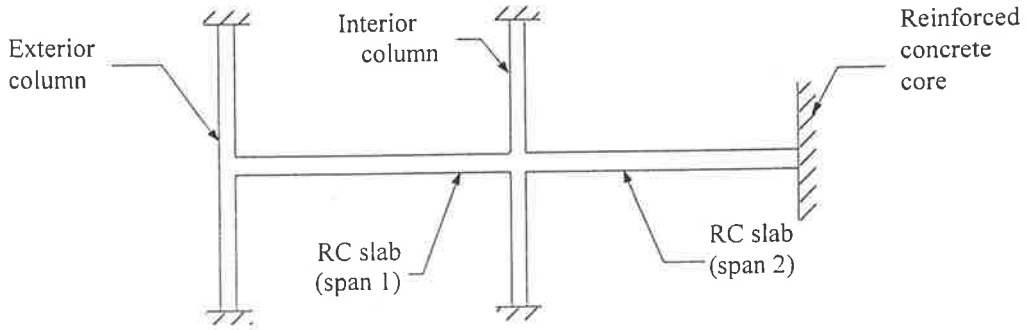

Figure 4.8 Two spans one-way reinforced concrete slab spanning between exterior column, interior column and a concrete core

For this analysis, the assumptions previously used in one-span reinforced concrete slab are applicable. The amount of restraint in the columns is represented by using a spring to represent the stiffness of each column. The deformation of each spring due to the restraining force depends on the spring stiffness and as a result, the structure can be simplified as shown in Figure 4.9.

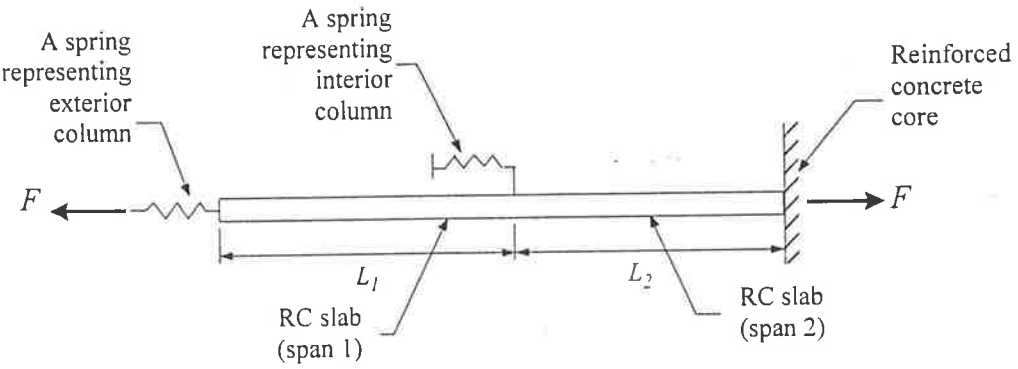

Figure 4.9 Springs are used to represent stiffness of columns

The analysis commences with an introduction of shrinkage strain into the structure similar to the single span reinforced concrete slab, resulting in restraining forces to develop at both column supports and rigid core. For the uncracked condition, both members are analysed using uncracked sections, but for post cracking condition, uncracked sections are only valid for regions which are not affected by cracking.

When the concrete begins to crack, the locations of the cracks depend mainly on the relative magnitude of the tensile forces in spans 1 and 2 and the stiffnesses of the members in the pre cracking and post cracking conditions. The first crack occurs in span 2. However, to determine subsequent cracking, it is necessary to predict the magnitude of the restraining forces in each span.

4.3.1 Creep effect is ignored

4.3.1.1 Uncracked case

The slabs are allowed to shrink freely by removing both springs as shown in Figure 4.10a. Once the slabs have fully shrunk, a force F is introduced into the springs and in the slabs to restore the compatibility. Thus, the slabs in both spans are only allowed to deform as shown in the Figure 4.10b. As can be seen from these figures, the notations used are explained as follows;

A = original position of section A

A' = position of section A, if span 1 and span 2 are free to shrink

A'' = position of section after span 1 and 2 are allowed to shrink, but are then reconnected to the springs at A and B

B = original position of section A

B' = position of section B, if span 1 and 2 are free to shrink

B'' = position of section after span 1 and 2 are allowed to shrink, but are then reconnected to the springs at A and B

C = position of section which does not move

According to Figure 4.10a, when the slabs are free to shrink in both spans, the following relationships can also be given as:

$$\delta_{sh_A} = (L_1 + L_2)\varepsilon_{sh} \tag{4.23}$$

$$\delta_{sh_B} = (L_2)\varepsilon_{sh} \tag{4.24}$$

where δ_{sh_A} = free shrinkage at A (compressive)

δ_{sh_B} = free shrinkage at B (compressive)

After spring A and B are reconnected to the slabs as shown in Figure 4.10b, they both deform at an amount δ_{sp_A} and δ_{sp_B} respectively. As a result, the following compatibility equations can be obtained as;

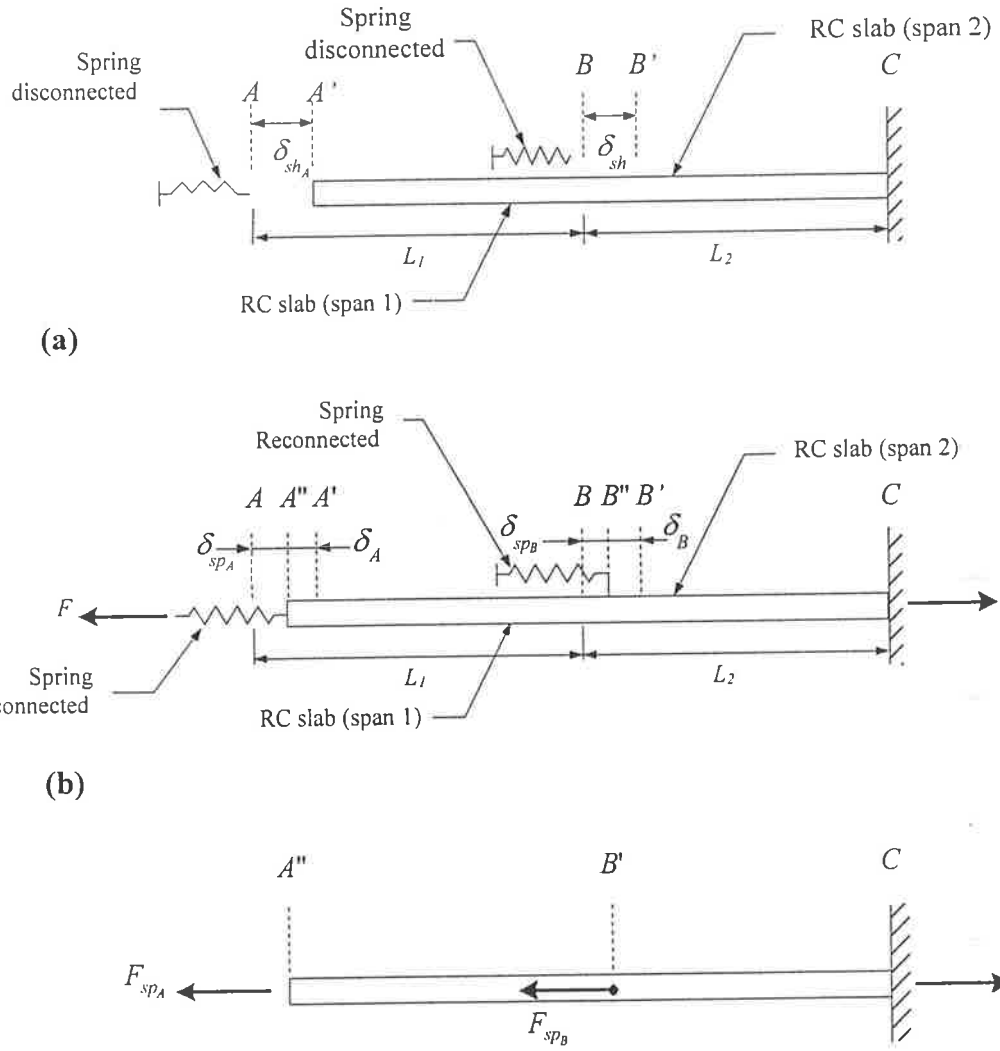

(c) Free body diagram of forces in the slabs

Figure 4.10 Postion of the slabs before and after the springs are reconnected to the structure

$$\delta_{sp_A} + \delta_A = \delta_{sh_A} \tag{4.25}$$

$$\delta_{sp_B} + \delta_B = \delta_{sh_B} \tag{4.26}$$

where δ_{sp_A} = deformation in spring A (tensile)

δ_{sp_B} = deformation in spring B (tensile)

δ_A = deformation of section A from shrinkage, zero force position

δ_B = deformation of section B from shrinkage, zero force position

In addition, the extension of span 1 is given by the relationship:

$$\delta_{slab1} = \delta_A - \delta_B \tag{4.27}$$

Similarly, the extension of span 2 is given by:

$$\delta_{slab2} = \delta_B \tag{4.28}$$

To solve for the restraining forces, the following **constitutive** equations can be written for both springs at position A and B and slabs in span 1 and 2:

$$F_{sp_A} = \delta_{sp_A} k_{sp_A} \tag{4.29}$$

$$F_{sp_B} = \delta_{sp_B} k_{sp_B} \tag{4.30}$$

$$F_{slab1} = k_{slab1} \delta_{slab1} \tag{4.31}$$

$$F_{slab1} = k_{slab1} (\delta_A - \delta_B) \tag{4.32}$$

$$F_{slab2} = k_{slab2} \delta_{slab2} \tag{4.33}$$

$$F_{slab2} = k_{slab2} \delta_B \tag{4.34}$$

where F_{sp_A} = tensile force in spring at A

F_{sp_B} = tensile force in spring at B

F_{slab1} = tensile force in span 1

F_{slab2} = tensile force in span 2

k_{sp_A} = stiffness of spring A

k_{sp_B} = stiffness of spring B

k_{slab1} = axial stiffness of span 1

k_{slab2} = axial stiffness of span 2

Note also that the transformed area sections are used to define the stiffness in both span 1 and 2. By using the equilibrium requirements as indicated in Figure 4.11a, 4.11b and 4.11c to satisfy the conditions at position *A*, *B*, and *C*, the following relationships can be expressed as:

At *A*

$$F_{sp_A} = F_{slab1} \text{ (both tension)} \tag{4.35}$$

At *B*

$$F_{slab1} + F_{sp_B} = F_{slab2} \tag{4.36}$$

At *C*

$$F_{slab2} = F_c \tag{4.37}$$

where F_c = reactive force at *C*

By substituting the constitutive equations into equation (4.25) and noting that $\delta_A = \delta_{slab1} + \delta_B$ and $F_{sp_A} = F_{slab1}$, the following equations are obtained:

$$\frac{F_{sp_A}}{k_{sp_A}} + \frac{F_{slab1}}{k_{slab1}} + \frac{F_{slab2}}{k_{slab2}} = \delta_{sh_A} \tag{4.38}$$

$$\frac{F_{slab1}}{k_{sp_A}} + \frac{F_{slab1}}{k_{slab1}} + \frac{F_{slab2}}{k_{slab2}} = \delta_{sh_A} \tag{4.39}$$

Simplifying further yields:

$$F_{slab1}\left(\frac{1}{k_{sp_A}} + \frac{1}{k_{slab1}}\right) + F_{slab2}\left(\frac{1}{k_{slab2}}\right) = \delta_{sh_A} \tag{4.40}$$

Similarly, by substituting the constitutive equations into equation (4.26) and noting that $\delta_B = \delta_{slab2}$, the following equations are obtained:

$$\frac{F_{sp_B}}{k_{sp_B}} + \frac{F_{slab2}}{k_{slab2}} = \delta_{sh_B} \tag{4.41}$$

It can be shown from equation (4.36) that $F_{sp_B} = F_{slab2} - F_{slab1}$, thus equation (4.41) can be re-written in terms of F_{slab1} and F_{slab2} as shown below:

$$\frac{F_{slab2} - F_{slab1}}{k_{sp_B}} + \frac{F_{slab2}}{k_{slab2}} = \delta_{sh_B} \tag{4.42}$$

Simplifying further yields:

$$F_{slab1}\left(\frac{-1}{k_{sp_B}}\right) + F_{slab2}\left(\frac{1}{k_{sp_B}} + \frac{1}{k_{slab2}}\right) = \delta_{sh_B} \tag{4.43}$$

From the above steps, it is now possible to calculate the unknowns, namely the restraining forces, F_{slab1} and F_{slab2}. By drawing an axial force diagram in both spans, it is obvious that the first crack forms in span 2. An equation similar to equation (4.8) can be used to solve for concrete stress just before the second crack occurs. Both span 1 and 2 is rewritten in general form as.

$$\sigma_c = \frac{F}{E_c(1+n\rho)} \tag{4.44}$$

where σ_c = concrete stress before 1st crack

E_c = modulus of elasticity of concrete

n = modular ratio of cross section

ρ = steel ratio of cross section

F = restraining force in the slab

By setting the concrete stress in span 2 equal to the tensile strength of concrete in equation (4.44) (i.e. $\sigma_{c2} = f_t'$), the restraining force F_{slab2} at first cracking can then be obtained. Once this is achieved, the restraining force F_{slab1} and the shrinkage strain at which first cracking occurs can be determined by substituting the value of F_{slab2} into equations (4.40) and (4.43) and solve both equations simultaneously.

4.3.1.2 After cracking

Further analysis is now carried out to determine the subsequent formation of the 2nd, 3rd cracks until no further cracks can form in either span. The formation of the first

Omit this page

Equilibrium conditions

At A

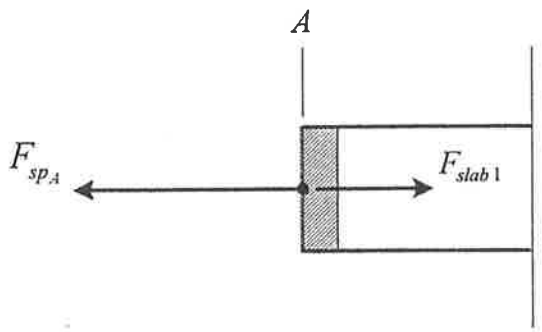

Figure 4.11(a) Free body diagram at position A

At B

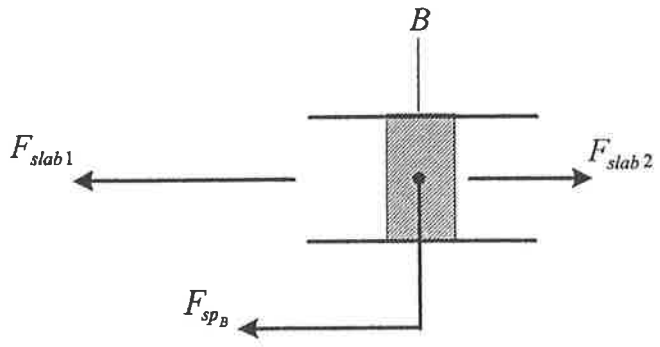

Figure 4.11(b) Free body diagram at position B

At C

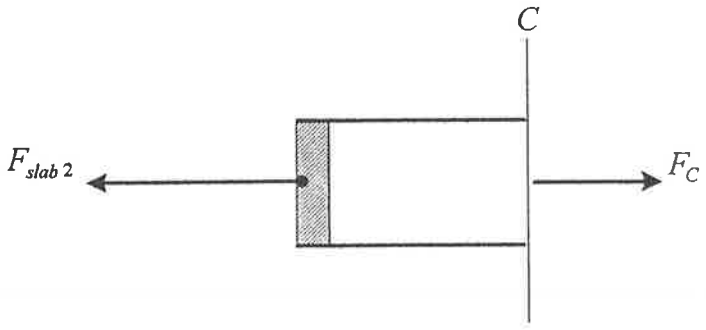

Figure 4.11(c) Free body diagram at position C

crack in span 2 causes a reduction in stiffness of the member and as a result, the magnitude of the restraining force F_{slab2} decreases quite significantly. To estimate a new axial stiffness of span 2, the same assumptions as those in Section 4.2.1.1 are adopted and an equation similar to equation (4.15) for the new axial stiffness in span 2 after a crack has occurred can be expressed as;

$$k_{nslab2} = \frac{\left(A_{c2}E_c / L_2\right)}{\left(\frac{W_{cr2}}{L_2}\right)\left(\frac{1}{n_2\rho_2}\right)+\left(1-\frac{W_{cr2}}{L_2}\right)\left(\frac{1}{1+n_2\rho_2}\right)} \tag{4.45}$$

The process of determining the restraining forces, F_{slab1} and F_{slab2} can now proceed using the same analysis as before, but with k_{slab2} now being replaced by k_{nslab2}. Furthermore, equation (4.23) and (4.24) are modified as shown below since the cracked region does not contribute to any free shrinkage when the springs are removed, even though the concrete within the crack region would undergo shrinkage:

$$\delta_{sh_A} = \left(L_1 + L_2 - W_{cr2}\right)\varepsilon_{sh} \tag{4.46}$$

$$\delta_{sh_B} = \left(L_2 - W_{cr2}\right)\varepsilon_{sh} \tag{4.47}$$

Thus, equation (4.40) and (4.43) can be re-written using equation (4.46) and (4.47) as;

$$F_{slab1}\left(\frac{1}{k_{sp_A}}+\frac{1}{k_{slab1}}\right)+F_{slab2}\left(\frac{1}{k_{nslab2}}\right)=\delta_{sh_A} \tag{4.48}$$

$$F_{slab1}\left(\frac{-1}{k_{sp_B}}\right)+F_{slab2}\left(\frac{1}{k_{sp_B}}+\frac{1}{k_{nslab2}}\right)=\delta_{sh_B} \tag{4.49}$$

By following the same procedures as the case before cracking, both F_{slab1} and F_{slab2} can be calculated and the location for the formation of a second crack can thus be predicted. Then it is possible to obtain the shrinkage strain simply by letting the stress of the uncracked concrete equals the tensile strength of concrete.

Once the second crack has taken placed, a new axial stiffness has to be defined. If the crack again appears in span 2, equation (4.45) only has to be modified slightly

by including a second cracked length W_{cr2} into the equation. (ie. W_{cr2} is replaced by $2W_{cr2}$). On the other hand, if the second crack occurs in span 1, the axial stiffness used in equation (4.48) must be replaced by a new stiffness. This is achieved by adopting the same method as in span 2 and can be given as follows:

$$k_{nslab1} = \frac{\left(A_{c1}E_c / L_1\right)}{\left(\frac{W_{cr1}}{L_1}\right)\left(\frac{1}{n_1\rho_1}\right)+\left(1-\frac{W_{cr1}}{L_1}\right)\left(\frac{1}{1+n_1\rho_1^*}\right)} \tag{4.50}$$

where k_{nslab1} = new axial stiffness in span 1

W_{cr1} = cracked length in span 1 and is equal to $2S_o$

Hence, it is obvious that as more cracks form in both spans, the analysis becomes very repetitive. Both spans are fully cracked when the number of cracks, m_1 and m_2 in span 1 and 2 reaches a state which no further cracking can form. Therefore, equation (4.45) and (4.50) can be rewritten to account for stiffness at different stages of cracking up to the fully cracked stage.

$$k_{nslab1} = \frac{\left(A_{c1}E_c / L_1\right)}{\left(\frac{m_1W_{cr1}}{L_1}\right)\left(\frac{1}{n_1\rho_1}\right)+\left(1-\frac{m_1W_{cr1}}{L_1}\right)\left(\frac{1}{1+n_1\rho_1^*}\right)} \tag{4.51}$$

$$k_{nspan2} = \frac{\left(A_{c2}E_c / L_2\right)}{\left(\frac{m_2W_{cr2}}{L_2}\right)\left(\frac{1}{n_2\rho_2}\right)+\left(1-\frac{m_2W_{cr2}}{L_2}\right)\left(\frac{1}{1+n_2\rho_2^*}\right)} \tag{4.52}$$

And similarly, the two free shrinkage strain equations can be expressed in general form as:

$$\delta_{sh_A} = \left(L_1 - m_1W_{cr1} + L_2 - m_2W_{cr2}\right)\varepsilon_{sh} \tag{4.53}$$

$$\delta_{sh_B} = \left(L_2 - m_2W_{cr2}\right)\varepsilon_{sh} \tag{4.54}$$

where m_1 = 0, 1, 2,.....maximum number of cracks where n is the maximum number of cracks in span 1

m_2 = 0, 1, 2,.....maximum number of cracks where n is the maximum number of cracks in span 2

4.3.2 Creep effect included

The method to include creep into the analysis is exactly the same as in one span reinforced concrete slab. Thus this topic will not be discussed in this section. Basically, the concrete modulus, E_c and the modular ratio, n terms in equation (4.51) and (4.52) are replaced by E_e and n_e terms respectively.

4.4 Determination of crack width

The analysis methods previously discussed in Section 4.2 and 4.3 allow the calculation of the restraining forces just before and immediately after each crack forms in a single span and two span reinforced concrete slab. In turn, these values can be used to calculate the corresponding tensile stresses in the reinforcement at the cracks during the process of shrinkage. Because the reinforcement alone carries the restraining force at the cracks, a general expression to calculate the tensile stress can be given as;

ie. $$\sigma_{s2} = F_{slab} A_s \tag{4.55}$$

In general, limiting the values of tensile stress in the reinforcement should ensure that crack widths through out the slabs do not become excessive. In addition, it was shown in Chapter 3 that the crack width depends on the tensile stress in the reinforcement along the crack region (ie. the length W_{cr} used in the analysis). Therefore, another useful relationship which can be established is the variation in crack width and reinforcement stress as a function of applied shrinkage strain. Beeby (1993) pointed that the crack width is greatest immediately before the formation of a further crack. This can be demonstrated in Figure 4.12a and 4.12b respectively.

To calculate the crack widths in the slabs, the equation given in Chapter 3 is used as follows.

$$w = 2\varsigma S_o(\varepsilon_{s2} - \varepsilon_{c2}) \tag{4.56}$$

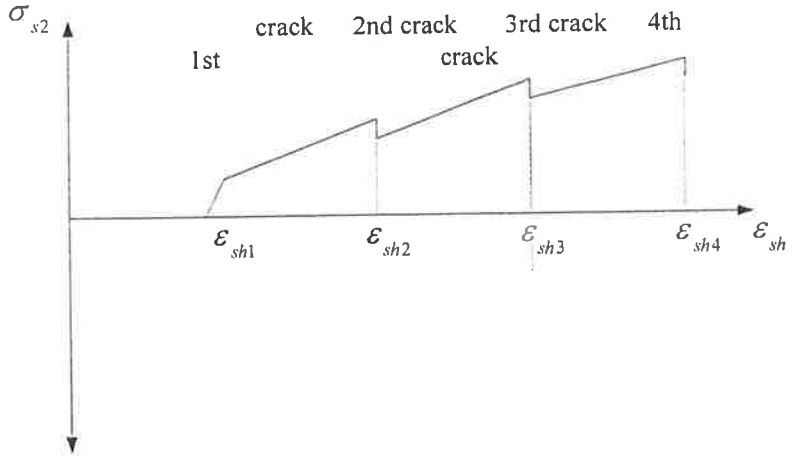

Figure 4.12a Variation of tensile stresses in the reinforcement at the cracks with shrinkage strains

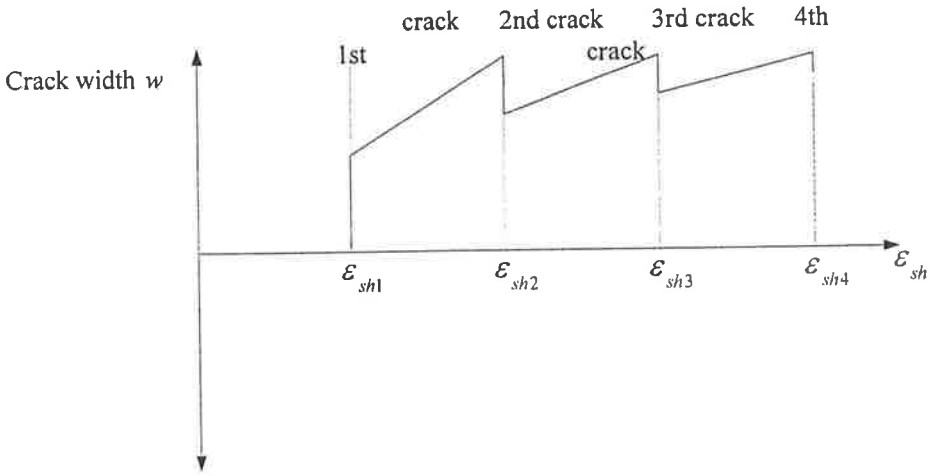

Figure 4.12b Development of crack widths with shrinkage strains

Table 4.1 Results of Example 1

	Hughes (1971,1972)	Leonhardt (1977)	Beeby (1979)	Rizkally & Hwang (1984)	CEB Manual (1985)	ACI 224 (1986)	Christiansen & Nelson (1997)
W_{cr} (mm)	402	348	174	244	206	121	300
No. of cracks at ε^*_{sh}	3	3	6	4	5	8	4
Reinforcement tensile stress at each crack, σ_{s2}(MPa)	298	300	343	330	347	372	327
Maximum crack width (mm)	0.6	0.52	0.30	0.40	0.36	0.22	0.49

Table 4.2 Results obtained using procedures from Gilbert (1991)

W_{cr} (mm)	No. of cracks at ε^*_{sh}	Reinforcement tensile stress at each crack, σ_{s2}(MPa)	Maximum crack width (mm)
625	6	312	0.38

From these results, the method predicted the number of cracks which developed until shrinkage strain of 600 $\mu\varepsilon$ is attained. Further cracking that developed beyond this range are ignored. Table 4.1 also shows the associated tensile stress in the reinforcement at each crack which in turn are used to determine the crack widths. By comparing these results with those calculated by Gilbert (1991) in Table 4.2, it can be seen that the number of cracks obtained using slab wall-wall sub-assemblage are varied from Gilbert's analysis by ± 2 cracks, depending on which crack spacing equation is used. Similarly, crack widths obtained, are ranged from 0.22mm to 0.6mm. Unlike Gilbert's analysis, creep effect was not considered in this example and therefore, the results could be over-estimated.

Example 2 Gilbert (1991)

Consider the same structure as in Example 1, but the reinforcement, A_s is now reduced from 750mm^2 per m to 375mm^2 per m. The main objective of this example

is to investigate the effect of reinforcement content on the development of cracking and the associated crack widths. Using the slab wall-wall sub-assemblage method, the results from the analyses as well as those from Gilbert (1991) are tabulated in Table 4.3 and 4.4 respectively.

Table 4.3 Results of Example 2

	Hughes (1971,1972)	Leonhardt (1977)	Beeby (1978)	Rizkally & Hwang (1984)	CEB Manual (1985)	ACI 224 (1986)	Christiansen & Nelson (1997)
W_{cr} (mm)	804	480	318	387	321	122	599
No. of cracks at ε^*_{sh}	1	1	1	1	1	1	2

Table 4.4 Results obtained using procedures from Gilbert (1991)

W_{cr} (mm)	No. of cracks at ε^*_{sh}	Reinforcement tensile stress at each crack, σ_{s2}(MPa)	Maximum crack width (mm)
625	1	reinforcement yielded	1.37

It can be seen from the results of tables that after the first crack has developed, the reinforcement yielded. As a result, excessive crack widths are obtained. This clearly demonstrates the need to ensure that sufficient reinforcement is provided in the member to avoid this type of serviceability failure.

Example 3

Consider the same one-way reinforced concrete slab in Example 1, but with different support conditions as shown below. The column is 6 m in height and also is assumed to be fixed at both ends. As shrinkage develops with time, the column provides partial restraint to the slab movement, while the rigid core does not allow any movements. The column sizes vary from 300mm × 300mm to 1000 mm × 1000mm. The final shrinkage strain is assumed to be 600 microstrains.

The main objective of this example is to investigate the effect of restraint provided by the end support. As a result, the slab column-wall sub-assemblage discussed in Section 4.2.1 is used to carry out the analysis. In each case, reinforced concrete columns of various cross-sections are analysed. The crack spacing equation suggested by CEB Manual (1985) is selected to calculate the length of cracked region, W_{cr}.

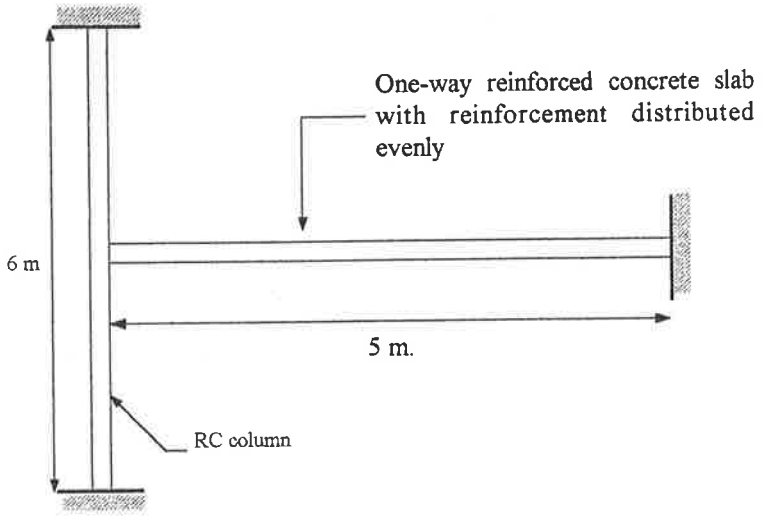

In effect, the results of these analyses are tabulated in Table 4.5 as shown. The results of CEB manual (1985) in Example 1 are also included for comparisons.

It can be seen that as the columns become smaller in size, the number of cracks significantly reduced. This is due to the fact that smaller columns provide less restraint against slab deformation due to shrinkage and therefore will tolerate more movement, resulting in smaller restraining forces at the same shrinkage strain. In fact, no cracks developed when the column sizes were reduced to 400mm by 400mm or smaller when the shrinkage strain reached 600 $\mu\varepsilon$. On the other hand, when the column sizes were increase to 900mm by 900mm, the number of cracks that occurred was similar to those with fully restraint supports.

Table 4.5 Results of Example 3

Column size	Number of cracks
400 mm × 400 mm	0
500 mm × 500 mm	0
600 mm × 600 mm	3
700 mm × 700 mm	4
800 mm × 800 mm	4
900 mm × 900 mm	5
1000 mm × 100 mm	5
1100 mm × 1100 mm	5
Example 1	5

Example 4

Consider two spans one-way reinforced concrete slabs as shown. The exterior and interior columns are assumed to be 500mm x 500mm in dimensions. The concrete and reinforcement properties are the same as Example 1 and apply to both spans. The ultimate shrinkage is assumed to develop to 600 $\mu\varepsilon$. As with Example 3, the crack spacing equation suggested by CEB Manual (1985) is selected to calculate the length of cracked region, W_{cr}

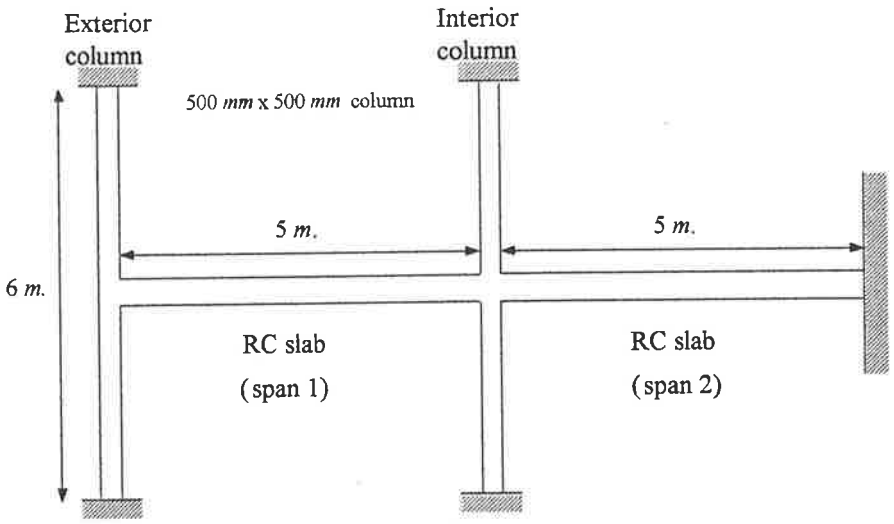

As shrinkage occurs in both spans, the magnitude of the restraining force would be higher in Span 2 due to the higher restraint. As a result, cracking would first appear in span 2 before developing in Span 1. The results of this analysis are tabulated in Table 4.6

Table 4.6 Results of Example 4

	Span 1	**Span 2**
W_{cr} (*mm*)	206	206
No. of cracks	3	6
Crack width (*mm*)	0.33	0.38

Based on these results, cracking would not develop in Span 1 until the restraining force is sufficient enough to cause the concrete tensile stress to exceed f_t'. The first 3 cracks only occur in Span 2 before causing the next cracks to develop in Span

Chapter 5

Control Recommendations for crack widths and crack control in restrained members with imposed deformations

5.1 Introduction

In Chapter 3, methods to calculate crack spacings and crack widths in reinforced concrete members subjected to shrinkage and temperature effects were presented. In this chapter, acceptable crack widths and methods for controlling crack widths to satisfy the required limits are considered. Crack control is basically achieved either by allocating sufficient reinforcement with appropriate details, or by introducing movement joints.

In regard to crack widths, a comparison is made of various guidelines and design provisions set out by design and building codes as well as those suggested by other independent researchers in control of cracking. However, it should be understood at the onset that "control of cracking" in this case relates to the service load which occurs as a result of restrained and imposed deformations.

The following guidelines and recommendations are those that are widely used and accepted by the majority of most designers and building authorities:

- CEB Manual (CEB, 1985)
- ACI 224 "Cracking in direct tension" (ACI, 1986)
- ACI 318-89 (ACI Committee, 1989)
- BS 8110: Structural use of concrete:1985 (BSI, 1993)
- CEB - FIP Model Code 1990 (CEB-FIP, 1993)
- AS 3600-1994 (SAA, 1994)

- Other researchers

For simplicity, the method suggested by the Australian Code AS3600-1994 (SAA, 1994) will be referred as AS3600, while the methods developed by CEB Manual and CEB - FIP Model Code (CEB-FIP, 1993) will be mentioned as CEB and the Code respectively. Likewise, the methods reported by ACI 318-89 (ACI Committee, 1989), ACI 224 (ACI, 1986) and BS 8110 Structural use of concrete: 1985 (BSI 1993) will be identified as ACI 318, ACI 224 and BS 8110.

5.2 CEB Manual (CEB, 1985)

CEB Manual (1985) provides several methods to control cracking due to axial tensile forces. These include direct calculation of both crack spacing and crack width. The procedures were already discussed in Chapter 3. Appropriate limits for crack width can then be used in conjunction with crack width calculations. Due to the semi-random process of crack formation and scatter in the material properties, the calculated crack width is factored. Thus, a design crack width, w_k (95 percent fractile) for a member with some restraint is taken as;

$$w_k = 1.3 w_m \tag{5.1}$$

where w_m = average crack width calculated using equation (3.69) in Chapter 3

As well as a limit on for crack width equation, CEB also specifies that a minimum amount of reinforcement should be provided so that the tensile stress in the reinforcement does not exceed the yield strength. This can be achieved by using the following relationships;

$$\rho_{min} = \frac{A_s}{A_{c,ef}} = \frac{f_t'}{f_{sy}} \tag{5.2}$$

The effective area of concrete, $A_{c,ef}$, is used instead of the gross area of the section and is based on the assumption that only a part of the gross section is affected by the distribution of tensile stress in the reinforcement. This is illustrated in Figure 5.1. It should be noted that the tensile strength of concrete should be the value at the time

of loading. For cracking due to shrinkage, the values at 3 to 7 days after casting are appropriate.

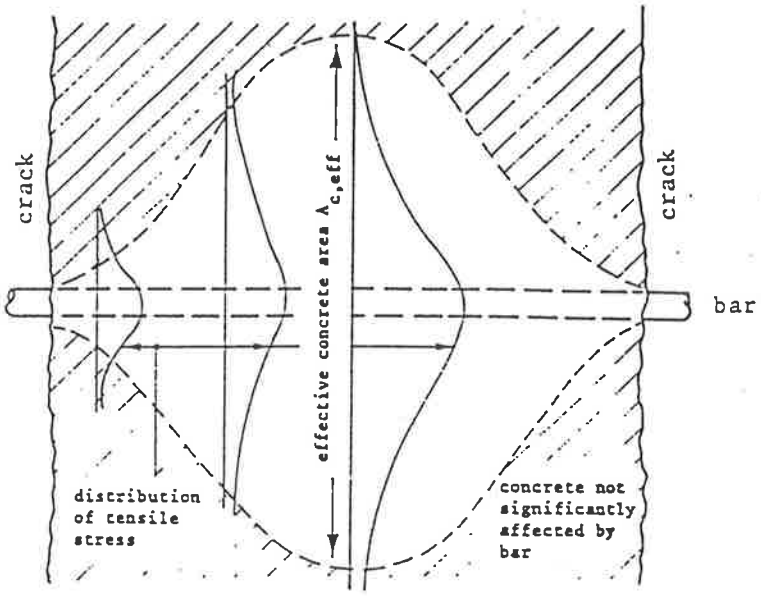

Figure 5.1 Dispersion of tensile stress into concrete between cracks (CEB Manual, 1985)

In addition, crack widths can be reduced by the use of smaller reinforcement at closer spacings. However, the possibility of reinforcement corrosion then increases. This is because the advantage gained by reducing the crack width in some particular cracks may be compromised by the overall increase in the quantity of reinforcement and larger number of cracks which in effect would contribute to the total risk for corrosion. In effect, CEB suggests an alternative method to reduce crack width by increasing the reinforcement ratio and reducing the tensile stress in the reinforcement.

As well as providing direct calculations for crack control, CEB develops a design chart which can be used to achieve adequate reinforcement ratios and minimum reinforcement size. This is reproduced in Figure 5.2. The derivation of the chart is based on the assumptions that concrete cover increases with increase in severity of the environment, as shown in Table 5.1 below, and reinforcement spacing should be the lesser of 15 times the reinforcement diameter or 300 *mm*.

Table 5.1 Crack width vs. concrete cover (reproduced from CEB Manual (1985))

Crack width (*mm*)	**Concrete cover (*mm*)**
0.1	35
0.2	25
0.4	20

Additionally, CEB suggests two methods of check for the crack limit state. These are represented in the Table 5.2 and 5.3 respectively.

Table 5.2 Crack control by limitation of bar diameter (reproduced from CEB Manual, 1985)

Allowable crack width (0.4 *mm*)		**Allowable crack width (0.2 *mm*)**	
Tensile stress in reinforcement, σ_s (MPa)	**Maximum reinforcement diameter (mm)**	**Tensile stress in reinforcement, σ_s (MPa)**	**Maximum reinforcement diameter (mm)**
200	50	100	50
240	25	120	25
280	20	200	12

where σ_s is the tensile stress in the reinforcement in the cracked section

Table 5.3 Maximum reinforcement spacing for crack control (reproduced from CEB Manual, 1985)

Design Crack width, w_k (mm)	**Tensile stress in reinforcement, σ_s (MPa)**					
	Maximum spacing (mm)					
	120	**160**	**200**	**240**	**280[1]**	**350[2]**
0.1	60	-	-	-	-	-
0.2	x	100	75	50	-	-
0.4	x	x	x	175	125	75

Note that: x indicates that any practical reinforcement spacing should be satisfactory

(1) 280 (2) 350 correspond to $0.7f_{sy}$ for reinforcement of 400 MPa

and 500 MPa respectively

In all methods recommended, CEB emphasised that the prediction of crack widths can only give rough estimates. However, these methods should ensure that the cracks developed would be below the calculated widths. Nevertheless it is not possible to ignore the possibility that some cracks will exceed this limit. These situations often arise in locations where there is a change in section or reinforcement is curtailed or lapped. To overcome this problem, special design provisions may be required.

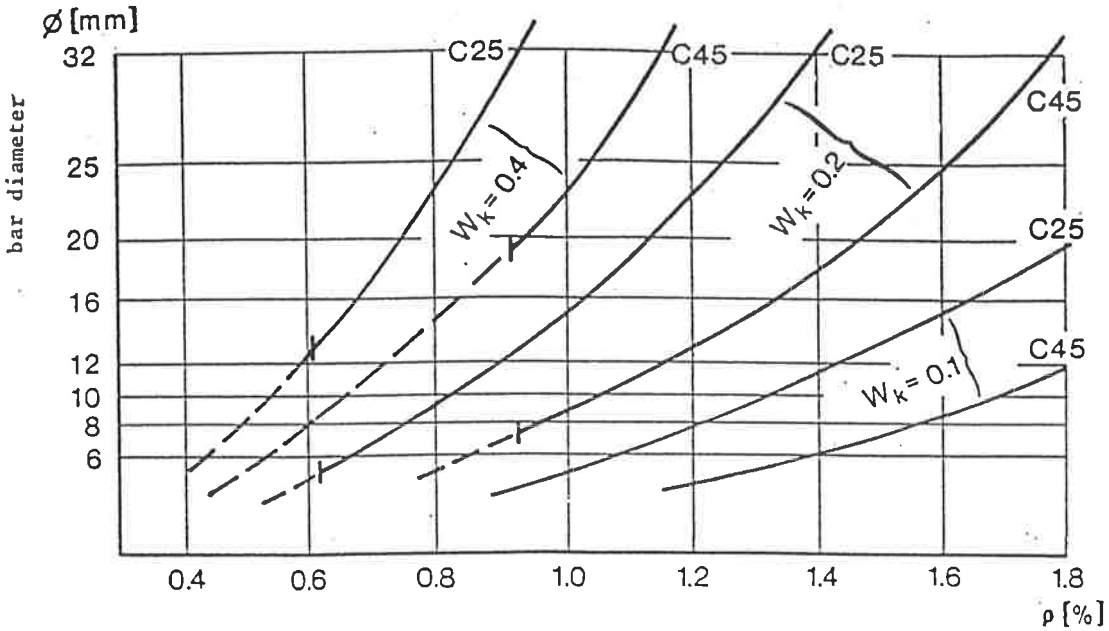

Figure 5.2 Design chart to calculate minimum reinforcement ratio and diameter (CEB, 1985)

When using methods suggested by CEB, it is necessary to understand that CEB specifies them for cracking which occurs as a result of axial tension. This may not be the same as axial tension caused by shrinkage and temperature changes. As an example, CEB accounted for the effect of restraints by modifying several factors in some of the equations, including the factor 1.3 in equation (5.1) instead of 1.7 for unrestrained members. Hence, it will be necessary to make some alterations in the analytical procedure in order to obtain appropriate results for crack widths.

5.3 ACI 224 " Cracking in direct tension" (1986)

ACI 224 treats control of cracking due to direct tension by minimising the maximum crack width. This is achieved at the design stage by providing sufficient reinforcement and at the construction stage by stage placing of concrete. The first provision is considered most effective when the reinforcement diameters as well as the spacings are kept as small as possible for a given total area of reinforcement. However, the report does not actually specify any limitations for the reinforcement in the member. The second provision is achieved by minimising shrinkage and temperature effects from taking place during and immediately after construction so that there is sufficient time for concrete to gain adequate strength. The methods in which these are carried out are described in many references concerning construction practices and guidelines, and therefore will not be elaborated further.

5.4 ACI 318-89 (ACI Committee, 1989)

The American Building code, ACI 318-89 gives provision for crack control in the slab due to shrinkage and temperature changes in the regions of low moment or where flexural stress is small. These situations can occur in the span direction where cracks caused by shrinkage or temperature changes can be accommodated by flexural cracks, while in the orthogonal span direction, additional reinforcement is needed to control these direct tension cracking.

As a result, ACI 318-89 requires designers to provide shrinkage and temperature reinforcement at right angle to the flexural reinforcement in a member where flexural actions are more significant. For shrinkage and temperature reinforcement, the following the minimum reinforcement ratios are recommended.

(a) Deformed bars with grade 40 or 50 in slabs	0.0020
(b) Deformed bars with grade 60 or welded wire fabric (plain or deformed) in slabs	0.0018
(c) Reinforcement with yield stress exceeding 60,000 psi measured at a yield strain of 0.35 % is used	$\frac{0.0018 \times 60{,}000}{f_{sy}}$

The above requirements do not have to be satisfied in every situation. Gilbert (1992) has commented that these values are merely the absolute minimum and reinforcement in excess of these may be necessary in some restrained members to provide adequate crack control.

5.5 BS 8110: 1985 (BSI, 1993)

BS 8110 gives allowance for cracking due to shrinkage and temperature changes by providing sufficient reinforcement to distribute the amount of cracks along the member. The majority of these provisions were given in reference with cracking which occurs in reinforced concrete walls. As a guide, the Code recommends a maximum crack width of 0.3mm, unless the environment to which the member is exposed to, is particular aggressive. To achieve this, the Code suggests minimum reinforcement ratios, $\rho_{\min}$, depending on the grade of reinforcement.

(a) For grade 460 and above $\rho_{min} = 0.0025$

(b) For grade 250 $\rho_{min} = 0.003$

The Code assumes that minimum reinforcement ratios should ensure that excessive cracking does not occur and the determination of crack widths is no longer necessary. As an alternative, the foregoing provisions can be ignored and crack widths can be calculated analytically to prove that they are satisfactory. However, the equation given applies to cracking due to flexure. BS 8110 suggested that cracking due to axial tension can also be used, but with "caution". By ensuring that the strain in the tension reinforcement is limit to $\frac{0.8 f_y}{E_s}$, the design surface crack width can be given in accordance to the following relationship;

$$w_k = \frac{3 a_{cr} \varepsilon_m}{1 + \frac{(a_{cr} - c_{min})}{h}} \qquad (5.3)$$

where a_{cr} = distance from the point considered to the surface of the nearest longitudinal reinforcement

c_{min} = minimum concrete cover

ε_m = average at the level considered

h = depth of the member

It should be noted that equation (5.3) is valid only for members subjected to axial tensile force. A similar expression for crack width for members under flexure is also available and can be found in the Code.

In addition, when the crack width being considered is directly above the reinforcement, (when $a_{cr} = c_{min}$), then equation (5.3) is reduced to;

$$w_k = 3c_{min}\varepsilon_m \tag{5.4}$$

On the other hand, when the distance a_{cr} is increased towards infinity ($a_{cr} \rightarrow \infty$), the crack width in equation (5.4) approaches;

$$w_k = 3h\varepsilon_m \tag{5.5}$$

By inspection, it can also be seen that the crack width can not exceed the value given below;

$$w_k = 3a_{cr}\varepsilon_m \tag{5.6}$$

BS 8110 advised that using either the empirical recommendations or the analytical calculations, should ensure that crack widths remain satisfactory. However, cracking is a semi-random process, occasionally, cracks which are larger than the one predicted, may occur. They can be treated as normal unless a significant number of these cracks exceed the calculated width.

5.6 CEB - FIP Model Code 1990 (CEB-FIP, 1993)

This Code stipulates that crack control is one of the criteria which must be satisfied for the serviceability state.

The Code requires that sufficient is provided to avoid yielding of the reinforcement after cracking. The satisfaction of this requirement eliminates the need to calculate crack widths. By appropriately choosing the size and spacing of the reinforcing bars using Table 5.4 given by the Code, the majority of crack widths occurring along reinforced concrete members should not exceed the value of 0.3 mm. In most

circumstances, this should satisfy the crack width limitation criterion (usually 0.3 mm).

The calculation of the tensile stress in the reinforcement in both cases can be carried out using the method discussed in Chapter 3. For cracking due to restraint, the maximum diameter of the reinforcing bar should be further modified using the equation given as;

$$d = d_{max} \frac{f_t'}{2.9} \tag{5.7}$$

where d_{max} = maximum diameter of reinforcing bar given in Table 5.4

f_t' = the Code recommends the use of mean tensile strength of concrete, at the time when crack occurs

Table 5.4 Maximum size and spacing of deformed bars in reinforced concrete section (CEB-FIP, 1993)

Tensile stress in the reinforcement (MPa)	Maximum reinforcing bar (mm)	Maximum reinforcing bar (mm)
160	32	300
200	25	250
240	20	200
280	14	150
320	10	100
360	8	60
400	6	
450	5	

Furthermore, for members with an overall depth less than or equal to 200 mm and only subjected to axial tension, the Code allows the maximum spacing not to be greater than 300 mm. even when a more accurate calculation is adopted.

In some extreme cases where excessive crack width is considered a major failure, it is necessary to explicitly calculate the crack widths in the reinforced concrete members. An example is where crack widths need to be maintained very small to ensure watertightness and to prevent corrosion of the reinforcement from an aggressive environment. The Code provides an analytical procedure to calculate the design crack width for transverse cracks based on the relationships between the maximum distance over cracked region which can be assumed as the maximum crack spacing, and the average tensile strain in the reinforcement and concrete and strain in the concrete caused by shrinkage over this distance.

ie. $$W_k = S_{max}(\varepsilon_{sm} - \varepsilon_{cm} - \varepsilon) \tag{5.8}$$

In the above expression, S_{max} can be determined by adopting either of the equations below;

For single crack formation

$$S_{max} = \frac{\sigma_{s2} d}{2\tau_{ave}}\left(\frac{1}{1 + n_e \rho_{eff}}\right) \tag{5.9}$$

or for a stabilised cracking stage

$$S_{max} = \frac{d}{3.6\rho_{eff}} \tag{5.10}$$

In both equation (5.9) and (5.10), the value of the average bond stress, τ_{ave} can be considered as 1.8 times the mean tensile strength of concrete at the time of cracking while the modulus ratio n_e and effective reinforcement ratio, ρ_{eff} can be obtained from the table and methods outlined in the Code respectively

In this case, minimum reinforcement ratio, ρ_{min} is equal to 0.0035 if the reinforcement containing 400 MPa is used.

5.8 Other researchers

A number of researchers including Hughes (1972) and (1973), Campbell-Allen and Hughes (1981) and Beeby (1979) proposed methods to calculate a minimum amount of reinforcement in the member. In all cases, they were developed for a reinforced concrete member with fully restrained supports subjected to shrinkage and temperature changes. A general equation for a minimum reinforcement ratio, ρ_{min} can be derived based on the following considerations:

First, consider a stage after which a crack has formed and equate forces in the regions of uncracked (region 1) and cracked (region 2) regions as shown in Figure 5.3.

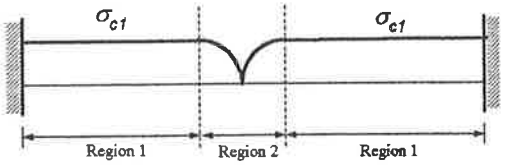

(a) Concrete stresses along the length of the slab

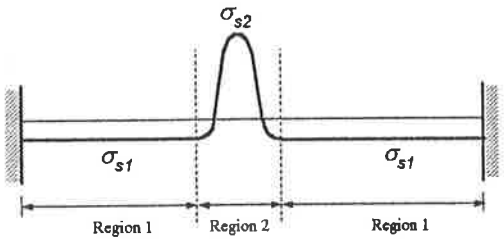

(b) Tensile stress in the reinforcement

Figure 5.3 Equilibrium of forces in uncracked and cracked region

An equilibrium equation can be obtained as shown;

$$A_s\sigma_{s2} = A_c\sigma_{c1} - A_s\sigma_{s1} \tag{5.13}$$

where σ_{s2} = the tensile stress in reinforcement in region 2

σ_{c1} = the tensile stress in concrete in region 1

σ_{s1} = the compressive stress in reinforcement in region 1

The reinforcement ratio is also defined as;

$$\rho = \frac{A_s}{A_c} \tag{5.14}$$

By rearranging equation (5.14) and substituting it into equation (5.13), the following relationship can be obtained as;

$$\rho = \frac{\sigma_{c1}}{\sigma_{s2} - \sigma_{c1}} \tag{5.15}$$

Therefore, a minimum reinforcement ratio, ρ_{min} can then be obtained by assuming that the tensile stresses in the reinforcement and concrete approach their yield strength simultaneously.

Hughes (1972) presented several techniques to determine the value σ_{c1}. The analysis by Brickell and Hoadley (1976) accounted for σ_{c1} by equating compatibility equation for the compressive strain in the bonded regions remoted from the crack. However since the value of σ_{c1} is much smaller that σ_{s2}, it is quite reasonable to ignore or approximate it to zero, (Hughes, 1978). Hence when $\sigma_{s2} = f_{sy}$ and $\sigma_{c1} = f_t^{'}$, the minimum reinforcement ratio can be given as;

$$\rho_{min} = \frac{f_t^{'}}{f_{sy}} \tag{5.16}$$

where $f_t^{'}$ = the tensile strength of concrete

f_{sy} = the yield strength of the reinforcement

Hughes (1978) further modified equation (5.16) to allow for the possible variation in material properties and adopted tensile strength of concrete after 3 days for $f_t^{'}$ value. Therefore, another equation for critical reinforcement ratio was proposed as follows,

$$\rho_{crit} = K_1 \frac{f_t'}{f_{sy}} \tag{5.17}$$

where K_1 = a factor to provide for the possible variation in materials properties, and in general can be taken as 1.1

Similarly, Campbell-Allen and Hughes (1981) suggested the following expression for the minimum reinforcement ratio,

$$\rho_{crit} = \frac{1.2 f_t'}{f_{sy}} \tag{5.18}$$

In general, direct tension cracking causes by these effects, develops when concrete is still immature. Therefore, tensile strength of concrete in its immature state must be used in equation (5.18). Brickell and Hoadley (1976) suggested that a first crack is likely to form after 24 hours of concrete casting. Hughes (1971) and (1972) recommended an expression for tensile concrete strength after 3 days as an upper limit should be substituted into the equation (5.18). Both Vetter and Evans, as reported by Brickell and Hoadley (1976) used concrete strength of either 7 or 28 day concrete strength to evaluate the minimum reinforcement ratios in their studies.

Most researchers, Evans and Hughes (1968), Hughes (1972) and (1973) and Campbell-Allen and Hughes (1981) agreed that yielding of reinforcement and the subsequent formation of wide cracks would not occur provided that ρ is kept above ρ_{min}. Brickell and Hoadley (1976) further commented that even though the critical reinforcement ratio is satisfied, crack widths may not be within limiting values for durability, serviceability or strength. In effect, additional reinforcement may be required to obtain finer cracks. Murray (1991) further advised that maximum tensile stress of 200 MPa should also be imposed in the reinforcement to ensure a reasonable crack widths.

As already discussed in Chapter 3, Base and Murray (1978) and (1982) disputed the accuracy and suitability of the traditional approaches (as suggested by Hughes (1972) and (1973) to control cracking. Hence they proposed an alternative method

which contradicts the traditional believes and assumptions in direct tension cracking.

So far in this review, the equations for minimum reinforcement ratio are directly depended on both the area of concrete A_c and area of reinforcement A_s. The problem lies whether to adopt the gross section area or just the effective area which contributes to the restraining action. Harrison (1981) explained that only a finite area within an effective zone around the reinforcement restrains the contraction of concrete. Therefore this effective zone must be used for area of concrete rather than the gross section. In addition, the use of concrete gross section of concrete in the design can be uneconomical and unnecessary for the control of surface crack widths. This is applicable in particular to a massive concrete section where strain distribution across the cross-section can not assumed to be uniform since shrinkage and thermal strains only occur close to the surface.

Hughes (1972) advised that the reinforcement ratio should be based on an effective "surface zone" where an effective thickness that only contributes to surface cracking be used in the analysis. These arguments generally agreed favourably with the recommendations from CEB Manual (1985) discussed in Section 5.2

5.9 Summary and conclusion

From this review, it can be seen that a minimum amount of reinforcement is typically specified by codes and standards to ensure that yielding of the reinforcement does not take place. The values may be influenced by subjective decisions made by the designers, as well as by the contribution from external factors such as environment, climate and exposure conditions.

In the design codes reviewed, CEB Manual (1985) provides the most comprehensive treatment for reinforced concrete members subjected to only axial tensile forces. Although, it is not as straight forward as some, the requirements apply to many situations where restrained and imposed deformations are the cause of cracking. A procedure is also given to calculate crack spacing and crack width for design, even though it is stated that for a restrained reinforced concrete member, it may not be necessary to carry out such calculations. This is because cracking in restrained

members may not actually reach a stabilising state. In addition, a minimum reinforcement ratio is specified, but an effective area section of concrete is used rather than the gross area section.

In many ways, the CEB-FIP 1990 (CEB-FIP, 1993) adopted similar design assumptions and analytical procedures to the CEB Manual (1985). As with the CEB Manual (1985), it was developed based on long experience and research output of the Euro-International Committee for Concrete (CEB) which carried extensive experimental investigations on this topic. As a result, it should be expected that fundamentally, both methods are closely related. In fact, the existing CEB-FIP 1990 (CEB-FIP, 1993) is a revision of the preceeding code published in 1978 to improve the understanding of the performance of concrete and improving the analytical and design techniques over the previous ones.

AS3600 (SAA, 1994) and ACI 318-89 (ACI Committee, 1989), on the other hand, briefly treat the topics of cracking due to shrinkage and temperature effects. Neither requires the calculation of crack width as a standard procedure. The correct interpretation of terms like "degree of restraint" and "primary and secondary" in AS 3600 can also have a large influence on the amount of reinforcement provided. Unlike AS3600, ACI 318-89 does not relate direct tension cracking to other factors such as degree of restraint, degree of crack control etc. In addition, both codes assume that the reinforcement for flexure in the span direction is sufficient to accommodate cracking caused by shrinkage and temperature effects, while in the direction orthogonal to the span, a minimum amount of reinforcement is specified. While ACI 224 (ACI, 1986) emphasises the importance of crack control due to direct tension, it does not impose any specific values for reinforcement. It does stress however that the reinforcement can be used to control both crack spacing and crack width most effectively when it is closely spaced and the diameters are kept as small as possible.

Likewise, BS8110 specifies a minimum reinforcement ratio to control shrinkage and temperature cracking. The Code assumes that a similar amount of reinforcement to reinforced concrete walls subjected to shrinkage and temperature should ensure similar satisfaction in other members. The analytical method to calculate crack

width is however more complicated. It seems that the equation was developed mainly for cracking due to flexure and, as is the case with other design codes, they tend to assume that cracking due to flexure is the primary concern. Once it is satisfied, cracking due to axial tension becomes a secondary concern which only has to satisfy the minimum reinforcement ratio.

Methods developed by Hughes (1972) and (1973), Hughes (1978), and Cambell-Allen and Hughes (1981) provide similar approaches to those of the design codes. Unlike some codes, however, they were specifically developed for shrinkage and temperature cracking rather than cracking due to axial tension. The experiments conducted were based on reinforced concrete walls subjected to shrinkage. Nevertheless, it should be applicable to other type of structures, including the slab system. The equations from Hughes (1978) and Cambell-Allen and Hughes (1981) are actually derivatives of the original equation from Hughes (1972) and (1973). Hughes (1978) refined the equation given by Hughes (1972) and (1973) by accounting for the possible variation in material properties and adopted tensile strength of concrete after 3 days for f_t' value.

In summary, it can be concluded that control of cracking due to restraint deformation is possible through the use of sufficient reinforcement in the member. A large number of literature and design codes reviewed, provide a minimum value of reinforcement to ensure that excessive cracking does not occur. As a result, it is not necessary to calculate the crack widths if this is satisfied. Table 5.5 summarises these recommendations to demonstrate their differences. Moreover, it is also a good practice to use the reinforcement with smallest diameter and spacing as practical as possible to effectively control the magnitude of crack spacing and crack widths.

Nevertheless, it should be understood also that designers should not merely accept these simple code methods for determining crack control reinforcement areas without questioning or understanding the limitations in certain cases.

Table 5.5 A summary of various minimum reinforcement ratio equations

Methods of crack control	**Minimum reinforcement ratio, ρ_{min}**
AS3600	ρ_{min} = 0.0063 for deformed bars with yield strength of 400 MPa where severe exposure condition is critical ρ_{min} = 0.005 for deformed bars with yield strength of 400 MPa where exposure condition is less critical
ACI 318-89	ρ_{min} = 0.002 for deformed bars with grade 40 or 50 in slabs ρ_{min} = 0.0018 for deformed bars with grade 6031 May, 1998 or welded wire fabric in slabs
CEB Manual (1985)	$\rho_{min} = \frac{f_t'}{f_{sy}}$
BS 8110	ρ_{min} = 0.0025 for reinforcement with grade 460 or above ρ_{min} = 0.003 for reinforcement with grade 250
Hughes (1972, 1973)	$\rho_{min} = \frac{f_t'}{f_{sy}}$
Campbell-Allen and Hughes (1981)	$\rho_{min} = \frac{1.2 f_t'}{f_{sy}}$
Hughes (1978)	$\rho_{min} = K_1 \frac{f_t'}{f_{sy}}$

Chapter 6

Design of reinforced concrete buildings for restrained and imposed deformations

6.1 Introduction

Design of a reinforced concrete building for restrained and imposed deformations must be considered in the preliminary stages to ensure that all the potential problems are properly examined. If a building is poorly designed or the effects of imposed deformations are neglected, problems associated with excessive cracking can occur.

In normal circumstances, design for restrained and imposed deformations becomes a specific and unique problem for each building since it is not possible to develop a general design technique to satisfy all potential distress conditions in all buildings.

Nevertheless, several strategies can be used to ensure that a good design is achieved. This chapter considers these design strategies and investigates how they can improve the design of reinforced concrete buildings to minimise the effects of restrained and imposed deformations.

The first strategy follows on from the findings of previous chapters. A trial design is analysed to calculate all the forces involved and whether the serviceability can be satisfied. A second strategy is to control the restrained and imposed deformations so that do not compromise the serviceability of the members. A third strategy is to allow for partial or total deformation at discrete locations within the building structure so that there is relief of the tensile stresses in the concrete. This is achieved

by incorporating movement joints. As a matter of fact, a combination of these strategies may be needed in order to come up with the most feasible design solution.

6.2 Strategy 1: Analysis of members using sub-assemblage systems.

For a trial design, it is best to consider a structural system that avoids the use or incorporates the least number of joints as possible. For such design, Jürgen (1995) suggested that existing tables and rules of thumb for estimating the necessary numbers of joints should be avoided. In order to estimate the magnitude of the imposed deformations and the restraining forces, the results from previous chapters can be used. This is achieved by considering sub-assemblages in critical regions of the structure. The crack widths and crack spacings are then calculated and compared with the design requirements. If the design requirements are not satisfied, then modification of the trial design can be made by increasing reinforcement content to provide adequate control of the cracking.

Usually, reinforcement exceeding the minimum requirement is needed to control excessive cracking in regions where the section of the member is weakened by service shafts and stairwells or by the reductions in member thickness and sizes. Rogers (1972) designed a very long horizontal structure, in which cracks were not permissible at all by over reinforcing so that they could withstand the effect of temperature changes. After many years in service, the structure was still reported to perform as intended.

6.3 Strategy 2: Limiting the restraining forces and deformations

There are several ways in which the restraining forces and deformations can be restricted to an acceptable level. Some are applied during the design phase; others during the construction phase, to achieve a satisfactory outcome.

6.3.1 Controlling the causes of deformations

Ruth (1995) suggested a number of possible means to reduce the effects of shrinkage and temperature change. Controlling the construction process can reduce deformation due to shrinkage in a structure. As long as it does not significantly affect the schedule, the completion of any shrinkage-sensitive regions should be

delayed so that tensile strength of concrete can gain sufficient strength to accommodate any high tensile stresses which develop. Furthermore, casting of the concrete in a foundation slab can be sequenced so that the shrinkage is minimised. This can be achieved by adopting a checkerboard pattern where only alternate squares are cast at the same time, but it is often difficult to access the casting areas and time consuming to split the formwork, (Ruth, 1995) and (Rainger, 1983). A better alternative may be to cast the slab in alternate long strips, approximately 4.5 to 5 m in width with longitudinal construction joints between strips, (Rainger, 1983). The two types of casting patterns are shown in Figure 6.1a and b.

In modern ground slab design for large warehouses where it is necessary to break up casting into a number of pours because of its large size, post tensioning is often used to control shrinkage and temperature cracking. This is achieved by partially prestressing the slab approximately after 24 hours after casting. The results ensure a ground slab relatively free of cracks and with fewer expansion joints. However the adjacent casting area must be left accessible for partial and full stressing before pouring can proceed.

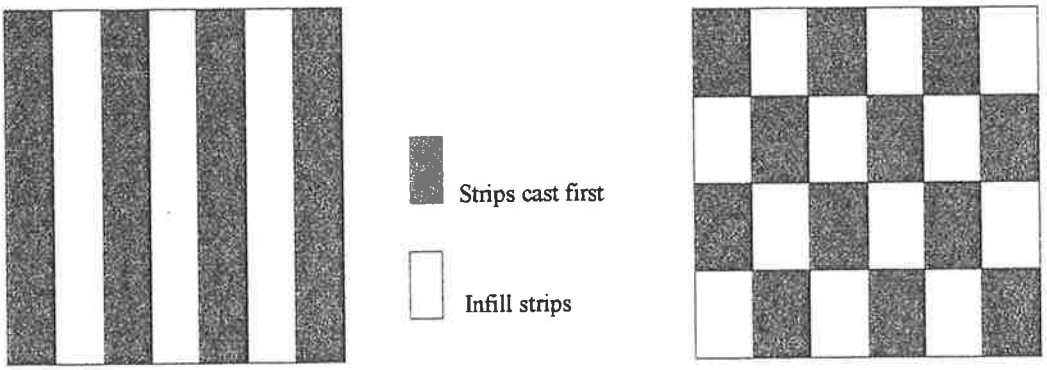

(a) Slabs casted in long alternate strips (b) Slabs casted in chequer board pattern

Figure 6.1 Two types of casting pattern to minimise restrained deformation in large ground floor slab

Another method which can be incorporated during construction is to reduce the effects of temperature which can contribute to large deformation. If possible, casting of members should commence when the temperature is at a medium level so that there is a smaller change in temperature experienced by the concrete. Casting in

extreme temperatures can also be alleviated by providing temporary thermal insulation to minimise the amount of moisture loss.

In addition, there are many factors that can influence the degree of shrinkage in concrete as already explained in Chapter 2. Thus, a suitable choice of concrete mix design can improve the tensile strength of concrete. Ruth (1995) recommended the concrete mixes with a low cement content and a low water/cement ratio.

6.3.2 Minimising the restraints and restraining forces

The position of structural members can greatly influence the degree of restraints and the development of restraining forces. Hence, it is important to carefully plan the locations of each member so that the interaction between members does not generate excessive restraining forces. To minimise the restraints, layout of stiff structural or members should be considered early in the design process. The positioning of shear walls, lift cores and other stiff lateral, load resisting members can be used to minimise restraint due to the induced deformations, (Alexander and Lawson, 1981).

Modern construction practice tends to brace building with shear walls or lift cores. These act as stiff regions, not only in resisting wind load, but also in resisting horizontal movement. A lift core generally offers great resistance to deformations in all directions while a wall would only does so in its own plane. Figure 6.2a illustrates cases where judicious positioning of these members is used to great advantage in reducing the restraint by allowing a greater degree of movement. Special attention should be drawn to the use of only one stiffening core and for shear walls perpendicular to the longitudinal facade. On the other hand, the arrangement of these members as indicated in Figure 6.2b illustrates poor designs which generate larger restraint amongst the structural members.

Restraints in the slabs normally originate externally from the supporting members, as well as internally from the reinforcement, but it is frequently very difficult to assess the amount of restraint provided by such supports precisely (Rainger, 1983). As already explained, the amount of restraint and restraining forces are largely dependent on the relative stiffnesses of the connected or adjacent members. It can be

shown that the problems caused by relative deformation between interior slabs and roof slabs can be minimised by introducing pin or hinged joints as shown in Figure 6.3 to permit some degree of free rotation.

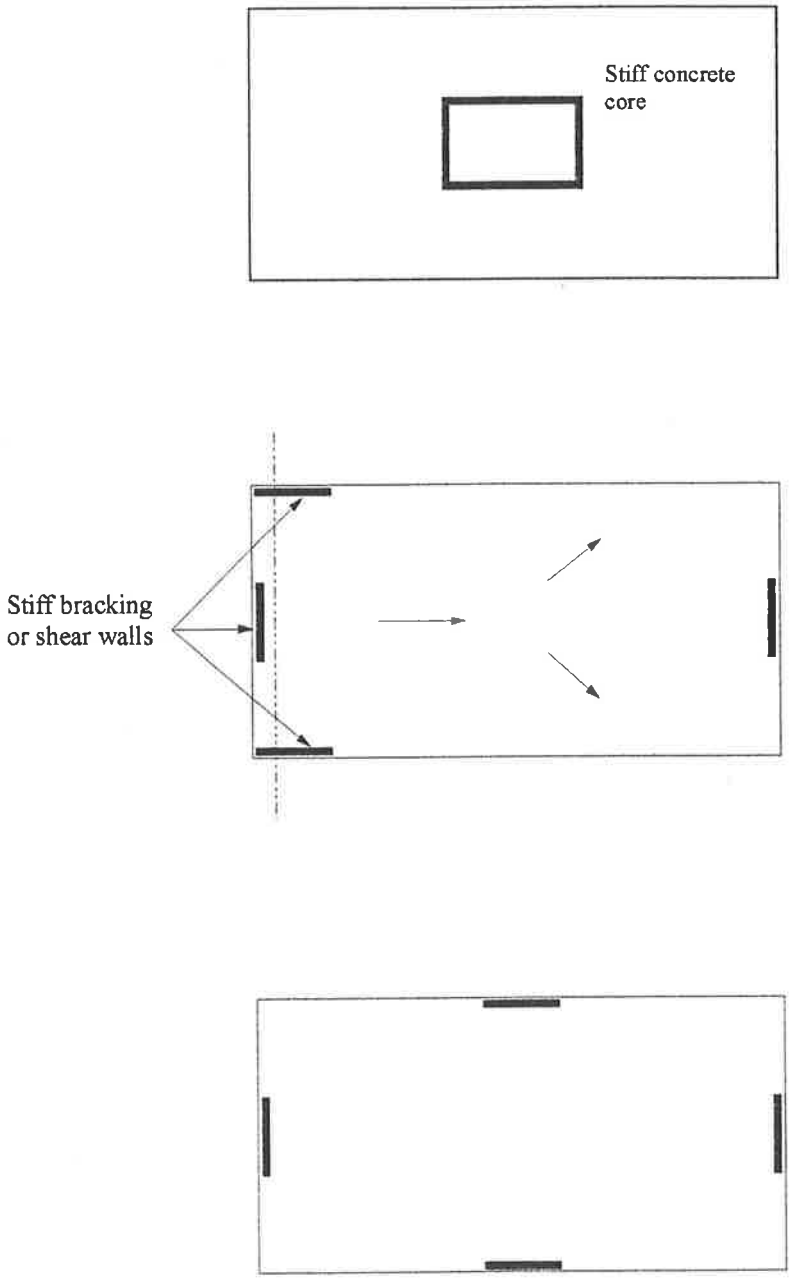

Figure 6.2a Correct positions of stiffening or bracing elements

In some situations, locations and type of connection of columns can affect the magnitude of restraining forces. Alexander and Lawson (1981) suggested that partial

connection of columns can reduce the build up of restraining forces in the structural system, in particular partially hinged columns can be more beneficial since they are less sensitive to temperature changes and thus should be used as long as the overall stability is not compromised.

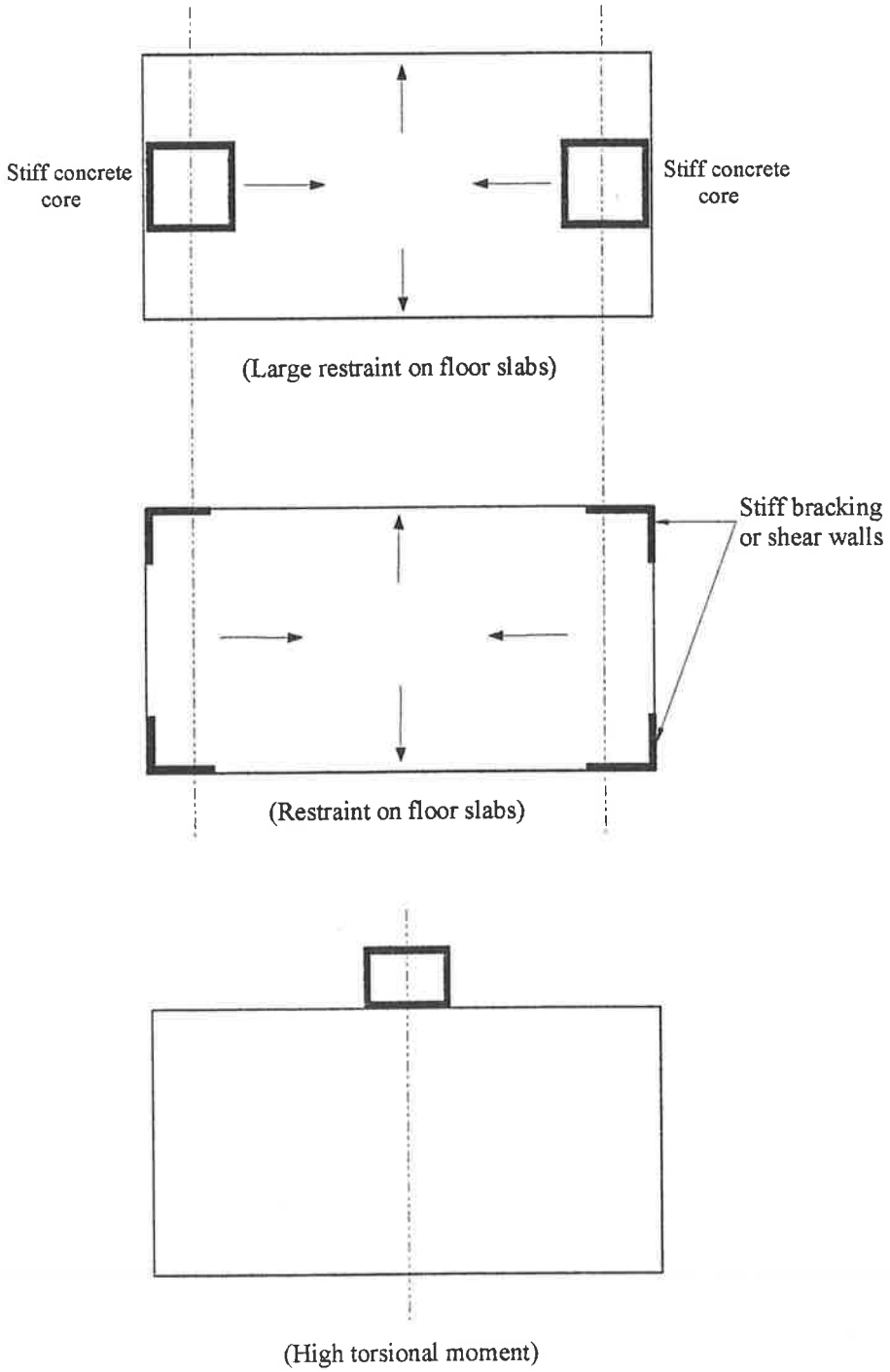

Figure 6.2b Incorrect positions of stiffening or bracing elements

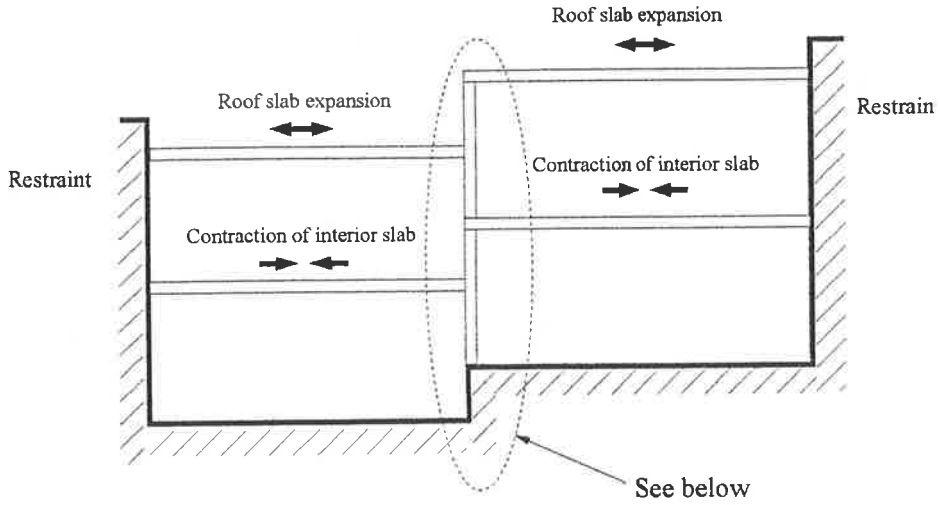

Slabs and colomns are rigidly attached to each other
(Reproduced from Figure 3.1a)

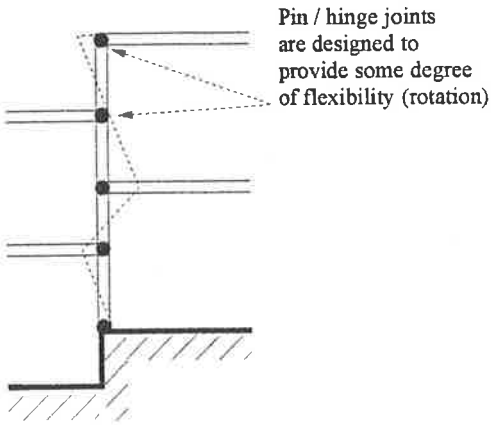

Figure 6.3 Pin or hinge joints incorporated to minimise restraint

Roofs are often subjected to higher temperature than the floors below, and columns should be design to move sympathetically. However, in car park construction, short columns adjacent to ramps may not, in practice be sufficiently flexible to permit this movement without cracking.

Research conducted by National Academy of Sciences (1974) also indicated that temperature effects on buildings with fixed columns based are likely to be more severe and cause more stress to the members than on buildings with hinged-column bases. Comparisons of two buildings indicated that induced stresses (shear forces,

axial forces and bending moments) caused by temperature effects at critical regions within the lowest story were almost double those at the corresponding locations in the hinged column building. Therefore, design of reinforced concrete buildings with a view to minimise restraint and resultant restraining forces, should consider the influence of the type of frame, type of connection to the foundation, and the stiffness against lateral displacement of the structural framing.

National Academy of Sciences further reported the influences of the symmetry of the building in terms of lateral stiffness against lateral displacement on the magnitude of stresses and deformations. They found that buildings, whose main structural frames provide identical stiffnesses against lateral displacement in both directions, are likely to develop smaller stresses and deformations than buildings whose main structural frames provide different stiffnesses against lateral displacement. The latter construction can exist in buildings where main structural frames such as columns or shear walls at one end offer significantly greater stiffness against horizontal displacement than the rest of columns.

With these two findings in mind, it is critical to investigate the influences of additional factors such as type of frame, type of connection to the foundation, and the stiffness against lateral displacement of the building structural frame (and the resultant restraining forces).

Good construction practice can also play a vital role in minimising restraints. Ideally, construction should proceed away from any likely restraint, and the restraints should be located towards the plan centre of the building so that large confining strains are not generated (Alexander and Lawson, 1981). In fact, designers should consult with the builder for some input in regard to method of construction or construction sequence during the design process when ever possible.

An example of construction of a slab spanning between concrete core and end restraints given by Alexander and Lawson (1981) can be used to illustrate this. For a single pour of slab spanning between rigid cores as shown in Figure 6.4a, restrained strain is induced according to the sum of the early-age temperature, in service temperature range and shrinkage strains. On the other hand, a slab which is poured

sequentially between the cores, can cause large lateral forces on the cores. The cores may not be able to provide sufficient restraint against such large forces, especially if the cores contain several blackouts and openings, which in this case may lead to shear cracking in the cores themselves (Figure 6.4b and c). Thus, it is recommended that the final pour should be relatively short, and delayed if possible to minimise the "locked in" strains.

6.3.3 Accommodation of restraining forces and restrained deformations

To some extent, the approach discussed in the previous section is adopted in the design so as to minimise or avoid the problem all together. In contrasting effects, the design strategy presenting here is used, possibly in combination with the previous strategies, to allow each member and the whole structure to be able to respond to imposed deformation in such a manner that its serviceability would not compromised.

As a consequence, this section investigates a number of design techniques used to accommodate for these restraining forces and deformations. Of cause, this task would not be possible to cover every design situations, but at least, this can be used to emphasise that clever design techniques always exist and can be cleverly applied in building structures to reduce or eliminate the problem.

One of the most notable efforts was by Khan and Fintel (1971) who presented several techniques to account for the effects of differential deformations in vertical members on other structural members such as slabs and walls. They suggested that it is possible and appropriate to design around the problem of these natures. Problem posed by differential deformations between the exterior columns and the shear walls and their adverse effects on the slab system can be avoided by forming hinges around the shear walls connecting to the slabs, at least in the upper stories, to avoid high moments (Figure 6.5a, b and c). Details shown in these figures can be used to eliminate the possibility of spalling due to overstress of the slab at the wall, Khan and Fintel (1971). In fact, this detail was successfully used in a 38 story building in USA from the 29th story onward.

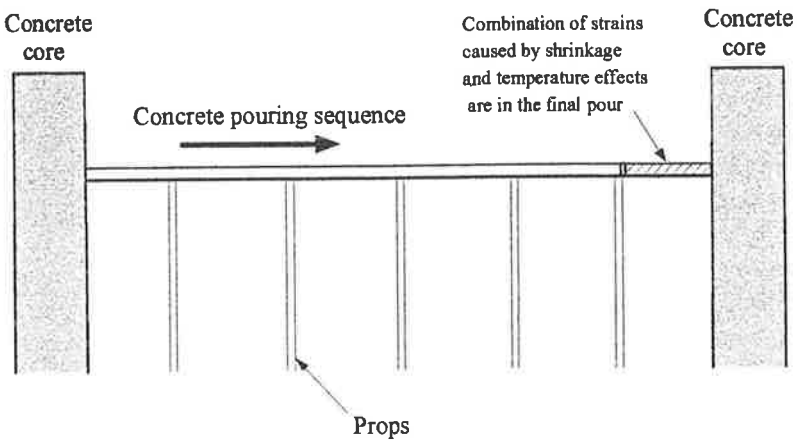

(a) Recommended slab construction sequence between concrete core (reproduced from Alexander and Lawson ,1981)

Plan of interior slab below roof slab

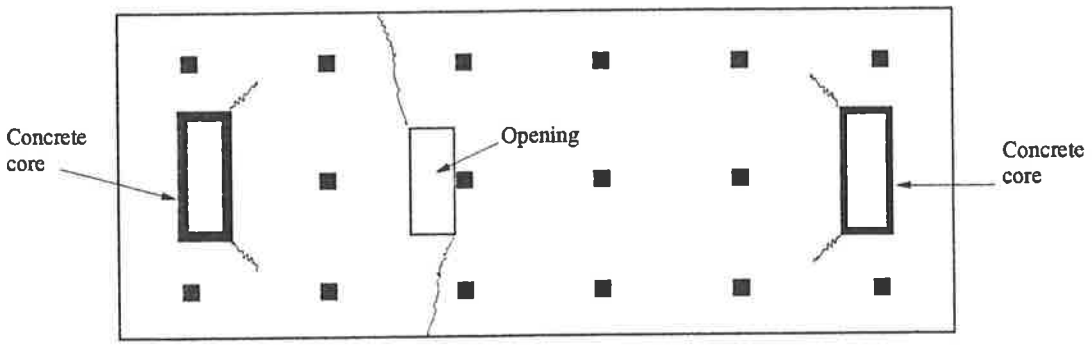

(b) Possible major cracks form at plane of concentration of strain

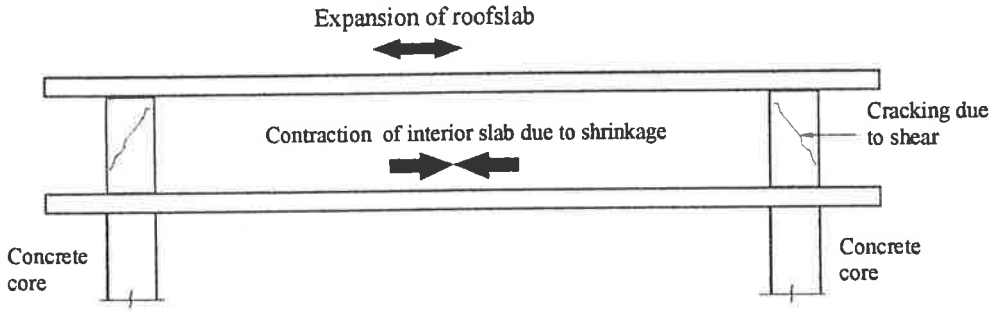

(c) Cracking as a result of different deformation between roof slab and interior slab

Figure 6.4 Cracking in slabs and walls due to imposed deformation (reproduced from Alexander & Lawson, 1981)

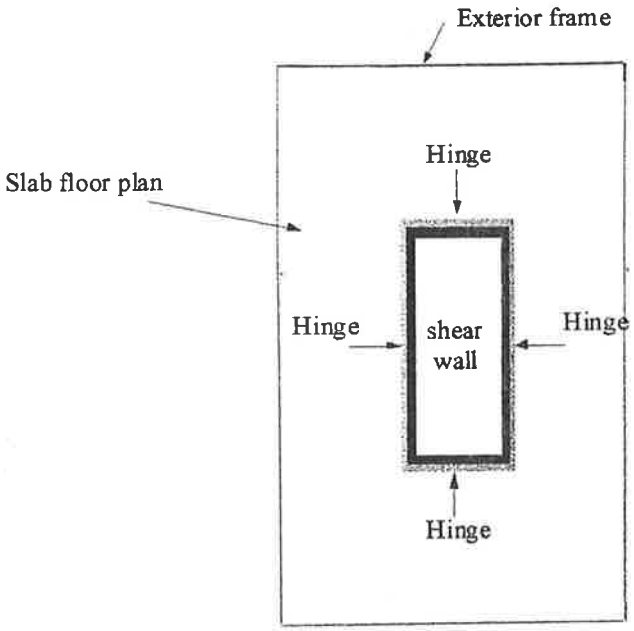

Figure 6.5a Hinging arrangment of slab around shear wall (based on drawing from Khan & Fintel, 1972)

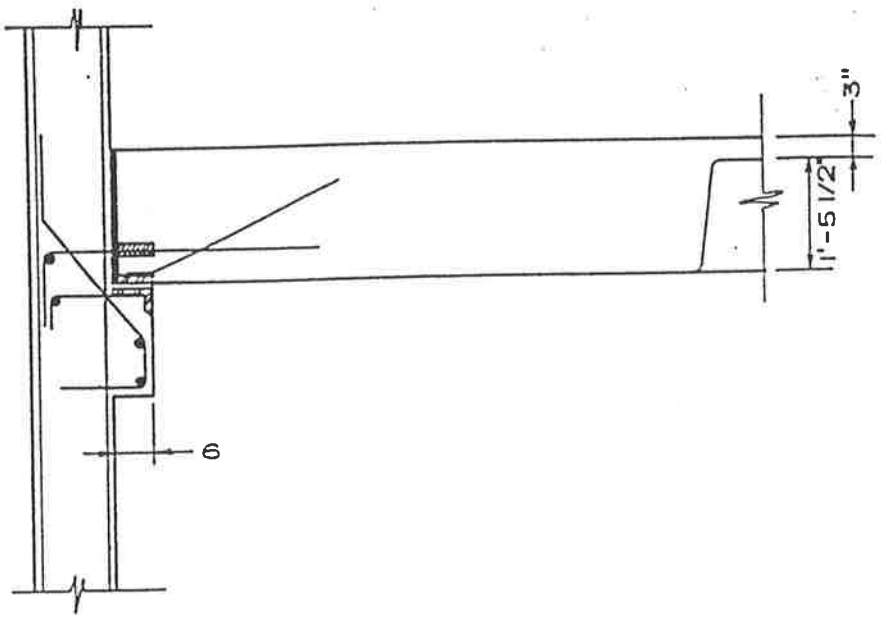

Figure 6.5b Hinge at joist section (reproduced from Khan & Fintel, 1971)

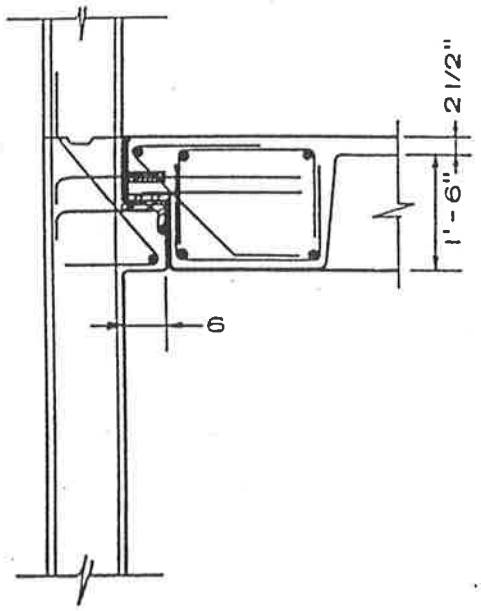

Figure 6.5c Hinge at waffle section (reproduced from Khan & Fintel, 1971)

However, problem concerning differential deformation in large interior columns close to shear walls requires different solution to the above. Khan and Fintel (1971) suggested that it could be overcome by connecting them with a deep beam which, in effect makes the columns act as parts of the shear wall. This is illustrated in Figure 6.6. The main function of the deep beam is to transfer loads from the shear wall into the adjacent columns, thus creating an equalising effect. As an alternative, a very heavy beams (story high) at the roof level or at intermediate and roof levels can be used to perform the same function.

Columns in reinforced concrete buildings which contain different percentages of reinforcement and different volume to surface ratio, are also more susceptible to differential shortening. In particular, buildings with over thirty stories can be over-stressed in the region close to the junction between slab system and column. In similar effect, rigid slab and beams can also be sensitive to differential vertical deformation at the supports due to differential foundation movements. As a result, it may be advisable to consider longer span between the rigid slab and the adjacent columns during the design stage to allow the structure with greater flexibility. Khan and Fintel (1971) recommended that structures with over thirty stories should be designed so that all interior columns have identical percentage of reinforcement.

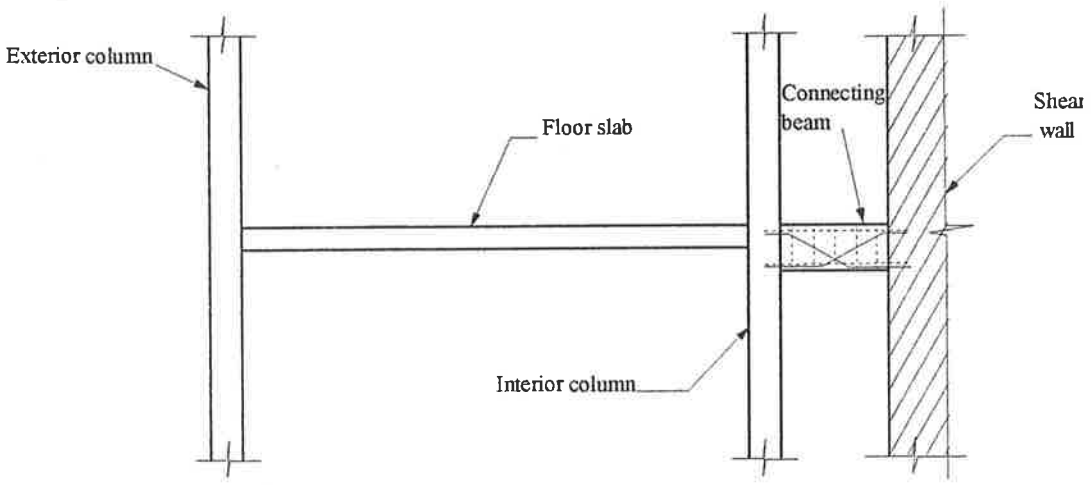

Figure 6.6 Connecting beam between interior column and shear wall (based on drawing from Khan and Fintel, 1971)

6.4 Strategy 3: Accommodation of deformations by incorporating movement joints

So far, strategy 1 and 2 concentrate on ways in which imposed deformations and restraining forces can be controlled or minimised. In other words, reinforced concrete buildings can be designed so as to avoid the problems or they can be designed to live with the problems. However, it is very often that the magnitude of imposed deformations and restraining forces in the members can remain very large even though all the design provisions have been adopted. In addition, if the reinforcement requirements are unacceptably high, due to cost or other adverse effects on performance, a compromise between the first two approaches has to be made. This is achieved by allowing greater deformations in the structure. A simplest way is to have a complete or physical discontinuity by introducing movement joints in the sub-assemblage which is being investigated.

A cost comparison of the alternative solutions, namely extra reinforcement, design modification, or a movement joint allows the most feasible design decision to be made. If movement joints are necessary, then a re-evaluation of the design is advisable in order to rationalise the locations of joints and to ensure that other requirements such as robustness are satisfied.

The topic of movement joint in reinforced concrete buildings is discussed in more detail in Chapter 7.

6.5 Summary

Design of reinforced concrete buildings to withstand restrained and imposed deformations requires the investigation of the material properties used in the buildings, causes and effects of imposed deformations, and how to control imposed deformations. It is however difficult to generalise a design approach to handle every distress conditions since each building is unique in many aspects, including structural layouts, design criteria, functional requirements and construction methods. Thus, each building structure needs to be assessed individually to evaluate the effects.

Three design strategies have been recommended which can be considered during the design process to design for restrained and imposed deformations. First is to use the procedures suggested in previous chapters (in particular Chapter 4) to evaluate the relevant forces involved. It is important to avoid the use of movement joints if possible. The crack width obtained is then checked against the design requirements. The second strategy studies different ways in controlling the magnitude of imposed deformations and the deformation itself. This is achieved by clever design which circumvent the problem of imposed deformations. The third strategy is to accommodate the deformations by incorporating movement joints.

In conclusion, it is apparent that control of restrained and imposed deformations requires more than just sufficient reinforcement to satisfy all the building code criteria. Planning for the locations of each member should be considered early so that the interactions between each member does not result in large build up of internal stresses or restraining forces. This can be achieved by understanding of how both structural and non-structural members responds to imposed deformations caused by time-dependent deformations so that early remedies can be provided. Being able to recognise all the important factors that affect the causes of deformations, is also another critical step which can lead to successful design of this type of structure.

Chapter 7

Movement Joints in RC Buildings

7.1 Introduction

Movement joints by many are considered as artificial cracks which are strategically placed to minimise cracking in other parts of the structure. By introducing movement joints, weak regions in the structure are created so that cracking occurs in these designated locations where it is of little importance, or produces little visual impact. For example, in situations where the use of additional reinforcement is not practical to control excessive cracking, movement joints can be used to concentrate the cracking in preformed grooves. As another example, movement joints are used in the sanitary structures to relieve tensile stresses associated with shrinkage and temperature changes (Rice, 1984 and Gogate, 1984) and hence to minimise crack width and leakage.

Movement joints are also used in many building structures to isolate various members so that they behave independently, in order to satisfy design constraints or to simplify of the analysis. Sometimes movement joints are used against existing construction to avoid excessive restraining forces. In precast construction where members have to be limited in size due to the restriction of crane capacity and the option of achieving continuity is not possible in the structure, movement joints have to be used.

As discussed in Chapter 7 by Rüth (1995), designers should first investigate all the possibility of eliminating the use of movement joints in building. If this is not possible, the number of joints used, should be kept to minimum and be as simple as possible. Problems also result because joints are given insufficient attention by designers both in terms of their locations and detailed design. In many aspects of

structural engineering, the most successful projects are based on well considered conceptual designs (Barton, 1989). It is crucial that designers properly identify and assess all the relevant factors during the early design stages.

Barton (1989) recommended that the following factors should be investigated prior to adopting movement joints in building structures;

a) magnitude of thermal, elastic, creep and shrinkage deformations without joints;
b) magnitude and locations of the restraining forces which develop in the structure;
c) building length compared with the empirical recommendations for joint spacing; and
d) effect of cracking on architectural elements and finishes.

After the investigations of the above factors are carried out, designers must decide whether a complete physical separation is required, or a partial separation with the transfer of some force components. Past experience has shown that joints which are completely separable are the most reliable and easiest to design and construct. Rüth (1995) pointed out that most damages observed in buildings indicated that the intended function of joints is not often achieved in practice because of an incorrect choice of joint detail and the precision needed for proper functioning of the joints can not be attained during construction. Sometimes a lack of supervision during construction results in design assumptions being different to the construction procedures. Therefore it is crucial that designer's participation in the project should continue right up to the completion of the building.

7.2 Types of movement joints (Review of current practice)

Various types of movement joints are used, depending on the type of movement to be allowed. In reinforced concrete buildings, they can be categorised into two major groups. The first group consists of joints that provide total physical separation between the adjacent members, and hence allow free translation and rotation in all directions of each member, thus relieving all tensile stresses in the region. These are referred to as expansion joints or isolation joints. The second group consists of

joints that only provide partial separation. In this group, reinforcement may be continued across the joint but the section is either reduced or debonded. The reason for this is to establish a plane of weakness to force the cracks to occur within the joint. These joints accommodate movement in one direction only, and are often referred as contraction joints or shrinkage control joints.

7.2.1 Expansion Joints or Isolation Joints

These joints are mainly used to reduce restraining forces which develop as a result of temperature changes. They are frequently located to isolate walls from floors or roofs, or to divide long concrete decks into shorter lengths. Expansion joints are also referred to as isolation joints (Barton, 1989). They are complicated and require routine maintenance to keep them functioning as intended. By properly locating the joints, the restraining forces can be largely eliminated by permitting the separated members of the building to expand and contract freely without affecting structural integrity or serviceability (ACI 224, 1995). The expansion joints thus isolate the building members and alleviate cracking due to contractions in the structure.

The width of the joints as recommended by ACI 224 (1995) should be in the range of 25 to 150 mm, depending on the maximum temperature rise. Nonetheless, it should be sufficient to withstand the largest relative movements occurring under extreme conditions such as earthquake and, the separated members must not come into contact at any times. CCAA (1996) also suggested that a joint width of at least 25 mm is needed to allow easy removal of formwork from the gap between the members.

In general, no reinforcement is usually taken through expansion joint but it is not unusual to include it to transfer shear and prevent differential deflection. These are shown in Figure 7.1. The reinforcement, if present, must be debonded to allow free axial movement as shown in Figure 7.1a. and are common locations at door openings or areas which are frequently accessed.

As stated earlier, expansion joints are mainly used so that the separated members can expand and contract freely due the temperature changes, but often they can also be used to accommodate differential foundation movements. The term "expansion

joint", as suggested by Potter (1969), is misleading since the overall shrinkage for a concrete structure is generally larger than the probable expansion due to temperature changes. Warner et al (1998) also reported that some designers argue that the contraction due to shrinkage effect would always exceed any expansion which can occur. As a result, expansion joints can be replaced by contraction joints in all normal structures.

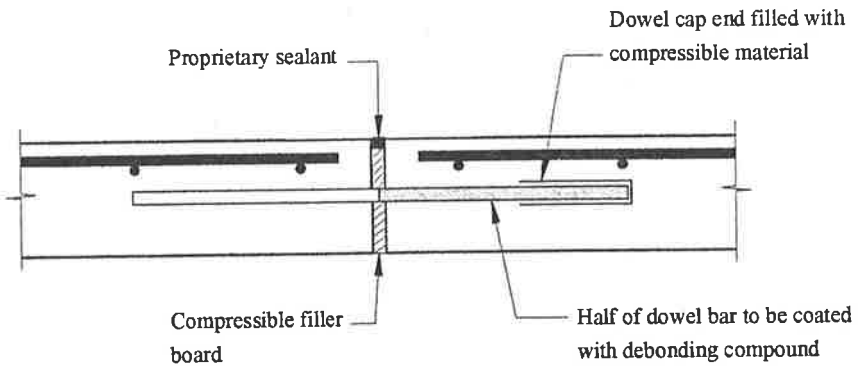

(a) Details of reinforced expansion joint

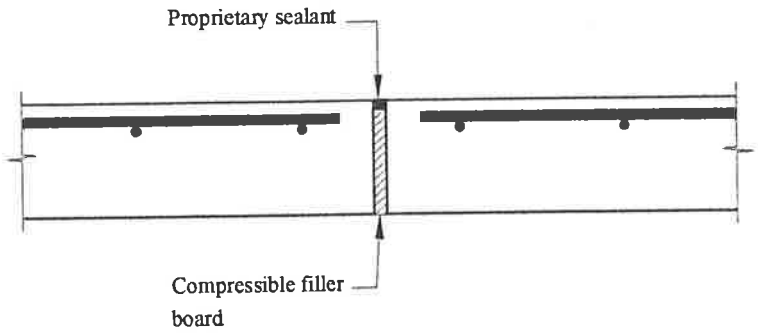

(b) Details of free expansion joint

Figure 7.1 Expansion joints in reinforced concrete structures

7.2.2 Contraction Joints

This type of joint is mainly used to reduce cracking caused by shrinkage and temperature changes in concrete members. A plane of weakness in the member

section is created by either reducing the concrete cross section and reinforcement, thereby forcing the cracks to occur in this region. In building structures, contraction joints are primarily used in walls and in slab-on-ground, but are not unusual in suspended slabs.

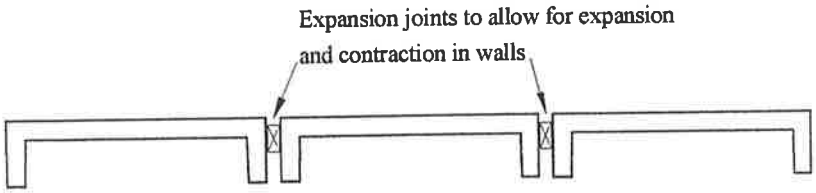

(c) Expansion joints in walls

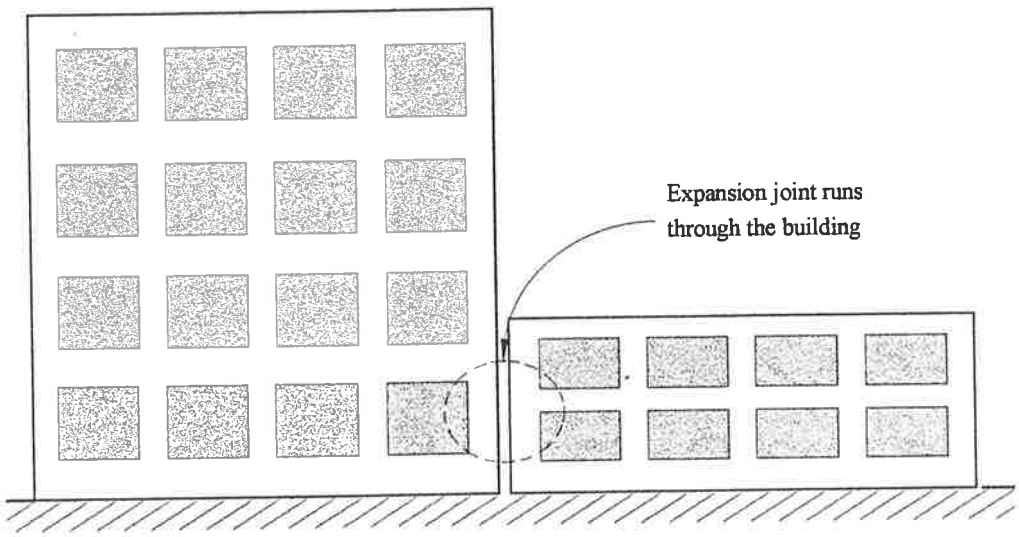

(d) Expansion joint in buildings

Figure 7.1 (continued) Expansion joints in reinforced concrete structures

In terms of reinforcement, contraction joints can be further divided into two types. One is where there is a complete termination of reinforcement at the joint as shown in Figure 7.2a. This is preferred in building construction. It is commonly found in liquid-containing structures to cater for early thermal movement and drying shrinkage where no load transfer or equalising of deflection in the plane of the joint

is wanted (Bussell & Cather, 1995). The second type is where part of the reinforcement extends across the joint, possibly for shear transfer and to maintain some structural stability or restrict differential deflections (refer to Figure 7.2b). Warner et al (1998) suggested that some moment could be transferred across the joint because the faces on the compressive side close if a moment is applied. Nonetheless, the moment at such a joint is substantially lowered by the reduced concrete area. This type of joint is also used in liquid-containing structures, but can be found in retaining walls and large ground-bearing slabs (Bussell & Cather, 1995). The plane of weakness in the section is maintained by debonding the reinforcement or reducing the area of concrete or reinforcement to satisfy the primary function of the joint. There are other types of contraction joints with different details but to serve the same functions. These include tied partial and keyed contraction joints which are illustrated in Figure 7.2c and d respectively.

7.3 Factors affecting the locations of joints

Movement joints should always be placed to relieve the high tensile stress which develops for the reasons discussed in Chapter 2. The main factors affecting the general locations of movement joints in building structures are discussed here. A more comprehensive discussion about movement joints and their locations with respect to each structural member in a building can be found in Rainger (1983), Bussell & Cather (1995) and ACI 224 (1995). Nevertheless, as a general rule, they should be located where there is an abrupt change in concrete element or building profile and plan (Figure 7.3a). Rainger (1983) also suggested that movement joints may be required in locations where there are changes of loading or loading capacity, changes of direction and at planes of change in construction material (Figure 7.3b and c).

High stress concentration often develops where a narrow region of the building is connected to a much wider and stiffer region of the building (Figure 7.4a). Expansion joints can normally be used to reduce the possibility of cracking. Similar problems can also arise in a floor or roof where differential horizontal movement may result in serious problems in the supporting columns or walls. A specially design pinned or hinged joint can then be incorporated (Rodin, 1969). This example

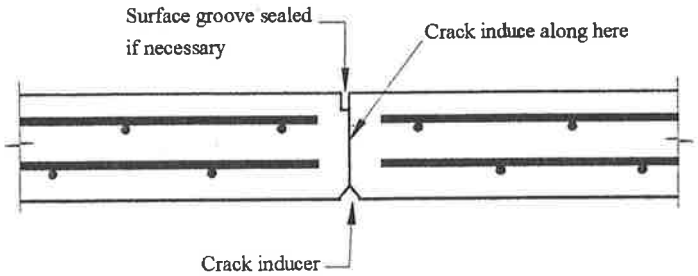

(a) Free contraction joint

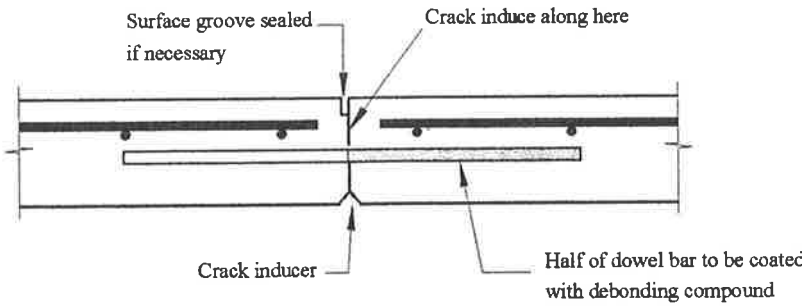

(b) Details of debonded partial contraction joint

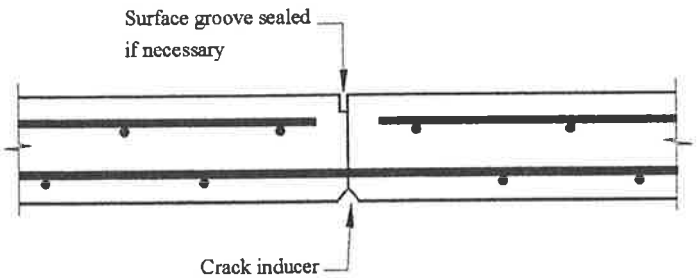

(c) Details of tied partial contraction joint

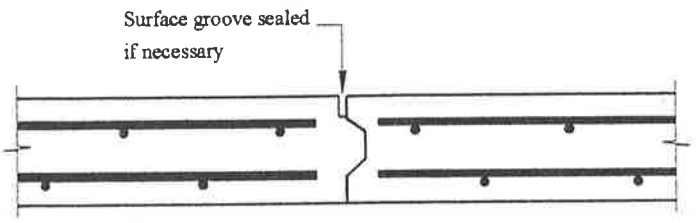

(d) Details of keyed contraction joint

Figure 7.2 Different types of contraction joints

is shown in Figure 7.4b. A recent study by Rüth (1995) recommended that the use of these joints should only be in critical regions of high stiffness where maximum forces develop. For example, movement joints may be used only in the lower floors where stiffness is at its highest and the inclusion of joints is most effective.

In addition, movement joints may be used to separate different systems within the same building or to separate the structure into two discrete structures (as in L-shape buildings). Provision should be made for the structures on either side to act independently and move with respect to each other. For example, the gap as indicated in Figure 7.6 must also be sufficient to accommodate the design earthquake deflections of both building (CCAA, 1996). Furthermore, Figure 7.5 (Bussell & Cather, 1995), demonstrates how a movement joint allows Block (a) with its stiff concrete core to undergo smaller deflection under wind load while Block (b) works as a frame and undergoes larger sidesway deflections. If the movement joint were not included in this structure, wind on the long face would generate torsional loading on the core and distortional movement would occur accordingly as shown in Block (c).

The other common area which may warrant movement joints in buildings is in the roof slabs or in floor slabs if the drying shrinkage is highly restrained. In these situations, thermal expansion of the concrete slab can dominate the overall deformation of the slab. In this case, EBS (1977) recommended that expansion joints should be incorporated in the slab otherwise overstressing and possibly damage may occur. Sometimes it may not be necessary to provide for movement in the remainder of the building. Boswell (1969) also suggested that subsequent expansion and contraction of the roof structure could be sufficient to cause failure by fatigue of the connection between roof slab and wall, hence it is critical that the connection is sufficiently designed against such failure. Figure 7.7 shows how rigidly attached wall panels can cause cracks on the external face of the building, simply because the roof area is not provided with expansion joints at suitable spacing (Boswell, 1969).

The influence of thermal effects in roof slabs should be investigated at an early stage in design so that the designers can decide where to locate the expansion joints. This

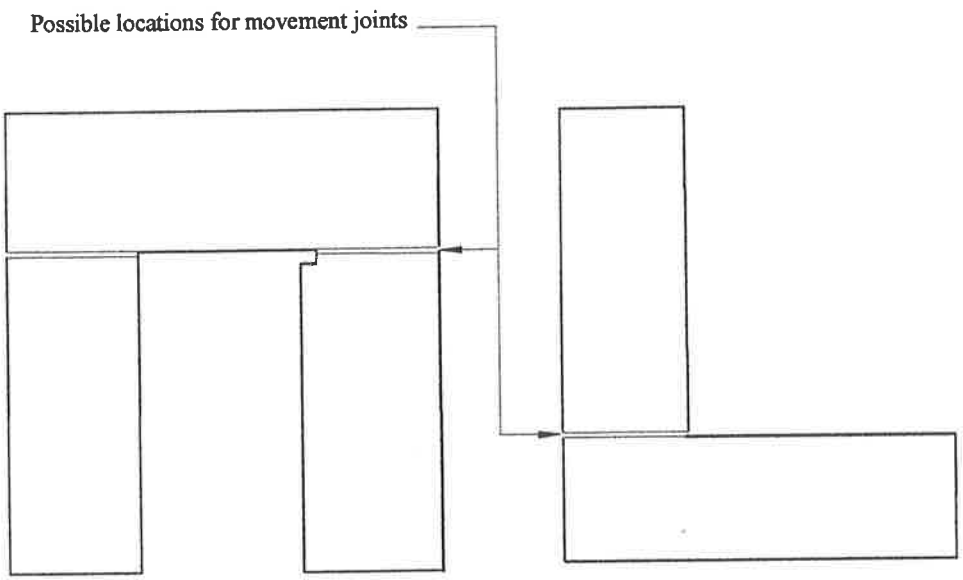

(a) Typical building plans with abrupt changes in plans/shapes

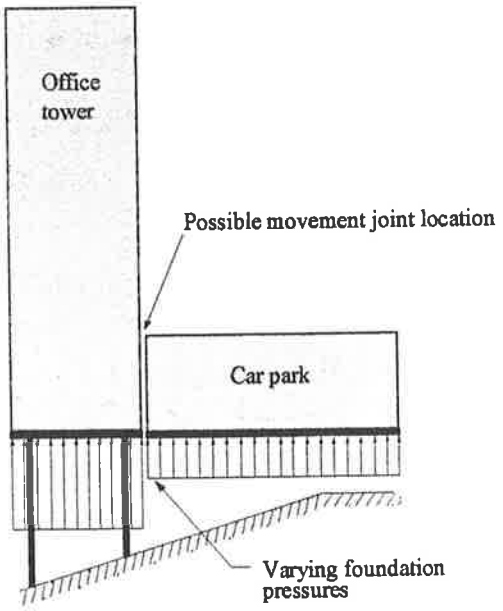

(b) Abrupt changes in loadings on foundation

(reproduced from Rainger (1993))

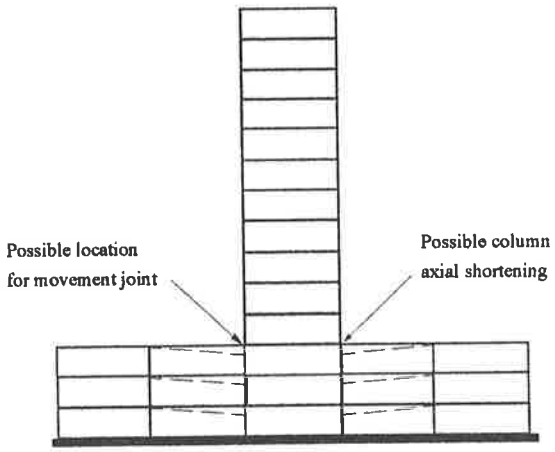

(c) Different loadings in columns

Figure 7.3 Various locations for movement joints in building structures

Furthermore, thermal movement may induce cracking in floor and ceiling finishes if they are of precast concrete (Boswell, 1969). Shrinkage effects are generally less severe in these areas because most of the shrinkage in precast concrete structures takes place in the factory yard. Nonetheless, differential shrinkage may contribute to serviceability problem if in-situ casting of concrete is also involved in the precast construction and should therefore be accounted for during design.

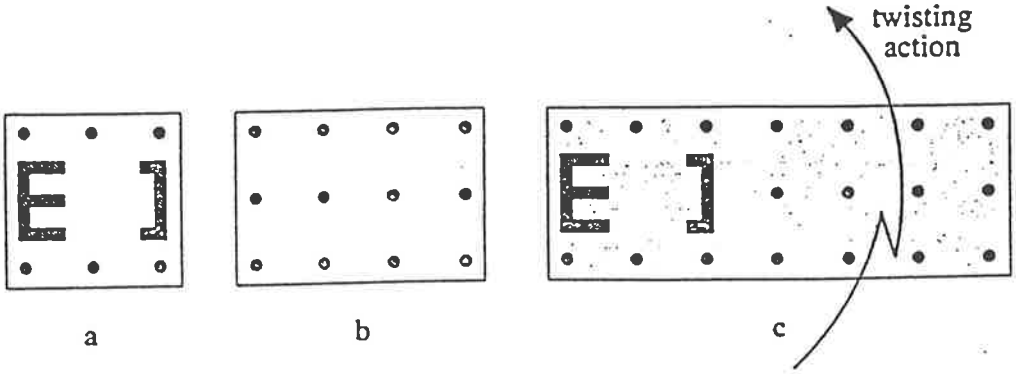

Figure 7.5 Movement joints for unsymmetrical structure (Bussell & Cather, 1995)

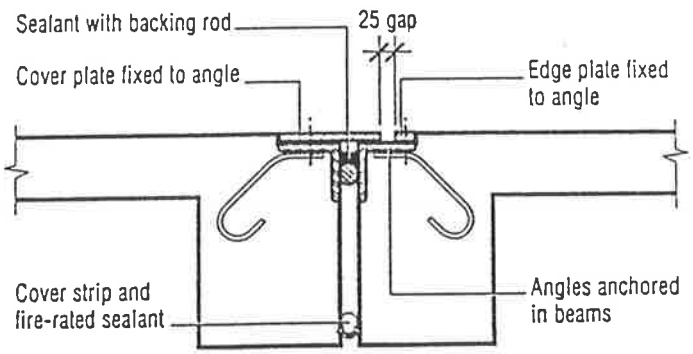

Figure 7.6 Gap between two members to allow for movement (CCAA, 1996)

Whenever expansion joints are used to cater for differential foundation movements, they should continue all the way through the structure. This can be carried out in practice by locating the joint in the slab on a line between twin rows of columns or between twin walls as shown in Figure 7.8a and b. The advantage of this design is that it permits movement in a number of directions. However the continuation of the joints may be terminated just above ground level if shrinkage and temperature effects are the main criteria because temperature changes are smaller and shrinkage takes place slower (therefore reduced by creep relaxation) in the ground floor (Bussell & Cather , 1995).

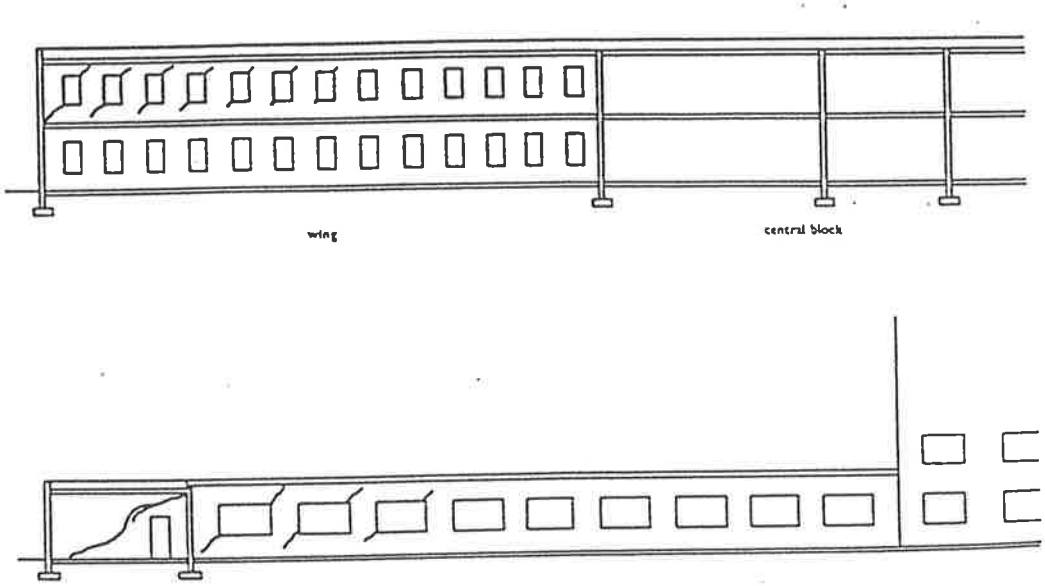

Figure 7.7 Examples of cracks on external of rigidly attached wall panels

Alternatively, expansion joints can be placed below single columns or single walls provided that one of the slab panels is attached to the column or wall while the other is supported on a sliding bearing.

In concrete slabs and walls, contraction joints may also be more desirable than expansion joints. If slabs are lightly reinforced, a large separating crack is likely to occur as the result of restrained deformation due to shrinkage. It has been well documented by various authors including Base and Murray (1978) that minimum reinforcement required for these effects generally is inadequate and as a consequence, contraction joints should be placed at regular intervals.

In cases where slabs extend beyond the building perimeter for example as external balconies, some consideration should be given to including expansion or contraction joints unless the transverse reinforcement is sufficient. It is well recognised that external balconies are prone to cracking perpendicular to their edges as a result of differential thermal movement and differential shrinkage of the concrete near the edge of the slab. Movement joint can also be used to relieve shrinkage between two cantilever slabs as shown in Figure 7.9, (Rainger, 1983).

In some situations, the introduction of movement joints may not be able to prevent cracking completely. Warner et al (1998) explained that cracking can still occur, in particular at re-entrant corners even when contraction joints are provided at regular spacing. A solution for this is to increase additional reinforcement and place it diagonally across the corners (refer to Figure 7.10). Warner et al (1998) further suggested that contraction joints should only be used where cracking is inevitable, in order to maintain the aesthetic of the member.

In USA, a number of building have been successfully built without expansion joints, but most authorities agree that it is good practice to place joints at changes in the plan cross section of the structure where stress concentrations are likely to develop.

7.4 Spacing of movement joints

There are no reliable rules which can be used to specify the spacing of movement joints. Each structure must be evaluated individually. For many years, the spacing is based on designers' judgement and previous experiences. If contraction joints are used, a choice needs to be made between joints at close spacing with relatively small amount of reinforcement, and joints at large spacing with high amount of reinforcement.

For walls and slabs with the reinforcement in the order of 2% of the total cross section area, contraction joints at close spacing are required to relieve the tensile stress caused by shrinkage and temperature. CIA (1989) suggested joint spacing in the range of 4 to 6 m where these lower reinforcement percentages are used and

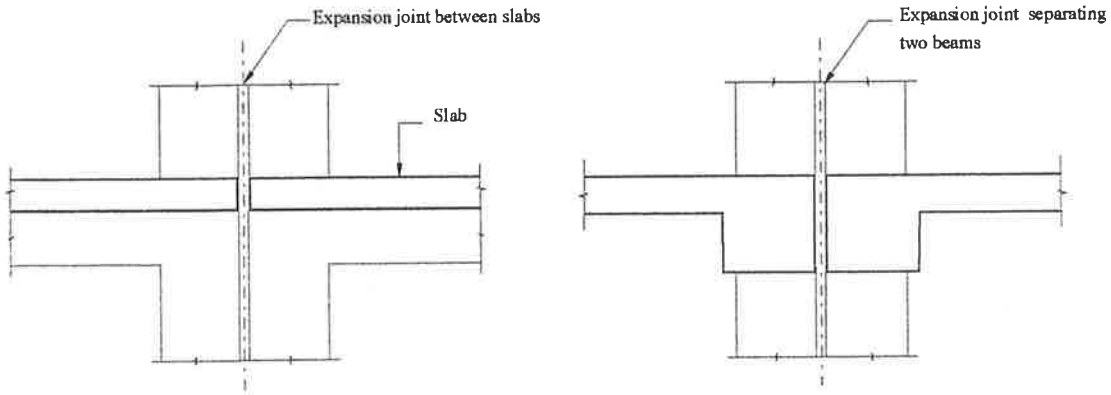

(a) Twin columns separating slabs (b) Twin columns and beams

Figure 7.8 Twin rows of column

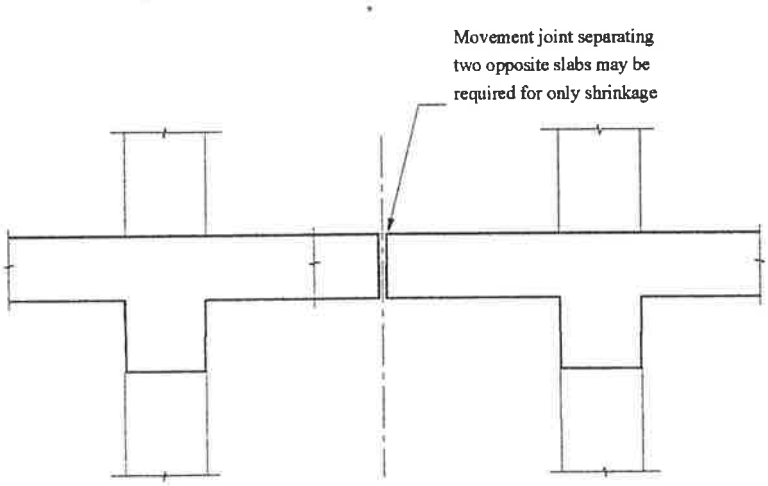

Figure 7.9 Cantilever slabs (based on drawings from Rainger (1983))

should not exceed 8m in concrete walls. ACI 224 (1995) suggested contraction joint spacing in the range of 4.6 to 9.2m. Portland Cement Association (1982) provided recommendations as to where to place contraction joints at opening in walls as illustrated in Figure 7.11. In addition, the panels enclosed between joints for both walls and slabs should have an aspect ratio of 1:1, with a maximum aspect ratio of 1:1.5. In areas where concrete surfaces directly expose to temperature variations and shrinkage, contraction joints at less than 3m spacing should be provided to minimise

cracking. This is particular applicable to external balcony slabs of buildings which are prone to cracking.

When expansion joints are used to isolate the movement of individual members, the maximum spacing depends on the exposure conditions and temperature variations in the structure. Barton (1989) suggested that a building greater than 45 to 50 m in length may require some movement joints to reduce cracking. Since there is no universal rules or accepted techniques to determine joint spacing, they can also varied from country to country. In Adelaide, Australia, a typical expansion joint spacing at Holdfast Shores Maria Pier Apartments is approximately 33 m. These are also chosen as construction joints. In UK, spacings of joints in large buildings are between 60 to 70m (Bussell & Cather, 1995). ACI 224 (1995) suggested a more conservative expansion joint spacing, varying from 9 to 60m depending on the type of structure. Nonetheless, ACI 224 (1995) found that in practice, the spacing is rarely less than 30m. When the structure is flexible in response to horizontal deformation, the spacing can also be increased. A flat roof slab supported by slender columns provides a good example for this situation. In contrast, an exposed structures supported on stiff elements may require a substantial closer joint spacing to reduce bending and horizontal shear force on the columns, (Bussell & Cather, 1995).

Moreover, local conditions can directly influence spacing of joints. Joint spacing used in cool, damp climate can be double of those in hot, dry climate regions. A study conducted by the US Building Research Advisory Board, as reported by Fintel (1974) and Bussell & Cather (1995), found that joint spacing up to as high as 180m could be feasible in framed symmetrical concrete structures for heated buildings in zones with very modest temperature ranges.

According to the review so far, the recommendations and guidelines for the joint spacings reviewed are varied and sometimes even contradicting. Table 7.1 and 7.2 contain summaries of movement joint spacings as recommended by a number of design codes and researchers. The references shown in these tables are given in ACI 224 (1995).

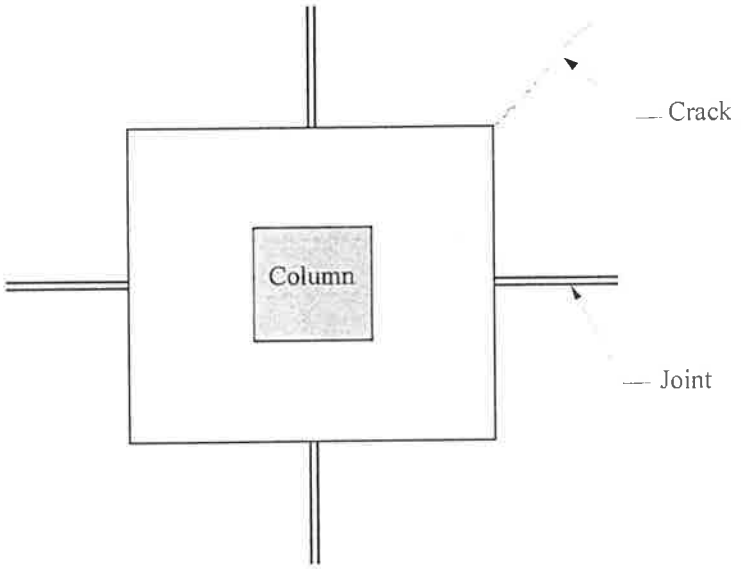

Figure 7.10 Crack at re-entrant corner (Warner et al, 1991)

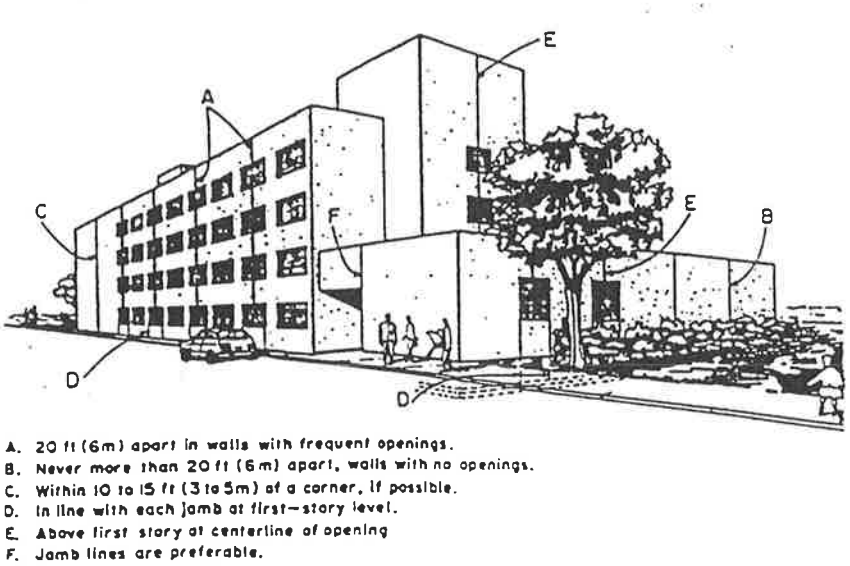

Figure 7.11 Recommendations for locations of contraction joints in building (ACI 224, 1986)

7.5 Analytical methods to calculate expansion joint spacing

As an alternative to choosing expansion joint spacings on the basis of past practice, a number of researchers have presented analytical methods to determine expansion joint spacing. The first method was by Martin and Acosta (1970) who developed an equation and design charts for calculating the maximum spacing of expansion joints in one-story frames with approximately equal spans. This method assumes that the factor of safety for vertical load also provides sufficient safety factor for the effect

Table 7.1 Contraction Joint spacing (ACI 224, 1995)

Author	Spacing
Merrill (1943)	6 m for walls with frequent openings, 7.5 m in solid walls.
Fintel (1974)	4.5 to 6 m for walls and slabs on grade.
Wood (1981)	6 to 9 m for walls.
PCA (1982)	6 to 7.5 m for walls depending on number of openings.
ACI 302.1R ta	4.5 to 6 m recommended until 302.1R-89, then changed to 24 to 36 times slab thickness
ACI 350R-83	9 m in sanitary structures.
ACI 350 R	Joint spacing varies with amount and grade of shrinkage and temperature reinforcement.
ACI 224R-92	one to three times the height of the walls in solid walls
Experimental Building Station (1977)	spacing depends on degree of movement control.
Barton (1989)	4 to 6m for members with minimum reinforcement (0.2%). Maximum of 8m for walls

Table 7.2 Expansion Joint spacing (ACI 224, 1995)

Author	Spacing
Lewerenz (1907)	23 m for walls
Hunter (1953)	25 m for walls and insulated roofs, 9 to 12 m for uninsulated roofs.
Billig (1960)	30 m maximum building length without joints.
Wood (1981)	30 to 35 m for walls
Indian Standard Institution (1964)	45 m maximum building length between joints
PCA (1982)	60 m maximum building length without joint
ACI 350R-83	36 m in sanitary structures partially filled with liquid (closer spacing required when no liquid present).
Experimental Building Station (1977)	20 to 30m in slabs
Barton (1989)	50 to 60m depending on the expected temperature.
Bussell and Cather (1995)	60 to 70m is common in UK. Also 20 to 40m for exposed floor slabs depending on degree of insulation.

of temperature changes. To avoid tedious computation for the specific temperature and shrinkage in the design, they determined that temperature and shrinkage forces should not exceed twenty percent of the dead load plus forty percent of the live load. From these values, expansion joint spacing was expressed as a function of the length and rigidity of the members and the temperature change in the location.

The design temperature change ΔT is considered as two-thirds of the difference between the extreme values of the normal daily maximum and minimum temperatures, T_{max} and T_{min}, at these locations. To account for drying shrinkage in

the concrete, a drop in temperature of about 30° F. (17° C.) is included to obtain the total design temperature change. This is expressed as;

$$\Delta T = \frac{2}{3}(T_{\max} - T_{\min}) + 30^{o} F \qquad (7.1)$$

Based on the above assumptions and equation (7.1), an equation to calculate expansion joint spacing L can be given as;

$$L = \frac{112{,}000}{R\Delta T} \qquad (7.2)$$

In the above equation

$$R = 144\frac{I_c}{h^2}\frac{(1+r)}{(1+2r)} \qquad (7.3)$$

where L = length of beam (ft.)

r = ratio of stiffness factor of column to stiffness factor of beam where $r = K_c/K_b$

h = column height (in.)

K_c = column stiffness factor and equals to I_c/h (in.^{3})

K_b = beam stiffness factor and equals to I_b/L (in.^{3})

I_c = moment of inertia of column (in.^{4})

I_b = moment of inertia of beam (in.^{4})

ΔT = total equivalent change in temperature (°F) including the temperature change due to shrinkage effect.

To prevent cracking in the exterior walls, Martin and Acosta (1970) also allowed a maximum lateral deflection of $\frac{h}{180}$ as an additional criterion for the spacing L. This is based on the assumption that the column provides little restraint to the floor system undergoing lateral deflection due to a temperature change (ACI 224, 1995). This limitation is given as:

$$L \le \frac{2000h}{\Delta T} \qquad (7.3)$$

Equation (7.3) is also based on the assumption that the lateral deflection of the floor system caused by a temperature change is not significantly restrained by the columns.

According to the analytical results, Martin and Acosta (1970) found that equation (7.2) yielded very conservative results, especially for very rigid structures. The critical moments also occurred in the exterior columns and beams. Pfeiffer and Darwin (1987) also investigated this method for two reinforced concrete frames. They criticised that method as being irrational, but they also found that it is easy to use and produce realistic joint spacing.

A second method was developed by the National Academy of Science (1974). Expansion joint spacing can be determined using a graph which expresses the spacing as a function of the design temperature change. The basis for this graphical representation consisted of a review of the procedures used by various federal agencies in the United States to select joint spacing, plus an analytical study comparing the theoretical effects of temperature change on two-dimensional elastic frames to the actual movements recorded during a one year period by the US Public Buildings Administration.

The purpose of the two-dimensional elastic frame analysis was to understand the distribution of stresses and the resulting frame deformations. As a result, nine beam-column frames subjected to a design temperature change of 100 °F were used in the study. By referring to Figure 7.12, the results from the analyses can be summarised as follows;

- the maximum axial forces in the beams were located near the centre of the frame, while the maximum bending moments and shear in the columns were located at the ends of the frame and at the beam-column joint respectively;
- buildings with fixed columns generated double the magnitude of shears;
- axial forces and bending moments were critical in sections within the lowest story when compared to buildings with hinged-columns; and

- the intensity of horizontal shear in the first story columns was largest at the ends of the frame and approaches zero towards the centre.

As illustrated in Figure 7.13, the graph expresses the allowable expansion joint spacing as a function of a design temperature change which also account for the types of building materials. The temperature change is assumed uniform throughout and is calculated for a specific site as the larger of;

$$\Delta T = T_w - T_m \tag{7.4}$$

where T_m = temperature during the normal construction season in the locality of the building and this is assumed to be thecontinuous period in a year during which the minimum daily temperature equals or exceeds 32 °F (0 °C),

T_w = temperature exceeded, on average, only 1 percent of the timen during the summer months of June throug September,

T_c = temperature equaled or exceeded, on average, 99 percent of the time during the winter months of December, January, and February.

The values of T_m, T_w, and T_c are given for various locations within the United States, but not for other countries otherwise.

Figure 7.13 is directly applicable to building structures with beam-column frame that contain columns hinged at the base and heated interiors. The applicability of this figure can be extended to cover a greater range of building structures by adding modification factors to account for different building configuration and stiffness, heating and cooling, and the type of column connection to the foundations. The modifications are as follows:

- joint spacing remains unchanged if the building is only subjected to heating and has hinged column bases;

- joint spacing is increased by 15 percent if the building is subjected to both heating and air-condition;
- joint spacing is decreased by 33 percent if the building is unheated;
- joint spacing is decreased by 15 percent if the building contains fixed column bases; and
- joint spacing is decreased by 25 percent if the building provides greater stiffness against lateral displacement at one end of the structure.

If one or more of the listed conditions occur, the total modification factor is the algebraic sum of the individual adjustment factors that apply.

A third analytical method to calculate maximum expansion joint spacing was proposed by Varyani and Radhaji as reported by Pfeiffer and Darwin (1987). The method can be used to predict joint spacing for symmetrical, single and multistory beam column frames subjected to temperature changes. Unlike the method by Martin and Acosta (1970), the design temperature is taken as two-thirds of the difference between maximum and minimum daily temperature for a single day rather than the difference in the extreme value of normal maximum and minimum daily temperatures.

In order to obtain joint spacing, Varyani and Radhaji's method requires the determination of the temperature-induced moment at the base of the corner columns with the moment due to gravity at the same point. They also considered only the first two stories of multistorey buildings to be critical in the analysis because only the first story columns and the beams supported by these columns are substantially affected by temperature change.

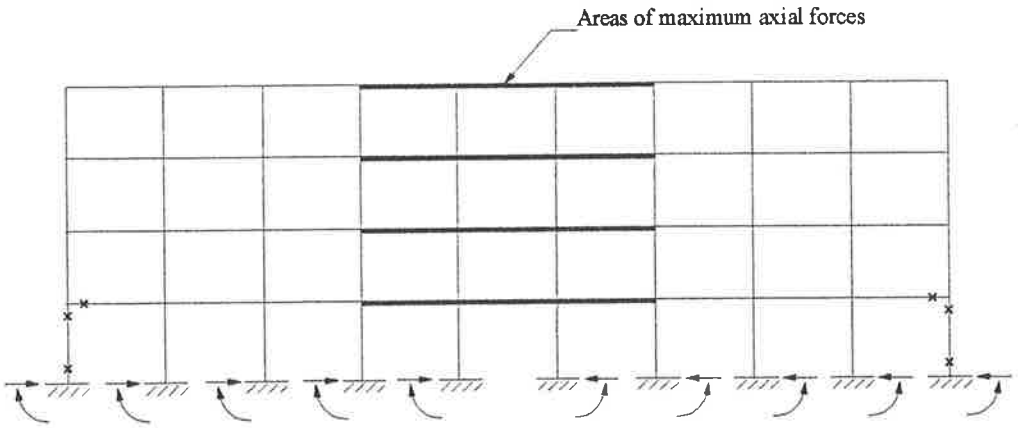

(a) Frame fixed at ground level

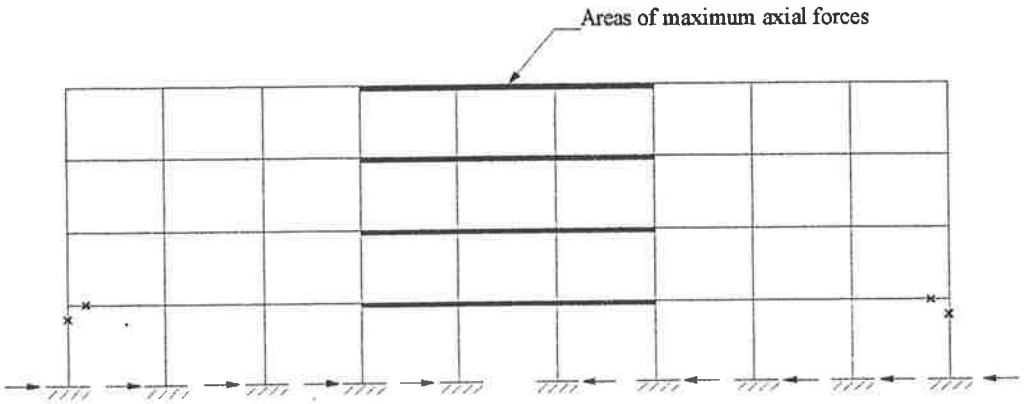

(b) Frame hinged at ground level

Figure 7.12 Analysis of multi-story and multi-span building frames subjected to uniform temperature change (x indicates maximum bending moments and maximum shear forces)

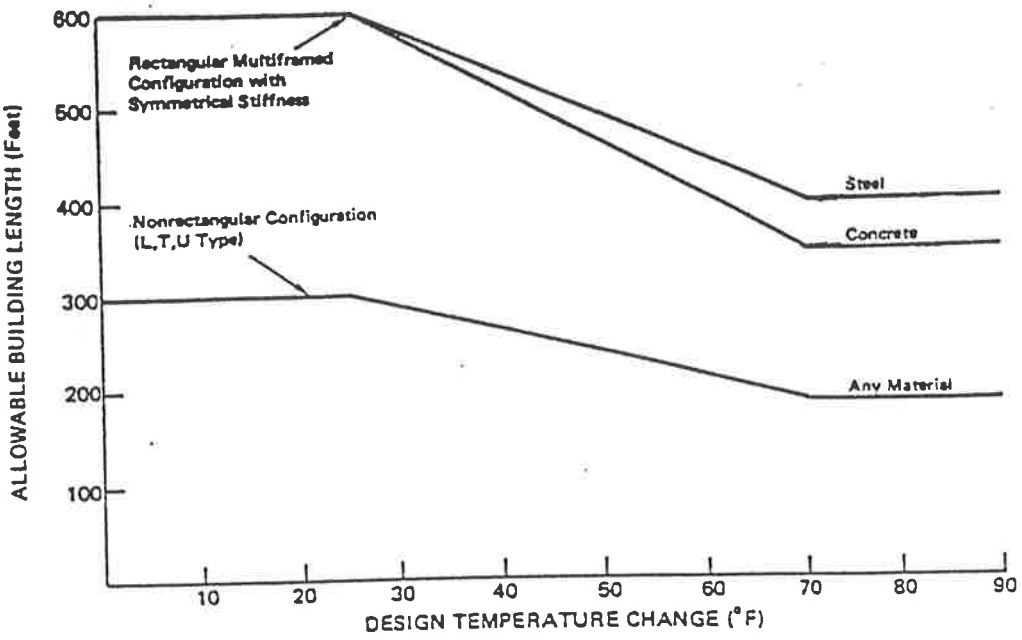

Figure 7.13 Recommended maximum allowable building length without expansion joints for different design temperatures (National Academy of Science, 1974)

Pfeiffer and Darwin (1987) demonstrated the use of all three analytical methods on a single story and multistorey reinforced concrete frame buildings. Some of the results of the calculations are shown here to assist the discussion of the relative merits of each method. Readers are referred to Pfeiffer and Darwin's work for full details of the calculations. As demonstrated in Table 7.3, the resulting expansion joint spacing varies between each method. In particular, results obtained using Vayani and Radhaji's method are extremely low while method by Martin and Acosta is more conservative than the one by the National Academy of Science. Since all three methods require the designers to make several assumptions for the calculations, these could be the cause leading to the disparity between them.

Nevertheless, of all the three methods, method proposed by Varyani and Radhaji, as reported by Pfeiffer and Darwin (1987) is the most complex and time consuming.

The results obtained from Pfeiffer and Darwin (1987) also indicate that this method is overconservative when compared with the previous two. Therefore this method may not be suitable for the designers. Although methods proposed by both Varyani and Radhaji and Martin and Acosta based the expansion joint spacing on the ability of the first level beams and columns to provide resistance to the temperature effects, Martin and Acosta's method is relatively simple and yet provides results which agree reasonably well with the current practice.

Table 7.3 Results of expansion joint spacing using methods by Martin and Acosta, Varyani and Radhaji and National Academy of Science.

Method of predicting	Single story	Multistorey
Martin and Acosta (1970)	251.1 ft.	Not applicable
National Academy of Science (1974)	340 ft.	340 ft.
Varyani and Radhaji as reported by Pfeiffer and Darwin (1987)	147.5 ft.	18.5 ft.

In contrast, method by the National Academy of Science (1974) does not require any rigorous calculations to obtain the joint spacing. The design temperature change can be determined simply by using the temperature data provided (only for United States). The review conducted by Pfeiffer and Darwin (1987) further suggests that it produces joint spacing which are in line with the current practice.

7.6 Summary

In summary, when movement joints are deemed necessary to control cracking or provide partial or full separation between members, the numbers ideally should be kept to minimum. The location and type of movement joints in buildings also become an essential element of the structure and design process. The decision should be given a primary consideration in the early stages of design. However, the general trend in design is to avoid expansion joints in buildings when ever possible because they are expensive to construct, impede the continuity of the structures and often provide maintenance problems due to inevitable poor construction practices.

After reviewing various guidelines, recommendations and analytical methods, it still remains that there are no reliable rules which can be used to specify the spacing of movement joints. Although, these recommendations can be used as guidelines, good engineering judgment still prevails. Each structure should be investigated individually by also considering various factors such as building configurations, type of construction, local conditions and sources of deformations. Prediction of contraction joint spacing is more or less a material problem, primarily governed by the low tensile strength of concrete and the bond stress between reinforcement and concrete. Prediction of expansion joint spacing on the other hand, requires considerations of the building structure as a whole.

So far, attempts have also been made to provide analytical methods to calculate expansion joint spacing, but all the results obtained, are varied and inconsistent with each other. In addition, each of the method either deals with only one specific type of structural arrangement or with only on criteria of performance. None of the methods appear to adequately deal with both of these factors. As an example, Both Martin and Acosta (1970) and Varyani and Radhaji, as reported by Pfeiffer and Darwin (1987) only concerned movement joints with the strength of the structure, but failed to address the subject of crack control. The method developed by National Academy of Science (1974) was based on a study of the performance of nine federal buildings over a period of one year, analyses of similar two dimensional frame buildings and a current practice of expansion joint spacing adopted by one federal agency in the United States. While this method addresses many problems and the associated factors which affect the joint spacing, the amount of field data is limited and these factors can be dealt with in a general manner.

A complete solution for the location and spacing of expansion joints must consider both strength and serviceability. When the members are restrained against deformation, limits should be imposed against the magnitude of the restraining forces and cracking in the members due to the effects of time dependent deformation.

Chapter 8

Conclusions and Recommendations

8.1 Summary of findings

The design of reinforced concrete buildings to allow for restrained and imposed deformations is a unique problem for each individual building. There are important factors such as building configuration and geometry, surrounding environment, construction methods and building materials which can contribute to the degree of restraint and the magnitude of the imposed deformations. Excessive cracking can occur in both structural and non structural components if imposed deformations are neglected or underestimated. Cracking of this type tends to propagate over the full depth of the member, and can seriously affect both the functionality and the aesthetics of the structure.

The main causes of deformations are shrinkage, creep, temperature effects and differential foundation movement, all of which have to be considered early in the design process in order to avoid further complications during the design life. Detailed literature reviews of shrinkage and creep indicated that these occurrences are dependent on various factors, namely type of aggregates and concrete, water/cement ratio, chemical admixtures, member shape and size, relative humidities, and type and duration of curing. Creep is further influenced by loading conditions and the influence of shrinkage itself. It was found that existing calculation techniques, including the current Australian Standard (AS 3600-1994) to estimate the magnitude of shrinkage and creep are quite adequate in providing

reasonable results, provided that the structure in question is not overly complex. Otherwise, a more rigorous procedure has to be adopted.

The study of cracking mechanisms of reinforced concrete members due to restrained and imposed deformations has shown that this type of cracking is different to that due to flexure. Thus, it was necessary to look for an alternative cracking theory which could be used to explain this phenomenon. This ultimately led to the reviews of two cases of cracking which occur as a result of two types of actions, namely direct applied tensile force and shrinkage and temperature effects.

Both cases of cracking involve a bond break down or slip at the reinforcement and concrete interface and the mechanism is different to cracking due to flexure. At the crack, the reinforcement is considered to carry the full tensile force while the stress in concrete is zero. Adjacent to both sides of the crack, the tensile stresses vary, and depend on the distribution of bond stress. As the tensile stresses are transferred from the reinforcement to the concrete by bond, the stress in the concrete increases, until at some distance S_o, from the crack, the concrete stress again resumes a constant value. In order to avoid the complexity of bond stress distribution over the distance, S_o, a constant or average bond stress can be assumed within this region. This assumption is quite reasonable, as it is very difficult to accurately analyse the bond stress within these regions.

Based on this simplification, a number of equations for crack spacing and crack width have been proposed. Another significant factor that influences the magnitude of crack spacing and crack width is the amount of reinforcement. In most cases, it is important that a minimum amount of reinforcement is included to ensure that cracking is not excessive. This suggestion is implemented in a number of design codes and research papers reviewed in this thesis. These include the latest Australian Standard, AS 3600-1994 (SAA, 1994) which recommends a minimum reinforcement ratio to prevent cracking caused by shrinkage and temperature.

In order to study the effects of restraining forces and cracking associated with restrained and imposed deformations, a slab column-wall sub-assemblage was analysed. All the forces involved were determined from first principles so that the

development of cracking from the first crack to the final crack at the stabilised cracking stage in the slab can be determined. This model indirectly allows the designer to achieve control of cracking by controlling the tensile stress in the reinforcement and ensuring that the maximum allowable crack width is not exceeded. It can be used as a simple design tool for checking the adequacy of a slab to resist the effects of restrained shrinkage. For single and two span slabs, a spread sheet program has been developed to perform the analysis. For multi-span members, a higher level computer language program would be needed. To simplify the analysis, the slab is assumed to be subjected to uniform shrinkage strain, and axial tensile stresses.

8.2 Recommendations

Findings from this research can be used to assist during the design process so that excessive cracking due to restraint and imposed deformation can be minimised during the life of the structure. The following recommendations are proposed to ensure early diagnosis of potential problems.

1) First, it is important to establish serviceability requirements such as allowable crack width, number of cracks and allowable deflections in the various building elements. As far as the cracking limitation is concerned, acceptable values range from 0.2 - 0.3 mm depending on the exposure classification and the intended use of the building. In normal situations, excessive cracking may be regarded as when maximum crack widths exceed the value of 0.3 mm.
2) The structural layout of the building and the preliminary sizing of members should be such that restraints are minimised and large internal tensile stresses do not develop. This is achieved by judicious placing of stiffening elements such as load bearing walls, stiffening cores and columns so that there is no large no restraint imposed on adjoining members such as beams and slabs.
3) Sufficient reinforcement must be specified in the members to ensure that yielding of the reinforcement does not take place due to whatever causes. Reinforcement is most effective to control both crack spacing and crack width when it is closely spaced and the diameters are kept as small as possible. This is because cracks

developed usually are more evenly distributed along the span and are also smaller in size.

4) All possible causes of deformations must be properly assessed and identified. Their magnitudes can be estimated using the methods explained in Chapter 2 if the deformations are due to shrinkage and creep. As a guide, most designers in Australia generally assume a final shrinkage strain between 500 to 700 $\mu\varepsilon$ after 56 days. This value also is in line with the latest Australian design code, AS 3600 (SAA, 1994) which suggests a median value of 700 $\mu\varepsilon$.

5) Once step 4 is determined, the structure or parts of the structure can be analysed to calculate the restraining forces. For a one-way reinforced concrete slab subjected to large imposed deformations, the method proposed in Chapter 4 can be adopted to predict the restraining forces and hence the extent of cracking. The method does not restrict designers to the use any particular crack spacing and crack width equations. Comparisons can therefore be made between the equations.

6) If the serviceability requirement is compromised due to excessive cracking, it may be necessary to alter the design by either increasing the amount of reinforcement or by modifying (decreasing) the member span. In most cases, the latter solution must be agreed by the architect or the client, otherwise different methods must be investigated to control the problem.

7) In many cases, it will be necessary to consider the inclusion of movement joints into the structure when other design provisions fail. Nevertheless, it is important to recognise that a complete solution for the location and spacing of expansion joints must consider both strength and serviceability. In addition the number must be kept absolutely to a minimum.

8) To obtain an optimum design, there has to be a compromise of continuity and articulation. As a matter of fact, it is possible to use the combination of both options in order to come up with the most feasible design solution. As a guide, movement joints are required when it is not feasible or practical to have a continuous structure because of excessive cracking. Movement joints such as expansion joint can be used a construction joint during the construction of structures.

8.3 Conclusion

It has been seen that the design of reinforced concrete buildings to accommodate restrained and imposed deformations requires the considerations of many factors. Two of the most important factors involve in determining the crack spacing and crack width. The results obtained in the numerical calculations using various equations are quite diverse. This indicates that the recommendations can only be used as an overall design guide. Good engineering judgement and experience must play an important role in deciding whether cracking will have detrimental outcomes on the structure. The model proposed in Chapter 4 is relatively at an early stage of development and it may be worthwhile to incorporate other effects such as bending moments and shears to further enhance the accuracy. Another area that has not been investigated is the effects of restrained and imposed deformations on prestressed concrete structures. Since this type of design is becoming very popular, it may be useful to consider it in future research.

Appendix

Numerical examples

The followings contain details of the calculations of examples presented in Chapter 4. A spread sheet program (Microsoft Excel) is used to carry out all the analyses, which also includes plotting of all the graphs

In all examples, the model presented in Chapter 4 requires the determination of the length of cracked region, W_{cr}. This is interpreted in terms of crack spacing as $2\varsigma S_o$.

Where S_o = minimum crack spacing obtained using various equations listed below

ς = coefficient suggested by CEB Manual (1985) to account for the tension stiffening, which is equal to 0.5 for member with restraint

The crack spacing equations are those contained in the following reference already discussed in Chapter 3:

- Hughes (1972, 1973)
- Leonhardt (1977)
- Beeby (1979)
- Rizkally & Hwang (1984)
- CEB Manual (1985)
- ACI 224 (1986)
- Christensen & Nielsen (1997)

Example 1 (Gilbert, 1992)

Consider a 5 m long and 150 mm thick reinforced concrete slab which is fully restrained at each end as shown . As shrinkage occurs in the concrete, restraining forces develop at each end, resulting in cracks though out the span.

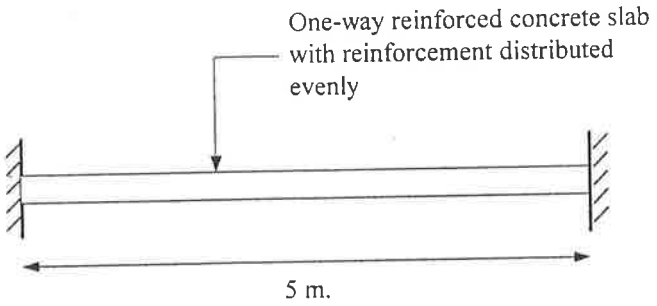

The structure has the following properties:

Concrete properties	
Tensile strength, f_t'	2 MPa
Young's modulus, E_c	25000 MPa
Cross sectional area , A_c	150000 mm^2/m
Concrete cover, c	30 mm

Reinforcement properties	
Yield strength, f_{sy}	400 MPa
Young's modulus, E_s	200000 MPa
Cross sectional area, A_s	750 mm^2/m
Reinforcement spacing, a	300 mm
Diameter, d	12 mm
Reinforcement ratio, ρ	0.005

Reference	Calculation	Results
	Example 1	
	Using the slab column-wall sub-assemblage model presented in Chapter 4, the following initial conditions can be determined in order to carry out the analysis for the development of cracking	
	(1) The restraining force just before the first crack can be calculated	
Eq (4.9)	$F_{cr} = A_c f_t'$	
	$\Rightarrow$	F_{cr} =**300 kN**
	(2) The bending stiffness of the column in Equation (4.17) has to be made infinitely large to represent the stiffness of the concrete core on the left hand side.	
	(3) Shrinkage strain at first cracking	
	Shrinkage strain at first cracking corresponds to the strain of concrete when f'_t is exceeded.	
	$\varepsilon_{sh1} = \frac{f_t'}{E_c}$	
	$\Rightarrow$	ε_{sh1} = **0.00008**
	(4) Calculation of the length of cracked region, W_{cr}	
	Since $W_{cr} = 2\varsigma S_o$, the followings equations calculate the values of W_{cr} using different crack spacing equations mentioned earlier.	
	Hughes (1972, 1973)	
Eq (3.94)	$S_{min} = \frac{f_t' d}{4\tau_{ave}\rho}$	
	where $\frac{f_t'}{\tau_{aver}}$ is assumed as 0.67	

Reference	Calculations	Results
	$\Rightarrow$	W_{cr} = **402 mm**
	Leonhardt (1977)	
Eq (3.39)	$S_{min} = (\frac{1}{2} l_o + S_o)$ $S_o = k_1(c,a) + k_2 k_3 \frac{d}{\rho_{eff}}$ where k_1 = 108 for $a > 2c$ k_2 = 0.4 k_3 = 0.25	
	Since it is necessary to calculate σ_{s2} prior to determination of l_o in equation (3.40), it is not possible using this model. Therefore, its value is ignored in this example. Nevertheless, it can be seen that the contribution of $\frac{1}{2} l_o$ is quite small and thus would not significantly affect the overall magnitude of W_{cr}	
	$\Rightarrow$	W_{cr} = **348 mm**
	Beeby (1979)	
Eq (3.44)	$S_m = K_1 c + K_2 \frac{d}{\rho}$ Assume that the probability of exceedance is approximately average, therefore k_1 = 1.33 k_2 = 0.08 Therefore S_m = 232 mm S_{min} = 174 mm	
	$\Rightarrow$	W_{cr} = **174 mm**

Reference	Calculation	Results
	Rizkally & Hwang (1984)	
Eq (3.66)	$S_m = 5(d - 7.2) + K_1(a,c) + 0.08\frac{d}{\rho}$	
	$S_m = 324$ mm	
	Thus, $S_{min} = 243$ mm	
	$\Rightarrow$	$W_{cr} = \underline{\mathbf{243\ mm}}$
	CEB Manual (1985)	
Eq (3.48)	$S_m = 2(c + \frac{a}{10}) + \kappa_1\kappa_2\frac{d}{\rho_r}$	
	where $k_1 = 0.4$	
	$k_2 = 0.25$	
	$\rho_r = 0.0078$	
	Therefore, $S_m = 274$ mm	
	$S_{min} = 206$ mm	
	$\Rightarrow$	$W_{cr} = \underline{\mathbf{206\ mm}}$
	ACI 224 (1986)	
Eq (3.52)	$S_{max} = 4t_e$ Where $t_e = c\sqrt{1+\left(\frac{a}{4c}\right)^2}$	
	Thus, $t_e = 81$ mm	
	and $S_{max} = 162$ mm	
	$S_{min} = 122$ mm	
	$\Rightarrow$	$W_{cr} = \underline{\mathbf{122\ mm}}$
	Christiansen & Nielson (1997)	
Eq (3.55)	$S_{\min} = (\frac{1}{2}l_o + S_o)$	

Reference	Calculations	Results
	where $S_o = \dfrac{0.5A_c}{N_{bar}\pi d}$ Since A_s = 750 mm^2/m, the number of bars per m = 6.63 bars Therefore, S_{min} = 300 mm $\Rightarrow$	W_{cr} = **300 mm**

After these initial conditions have been determined, the analysis now proceeds to investigate the development of cracking as shrinkage in the concrete increases with time. The following spread sheets show the analysis for each length of cracked region as shrinkage increases with time.

Table A.1 Development of cracking due to shrinkage using equation by Hughes (1972, 1973)

Hughes (1972, 1973)						
No. of cracks	**k_{slab} (N.mm)**	**ε_{sh} at cracking**	***F.* immediately after each crack (kN)**	***F.* just before each crack (kN)**	**σ_{s2} at crack (MPa)**	**Crack width (mm)**
0	780000	0.00008	Conditions before cracks	300		0
1	259136	0.000082	94	312	126	0.25
2	155378	0.000289	188	312	250	0.50
3	110955	0.000532	223	312	298	0.60
4	86283	0.000832	243	312	324	0.65
5	70588	0.001213	255	312	341	0.68
6	59724	0.001712	264	312	352	0.71
7	51758	0.002395	270	312	361	0.72
8	45667	0.003385	275	312	367	0.74
9	40859	0.004951	279	312	372	0.75
10	36967	0.007803	282	312	376	0.76
11	33752	0.014620	285	312	380	0.76
12	31051	0.052583	287	312	383	0.77

Note that the maximum number of cracks can not exceed 12 since 13 times W_{cr} is greater than the 5 m span of the slab

Table A.2 Development of cracking due to shrinkage using equation by Leohardt (1977)

Leohardt (1977)						
No. of cracks	**k_{slab} (N.mm)**	**ε_{sh} at cracking**	***F.* immediately after each crack (kN)**	***F.* just before each crack (kN)**	**σ_{s2} at crack (MPa)**	**Crack width (mm)**
0	780000	0.000080	Conditions before cracks	300		0
1	284672	0.000080	105	300	140	0.24
2	174107	0.000257	192	312	255	0.44
3	125402	0.000456	225	312	300	0.52
4	97990	0.000692	244	312	325	0.57
5	80412	0.000980	256	312	342	0.59
6	68182	0.001336	265	312	353	0.61
7	59181	0.001789	271	312	361	0.63
8	52279	0.002384	276	312	368	0.64
9	46819	0.003200	279	312	373	0.65
10	42391	0.004391	283	312	377	0.66
11	38729	0.006289	285	312	380	0.66
12	35649	0.009789	287	312	383	0.67
13	33023	0.018409	289	312	385	0.67
14	30757	0.073895	291	312	387	0.67

Note that the maximum number of cracks can not exceed 14 since 15 times W_{cr} is greater than the 5 m span of the slab

Table A.3 Development of cracking due to shrinkage using equation by Beeby (1979)

Beeby (1979)						
No. of cracks	**k_{slab} (N.mm)**	**ε_{sh} at cracking**	***F.* immediately after each crack (KN)**	***F.* just before each crack (KN)**	**σ_{s2} at crack (MPa)**	**Crack width (mm)**
0	780000	0.000080	Conditions before cracks	300		0
1	417112	0.000080	159	300	212	0.18
2	284672	0.000157	214	312	285	0.25
3	216066	0.000238	237	312	316	0.28
4	174107	0.000325	252	312	336	0.29
5	145794	0.000419	262	312	349	0.30
6	125402	0.000521	269	312	358	0.31
7	110014	0.000632	274	312	365	0.32
8	97990	0.000753	278	312	371	0.32
9	88335	0.000885	281	312	375	0.33
10	80412	0.001032	284	312	379	0.33
11	73794	0.001193	286	312	382	0.33
12	68182	0.001373	288	312	384	0.33
13	63363	0.001575	290	312	387	0.34
14	59181	0.001802	291	312	389	0.34
15	55516	0.002060	293	312	390	0.34

Note that the maximum number of cracks can not exceed 27 since 28 times W_{cr} is greater than the 5 m span of the slab

Table A.4 Development of cracking due to shrinkage using equation by Rizkally & Hwang (1984)

Rizkally & Hwang (1984)						
No. of cracks	**k_{slab} (N.mm)**	**ε_{sh} at cracking**	***F.* immediately After each crack (kN)**	***F.* just before each crack (kN)**	**σ_{s2} at crack (MPa)**	**Crack width (mm)**
0	780000	0.000080	Conditions before cracks	312		0
1	352144	0.000080	132	300	177	0.21
2	227405	0.000199	202	312	270	0.33
3	167922	0.000324	231	312	308	0.37
4	133166	0.000464	248	312	330	0.40
5	110247	0.000622	259	312	345	0.42
6	94089	0.000802	266	312	355	0.43
7	82062	0.001008	272	312	363	0.44
8	72761	0.001248	277	312	369	0.45
9	65354	0.001528	280	312	374	0.45
10	59316	0.001862	283	312	378	0.46
11	54299	0.002265	286	312	381	0.46
12	50064	0.002762	288	312	384	0.47
13	46442	0.003391	289	312	386	0.47
14	43309	0.004211	291	312	388	0.47

Note that the maximum number of cracks can not exceed 20 since 21 times W_{cr} is greater than the 5 m span of the slab

Table A.5 Development of cracking due to shrinkage using equation by CEB Manual (1985)

CEB Manual (1985)						
No. of cracks	**k_{slab} (N.mm)**	**ε_{sh} at cracking**	***F.* immediately after each crack (kN)**	***F.* just before each crack (kN)**	**σ_{s2} at crack (MPa)**	**Crack width (mm)**
0	780000	0.000082	Conditions before cracks	300		0
1	384236	0.000082	145	300	194	0.20
2	254902	0.000179	208	312	277	0.29
3	190709	0.000282	234	312	312	0.32
4	152344	0.000394	250	312	333	0.34
5	126829	0.000519	260	312	347	0.36
6	108635	0.000656	267	312	357	0.37
7	95006	0.000810	273	312	364	0.37
8	84416	0.000983	277	312	370	0.38
9	75949	0.001178	281	312	374	0.39
10	69027	0.001401	284	312	378	0.39
11	63260	0.001657	286	312	381	0.39
12	58383	0.001955	288	312	384	0.40
13	54204	0.002306	290	312	386	0.40
14	50584	0.002725	291	312	388	0.40

Note that the maximum number of cracks can not exceed 24 since 25 times W_{cr} is greater than the 5 m span of the slab

Table A.6 Development of cracking due to shrinkage using equation by ACI 224 (1986)

ACI 224 (1986)						
No. of cracks	**k_{slab} (N.mm)**	**ε_{sh} at cracking**	***F.* immediately after each crack (kN)**	***F.* just before each crack (kN)**	**σ_{s2} at crack (MPa)**	**Crack width (mm)**
0	780000	0.000080	Conditions before cracks	300		0
1	484472	0.000080	186	300	248	0.15
2	351351	0.000138	227	312	303	0.18
3	275618	0.000190	245	312	327	0.20
4	226744	0.000253	257	312	343	0.21
5	192593	0.000316	265	312	354	0.22
6	167382	0.000382	271	312	362	0.22
7	148008	0.000452	276	312	368	0.22
8	132653	0.000526	280	312	373	0.23
9	120185	0.000605	283	312	377	0.23
10	109859	0.000690	285	312	380	0.23
11	101167	0.000779	287	312	383	0.23
12	93750	0.000875	289	312	386	0.24
13	87346	0.000978	291	312	388	0.24
14	81761	0.001088	292	312	389	0.24
15	76847	0.001207	293	312	391	0.24

Note that the maximum number of cracks can not exceed 24 since 25 times W_{cr} is greater than the 5 m span of the slab

Table A.7 Development of cracking due to shrinkage using equation by Christensen & Nielsen (1997)

Christensen & Nielsen (1997)						
No. of cracks	**k_{slab} (N.mm)**	**ε_{sh} at cracking**	***F.* immediately after each crack (kN)**	***F.* just before each crack (kN)**	**σ_{s2} at crack (MPa)**	**Crack width (mm)**
0	780000	0.000080	Conditions before cracks	300		0
1	312000	0.000080	116	300	155	0.23
2	195000	0.000230	196	312	261	0.39
3	141818	0.000393	227	312	303	0.45
4	111429	0.000582	245	312	327	0.49
5	91765	0.000803	257	312	343	0.51
6	78000	0.001066	265	312	354	0.53
7	67826	0.001383	271	312	362	0.54
8	60000	0.001773	276	312	368	0.55
9	53793	0.002265	280	312	373	0.56
10	48750	0.002905	283	312	377	0.57
11	44571	0.003771	285	312	380	0.57
12	41053	0.005008	287	312	383	0.57
13	38049	0.006919	289	312	386	0.58
14	35455	0.010263	291	312	388	0.58
15	33191	0.017621	292	312	389	0.58

Note that the maximum number of cracks can not exceed 16 since 17 times W_{cr} is greater than the 5 m span of the slab

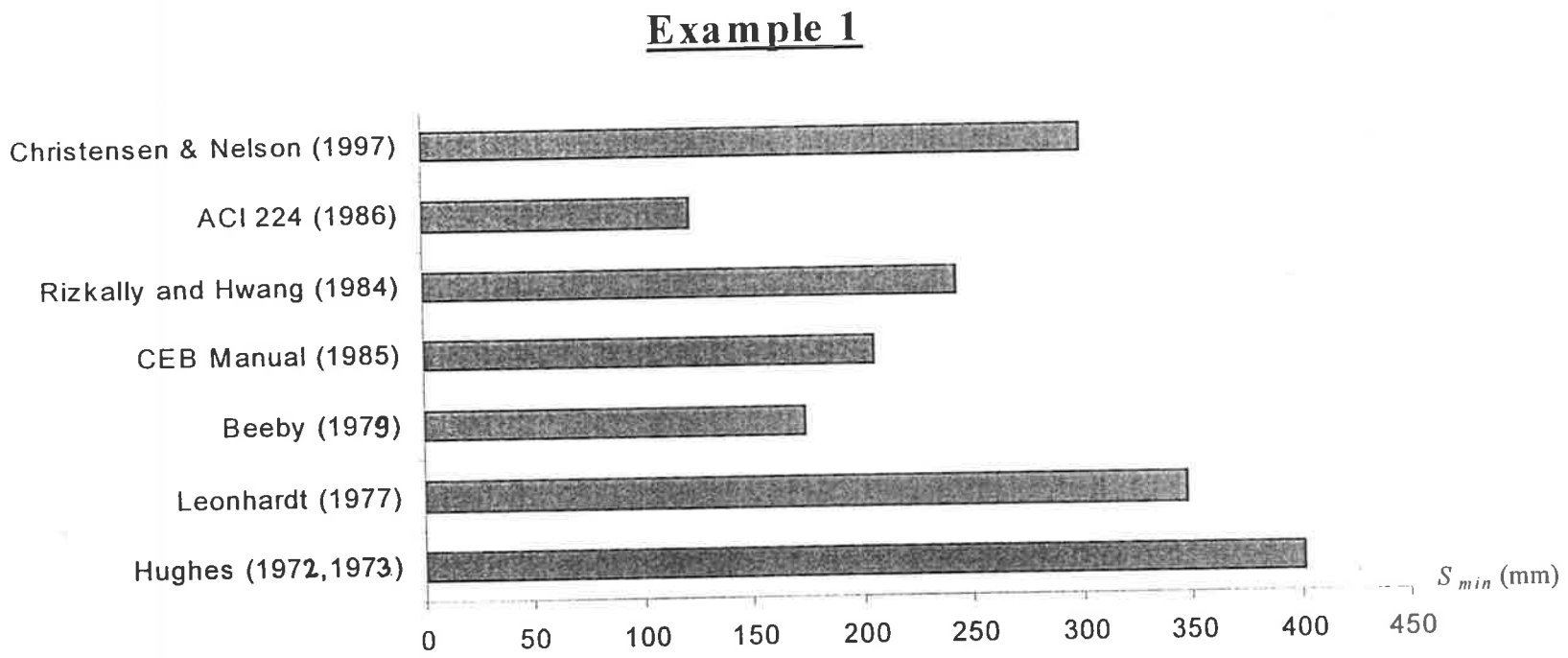

Figure A.1 Minimum crack spacing obtained using different equations

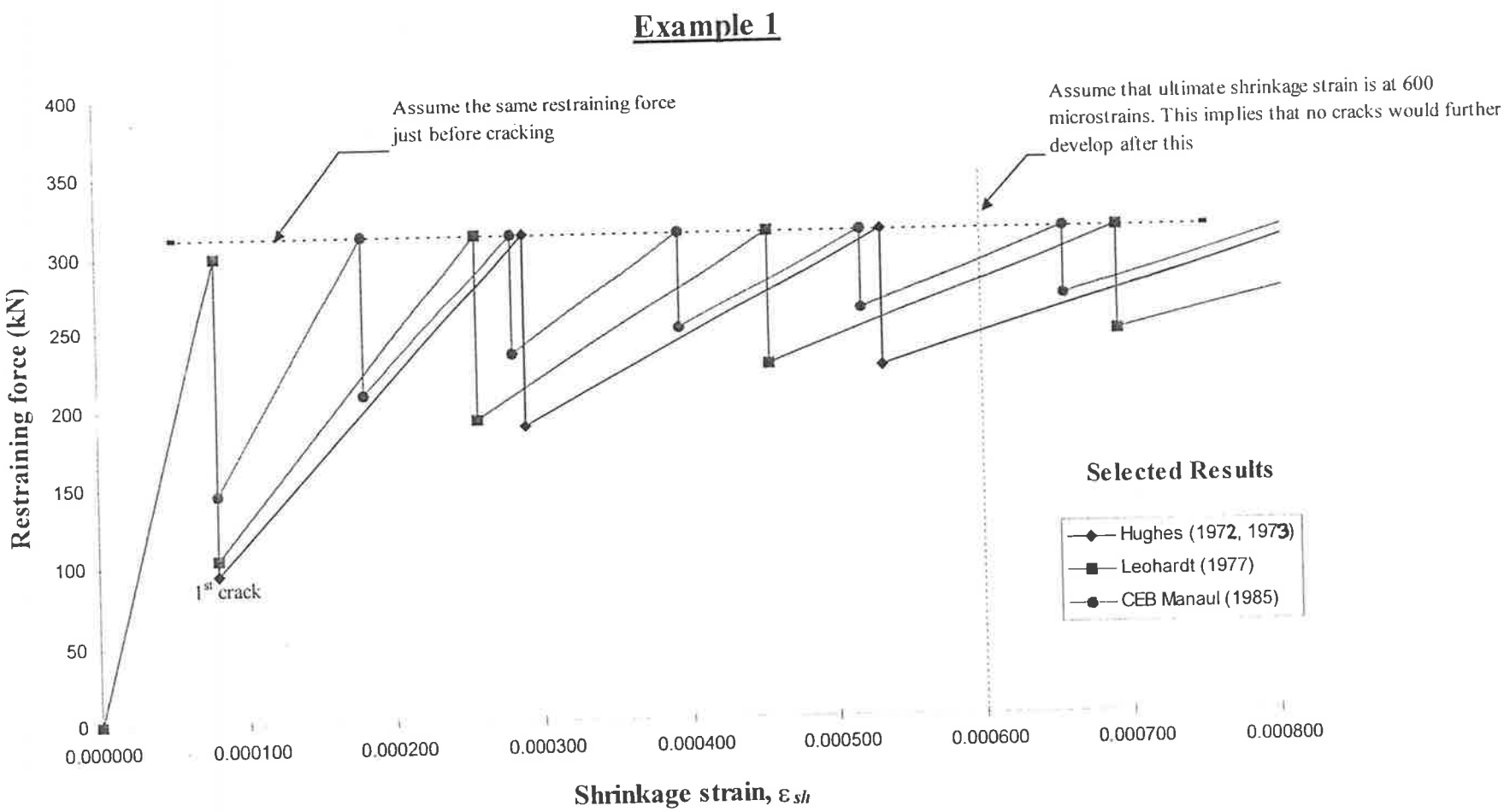

Figure A.2 Plots of restraining force vs. shrinkage strain calculated using different W_{cr}

Example 1

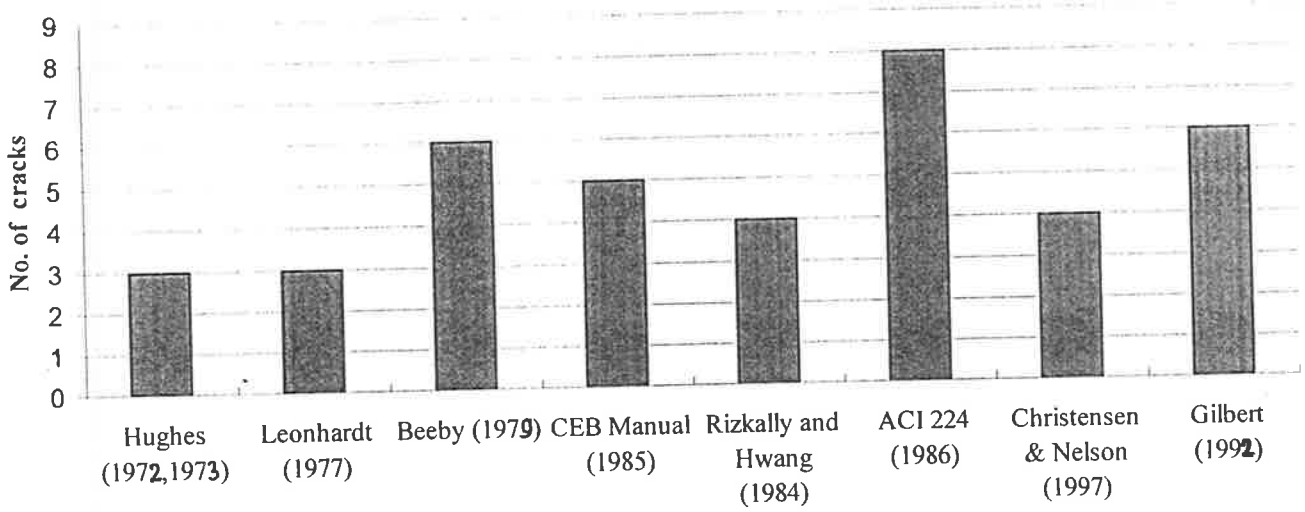

Figure A.3 Different number of cracks obtained when shrinkage strain is at 600 με

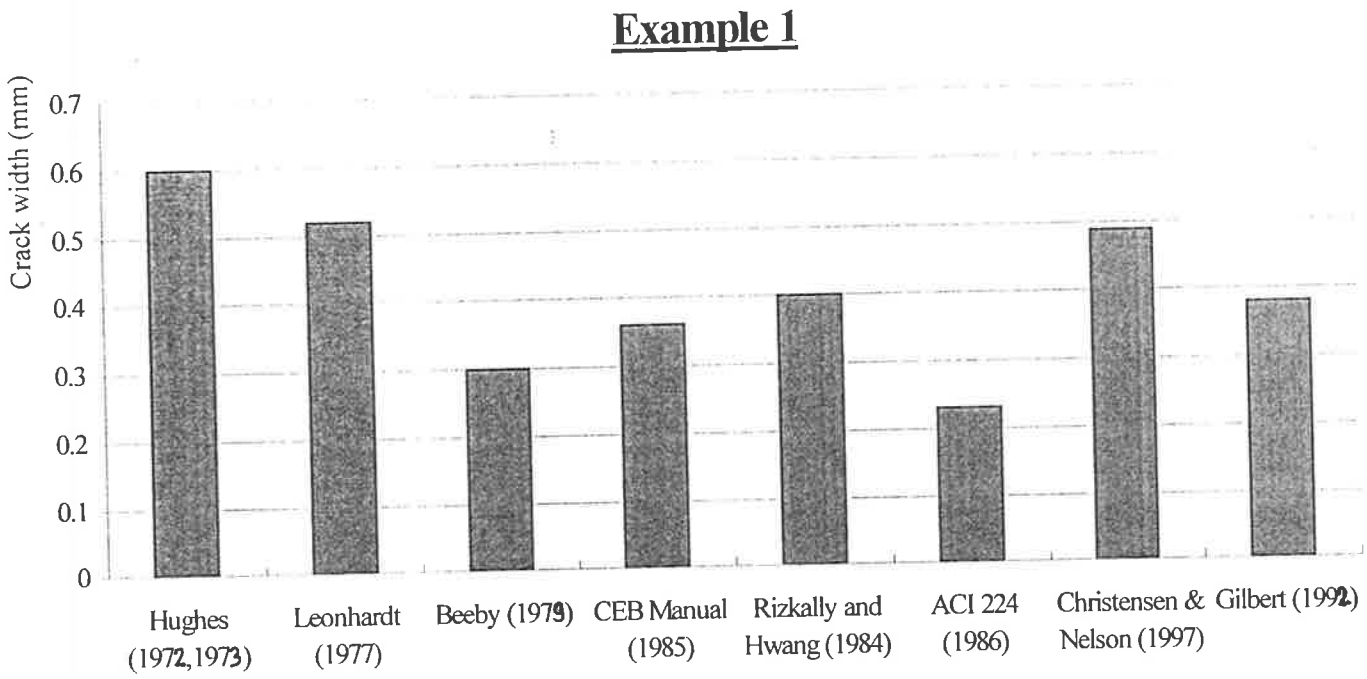

Figure A.4 Crack widths obtained using different equations

Note that each crack width is calculated, using the magnitude of tensile stress in the last crack which developed prior to the termination of shrinkage.

Example 2 (Gilbert, 1992)

In this example, again consider the same 5 m long and 150 mm thick reinforced concrete slab which is fully restrained at each end. As shrinkage occurs in the concrete, restraining forces develop at each end, resulting in cracks though out the span. However the amount of reinforcement A_s, is now reduced to 375 mm^2/m in the slab. The rest of the member properties remain unchanged as Example 1.

Reference	Calculation	Results
	Example 2 Similar to Example 1, the following initial conditions must be determined in order to carry out the analysis for the development of cracking	
Eq (4.9)	(1) The restraining force just before the first crack is calculated as shown $F_{cr} = f_t' A_c$ $\Rightarrow$	F_{cr} =**300 kN**
Example 1	(2) The bending stiffness of the column in Equation (4.17) has to be made infinitely large to represent the stiffness of the concrete core on the left hand side. (3) Shrinkage strain at first cracking is also unchanged $\varepsilon_{sh1} = \frac{f_t'}{E_c}$ $\Rightarrow$	ε_{sh1} = **0.00008**

Reference	Calculations	Results
	(4) Calculation of the length of cracked region, W_{cr}	
	In this case, the reinforcement ratio, ρ is reduced from 0.005 to 0.0025	
	Hughes (1972, 1973)	
Eq (3.94)	$S_{\min} = \dfrac{f_t' d}{4\tau_{ave}\rho}$	
	where $\dfrac{f_t'}{\tau_{aver}}$ is assumed as 0.67	
	$\Rightarrow$	W_{cr} = **804 mm**
	Leohardt (1977)	
Eq (3.39)	$S_{\min} = (\dfrac{1}{2} l_o + S_o)$ $S_o = k_1(c,a) + k_2 k_3 \dfrac{d}{\rho_{eff}}$ where $k_1 = 108$ for $a > 2c$ $k_2 = 0.4$ $k_3 = 0.25$	
	Since it is necessary to calculate σ_{s2} prior to determination of l_o in equation (3.40), it is not possible using this model. Therefore, its value is ignored in this example. Nevertheless, it can be seen that the contribution of $\dfrac{1}{2} l_o$ is quite small and thus would not significantly affect the overall magnitude of W_{cr}	
	$\Rightarrow$	W_{cr} = **480 mm**

Reference	Calculation	Results
	Beeby (1979)	
Eq (3.44)	$S_m = K_1 c + K_2 \frac{d}{\rho}$	
	Assume that the probability of exceedance is approximately average, therefore	
	$k_1 = 1.33$	
	$k_2 = 0.08$	
	Therefore $S_m = 424$ mm	
	$S_{min} = 318$ mm	
	$\Rightarrow$	$W_{cr} = \underline{\mathbf{318\ mm}}$
	Rizkally & Hwang (1984)	
Eq (3.66)	$S_m = 5(d - 7.2) + K_1(a,c) + 0.08\frac{d}{\rho}$	
	$S_m = 516$ mm	
	Thus, $S_{min} = 387$ mm	
	$\Rightarrow$	$W_{cr} = \underline{\mathbf{387\ mm}}$
	CEB Manual (1985)	
Eq (3.48)	$S_m = 2(c + \frac{a}{10}) + \kappa_1 \kappa_2 \frac{d}{\rho_r}$	
	where $k_1 = 0.4$	
	$k_2 = 0.25$	
	$\rho_r = 0.0039$	
	Therefore, $S_m = 428$ mm	
	$S_{min} = 321$ mm	
	$\Rightarrow$	$W_{cr} = \underline{\mathbf{321\ mm}}$
	ACI 224 (1986)	
Eq (3.52)	$S_{max} = 4t_e$ Where $t_e = c\sqrt{1 + \left(\frac{a}{4c}\right)^2}$	

Reference	Calculations	Results
	Thus, $t_e \doteq 81$ mm and $S_{max} = 162$ mm $S_{min} = 122$ mm $\Rightarrow$	$W_{cr} = \underline{\mathbf{122\ mm}}$
Eq (3.55)	Christiansen & Nielson (1997) $S_{\min} = (\frac{1}{2} l_o + S_o)$ where $S_o = \frac{0.5 A_c}{N_{bar} \pi d}$ Since $A_s = 375$ mm^2/m, the number of bars per m = 3.32 bars Therefore, $S_{min} = 599$ mm $\Rightarrow$	$W_{cr} = \underline{\mathbf{599\ mm}}$

After these initial conditions have been determined, the analysis now proceeds to investigate the development of cracking as shrinkage in the concrete increases with time. The following spread sheets show the analysis of cracking for each length of cracked region as shrinkage increases with time.

Table A.8 Development of cracking with reinforcement reduced using method by Hughes (1972, 1973)

Hughes (1972, 1973)						
No. of cracks	**k_{slab} (N.mm)**	**ε_{sh} at cracking**	***F.* immediately after each crack (kN)**	***F.* just before each crack (kN)**	**σ_{s2} at crack (MPa)**	**Crack width (mm)**
0	765000	0.000080	Conditions before cracks	300		0
1	84624	0.000080	28	300	76	0.31
2	44789	0.001069	162	306	Steel yielded	1.61

Note that the development of third crack is not possible since the reinforcement would have yielded prior to this

Table A.9 Development of cracking with reinforcement reduced using method by Leonhardt (1977)

Leonhardt (1977)						
No. of cracks	**k_{slab} (N.mm)**	**ε_{sh} at cracking**	***F.* immediately after each crack (kN)**	***F.* just before each crack (kN)**	**σ_{s2} at crack (MPa)**	**Crack width (mm)**
0	765000	0.000080	Conditions before cracks	300		0
1	131897	0.000080	49	300	130	0.31
2	72170	0.000577	168	306	Steel yielded	0.96

Note that no further cracks can develop since the reinforcement is just at yield.

Table A.10 Development of cracking with reinforcement reduced using method by Beeby (1979)

Beeby (1979)						
No. of cracks	**k_{slab} (N.mm)**	**ε_{sh} at cracking**	***F.* immediately after each crack (kN)**	***F.* just before each crack (kN)**	**σ_{s2} at crack (MPa)**	**Crack width (mm)**
0	765000	0.000082	Conditions before cracks	300		0
1	183014	0.000080	68	300	182	0.29
2	103940	0.000386	174	306	Steel yielded	0.64

Note that the development of second crack is not possible since the reinforcement would have yielded prior to this

Table A.11 Development of cracking with reinforcement reduced using method by Rizkally & Hwang (1984)

Rizkally & Hwang (1984)						
No. of cracks	**k_{slab} (N.mm)**	**ε_{sh} at cracking**	***F.* immediately after each crack (kN)**	***F.* just before each crack (kN)**	**σ_{s2} at crack (MPa)**	**Crack width (mm)**
0	765000	0.000080	Conditions before cracks	300		0
1	157084	0.000080	58	300	154	0.30
2	87529	0.000463	171	306	Steel yielded	0.77

Note that the development of second crack is not possible since the reinforcement would have yielded prior to this

Table A.12 Development of cracking with reinforcement reduced using method by CEB Manual (1985)

CEB Manual (1985)						
No. of cracks	**k_{slab} (N.mm)**	**ε_{sh} at cracking**	***F.* immediately after each crack (kN)**	***F.* just before each crack (kN)**	**σ_{s2} at crack (MPa)**	**Crack width (mm)**
0	765000	0.000080	Conditions before cracks	300		0
1	181710	0.000080	68	300	180	0.29
2	103100	0.000389	174	306	464	0.64

Note that the development of second crack is not possible since the reinforcement would have yielded prior to this

Table A.13 Development of cracking with reinforcement reduced using method by ACI 224 (1986)

ACI 224 (1986)						
No. of cracks	**k_{slab} (N.mm)**	**ε_{sh} at cracking**	***F.* immediately after each crack (kN)**	***F.* just before each crack (kN)**	**σ_{s2} at crack (MPa)**	**Crack width (mm)**
0	765000	0.000082	Conditions before cracks	306		0
1	344595	0.000082	136	306	364	0.22
2	222384	0.000189	198	306	529	0.33

Note that the development of second crack is not possible since the reinforcement would have yielded prior to this

Table A.14 Development of cracking with reinforcement reduced using method by Christiansen & Nielsen (1997)

Christiansen & Nielson (1997)						
No. of cracks	**k_{slab} (N.mm)**	**ε_{sh} at cracking**	***F.* immediately after each crack (kN)**	***F.* just before each crack (kN)**	**σ_{s2} at crack (MPa)**	**Crack width (mm)**
0	765000	0.000082	Conditions before cracks	306		0
1	109442	0.000082	39	306	105	0.31
2	58937	0.000638	143	306	380	1.14
3	40327	0.001368	177	306	471	1.41

Note that the development of third crack is not possible since the reinforcement would have yielded prior to this

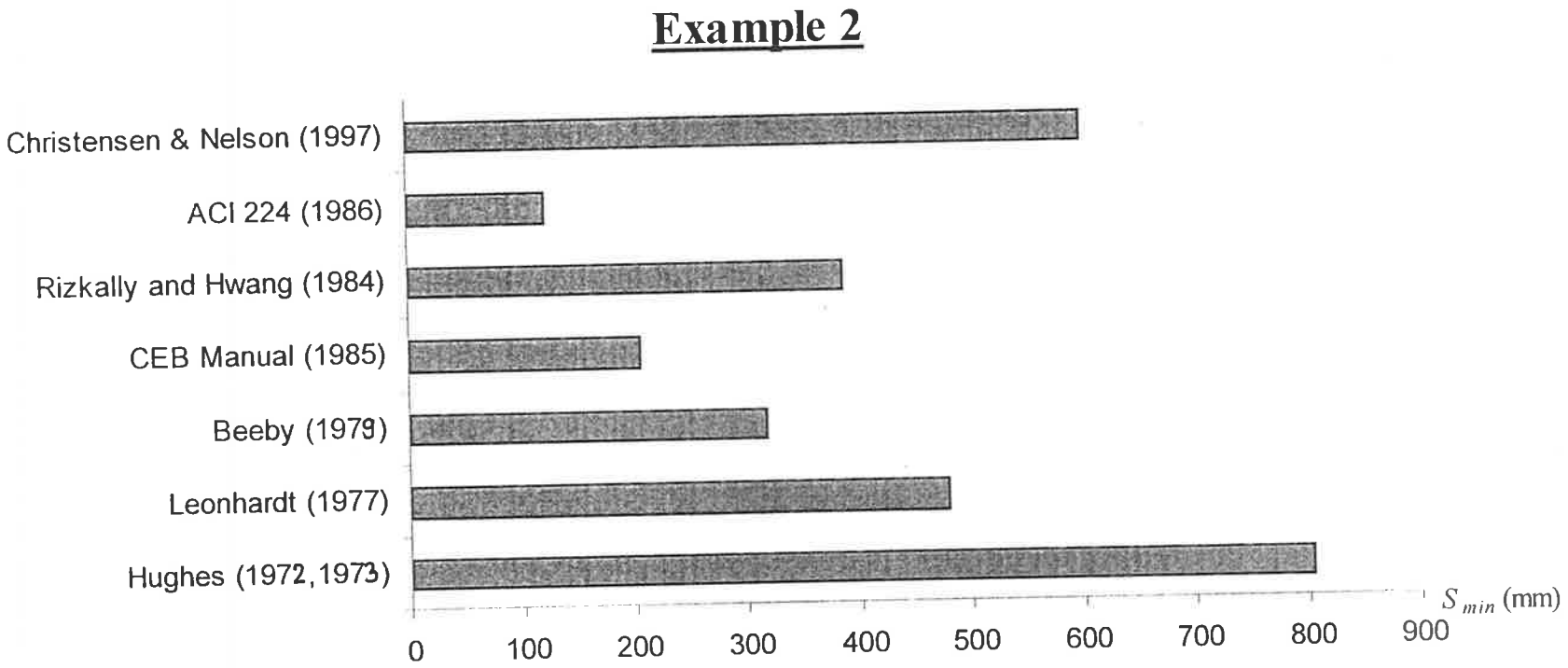

Figure A..5 Crack spacings obtained when the amount of reinforcement is halved

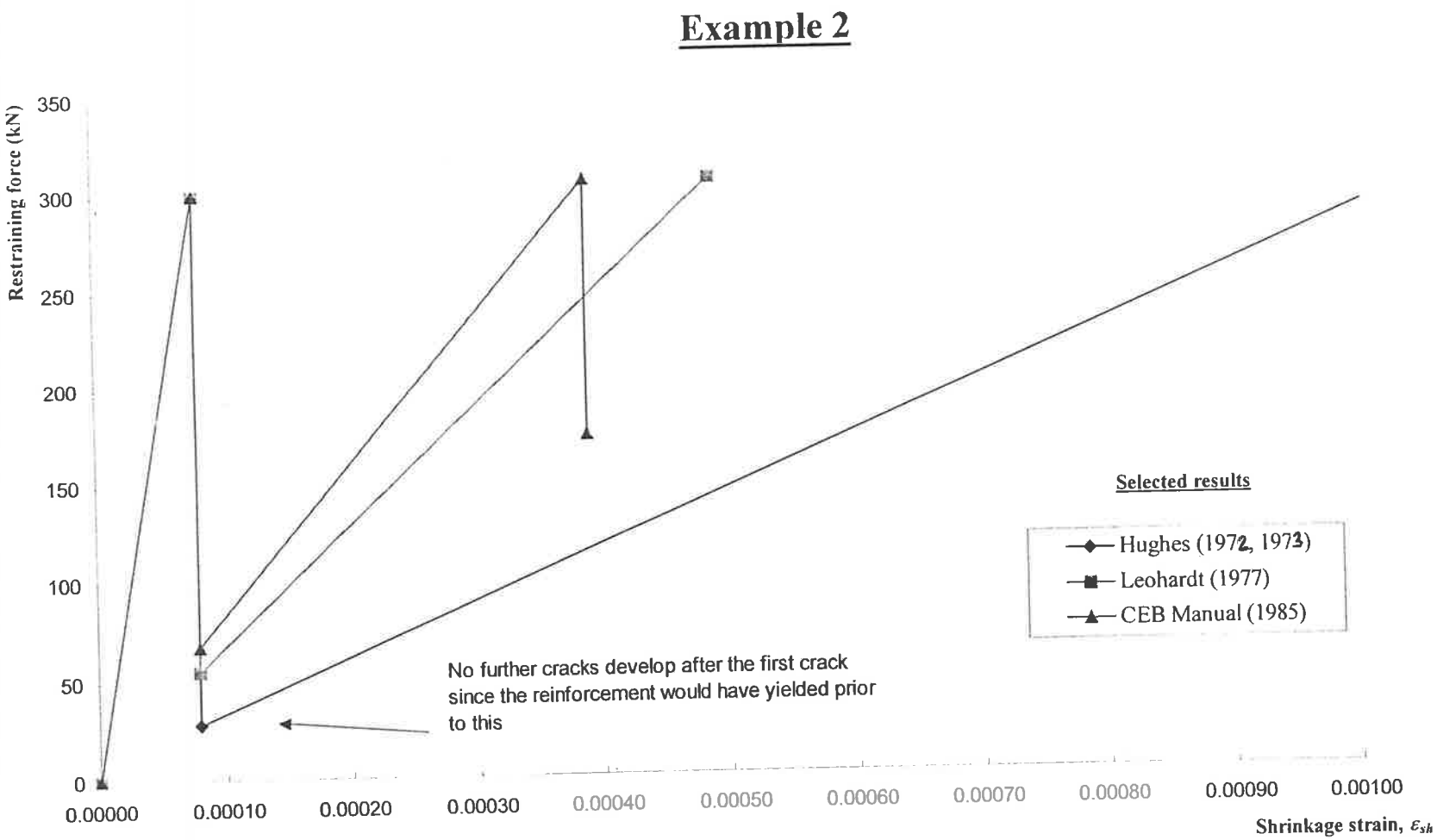

Figure A.6 Plots of restraining force vs. shrinkage strain calculated using different W_{cr}

Example 2

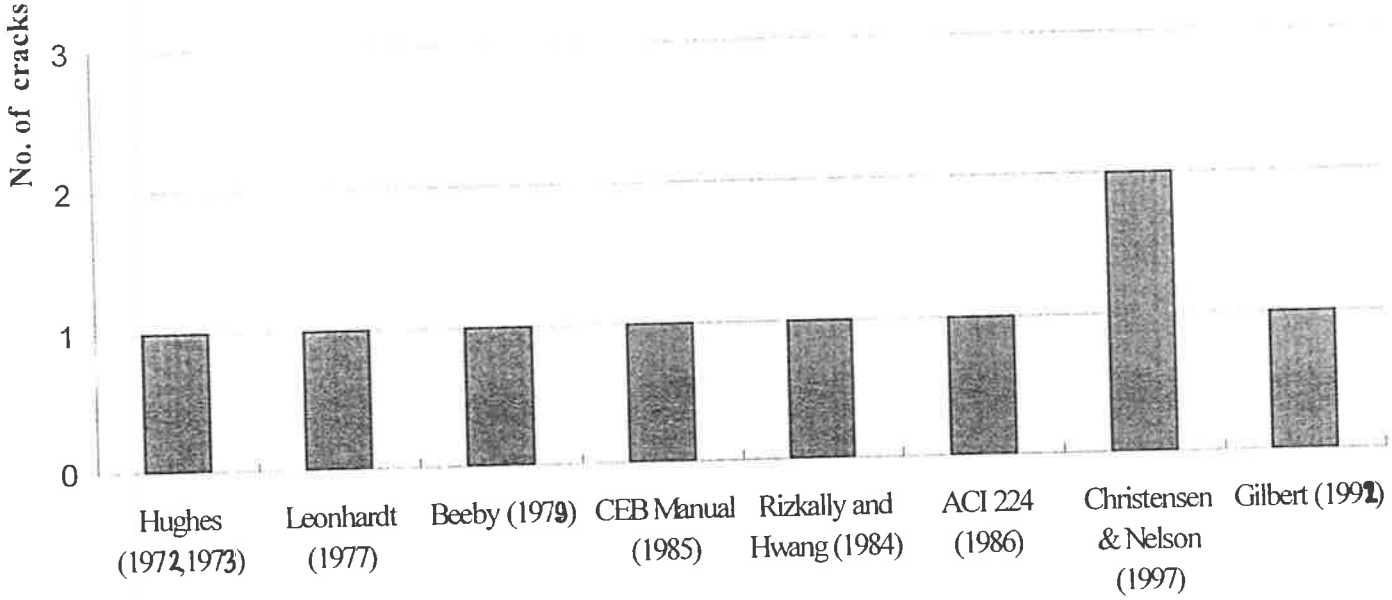

Figure A.7 Different number of cracks obtained when the amount of reinforcement is halved

Example 3

Consider the same one-way reinforced concrete slab in Example 1, but with different support conditions as shown below. The column is 6 m in height and also is assumed to be fixed at both ends. As shrinkage develops with time, the column provides partial restraint to the slab movement, while the rigid core does not allow any movements. The column sizes vary from 300mm × 300mm to 1000 mm × 1000mm. The final shrinkage strain is assumed to be 600 microstrains.

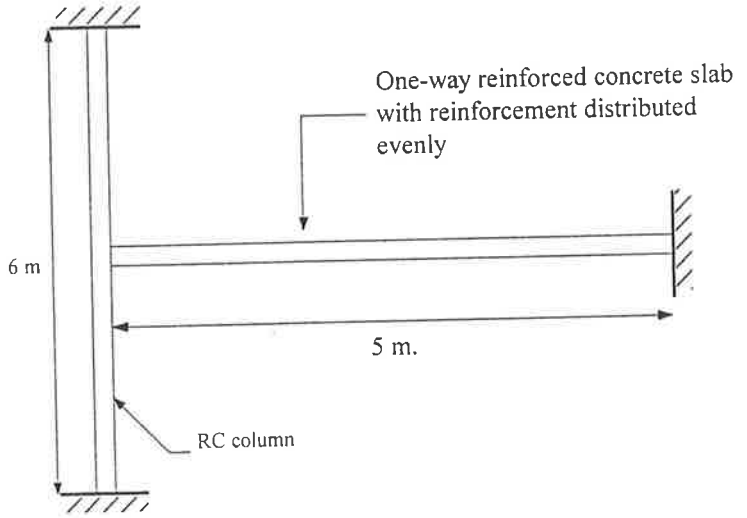

The structure has the following properties:

Concrete properties	
Tensile strength, $f_t^{'}$	2 MPa
Young's modulus, E_c	25000 MPa
Cross sectional area , A_c	150000 mm^2/m
Concrete cover, c	30 mm
Ultimate creep coefficient, ϕ^*	2.5

Reinforcement properties	
Yield strength, f_{sy}	400 MPa
Young's modulus, E_s	200000 MPa
Cross sectional area, A_s	750 mm^2/m
Reinforcement spacing, a	300 mm
Diameter, d	12 mm
Reinforcement ratio, ρ	0.005

As with previous examples, the following initial conditions need to be determined before proceeding with the analysis.

Reference	Calculation	Results
	Example 3 Using the slab column-wall sub-assemblage model presented in Chapter 4, the following initial conditions can be determined in order to carry out the analysis for the development of cracking (1) The restraining force just before the first crack can be calculated	
Eq (4.9)	$F_{cr} = f_t' A_c$ $\Rightarrow$	F_{cr} = **<u>300 kN</u>**
	(2) The bending stiffness of the column which are fixed at both ends in Equation (4.17) can be calculated as: $k_{sp} = \frac{192 E_c I}{h^3}$ where I = moment of inertia of a column	

Reference	Calculation	Results
	The assumption is also made that the column remains uncracked when subjected to restraining force Hence, the bending stiffnesses of various column sizes are as shown: Column 300 mm by 300 mm $\Rightarrow$ k_{sp} = **15000 N.mm** Column 400 mm by 400 mm $\Rightarrow$ k_{sp} = **47400 N.mm** Column 500 mm by 500 mm $\Rightarrow$ k_{sp} = **116000 N.mm** Column 600 mm by 600 mm $\Rightarrow$ k_{sp} = **240000 N.mm** Column 700 mm by 700 mm $\Rightarrow$ k_{sp} = **445000 N.mm** Column 800 mm by 800 mm $\Rightarrow$ k_{sp} = **759000 N.mm** Column 900 mm by 900 mm $\Rightarrow$ k_{sp} = **122000 N.mm** Column 1000mm by 1000mm $\Rightarrow$ k_{sp} = **185000 N.mm** (3) Shrinkage strain at first cracking By substituting value of the restraining force just before cracking calculated earlier into equation (4.17) and solve for ε_{sh}, the shrinkage strain at first cracking can be determined as: $$\varepsilon_{sh1} = \frac{F_{cr}\left(\frac{1}{k_{sp}} + \frac{1}{k_{slab}}\right)}{L}$$ The shrinkage strain at first cracking for various column sizes are as shown: Column 400 mm by 400 mm $\Rightarrow$ ε_{sh1} = 0.001396 Column 500 mm by 500 mm $\Rightarrow$ ε_{sh1} = 0.000842	

Reference	Calculation	Results
	Column 600 mm by 600 mm $\Rightarrow$ $\varepsilon_{sh1} = 0.000340$ Column 700 mm by 700 mm $\Rightarrow$ $\varepsilon_{sh1} = 0.000220$ Column 800 mm by 800 mm $\Rightarrow$ $\varepsilon_{sh1} = 0.000162$ Column 900 mm by 900 mm $\Rightarrow$ $\varepsilon_{sh1} = 0.000131$ Column 1000 mm by 1000 mm $\Rightarrow$ $\varepsilon_{sh1} = 0.000114$ Column 1100 mm by 1100 mm $\Rightarrow$ $\varepsilon_{sh1} = 0.000103$ (4) Calculation of the length of cracked region, W_{cr} The equation suggested by CEB Manual (1985) is used to calculated the minimum crack spacing, S_{min} From Example 1, it was calculated as $S_{min} = 206$ mm Since $W_{cr} = 2\varsigma S_o$, Thus $\Rightarrow$	$W_{cr} =$ **206 mm**

As with previous examples, Microsoft Excel is used to perform the analysis for each column size. The number of cracks developed, are then compared with the one in Example 1. It should be noted that the analysis assumes that shrinkage no longer takes place when the shrinkage strain approaches 600 $\mu\varepsilon$

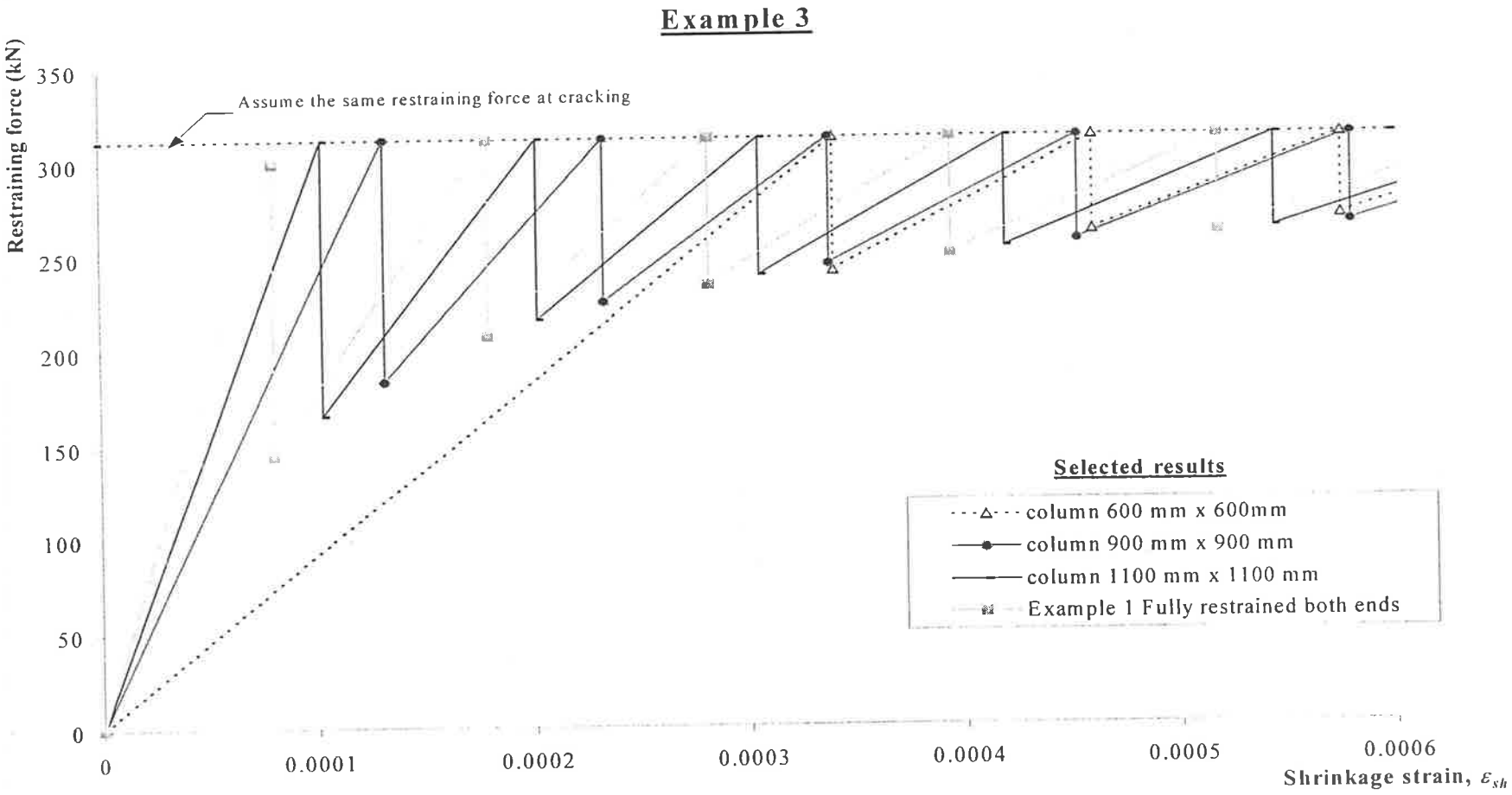

Figure A.8 Restraining force in slab vs. shrinkage strain of members from various column size

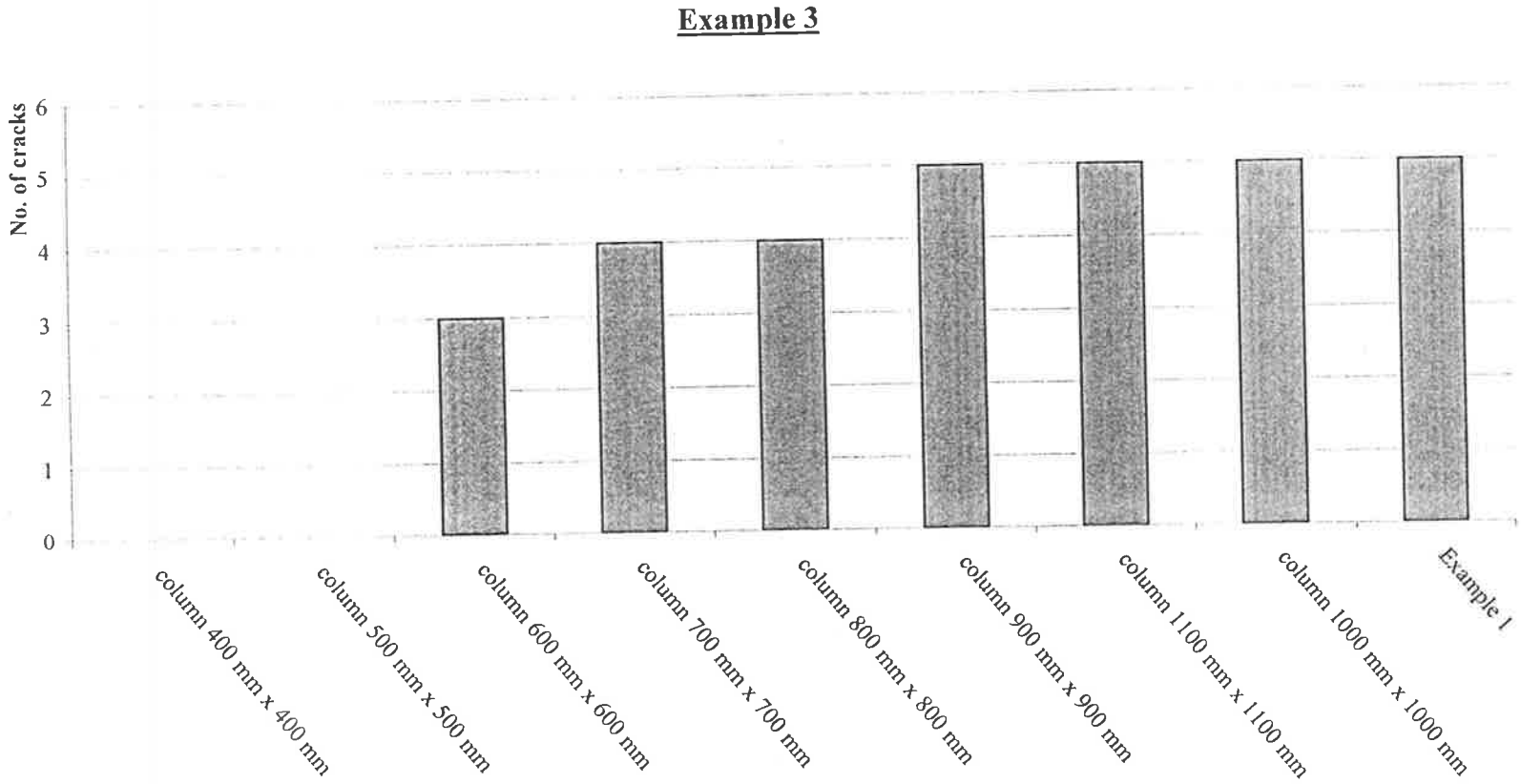

Figure A.9 Comparison of number of cracks obtained with different column sizes

Example 4

Consider two spans one-way reinforced concrete slabs as shown. The exterior and interior columns are assumed to be 500mm x 500mm in dimensions. The concrete and reinforcement properties are the same as in Example 1.

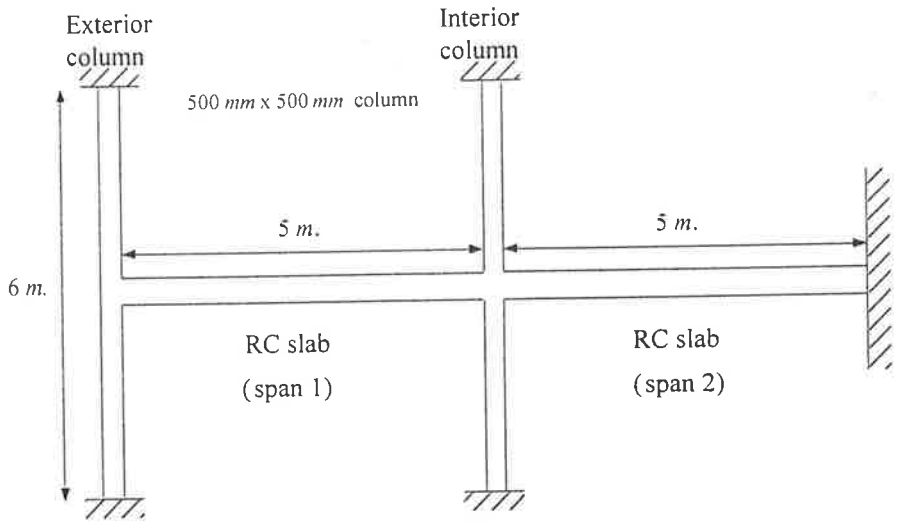

The following calculations are calculated below.

Reference	Calculation	Results
	Example 4 **<u>Condition before cracking</u>** (1) Axial stiffness of the slab The axial stiffnesses of the slabs in span 1 and 2 are identical and are calculated by: $$k_{slab1} = \frac{A_c E_c (1 + n\rho)}{L_1}$$ Likewise $$k_{slab2} = \frac{A_c E_c (1 + n\rho)}{L_2}$$ $\Rightarrow k_{slab1}$ = **<u>780,000 N.mm</u>** $\Rightarrow k_{slab2}$ = **<u>780,000 N.mm</u>**	

Reference	Calculation	Results
Example 3	(2) Bending stiffness of column 500 mm by 500 mm The bending stiffness for both exterior and interior columns are similar to Example 3 $\Rightarrow k_{spA} =$ **240,000 N.mm** $\Rightarrow k_{spB} =$ **240,000 N.mm**	
	(3) Restraining force before cracking It can be seen that the first crack would occur in the slab of span 2 because of larger restraint. Assuming the transformed area of concrete, the restraining force just before the first crack occurs when tensile strength of concrete is reached and can be calculated as:	
Eq. (4.44)	$F_{slab2} = f_t' A_c (1 + n\rho)$	
	$\Rightarrow$	$F_{slab2} =$ **312 kN**
	(4) Restraining force in span 1 and shrinkage strain at first cracking By substituting the value of F_{slab2} into equations (4.40) and (4.43), and solve both equations for F_{slab1} and ε_{sh1} simultaneously,	
Eq. (4.40)	$F_{slab1}(\frac{1}{k_{sp_A}} + \frac{1}{k_{slab1}}) + F_{slab2}(\frac{1}{k_{slab2}}) = \delta_{sh_A}$	
Eq. (4.43)	$F_{slab1}(\frac{-1}{k_{sp_B}}) + F_{slab2}(\frac{1}{k_{sp_B}} + \frac{1}{k_{slab2}}) = \delta_{sh_B}$	
	where $\delta_{sh_A} = (L_1 + L_2)\varepsilon_{sh1}$ $\delta_{sh_B} = (L_2)\varepsilon_{sh1}$	
	$\Rightarrow$	$F_{slab1} =$ **218 kN**
	$\Rightarrow$	$\varepsilon_{sh1} =$ **0.000159**
	It can be seen that at this stage, the restraining force in Span 1 is insufficient to cause any cracks.	

Reference	Calculation	Results
Example 1	**After the first crack** Immediately after the first crack, the axial stiffness of the slab in Span 2 reduced significantly and the stiffness term k_{slab2} is replaced by equation 4.45. $$k_{nslab2} = \frac{\left(A_{c2}E_c / L_2\right)}{\left(\frac{W_{cr2}}{L_2}\right)\left(\frac{1}{n_2\rho_2}\right) + \left(1 - \frac{W_{cr2}}{L_2}\right)\left(\frac{1}{1+n_2\rho_2}\right)}$$ where W_{cr2} = 206 mm This gives $\Rightarrow k_{nslab2}$ = **384236 N.mm** Also the restraining force is reduced to , F_{slab2} = **103 kN** The analysis for further cracking can proceed by solving simultaneous equations as the case before cracking. This can be achieved by using spread sheet as shown. It can be seen that as shrinkage strain increases, the restraining force in Span 1 continues to increase and the first crack developed when the restraining force exceeds 312 kN. Then cracks continue to develop in both spans until the assumed ultimate shrinkage strain is attained.	

Table A.15 Development of cracking due to shrinkage in two span reinforced concrete structure

No. of cracks									Crack width (mm)	
Span 1 (m_1)	Span 2 (m_2)	k_{slab2} (N.mm)	k_{slab1} (N.mm)	Shrinkage Strain, ε_{sh}	F_{slab2} Before (kN)	F_{slab2} After (kN)	F_{slab1} Before (kN)	F_{slab1} After (kN)	Span 1	Span 2
0	0	780000	780000	0.000159	312	NA	218	NA	Uncracked	Uncracked
0	1	384236	780000	0.000159	312	103	218	139	Uncracked	0.14
0	2	254902	780000	0.000222	312	150	251	187	Uncracked	0.21
0	3	190709	780000	0.000290	312	197	286	233	Uncracked	0.27
1	4	152344	384236	0.000362	312	205	312	223	0.31	0.28
2	5	126829	254902	0.000475	312	245	312	233	0.32	0.34
3	6	108635	190709	0.000600	312	280	312	240	0.33	0.38
End of analysis due to ultimate shrinkage strain in concrete has occurred										

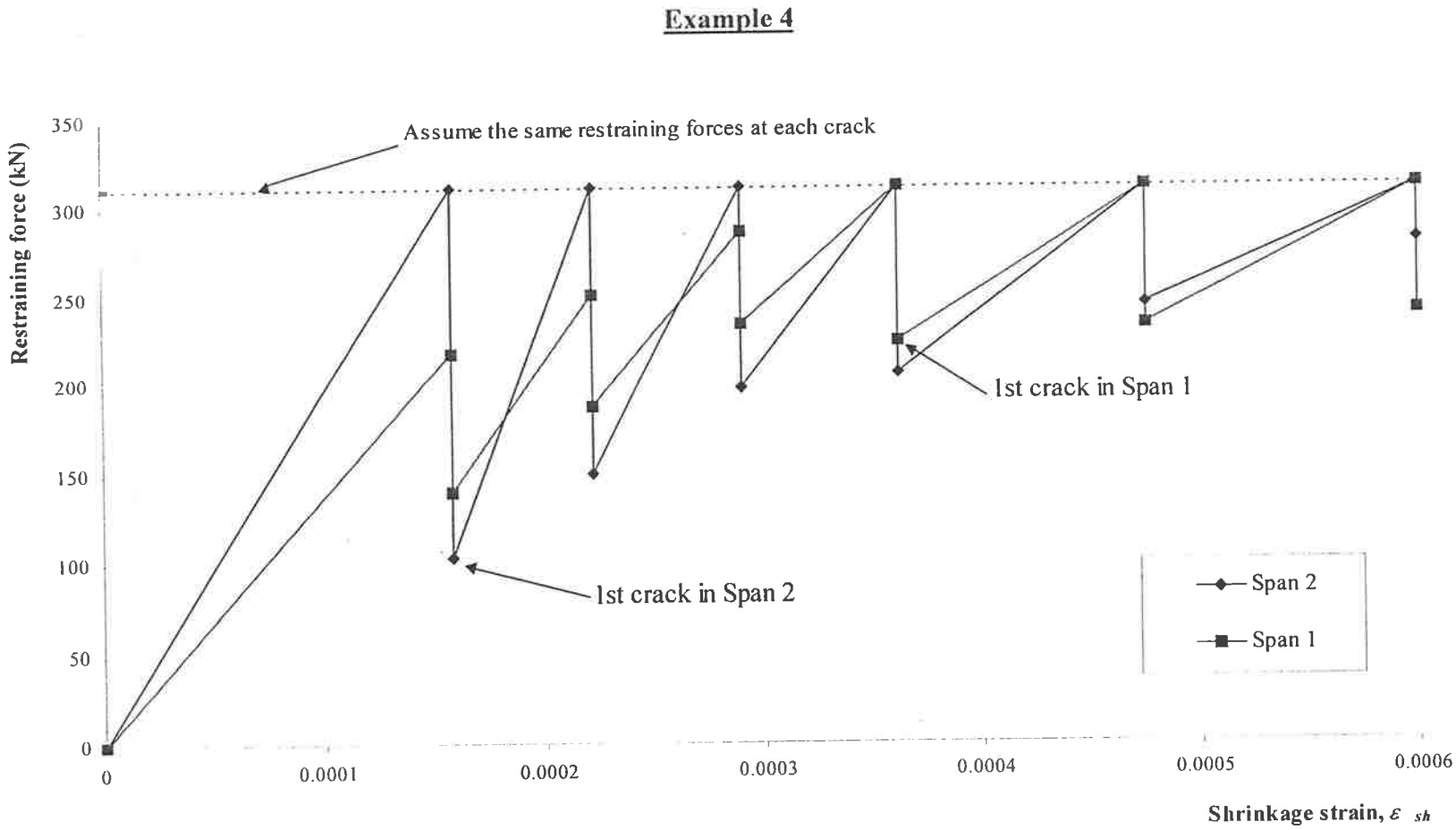

Figure A.10 Restraining forces in two span reinforced concrete slabs vs. shrinkage strain

Bibliography

1. ACI COMMITTEE 209 (1971) Prediction of creep, shrinkage and time effects in concrete structures, paper SP27-3. *Designing for effects of creep, shrinkage, temperature in concrete structures, ACI Publication SP-27.* American concrete institute, Detroit, pp. 51-93. *SP-27.*
2. ACI COMMITTEE 209 (1982) Prediction of creep, shrinkage, and temperature effects in concrete structures, ACI 209R-82, SP 76-10. *Designing for creep and shrinkage in concrete structures*, A tribute to Adrian Pauw, publication SP-76, American concrete institute, Detroit, pp.193-300.
3. ACI COMMITTEE 224 (1986) *Cracking of concrete member in direct tension* (ACI 224.2R-86, p 11). American concrete institute, Detroit,
4. ACI COMMITTEE 224 (1989) *Control of cracking in concrete structures (ACI 224R-89*, p 43). Detroit, American concrete institute.
5. ACI COMMITTEE 224 (1995) *Joints in concrete Construction (ACI 224.3R-95)*, Detroit, American concrete institute.
6. ALEXANDER, M. A. & LAWSON, R. M. (1981*) Design of movement in building*, p54. Construction industry research and information association, London.
7. AL RAWI, R. S. & KHEDER, G. F. (1990) Control of cracking due to volume change in base-restrained concrete members", *ACI structural journal*, July/August, pp. 397-405.
8. AL-SULAIMANI, G. J., KALEEMULLAH, M., BASUNBUL, I. A. & RASHEEDUZZAFAR (1990) Influence of corrosion and cracking on bond behaviour and strength of reinforced concrete members. *ACI Structural journal*, March-April, Vol. 87, No. 2, pp. 220-231.

9. AMERICAN CONCRETE INSTITUTE (ACI) (1989) *Building code requirements for reinforced concrete (ACI 318-89) and commentary - ACI 318R-89*,Detroit, USA American concrete institute.
10. ARUMUGASAAMY, P. & SWAMY, R. N. (1989) A simple design aid for predicting shrinkage and creep strains in buildings and bridges, SP117-11. *Long-term serviceability of concrete structures*, Eds. Farah, A., Detroit, American concrete institute, pp. 227-248.
11. BAKOSS, S. L., GILBERT, R. I., FAULKES, K. A. & PULMANO, V. A. (1982) Long term deflection of reinforced concrete beams. *Magazine of concrete research*, December, Vol. 34, No.121, pp.203- 212.
12. BARTON, L. (1989) Joints in concrete buildings. *Concrete Institute of Australia, Queensland Branch, Seminar*, October, p.8
13. BASE, G.D. (1981) Bond, and control of cracking in reinforced concrete. *Bond in Concrete*, Eds. Bartos, P. pp 446-457.
14. BASE, G. D. (1985) Shrinkage cracking-how they form-detailing reinforcement to control shrinkage cracking. Cracking of concrete-its importance, prediction and control, Concrete Institute of Australia, November 4.
15. BASE, G. D. & MURRAY, M. H. (1978a) Controlling shrinkage cracking in restrained reinforced concrete. Pavements and structures, The Ninth ARRB Conference, University of Queensland 21-25 August, Australian Road Research Board, Vol. 9 Part 4, pp. 167-173
16. BASE, G. D. & MURRAY, M. H.(1978b) Control of shrinkage cracking in reinforced concrete", Department of Civil Engineering, University of Melbourne, 7 pp.
17. BASE, G. D. & MURRAY, M. H. (1982) A new look at shrinkage cracking. *Civil engineering transactions*, The institute of engineers, Australia, Vol. CE24, No.2, pp 171-176.
18. BAZANT, Z. P. (1986) Physical mechanisms and their mathematical descriptions, Chapter1. Fourth RILEM international symposium on Creep and shrinkage of concrete: mathematical modelling, Northwestern University, Illinios, USA.

19. BAZANT, Z. P. & PANULA, L. (1978) Practical prediction of time-dependent deformations of concrete, Part 1 and 2. *Materials and structures*, September-October, Vol. 11, No. 65, pp. 305-228.
20. BAZANT, Z. P. & PANULA, L. (1978) Practical prediction of time-dependent deformations of concrete, Part 3. *Materials and structures*, November-December, Vol. 11, No. 66, pp. 415-434.
21. BAZANT, Z. P. & PANULA, L. (1982) New model for practical prediction of creep and shrinkage. *Designing for creep and shrinkage in concrete structures, ACI SP-76*. American concrete institute, Detroit, pp. 7-23.
22. BAZANT, Z. P. & PANULA, L. (1984) Practical prediction of creep and shrinkage of high strength concrete. *Materials and structures*, September-October, Vol. 17, No. 101, pp. 375-378.
23. BAZANT, Z. P., OSMAN, E. & THONGUTHAI, W. (1976) Practical formulation of shrinkage and creep of concrete. *Materials and structures*, November-December, Vol. 9, No. 54, pp. 395-406.
24. BAZANT, Z. P. & WITTMANN, F. H. (1982) *Creep and shrinkage in concrete structures*, p 363,New York. Wiley.
25. BEEBY, A. (1985) Cracking of concrete-prediction and control of flexural and direct tension cracking. Cracking of concrete-its importance, prediction and control, Concrete Institute of Australia, November 4.
26. BEEBY, A. W. (1979), The prediction of crack widths in harden concrete. *The structural engineer*, January, Vol. 57A, No.1, London, pp 9-17.
27. BERNHARDT, C. J. (1969) Creep and shrinkage of concrete. *Materials and structures*, Vol. 2, No. 8, pp. 145-148.
28. BOSWELL, P. (1969) Detailing for movement in precast concrete structures, Paper 5, Session b: Design and detailing for movement, p. 13. *Design for movement in buildings.*
29. BOWLES, J. E. (1988) *Foundation analysis and design, International edition, 4th edition*, p.1004, Singapore. McGraw-Hill Book Co.
30. BRICKELL, A. & HOADLEY, P. J. (1976) Thermal and shrinkage cracking in reinforced concrete slabs. *Civil engineering transactions*, The institute of engineers, Australia, Vol. CE18, No.1, pp. 24-28.

31. BRISTISH STANDARDS INSTITUTION (1993) *BS8110: Structural use of concrete:1985*. London

32. BROMS, B. B. & LUTZ, L. A. (1965) Effects of arrangements of reinforcement on crack width and crack spacing of reinforced concrete members. *Journal of the American concrete institute, proceedings*, Vol. 62, Nov., pp. 1395-1410.

33. BRUGGELLING, A. S. G. (1991) *Structural concrete, Theory and its application*, p. 470. Netherlands, A.A. Balkema.

34. BUSSELL, M. N. & CATHER, R. (1995) *Design and construction of joints in concrete structures, Report 146*, p. 79. London. Construction industry research and information association (CIRIA).

35. CAMPBELL-ALLEN, D. (1973) The prediction of shrinkage for Australian concrete. *Civil engineering transactions*, Institute of engineers, Australia, Vol. 15, No.1 & 2 pp. 53-57, 62.

36. CAMPBELL-ALLEN, D. (1979) *The reduction of cracking in concrete*. School of civil engineering, University of Sydney in association with cement and concrete of Australia, May, p.165.

37. CAMPBELL-ALLEN, D. (1992) Properties of hardened concrete. *Australian concrete technology*. Eds RYAN, W.G.& SAMARIN, A., chapter 10. Longman Cheshire, p.197.

38. CAMPBELL-ALLEN, D & HUGHES, G. W. (1981) Reinforcement to control thermal and shrinkage cracking. *IEAust, Civil Engineering Transactions*, Vol. CE23, No. 3, August, pp. 158-165.

39. CEB-FIP (1993*) CEB-FIP Model Code 1990, Design code*, p. 437, London. Thomas Telford.

40. Cement and Concrete Association of Australia (1996). *Joints in Concrete Buildings, Concrete Information Technical Note 63*, 6 pp.

41. CHAN, H. C., CHEUNG, Y. K. & HUANG, Y. P. (1992) Crack analysis of reinforced concrete tension members. Journal of structural engineering, August, Vol. 118, No. 8, pp. 2118-2132.

42. CHRISTIANSEN, M. B. & NIELSEN, M. P. (1997) Modelling tension stiffening in reinforced concrete structures - Rods, beams and disks.

Department of structural engineering and materials, Technical University of Denmark, Series R, No. 22

43. COMITE' EURO-INTERNATIONAL DU BETON (1985) *CEB design manual on cracking and deformations, English edition*, Eds Beeby, A. W., Farve, R., Koprna, M. & Jaccoud, J. P., Lausanne, Swiss Federal Institute of Technology.
44. COURCY, J.W. (1969a) Movement in concrete structures, Regional recommendations and standards for design and construction: Part 1. *Concrete*, Vol. 3, No. 2, pp. 241-246.
45. COURCY,J. W. (1969c) Movement in concrete structures, Regional recommendations and standards for design and construction: Part 3. *Concrete*, Vol. 3, No. 2, pp.335-338.
46. COURCY,J.W. (1969b) Movement in concrete structures, Regional recommendations and standards for design and construction: Part 2. *Concrete*, Vol. 3, No. 2, pp.293-296.
47. EDWARDS, A. D. & PICARD, A. (1972) Theory of cracking in concrete members. *Journal of structural division*. Proceedings of the American Society of Civil Engineers, December, Vol.98, No. ST12, pp. 2687-2700.
48. ELBADRY, M. & GHALI, A. (1995) Control of thermal cracking of concrete structures. *ACI structural journal*, July/August, Vol. 92, No. 4, pp. 435-450.
49. EVANS, E. P. & HUGHES, B.P. (1968) Shrinkage and thermal cracking in a reinforced concrete retaining wall. *Proc. institute of civil engineers*, Vol. 39, pp111-125.
50. EXPERIMENTAL BUILDING STATION (1977) Joints in suspended concrete floor slabs (Revised). *EBS Notes on the science of building, NSB 112*. Department of Housing and Construction, May, p. 4.
51. FENWICK, R. C. (1973) Assessment of the influence of creep and shrinkage on concrete structures. Movement in concrete, Proceedings of a seminar held at the New Zealand Concrete Research Association in Wednesday, August 8bth, pp. 30-53.
52. FINTEL, M. & GHOSH, S. K. (1983) Economics of long-span concrete slabl systems for office buildings - A survey. Concrete international, February, pp.21-34.

53. FINTEL, M. (1974) *Handbook of concrete engineering*, pp. 94-110. New York, Van Nostrand Reinhold Company.
54. FIP RECOMMENDATIONS () *Design of multi-story precast concrete structures*, Thomas Telford.
55. FLOEGL, H. & MANG, H. A. (1982) Tension stiffening concept based on bond slip. *Journal of structural division.* Proceedings of the American Society of Civil Engineers, December, Vol.108, No. ST12, pp. 2681-2700.
56. GHALI, A. & FAVRE, R. (1986) *Concrete structures: stresses and deformations*, USA, 352 pp, Chapman and Hall Ltd.
57. GILBERT, R. I. (1988) *Time effects in concrete structures*, p. 321, The Netherlands. Elsevier Science Publishers B.V.
58. GILBERT, R. I. (1992) Shrinkage cracking in fully restrained concrete members. *ACI structural journal*, March-April, pp 141-149.
59. GOGATE, A. B. (1984) An analysis of ACI Committee 350's recommended design standards. *Concrete International*, Vol. 6, No. 10, October, pp. 17-20.
60. GOTO, Y. (1971) Cracks formed in concrete around deformed tension bars. *ACI Journal*, April, Vol. 68, No. 4, pp. 244-251.
61. GUPTA, A. K. & MAESTRINI, S. R. (1990) Tension-stiffness model for reinforced concrete bars. *Journal of structural engineering*, ASCE Structural division, March, Vol. 116, No. 3, pp. 769-790
62. HARRISON, T. A. (1981) *Report 91, Early-age thermal crack control in concrete*. Construction industry research and information association, London (CIRIA), 48 pp.
63. HUGHES, B. P. (1972) *Limit State Theory for Reinforced Concrete*, London, pp. 431. Pitman Publishing.
64. HUGHES, B. P. (1973) Early thermal movement and cracking of concrete. *Concrete,* May, pp. 43-44.
65. HUGHES, B. P. (1974) Early thermal stresses in massive RC structures. *Building Research and Practice*, May/June, pp 165-171.
66. HUGHES, G.W. (1978) *Reinforcement to control thermal and shrinkage cracking, Thesis*, Master of Engineering Science, University of Sydney

67. JIENG, D. H., SHAH, S. P. & ANDONIAN, A. T. (1984) Study of the transfer of tensile forces by bond. *ACI Journal, Proceedings*, vol. 81, No. 3, pp. 251-259

68. KANKAM, C. K. (1997) Relationship of bond stress, steel stress, and slip in reinforced concrete. *Journal of structural engineering* , January, Vol. 123, No. 1, pp 75-85.

69. KEMP, E. L. & WILHELM, W. J. (1979) Investigation of the parameters influencing bond cracking. ACI Journal, January, Vol. 76, No. 1, pp. 47-55.

70. KHAN, F. R. & FINTEL, M. (1971) Conceptual details for creep, shrinkage, and temperature in ultra high rise buildings. *Designing for the effects of creep and shrinkage in concrete structures, SP-27.* American Concrete Institute. pp.215-218.

71. LEONHARDT, F. (1977) Crack control in concrete structures, p26. IABSE Surveys No. S-4/77, *International association for bridge and structural engineering*, Zurich, August.

72. LUTZ, L. & GERGELY, P. (1967) Mechanics of bond and slip of deformed bars in concrete. *ACI Journal*, November, Vol. , No. pp. 711-721.

73. MANN, O. CLARKE (1970) Expansion-contraction joint locations in a concrete structure. *Designing for the effects of creep and shrinkage in concrete structures,* American Concrete Institute. pp. 311-322

74. MARTIN, I. & ACOSTA, J. (1970) Effect of thermal variations and shrinkage on one story reinforced concrete buildings. *Designing for the effects of creep and shrinkage in concrete structures, SP-27.* American Concrete Institute. pp.229-241.

75. McDONALD, D. B. & ROPER, H. (1993) Accuracy of prediction models for shrinkage of concrete. *ACI Materials journal*, American concrete institute, May-June, Vol. 90, No. 3, pp. 265-271.

76. MAYER, H & RUSCH, H (1970) Building damage caused by deflection of reinforced concrete building components. *Technical translation 1412.* National research council, Ottawa, Canada.

77. MULLER, H. S. & HILSDORF, H. K. (1982) Comparison of prediction methods for creep coefficients of structural concrete with experimental data.

Fundamental research on creep and shrinkage of concrete. Eds WITTMAN, F. H., Martinus Nijhoff Publishers, The Hague.

78. MULLER, H. S. & PRISTL, M. (1993) Creep and shrinkage of concrete at variable ambient conditions. *Creep and shrinkage of concrete, Proceedings of the fifth international RILEM symposium*, Eds BAZANT, B. P. & CAROL, I. , 6-9 September, Barcelona, Spain, E & FN SPON, Great Britain, pp.l 5 – 26.
79. MURRAY, M.H. (1991) Shrinkage crack control in AS3600. *Australian civil engineering transactions*, December, Vol. CE33, No.4, pp 225-232.
80. NATIONAL ACADEMY OF SCIENCES (1974) *Expansion joints in buildings, Technical report No. 65*, Washington, D.C., pp. 43.
81. NEVILLE, A. M. (1973) Summary of the address given by Professor A.M. Neville. Movement in concrete, Proceedings of a seminar held at the New Zealand Concrete Research Association in Wednesday, August 8bth, pp. 3-19.
82. NEVILLE, A. M. (1981) *Properties of concrete, 3rd edition*, p.779, Great Britain. Longman Scientific & Technical.
83. NEVILLE, A. M., DILGER, W. H. & BROOKS, J. J. (1983) *Creep of plain and structural concrete*, p 361. London, Construction Press.
84. NEVILLE, A. M. & BROOKS, J.J (1987) *Concrete technology*, p.438, England. Longman Scientific & Technical.
85. NEWBEGIN, J. D. & BRUERE, G. M. (1992) Chemical admixtures. *Australian concrete technology*. Eds RYAN, W.G.& SAMARIN, A., chapter 4. Longman Cheshire, p.197.
86. NGAB, A. S., NILSON, A. H. AND SLATE, F. O. (1981) Shrinkage and creep of high strength concrete. *ACI Journal, Proceedings*, vol. 78, No. 4, pp. 255-261
87. NIELSEN, L. F. (1982) The Improved Dishinger method as related to other methods and practical applicability. *Designing for creep & shrinkage in concrete structures, a tribute to Adrain Pauw, Publication SP-76*, American concrete institute, Detroit, pp. 169-191.
88. NILSON, A. H. (1972) Internal measurement of bond slip. *ACI Journal*, July, Vol. 69, No. , pp. 439-441.

89. OESTERLE, R. G., GLIKIN, J. D. & LARSON, S. C. (1989) *Design of precast prestressed bridge girders made continuous, National Cooperative Highway Research Program, Report 322*, Transport Research Board, National research council, Washington D.C., November, 97 pp.

90. O'MOORE, L. M. (1996) *Time-dependent behaviour of reinforce and plain high-strength concrete columns, PhD Thesis*. Department of Civil Engineering, The University of Queensland, August.

91. OUYANG, C., KULKARNI, S. M. & SHAH, S. P. (1997) Prediction of cracking response of reinforced concrete tensile members. *Journal of structural engineering*, January, Vol. 123, No. 1, pp. 70-78.

92. PARK & PAULAY (1975) *Reinforced concrete structures*. John Wiley & Sons, Inc.

93. PECK, R. B., HANSON, W. E. & THORNBURN, T. H. (1974) *Foundation engineering*, p. 514, New York. John Wiley & Sons Inc..

94. PERRY, E. S. & THOMSON, J. N. (1966) Bond stress distribution on reinforcing steel in beams and pullout specimens. *ACI Journal*, August, Vol. 63. No. 8, pp 865-876.

95. PFEIFFER, M. J. & DARWIN, D. (1987) *Joint design for reinforced concrete buildings, SM Report No. 20*, University of Kansas Center for research, Lawrence, KS, December, pp. 73.

96. POTTER, R. J. (1969) The detailing of structures, cladding and non-structural components for movement.

97. POTTER, R. J. (1997) Joints in concrete buildings. *Concrete Information, Technical Note 63*. Cement and Concrete Association of Australia, p. 6.

98. PRECAST AND PRESTRESSED CONCRETE (1995) PCI design handbook, third edition, section 4.3, Illinois, Chicago, Prestressed concrete institute.

99. RAINGER, P. (1983) *Movement control in the fabric buildings*, p. 216. London, Batsford Academic and Educational LTD.

100. REINHARDT, H. W. (1991) Imposed deformation and cracking. *IABSE Colloquium Stuttgart 1991, Structural concrete*, International association for bridge and structural engineering, pp. 101-110.

101. RICE, P. F. (1984) Structural design of concrete sanitary structures. *Concrete international*, Vol. 6, No. 10, October, pp.14-16.

102. RICHARDSON, M. G. () Cracking in reinforced concrete buildings. *Concrete international*, January, pp. 21-23.

103. RIZKALLA, S. H. & HWANG, L. S. (1984) Crack prediction for members in uniaxial tension. ACI Journal, November-December, Vol. 81, No. 6, pp.572-579.

104. RODIN, J. (1969) The implications of movement on structural design, Paper 4, Session b: Design and detailing for movements, p. 25. Design of movement in buildings.

105. ROPER, H. (1966) Dimensional changes as a factor in selection of rock types for use as concrete aggregates. *Construction review,* Vol. 39, No. 7, pp. 22-23

106. ROPER, H. (1974a) Shrinkage, tensile creep and cracking tendency of concretes. *Australian road research*, December, Vol. 5, No. 6, pp. 26-35.

107. ROPER, H. (1974b) The properties of concrete manufactured with coarse aggregate of the Sydney Area. *Australian road research*, December, Vol. 5, No. 6, pp. 40-50.

108. ROPER, H. (1974c) Studies of the deformation and cracking characteristics of Sydney concrete under site conditions. *Australian road research*, December, Vol. 16, No. 2, pp. 179-185.

109. RUSSO, G. & ROMANO, F. (1992) Cracking response of RC members subjected to uniaxial tension. *Journal of structural engineering*, May, Vol. 118, No. 5, pp. 1172-1190.

110. RUTH, JÜRGEN. (1995) Movement joints: a necessary evil or avoidable?. *Large Concrete Buildings* Eds. Rangan, B.V. & Warner, R.F. Chapter 10.

111. SAMARIN, A. (1985) Prehardening cracking in concrete. Cracking of concrete-its importance, prediction and control, Concrete Institute of Australia, November

112. SAMARIN, A. (1996) Concrete shrinkage-causes and effects to be considered in a structural design. *Concrete in Australia, Concrete Institute of Australia*, vol.22, no.1, April, pp.18-23.

113. SOMAYAJI, S. & SHAH, S. (1981) Bond stress versus slip and cracking response of tension members. *ACI Journal, Proceedings*, May-June, Vol. 78, No. 3, pp. 217-225.

114. STANDARD AUSTRALIA. AS3600 (1994) *Concrete Structures*, Standard Australia, Sydney.

115. TASSIOS, T. P. & YANNOPOULOS, P. J. (1981) Analytical studies on reinforced concrete members under cyclic based on bond stress-slip relationships. *ACI Journal, Proceedings*, May-June, Vol. 78, No. 3, pp. 206-216.

116. TECHNICAL SUB-COMMITTEE (1989) *Design of joints in concrete buildings*. C.I.A. NSW Branch, August, p.9.

117. THORNTON, C. H. & LEW, I. P. (1982) Analysis of restrained concrete structures for creep and shrinkage, pp.305-321. *Fundamental research on creep and shrinkage of concrete*. Eds WITTMAN, F. H., Martinus Nijhoff Publishers, The Hague.

118. VENKATESWARLU, B. & GESUND, H. (1972) Cracking and bond slip in concrete beams. *Journal of structural division*. Proceedings of the American Society of Civil Engineers, December, Vol.98, No. ST12, pp. 2663-2685.

119. WALSH, P. (1988) *Use of the Australian Standard for concrete structures*, Australia, CSIRO.

120. WARNER, R. F., RANGAN, B. V. & HALL, A. S. (1989) *Reinforced concrete, 3rd edition*, p. 553, Melbourne. Longman Cheshire Ltd.

121. WARNER, R. F., Rangan, B. V., HALL, A. S. & FAULKES, K. A. (1998) *Concrete structures*, p 781, Melbourne. Addison Westley Longman Australia Pty. Limited.

122. WHITE, C. (1985) Drying shrinkage-what happens before?- Cement aspects. Cracking of concrete-its importance, prediction and control, Concrete Institute of Australia, November 4.

123. WICKE, M. (1991) Cracking and deformation in structural concrete. *IABSE Colloquium Stuttgart 1991, Structural concrete*, International association for bridge and structural engineering, pp. 50-57.

124. WITTMANN, F. H. (1982) Creep and shrinkage mechanisms, pp. 129-161 *Creep and shrinkage in concrete structures*, Eds BAZANT, B. P. & WITTMAN, F. H., John Wiley & Sons Ltd., Belfast.

125. WOOD, R. H. (1981) Joints in sanitary engineering structures. *Concrete international*, April, pp. 53-56

126. YANG, S. & CHEN, J. (1988) Bond slip and crack width calculations of tension members. ACI structural journal, July-August, Vol. 85, No. 4, pp. 441-422.

127. YANNOPOULOS, P. J. (1989) Variation of concrete crack widths through the concrete cover to reinforcement. *Magazine of concrete research*, June, Vol. 41, No. 147, pp. 63-68.

Errata

Page vi	**Last line**
Replace	Crack due an applied tensile force
With	Crack due to an applied tensile force
Page xix	**line2**
Replace	Effect cross section
With	Effective cross section
Page 108	**line 2**
Replace	Equation (3.95)
With	Equation (3.96)
Page 176	**line 6**
Replace	Jürgen (1995)
With	Ruth (1995)